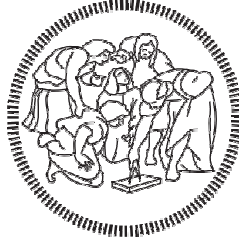


POLITECNICO DI MILANO

Department of Architecture, Built Environment and Construction Engineering  
ABC-PhD XXIX Cycle



**Building Simulation Models in Control Systems for Energy Efficiency**

PhD Dissertation by  
Giorgia Marenzi

Supervisor: Massimiliano Manfren  
Tutor: Niccolò Aste

Head of PhD Program: Enrico De Angelis



A Massimiliano, Dario e Lavinia



## INDEX

Abstract .....	4
1. Introduction.....	5
List of References .....	7
2. Problem and Claim.....	10
2.1. Performance Gap.....	10
2.2. Data Analytics and Simplified Building Modeling.....	11
List of References .....	13
3. State of the Art of BACS for performance optimization .....	15
3.1. Building Automation and Control Systems .....	17
3.2. Control Fundamentals, Strategies and Schemes .....	19
3.3. Control Devices, Networks and Systems Integration .....	21
3.3.1. Occupancy Detection and Behavioral Modeling .....	23
3.3.2. Indoor Environmental Quality Control and Analysis .....	24
3.4. Control Modes and Strategies .....	25
3.4.1. Rule Based Control (RBC) and Model Based Control (MBC).....	27
3.4.2. Adaptive Control and Learning Techniques .....	28
3.4.3. Model Predictive Control.....	29
3.5. Buildings and Control Models .....	30
3.5.1. White-Box Models.....	32
3.5.2. Grey-Box Models.....	33
3.5.3. Black-Box Models .....	33
3.6. BACS and Building Energy Management .....	34
3.6.1. Load Management and Performance Optimization .....	35
3.6.2. Performance Monitoring, Tracking and Data Analysis .....	37
3.7. Discussion .....	38
List of References .....	40

4. Reduced Order Building Energy Models.....	49
4.1. Fundamental Definitions in Modeling.....	50
4.1.1. Linear and Non-Linear Models.....	50
4.1.2. Time Variant and Time Invariant Models.....	51
4.1.3. Discrete and Continuous Time Models.....	51
4.1.4. Direct and Inverse Models.....	51
4.2. Building Energy Dynamics.....	53
4.2.1. Input and Output Data of Model.....	55
4.2.2. Energy Balance of Nodes.....	58
4.2.3. Temperature of Nodes.....	58
4.2.4. Internal and Solar Gains.....	59
4.2.5. Heat Transfer in Building.....	61
4.2.6. Factors for Nodal Energy Gains of Technical Systems.....	63
4.2.7. Climate Data Analysis.....	63
4.2.8. Intermittent Operation Accounting.....	64
4.3. Optimization Model Formulation.....	65
4.3.1. Non Linear Time Variant Model Objective Function.....	66
4.3.2. Linear Time-Variant Model Objective Function.....	68
4.3.3. Linear Time Invariant Model (2 States, 1 Hidden State) Objective Function.....	68
4.3.4. Linear Time Invariant Model (1 States, 2 Hidden State) Objective Function.....	70
4.4. Dynamic Model Validation.....	71
4.5. Operation Data Analysis.....	74
4.5.1. Parameters Estimation Procedure and Uncertainty Analysis.....	75
4.5.2. Simplified Direct Model.....	78
4.5.3. Simplified Inverse Model.....	80
4.6. Model Predictive Control.....	82
4.6.1. Optimization Model for MPC.....	83
4.6.2. Comfort Model.....	84
4.7. Model Output and Visualization of Relevant Quantities.....	86
List of References.....	88
5. Applications.....	91
5.1. Case Study Description.....	91
5.2. Building Energy Simulations.....	94
5.2.1. Detailed Simulation.....	95

5.2.2. Simplified Simulation .....	102
5.2.3. Comparisons.....	105
5.3. Performance Monitoring, Tracking and Data Analysis .....	108
5.3.1. Monthly Energy Needs Analysis – Heat Transfer Coefficient Investigation .....	108
5.3.2. On Site Measurements – Experimental Analysis.....	119
5.3.3. Free Floating Temperature Analysis – Thermal Capacity Investigation .....	122
5.3.4. Model Calibration .....	123
5.3.5. Parameter Identification with Inverse Models .....	127
5.4. Load Management and Performance Optimization .....	130
5.4.1. General Statements .....	131
5.4.2. Seasonal Energy Saving.....	132
5.4.3. Seasonal Comfort Analysis .....	134
5.4.4. Daily and Hourly Analysis.....	141
5.4.5. Sensitivity Analysis.....	149
5.5. Discussion .....	153
List of References .....	155
6. Conclusion .....	156

## **ABSTRACT**

The pressing global environmental issues are fostering a rapid change in the energy and sustainability policies for the built environment. New paradigms are emerging, such as “Nearly Zero Energy Building” (nZEB), and sustainability assessment schemes are progressively evolving and diffusing. However, empirical studies show how, very often, the gap between the predicted (design phase) and measured (operation phase) energy performance is very large, due to design phase, construction phase, commissioning and operation phase errors. This performance gap creates a problem of credibility in the building industry and, more in general, in sustainability practices.

Current design and operation practices for building performance optimization should evolve to ensure adequate performance in spite of possible changes in climatic conditions (e.g. climate change adaptation) and occupants’ behavioral patterns. Optimal control and data analytics can play a key role in this sense. For these reasons, a framework for the analysis of the potential of Building Automation and Control Systems for performance optimization is proposed, specially on predictive control. This framework aims to highlight, in particular, the possibility of establishing an effective methodological continuity among building performance simulation, control and data analytics, not recognizable in present practices.

In predictive control systems the main problem is related to the building model used and its calibration phase and not to the optimization algorithm. There are many detailed physical dynamic models developed to simulate building behavior, however, many of these models need detailed information, very high computation power and memory space. An alternative is represented by data driven models: statistical and machine learning techniques can help determining input/output relationships without detailed a priori knowledge of the phenomena themselves. In models obtained solely by statistical methods, therefore, the identified parameters tend to lose physical insights and sometimes their values contradict physical phenomena. In order to avoid this, hybrid models, mixing knowledge-based and statistical approaches, are introduced. These models are also called simplified or gray-box models.

In conclusion, the aim of the research, therefore, is to find a simple and understandable method able to create a dialogue with both control and energy simulation fields in order to fill the gap between the predicted (design phase) and measured (operation phase) energy performance. Furthermore, a very important intend is to find the main data needed by the building model in order to guarantee a good control result (in a predictive perspective) and a calibration method able to verify whether the model simulates effectively the actual trend.

## 1. INTRODUCTION

Energy services have a large impact both in economic and environmental terms. The residential and commercial sectors use 154 quadrillion Btu (3.9 trillion TOE) in energy (includes losses in electricity generation, transmission, and distribution), which accounts for almost 30% of final energy use in the world (524 quadrillion Btu, 13 trillion TOE) [1]. The energy demand related to heating, cooling and ventilation is often the predominant part, although the incidence of the energy used for appliances and lighting should not be underestimated, in particular in commercial buildings, but also in residential ones, depending on country specific characteristics. In U.S. homes about 40% of this energy is due to space heating [2] while in Europe the value rises up at 70% [3]. Another important part of final energy consumption is represented by electricity; 35% of total energy use in the U.S. homes [2] and 15% in Europe [3] is related to appliance, lighting and electronics, and the energy consumption, in absolute term, is increasing.

Today, the reduction of the environmental impact determined by building technologies and services is fundamental for global sustainability. There exist important ongoing initiatives for the built environment involving sustainability assessment [4,5], energy efficiency of products and practices [6] and energy policy [7]. European Commission, in fact, has underlined the importance of the issue by adopting an *Action Plan for energy efficiency* aiming to 20% reduction by 2020 [7]. Beyond the reduction of CO<sub>2</sub> emissions and primary energy consumptions, the Directives [6,8], emphasize the importance of energy efficiency, energy management and commissioning.

In this framework, a new building paradigm has been conceived, that of “nearly Zero Energy Building” or “nZEB” [8-13]. According to the objectives of the Energy Performance Building Directive (EPBD) 2010/31/EU, in fact, all new buildings shall be nearly Zero Energy. The nZEB paradigm will involve both new and refurbished buildings, in order to promote a radical renovation of the built environment. Several different regulatory definitions have been developed in EU countries [14], but, in general, nearly Zero Energy Buildings should combine very low energy demand with relevant onsite renewable energy production and should be able to reduce, as much as possible, the mismatch between demand and onsite production [15-19]. Design choices in nZEBs should be optimal from the techno-economic point of view [20-24] considering not merely the initial investment cost, but also the energy-related running costs, with a coherent methodology.

Further, in order to facilitate the successful integration of building within “intelligent” energy infrastructures [25-27], operational flexibility and optimal dispatch (generation, storage, exchange with the grid, etc.) of onsite resources [28-35], become extremely relevant. At the same time, the infrastructural systems will have necessarily to be able to interact positively with the end-users and the built environment to maximize overall efficiency and to minimize the risk of failures and outages.

On the market side, it is worth noticing that the total BAC (Building Automation, Controls and Building Management) market is expected to reach 49.5 billion dollars by the year 2018 and the annual growth rate (CAGR: Compound Annual Growth Rate) calculated from 2013 and projected to 2018 resulting in double digit [36]. These number are referring to the entire BAC market and, in particular, includes the following areas: lighting, security and access control, HVAC, external controls and BEMS (Building Energy Management Systems). The significant part of the target market is about the energy management: the total world sales of BEMS, relative to 2013, is approximately

16.7 billion dollars and, according to some forecasts, it will grow up to 23.14 billion dollars by 2017 [37]. National and international policies are among the most important "driving feature" that characterize this market; the regulations imposed by governments and supported with financial incentives (e.g. grants, loans, tax relief, etc.), have increased the demand for innovative solutions to reduce "operating costs" in buildings construction [38,39].

Actually, within a scenario where new buildings are nearly Zero Energy and the grid is "smart", the possibility of operating them in an intelligent way becomes more and more important. A proper commissioning and management during the operational phase is essential to ensure monitoring and optimization of all energy flows in the real-time operation of the building [40,41]. In this sense, Building Automation and Control Systems (BACS) for performance optimization and Technical Building Management (TBM) for monitoring and performance tracking, are an essential elements for the evolution of the built environment.

Thermal control in buildings, however, received less attention from control engineering communities than other application fields, like aerospace, petro-chemical, electronics or automotive [42]. One of the reason is that, while control systems in these fields have always had a fundamental role for the improvement of the efficiency in the controlled system, in buildings, the efficiency was associated mainly just to envelope and/or technical systems improvement. Therefore, buildings waste large amount of energy due to poor control performance and have a large potential for savings by improving it [42,43]. Further, another problem related to the building sector compared to the others, is the lack of data and, therefore, to the data analysis phase; it is known that while monitoring strategies are mostly aimed at anomaly detection [44-46], other fundamental insights can be learned from data, by employing calibrated energy simulation models [47-52] and inverse modeling techniques [40,53,54]. The analysis of high-resolution data measured in buildings requires modeling techniques able to describe the energy dynamics effectively and several strategies are possible at the state of the art [55-59]. An important issue, therefore, is related to the balance between available actual data and data needed by the models used. A strategy that allows energy performance characterization without a detailed description of the building while retaining a physical interpretation is grey-box modeling. The absence of physical interpretation, typical for example of black-box models, creates significant problems in the effective implementation of the energy and emission saving strategies. In conclusion, a simplified physical-statistical approach can be a more suitable option. This is an approach already successfully tested in full scale dynamic modeling [60] and model predictive control [61,62].

The final goal, therefore, is to investigate different models and techniques in order to identify a whole workflow able to link the various fundamental control moments in the operational phase of the building, starting from the energy simulation, to the monitoring and data analysis until the optimization phase.

## LIST OF REFERENCES

- [1] U.S. Energy Information Administration, International Energy Outlook 2013.
- [2] U.S. Energy Information Administration, Residential Energy Consumption Survey (RECS) 2009, Release Date: January 11, 2013.
- [3] European Environment Agency (EEA), Household Energy Consumption By End-Use In The Eu-27, 2012.
- [4] CESBA - Common European Sustainable Building Assessment ([http://wiki.cesba.eu/wiki/main\\_page](http://wiki.cesba.eu/wiki/main_page)).
- [5] Dodd, S. Donatello, E. Garbarino, M. Gama-Caldas, Identifying macro-objectives for the life cycle environmental performance and resource efficiency of EU buildings, JRC EU Commission, 2015.
- [6] Energy Efficiency Directive, 2012/27/EU.
- [7] Commission Of The European Communities, Action Plan For Energy Efficiency: Realizing The Potential, Brussels, October 19, 2006.
- [8] Energy Performance Building Directive (EPBD), 2010/31/EU.
- [9] International Energy Agency (IEA - EBC), Annex 52: Towards Net Zero Energy Solar Buildings.
- [10] Marszal Aj, Heiselberg P, Bourrelle Js, Musall E, Voss K, Sartori I, Et Al. Zero Energy Building – A Review Of Definitions And Calculation Methodologies. *Energy And Buildings*. 2011;43:971-9.
- [11] Sartori I, Napolitano A, Voss K. Net Zero Energy Buildings: A Consistent Definition Framework. *Energy And Buildings*. 2012;48:220-32.
- [12] Annunziata E, Frey M, Rizzi F. Towards Nearly Zero-Energy Buildings: The State-Of-Art Of National Regulations In Europe. *Energy*. 2013;57:125-33.
- [13] Attia S, Hamdy M, O'brien W, Carlucci S. Assessing Gaps And Needs For Integrating Building Performance
- [14] Nearly Zero Energy Buildings, Definitions Across Europe (Factsheet). Buildings Performance Institute Europe (BPIE), 2015.
- [15] Lund H, Marszal A, Heiselberg P. Zero Energy Buildings And Mismatch Compensation Factors. *Energy And Buildings*. 2011;43:1646-54.
- [16] Frontini F, Manfren M, Tagliabue Lc. A Case Study Of Solar Technologies Adoption: Criteria For Bipv Integration In Sensitive Built Environment. *Energy Procedia*. 2012;30:1006-15.
- [17] Baetens R, De Coninck R, Van Roy J, Verbruggen B, Driesen J, Helsen L, Et Al. Assessing Electrical Bottlenecks At Feeder Level For Residential Net Zero-Energy Buildings By Integrated System Simulation. *Applied Energy*. 2012;96:74-83.
- [18] Dar Ui, Sartori I, Georges L, Novakovic V. Advanced Control Of Heat Pumps For Improved Flexibility Of Net-Zeb Towards The Grid. *Energy And Buildings*. 2014;69:74-84.
- [19] Cao S, Hasan A, Sirén K. Matching Analysis For On-Site Hybrid Renewable Energy Systems Of Office Buildings With Extended Indices. *Applied Energy*. 2014;113:230-47.
- [20] Kapsalaki M, Leal V, Santamouris M. A Methodology For Economic Efficient Design Of Net Zero Energy Buildings. *Energy And Buildings*. 2012;55:765-78.
- [21] Corgnati Sp, Fabrizio E, Filippi M, Monetti V. Reference Buildings For Cost Optimal Analysis: Method Of Definition And Application. *Applied Energy*. 2013;102:983-93.
- [22] Aste N, Adhikari Rs, Manfren M. Cost Optimal Analysis Of Heat Pump Technology Adoption In Residential Reference Buildings. *Renewable Energy*. 2013;60:615-24.
- [23] Hamdy M, Hasan A, Siren K. A Multi-Stage Optimization Method For Cost-Optimal And Nearly-Zero-Energy Building Solutions In Line With The Epbd-Recast 2010. *Energy And Buildings*. 2013;56:189-203.
- [24] Ferrara M, Fabrizio E, Virgone J, Filippi M. A Simulation-Based Optimization Method For Cost-Optimal Analysis Of Nearly Zero Energy Buildings. *Energy And Buildings*. 2014;84:442-57.
- [25] Wissner M. The Smart Grid – A Saucerful Of Secrets? *Applied Energy*. 2011;88:2509-18.

- [26] Asmus P. Microgrids, Virtual Power Plants And Our Distributed Energy Future. *The Electricity Journal*. 2010;23:72-82.
- [27] Katz Rh, Culler De, Sanders S, Alspaugh S, Chen Y, Dawson-Haggerty S, Et Al. An Information-Centric Energy Infrastructure: The Berkeley View. *Sustainable Computing: Informatics And Systems*. 2011;1:7-22.
- [28] Parisio A, Rikos E, Tzamalís G, Glielmo L. Use Of Model Predictive Control For Experimental Microgrid Optimization. *Applied Energy*. 2014;115:37-46.
- [29] Fazlollahi S, Mandel P, Becker G, Maréchal F. Methods For Multi-Objective Investment And Operating Optimization Of Complex Energy Systems. *Energy*. 2012;45:12-22.
- [30] Menon Rp, Paolone M, Maréchal F. Study Of Optimal Design Of Polygeneration Systems In Optimal Control Strategies. *Energy*. 2013;55:134-41.
- [31] Fazlollahi S, Bungener Sl, Mandel P, Becker G, Maréchal F. Multi-Objectives, Multi-Period Optimization Of District Energy Systems: I. Selection Of Typical Operating Periods. *Computers & Chemical Engineering*. 2014;65:54-66.
- [32] Fazlollahi S, Becker G, Maréchal F. Multi-Objectives, Multi-Period Optimization Of District Energy Systems: Ii—Daily Thermal Storage. *Computers & Chemical Engineering*. 2014;71:648-62.
- [33] Fazlollahi S, Becker G, Maréchal F. Multi-Objectives, Multi-Period Optimization Of District Energy Systems: Iii. Distribution Networks. *Computers & Chemical Engineering*. 2014;66:82-97.
- [34] Stadler M, Groissböck M, Cardoso G, Marnay C. Optimizing Distributed Energy Resources And Building Retrofits With The Strategic Der-Camodel. *Applied Energy*. 2014;132:557-67.
- [35] Beccali M, Brunone S, Cellura M, Franzitta V. Energy, Economic And Environmental Analysis On Ret-Hydrogen Systems In Residential Buildings. *Renewable Energy*. 2008;33:366-82.
- [36] marketsandmarkets.com, "Building Automation & Controls Market (2013 – 2018): By Product (Lighting, Security & Access, HVAC, Entertainment, Outdoor, Elevator Controls, Building Management Systems (BMS)), Application & Geography (Americas, Europe, Apac, And Row)".
- [37] memoori.com, "The Market For BEMS And Enterprise Energy Management 2013 To 2017".
- [38] EU Commission, Communication 6317/2015, Towards an Integrated Strategic Energy Technology (SET) Plan: Accelerating the European Energy System Transformation.
- [39] EEFIG, Energy Efficiency – the first fuel for the EU Economy, How to drive new finance for energy efficiency investments, 2015.
- [40] International Energy Agency (IEA), Annex 58: Reliable Building Energy Performance Characterization Based On Full Scale Dynamic Measurement, EBC Programme, 2015.
- [41] European Commission, Programme IEE (Intelligent Energy Europe), Building Eq - The EPBD And Continuous Commissioning - Tools And Methods For Linking EPDB And Continuous Commissioning. 2007.
- [42] Hazyuk I, Ghiaus C, Penhouet D. Optimal Temperature Control Of Intermittently Heated Buildings Using Model Predictive Control: Part I – Building Modeling. *Building And Environment*. 2012;51:379-87.
- [43] Nguyen Ta, Aiello M. Energy Intelligent Buildings Based On User Activity: A Survey. *Energy And Buildings*. 2013;56:244-5.
- [44] Bynum Jd, Claridge De, Curtin Jm. Development And Testing Of An Automated Building Commissioning Analysis Tool (Abcat). *Energy And Buildings*. 2012;55:607-17.
- [45] Lin G, Claridge De. A Temperature-Based Approach To Detect Abnormal Building Energy Consumption. *Energy And Buildings*. 2015;93:110-8.
- [46] Sklavounos D, Zervas E, Tsakiridis O, Stonham J. A Subspace Identification Method For Detecting Abnormal Behavior In Hvac Systems. *Journal Of Energy*. 2015;2015:12.
- [47] Raftery P, Keane M, O'donnell J. Calibrating Whole Building Energy Models: An Evidence-Based Methodology. *Energy And Buildings*. 2011;43:2356-64.
- [48] Manfren M, Aste N, Moshksar R. Calibration And Uncertainty Analysis For Computer Models – A Meta-Model Based Approach For Integrated Building Energy Simulation. *Applied Energy*. 2013;103:627-41.
- [49] Li X, Wen J. Review Of Building Energy Modeling For Control And Operation. *Renewable And Sustainable Energy Reviews*. 2014;37:517-37.

- [50] Coakley D, Raftery P, Keane M. A Review Of Methods To Match Building Energy Simulation Models To Measured Data. *Renewable And Sustainable Energy Reviews*. 2014;37:123-41.
- [51] Royapoor M, Roskilly T. Building Model Calibration Using Energy And Environmental Data. *Energy And Buildings*. 2015;94:109-20.
- [52] Fabrizio E, Monetti V. Methodologies And Advancements In The Calibration Of Building Energy Models. *Energies*. 2015;8:2548.
- [53] Kramer R, Van Schijndel J, Schellen H. Simplified Thermal And Hygric Building Models: A Literature Review. *Frontiers Of Architectural Research*. 2012;1:318-25.
- [54] Kramer R, Van Schijndel J, Schellen H. Inverse Modeling Of Simplified Hygrothermal Building Models To Predict And Characterize Indoor Climates. *Building And Environment*. 2013;68:87-99.
- [55] M. Kavgic, A. Mavrogianni, D. Mumovic, A. Summerfield, Z. Stevanovic, M. Djurovic-Petrovic, A review of bottom-up building stock models for energy consumption in the residential sector, *Building and Environment*. 2010;45:1683-1697.
- [56] H. Zhao, F. Magoulès, A review on the prediction of building energy consumption, *Renewable and Sustainable Energy Reviews*. 2012;16:3586-3592.
- [57] A. Fouquier, S. Robert, F. Suard, L. Stéphan, A. Jay, State of the art in building modelling and energy performances prediction: A review, *Renewable and Sustainable Energy Reviews*. 2013;23:272-288.
- [58] N. Fumo, A review on the basics of building energy estimation, *Renewable and Sustainable Energy Reviews*. 2014;31:53-60.
- [59] D. Coakley, P. Raftery, M. Keane, A review of methods to match building energy simulation models to measured data, *Renewable and Sustainable Energy Reviews*. 2014;37:123-141.
- [60] IEA-EBC Annex 58, Reliable Building Energy Performance Characterisation Based on Full Scale Dynamic Measurements ([www.kuleuven.be/bwf/projects/annex58](http://www.kuleuven.be/bwf/projects/annex58))
- [61] Oldewurtel F, Parisio A, Jones CN, Gyalistras D, Gwerder M, Stauch V, et al. Use of model predictive control and weather forecasts for energy efficient building climate control. *Energy and Buildings*. 2012;45:15-27.
- [62] Lehmann B, Gyalistras D, Gwerder M, Wirth K, Carl S. Intermediate complexity model for Model Predictive Control of Integrated Room Automation. *Energy and Buildings*. 2013;58:250-62

## **2. PROBLEM AND CLAIM**

### **2.1. PERFORMANCE GAP**

While new paradigms for the construction sector are emerging, such as that of “Nearly Zero Energy Building” and sustainability assessment schemes are progressively evolving and becoming more common, empirical studies show how, very often, the gap between the predicted (design phase) and measured (operation phase) energy performance could be very large [1]. This issue is generally addressed with the term “performance gap” [2], as simulation results tend to be generally optimistic. The “performance gap” can be fundamentally caused by design phase, construction phase, commissioning and operational phase errors.

Generally, the decisions that have the greatest impact on total facility cost and energy demand are made early in the design process [3], without understanding their overall impact of performance during building life cycle. Prioritization with respect to multiple objectives and initial investment cost remain critical dimensions for practitioners, because buildings are generally designed, constructed and operated by different entities (often with conflicting needs and different responsibilities). A technical issue is determined by the lack of software to quickly and accurately simulate building energy performance, considering appropriately the uncertainty of the input data assumed. In fact, in the Architecture, Engineering and Construction (AEC) sector, several computational tools are used in the design phase but they lack integration, although several efforts are ongoing to include more advanced features in Building Information Modeling (BIM) [4]. Further, Building Energy Modeling (BEM) tools are not generally used at present for the design of control and diagnostic systems suitable for operation phase, although research activities are ongoing [4]. Additionally, building simulation tools are not generally used throughout the life cycle for the verification and benchmarking of building performance due to the difficulties in model calibration and comparison. Therefore, there is a missing link among models suitable for performance optimization and monitoring across life cycle phases [5].

This situation creates a problem of credibility in the building industry and, more in general, in sustainability practices because the errors committed can directly reflect on energy performance and, consequently on the running costs and on global cost optimality. A good energy and environmental design, in fact, cannot guarantee an appropriate performance during whole life cycle without proper commissioning and management [6,7]. The gap can also create immediate problems where Energy Performance Contracting (EPC) [8,9] formulas are present for energy services.

Bridging the gap between simulated and real energy usage requires the presence of embedded control and fault detection applications that have to be adaptive, self-calibrating and conceived to enable a model based interpretation of measured data, for performance benchmarking. Currently, in the AEC sector, state-of-the-art methods and models used in other sectors, such as optimization techniques for design [10,11] and advanced control [12,13], are not widely used. More specifically, on

the design side, the inability to evaluate quickly different configurations determines generally a preference for business-as-usual solutions. On the control side, specific knowledge can contribute to the evolution of the building design process, including principles and methods that can be useful to maintain the requested level of performance by adapting building operation to a rapidly changing environment [14]. These elements are particularly relevant if we think that one of the fundamental issues related to the “performance gap” is the design of buildings which are “climate change proof” [15] and “occupant proof” [16]. Further, with respect to the interaction of buildings with energy infrastructures and communities, several topics are emerging such as load matching, load shifting, storage management and building flexibility [6, 17-20]. The optimization of the dynamic operation of a building or of a cluster of buildings requires the definition of suitable models that can be solved by high performance solvers in real-time. Of course, domain specific model reduction techniques are required [21-23] and uncertainty and sensitivity analysis should be taken into account as well in model verification, validation and calibration [24-26]. It is not sufficient to simulate just a few trajectories but the dynamics of the coupled systems should be thoroughly explored and understood. Finally, data driven models for fault detection, diagnosis and prognostics are generally not conceived for multi-scale applications and for being integrated and synergy with optimization models. Therefore, a further effort of integration in this sense is necessary.

## **2.2. DATA ANALYTICS AND SIMPLIFIED BUILDING MODELING**

In order to contain the errors (causes of the “performance gap”) within acceptable and quantifiable performance ranges, adequate indicators and benchmarking strategies should be applied during whole building life cycle [27]. In this sense, the analysis of the measured performance is the starting point for reducing the gap and, therefore, applications aimed at monitoring energy flows [28,29] and operation parameters are essential.

Analysis of trends in energy consumptions and anomaly detection is a recurring problem in building performance simulation and monitoring. Simulations can be used to determine different operational trajectories to be compared with the real one. In other word, extraction of information from parametric simulation data can facilitate, on the one hand, operational malfunctioning and faults identification [30,31], on the other hand, energy performance model calibration [24, 32-36].

Performance benchmarking by means of energy models is essential to detect performance degradation at multiple levels(system, subsystem and device). Therefore, the development of data analytics is essential to ensure efficient building operation during the whole life cycle [5,14]. Additionally, advanced data analytics aimed at multi-scale applications can fundamentally contribute to an evolution towards a sustainable built environment, more effectively integrated with large scale infrastructures [37] and more useful for the building sector as a whole [38].

Of course, several issues are present when facing uncertain multi-scale problems, in particular the probabilistic criteria and the robustness of methods used for design and control strategies.

As expressed before, the role of data analytics can be on two sides, design and operation of buildings. First, operation can be improved by performance tracking [39,40] (i.e. reducing commission-

ing and operation errors) and, after that, design practices can be improved by learning from errors in a more transparent way through data analytics [30,41], unveiling typical and recurrent design and construction errors. At present, in the design phase little attention is paid to diagnostics at the system level; current practices focus mainly at the component level, employing traditional Fault Detection and Diagnosis (FDD). Low energy buildings present a much tighter coupling and dependency among system, subsystem and device performance levels. Therefore, new tools must be developed to dynamically extract information from data for diagnostics and prognostics aimed at global efficiency, while the current state-of-the-art is to control the performance mainly at subsystem levels. The fundamental steps of performance tracking are the following ones:

1. acquiring data and track the performance with adequate indicators at the system, subsystem and component level;
2. identifying anomalies, malfunctioning, faults, etc. through diagnostics;
3. identifying solutions;
4. applying solutions to fix problem and verify results.

From the methodological point of view, three basic elements have to converge in order to foster performance tracking:

- utility bill data analysis;
- metering and data acquisition from BACS;
- performance benchmarking methodologies.

A centralized data acquisition and analysis system is therefore necessary to seamlessly integrate these practices with commissioning procedures.

In conclusion, the research and the definition of models to be employed for multiple tasks across the building life cycle has the purpose to unite, in a circular approach, various aspects related to building performance analysis, considering first operational optimization and diagnostics. The main steps are the following:

1. energy simulation with a lumped parameter model;
2. model calibration with building operation data;
3. exploration of building energy management strategies and predictive control potential.

The methodology used for the research, therefore, seeks to unite these steps through the choice of effective tools, able to interact each other. A current problem, in fact, is the difficulty to link the steps indicated above because of several issues (e.g. technological limitations, sectorial view, practitioners training, etc.). The research project, therefore, has the ultimate goal of trying to unify methods and models used in different fields and understand how to make them usable in an effective workflow across life cycle phases.

## LIST OF REFERENCES

- [1] de Wilde P. The gap between predicted and measured energy performance of buildings: A framework for investigation. *Automation in Construction*. 2014;41:40-9
- [2] Lewry A, Ortiz J, Nabil A, Schofield N, Vaid R, Hussain S, et al. Bridging the gap between operational and asset ratings – the UK experience and the green deal tool. 2014
- [3] Bleil de Souza C. Studies into the use of building thermal physics to inform design decision making. *Automation in Construction*. 2013;30:81-93
- [4] International Energy Agency (IEA - EBC), Annex 60: New Generation Computational Tools for Building & Community Energy Systems
- [5] Miller C, Schlueter A. Applicability of lean production principles to performance analysis across the life cycle phases of buildings. CLIMA 2013: 11th REHVA Congress and 8th International Conference on IAQVEC2013
- [6] Lund H, Marszal A, Heiselberg P. Zero energy buildings and mismatch compensation factors. *Energy and Buildings*. 2011;43:1646-54
- [7] Cao S, Hasan A, Sirén K. On-site energy matching indices for buildings with energy conversion, storage and hybrid grid connections. *Energy and Buildings*. 2013;64:423-38
- [8] Zhang X, Gao H. Optimal Performance-Based Building Facility Management. *Computer-Aided Civil and Infrastructure Engineering*. 2010;25:269-84.
- [9] Almeida N, Sousa V, Alves Dias L, Branco F. A framework for combining risk-management and performance-based building approaches. *Building Research & Information*. 2010;38:157-74
- [10] Talbourdet F, Michel P, Andrieux F, Millet J-R, Mankibi M, Vinot B. A knowledge-aid approach for designing high-performance buildings. *Build Simul*. 2013;6:337-50.
- [11] Chantrelle FP, Lahmidi H, Keilholz W, Mankibi ME, Michel P. Development of a multicriteria tool for optimizing the renovation of buildings. *Applied Energy*. 2011;88:1386-94
- [12] Li X, Wen J. Review of building energy modeling for control and operation. *Renewable and Sustainable Energy Reviews*. 2014;37:517-37
- [13] Henze GP. Model predictive control for buildings: a quantum leap? *Journal of Building Performance Simulation*. 2013;6:157-8
- [14] Brown DL, Burns JA, Collis S, Grosh J, Jacobson CA, Johansen H, et al. *Applied & Computational Mathematics - Challenges for The Design and Control of Dynamic Energy Systems*. 2011
- [15] de Wilde P, Coley D. The implications of a changing climate for buildings. *Building and Environment*. 2012;55:1-7
- [16] Wei S, Jones R, de Wilde P. Driving factors for occupant-controlled space heating in residential buildings. *Energy and Buildings*. 2014;70:36-44
- [17] Frontini F, Manfren M, Tagliabue LC. A Case Study of Solar Technologies Adoption: Criteria for BIPV Integration in Sensitive Built Environment. *Energy Procedia*. 2012;30:1006-15.
- [18] Baetens R, De Coninck R, Van Roy J, Verbruggen B, Driesen J, Helsen L, et al. Assessing electrical bottlenecks at feeder level for residential net zero-energy buildings by integrated system simulation. *Applied Energy*. 2012;96:74-83.
- [19] Dar UI, Sartori I, Georges L, Novakovic V. Advanced control of heat pumps for improved flexibility of Net-ZEB towards the grid. *Energy and Buildings*. 2014;69:74-84.
- [20] Cao S, Hasan A, Sirén K. Matching analysis for on-site hybrid renewable energy systems of office buildings with extended indices. *Applied Energy*. 2014;113:230-47
- [21] Fazlollahi S, Mandel P, Becker G, Maréchal F. Methods for multi-objective investment and operating optimization of complex energy systems. *Energy*. 2012;45:12-22.
- [22] Menon RP, Paolone M, Maréchal F. Study of optimal design of polygeneration systems in optimal control strategies. *Energy*. 2013;55:134-41.

- [23] Lehmann B, Gyalistras D, Gwerder M, Wirth K, Carl S. Intermediate complexity model for Model Predictive Control of Integrated Room Automation. *Energy and Buildings*. 2013;58:250-62.
- [24] Coakley D, Raftery P, Keane M. A review of methods to match building energy simulation models to measured data. *Renewable and Sustainable Energy Reviews*. 2014;37:123-41.
- [25] Coleman HW, Steele WG. *Experimentation, Validation, and Uncertainty Analysis for Engineers*: Wiley; 2009.
- [26] Oberkampf WL, Roy CJ. *Verification and Validation in Scientific Computing*: Cambridge University Press; 2010.
- [27] Beccali M, Cellura M, Fontana M, Longo S, Mistretta M. Energy retrofit of a single-family house: Life cycle net energy saving and environmental benefits. *Renewable and Sustainable Energy Reviews*. 2013;27:283-93
- [28] International Energy Agency (IEA - EBC), Annex 58: Reliable Building Energy Performance Characterization based on full scale dynamic measurement.
- [29] European Commission, Programme IEE (Intelligent Energy Europe), Building EQ - The EPBD and Continuous Commissioning - Tools and methods for linking EPDB and continuous commissioning. 2007
- [30] Miller C, Nagy Z, Schlueter A. Automated daily pattern filtering of measured building performance data. *Automation in Construction*. 2015;49, Part A:1-17.
- [31] de Wilde P, Martinez-Ortiz C, Pearson D, Beynon I, Beck M, Barlow N. Building simulation approaches for the training of automated data analysis tools in building energy management. *Advanced Engineering Informatics*. 2013;27:457-65.
- [32] Raftery P, Keane M, O'Donnell J. Calibrating whole building energy models: An evidence-based methodology. *Energy and Buildings*. 2011;43:2356-64.
- [33] Manfren M, Aste N, Moshksar R. Calibration and uncertainty analysis for computer models – A meta-model based approach for integrated building energy simulation. *Applied Energy*. 2013;103:627-41.
- [34] Korolija I, Marjanovic-Halburd L, Zhang Y, Hanby VI. UK office buildings archetypal model as methodological approach in development of regression models for predicting building energy consumption from heating and cooling demands. *Energy and Buildings*. 2013;60:152-62.
- [35] Calleja Rodríguez G, Carrillo Andrés A, Domínguez Muñoz F, CejudoLópez JM, Zhang Y. Uncertainties and sensitivity analysis in building energy simulation using macroparameters. *Energy and Buildings*. 2013;67:79-87.
- [36] Yang Z, Becerik-Gerber B. A model calibration framework for simultaneous multi-level building energy simulation. *Applied Energy*. 2015;149:415-31.
- [37] INFERLab - Intelligent Infrastructure Research Lab (<http://inferlab.org/>).
- [38] Dodd, S. Donatello, E. Garbarino, M. Gama-Caldas, Identifying macro-objectives for the life cycle environmental performance and resource efficiency of EU buildings, JRC EU Commission, 2015.
- [39] Bynum JD, Claridge DE, Curtin JM. Development and testing of an Automated Building Commissioning Analysis Tool (ABCAT). *Energy and Buildings*. 2012;55:607-17.
- [40] Lin G, Claridge DE. A temperature-based approach to detect abnormal building energy consumption. *Energy and Buildings*. 2015;93:110-8.
- [41] Maile T, Bazjanac V, Fischer M. A method to compare simulated and measured data to assess building energy performance. *Building and Environment*. 2012;56:241-51.

### 3. STATE OF THE ART OF BACS FOR PERFORMANCE OPTIMIZATION

The chapter aims to give a general framework for the analysis of BACS for building performance optimization, considering the general objectives of BACS and the necessary improvements in building design, construction, commissioning and operation practices, needed to bridge the “performance gap”. As first, it is important to recall the most relevant design choices and measures for the performance optimization of building (both new and refurbished ones), summarized in Table 1, showing, in particular, the basic elements related to control. After that, the elements whose variability is difficult to assess in the design phase, from the building modeling point of view, are summarized in Table 2. Many of these elements are intimately related furthermore to commissioning, operation and control. Finally, the fundamental sensors and meters data for control and building performance tracking are reported in Table 3. These three tables illustrates the cross-disciplinary role of data, highlighting the most relevant dimensions to be considered for the improvement of building performance.

**Tab. 1 - Design choices and energy efficiency measures for different systems in buildings.**

<b>System</b>	<b>Design/efficiency measure</b>
Building fabric	Improve opaque building component performance (thermal transmittance, admittance, etc.)
	Improve transparent building component performance (thermal transmittance, gain coefficient, etc.)
	Decrease infiltration
	Optimize transparent/opaque surface ratio
	Improve shading systems (solar gain control, visual comfort, integrate daylighting integration, etc.)
Appliances	Reduce plug loads and improve efficiency
Lighting systems	Reduce lighting loads and improve efficiency
	Exploit daylighting
Technical systems	Increase cooling system efficiency
	Increase heating system efficiency
	Increase ventilation system efficiency
	Increase DHW system efficiency
	Decrease size of auxiliary systems
	Use heat recovery
	Use economizers
Use thermal storage (active/passive)	
Distributed generation	Install Photovoltaic System
	Install Wind Power System
	Install Combined Heating and Power, Combined Heating, Cooling and Power
Automation and Control	Increase cooling set-points
	Decrease heating set-points
	Decrease DHW set-points

	Adjust operating schedules (heating, cooling, ventilation, DHW, lighting, etc.)
	Adjust outdoor fresh air rate with respect to occupancy and IAQ
	Adjust economizers settings
	Optimize partial load operation of heating/cooling/DHW systems
	Optimize partial load operation of auxiliary systems
	Optimize thermal storage operation (load shifting, peak shaving, etc.)
	Optimize integration of natural and artificial lighting systems
	Optimize shading system operation with respect to lighting and heat gains (heating/cooling)

**Tab. 2 - Uncertain parameters and boundary conditions in building energy modeling.**

<b>System</b>	<b>Uncertain Parameter and Boundary Condition</b>
Building fabric	Building materials
	Components and assembly (thermal transmittance, thermal bridges, etc.)
	Air Change Rate for infiltration and natural ventilation
	Shading system operation
Appliances	Installed power and efficiency
	Operation schedule appliances - Daily/Weekly
Lighting systems	Installed power and efficiency
	Operation schedule lighting - Daily/Weekly
Technical systems	Heating set-point temperature
	Operation schedule heating - Daily/Weekly
	Heating system efficiency
	Cooling set-point temperature
	Operation schedule cooling - Daily/Weekly
	Cooling system efficiency
	Air Change Rate for mechanical ventilation
	Operation schedule ventilation - Daily/Weekly
	DHW set-point temperature
	Operation schedule DHW - Daily/Weekly
	DHW system efficiency
	Ventilation system efficiency
	Auxiliary systems efficiency
	Heat recovery systems efficiency
	Economizer settings
Thermal storage efficiency	
Distributed generation	Photovoltaic power output
	Wind system power output
	Combined Heating and Power, Combined Heating, Cooling and Power operation

**Tab. 3 - Sensor and meters data for control and performance tracking.**

<b>Element</b>	<b>Quantity</b>	<b>Unit</b>	<b>Description</b>
Consumption	Total fuel consumptions	Wh, kWh, MWh, m <sup>3</sup> , l, kg	Cumulative value from meter reading
	Total energy consumption (heating and cooling)	Wh, kWh, MWh	

	Total electricity consumption		
	Total water consumption	m <sup>3</sup> , l	
Weather	Outdoor temperature	°C	Value from on-site weather station or weather data provider
	Outdoor relative humidity	%	
	Global irradiation on horizontal surface	W/m <sup>2</sup>	
Indoor conditions	Indoor temperature	°C	Value from selected reference zone
	Indoor relative humidity	%	
	CO <sub>2</sub> concentration	ppm	
	Luminance	lux	
Systems	Supply/return air temperature - water circuits	°C	Value from system of the selected reference zone
	Supply/return air temperature - AHU		
	Supply/return air relative humidity - AHU	%	
	Flow meters	l/s, m <sup>3</sup> /h	
	Pressure meters	kPa, Pa	
	Control signals for pumps and fans	0-100%, 0-1, ON/OFF, 0/1	
	Control signals for presence sensors		
	Control signals for CO <sub>2</sub> sensors		
Sampling and analysis interval	Data polling interval	s, min, h, day	Value depending on type of data analysis
	Data acquisition length period	day, month, year	

### 3.1. BUILDING AUTOMATION AND CONTROL SYSTEMS

Building Automation and Control Systems are usually defined by the acronym BACS. Commonly, buildings that have BACS and Technical Building Management (TBM) are addressed with the term “intelligent” or “smart” buildings [1,2]. Although these terms are rather generic, they can state that the intelligence of building resides in its ability to provide building services (thermal comfort, indoor air quality, lighting, etc.) while maximizing efficiency and cost savings and minimizing environmental impact [2-4]. More precise definitions related to building automation are presented in [5]. Particularly relevant are the definitions of Building Automation and Control (BAC), BACS and TBM:

- BAC are product, software, and engineering services for automatic controls, monitoring and optimization, human intervention and management to achieve energy-efficient, economical and safe operation of buildings services equipment. BACS comprise all products and engineering services related to BAC and it is a term used alternatively to BACS is Building Management System (BMS).
- TBM involves all the processes and services related to operation and management of buildings and technical systems through the interrelationships between the different disciplines and trades. Building Management (BM) can be assigned as part of Facility Management [6]. TBM involves not only the presence of automation and control systems but also their effective integration [7]. All these definitions clarify the multidisciplinary role of automation and control, involving hardware and software.

The control functions in BACS belong generally to the following main areas:

- heating, ventilation and air conditioning systems (HVAC);
- domestic hot water (DHW);
- lighting system control;
- shading systems control;
- energy conversion and storage (heating and cooling);
- onsite power generation;
- monitoring and data acquisition;
- communications and security management.

As defined in the previous, BACS are aimed at energy-efficient building operation and, therefore, control and energy management functions are partially overlapping. As a consequence, BACS are also indicated as Energy Management and Control Systems (EMCS) [8].

Wang in [9] outlines an evolution pathway of these systems through the following steps:

1. *Dedicated Systems* (1980-85 all subsystems characterized by individual functions);
2. *Integrated Multifunction Systems* (1985-90 the individual subsystems were grouped into functional areas);
3. *Building Level Integrated Systems* (1990-95 first phase of integration at the building level of automation, BAS, and communication, ICT);
4. *Computer Integrated Building* (1995-2002, exploiting the capabilities of network technologies);
5. *Enterprise Network Integrated System* (ENIS) (after 2002 the integration is carried out at a higher level to connect even more buildings).

This evolution pathway determined an increasing level of integration among components, devices, systems and services, as summarized in Figure 1.

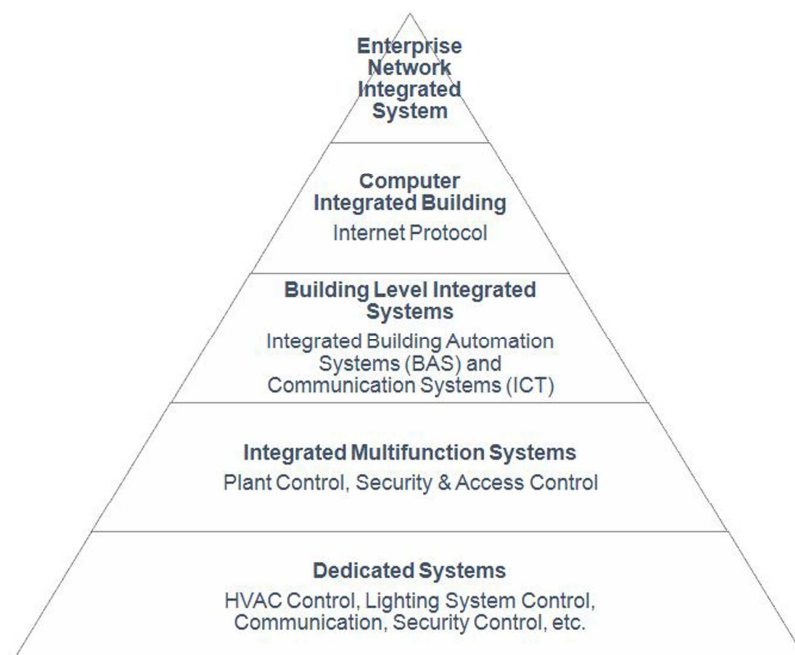


**Figure 1. Evolution pathway of Building Automation and Control Systems.**

Nowadays, the digital revolution, which contributed to a major change in our behavior and started to reshape the way we approach our “physical” objects, is bringing in a new concept, the “Internet of Things” (IoT). IoT is really about connecting devices, acquiring data and performing computational processes, either in the devices themselves (by embedded computers) or in the cloud by means of applications and services. By leveraging the possibilities of web technologies, ICT solutions can be economically competitive, easily deployable on the market and effectively supporting the adoption of clean technologies and sustainable behaviors. In this sense, IoT could effectively support the future evolution of BACS and TBM. Further, in a resource-constrained horizon, our infrastructural systems (Internet, Smart Grid, etc.) will necessarily have to be able to interact positively with the end-users and the built environment to maximize overall efficiency and minimize the risk of failures and outages.

The development of advanced algorithms, applications and services in buildings is not new [10,11] and the ability to learn and adapt is already present in several products [12]; a review about computational intelligence and automation can be found in [10]. However, the present challenges in terms of energy efficiency and integration of buildings within energy and communication infrastructures determine the need for a research effort with a much wider scope [13,14].

### **3.2. CONTROL FUNDAMENTALS, STRATEGIES AND SCHEMES**

Control theory and process control represent a mixture of mathematical, physical and engineering knowledge. Control applications are naturally cross-disciplinary as they deal fundamentally with two main aspects, maintaining a certain process or system in controlled operational conditions and set-point and manage the transition from one operational state to another.

In the first case, the objective of control is to guarantee that a certain process or system remains within definite conditions (e.g. performance criteria such as efficiency, cost, safety, etc.) depending on its specific characteristics. In the second case, the objective is to be able to switch from one operational state to another and, therefore, to adapt the operation of the process or system to a variety of possible conditions and constraints. There are several definitions and terminologies related to control applications, but the most basic ones are:

- input variables;
- output variables.

Input variables show the effect of the external elements on the system (e.g. factor and variables that influence a process). Some of the input variables are controllable and some are not; they are called, respectively, manipulated inputs (controlled by the control system or by an operator) and disturbances (inputs that cannot be controlled neither by the control system nor by the operator) that can be measurable and non-measurable. Output variables are often indicated as control variables as they are the output of the process or system.

Further, two main control structures can be present:

- Single Input - Single Output (SISO), where a single control variable and a single manipulated input are present;

- Multiple Input - Multiple Output (MIMO), where multiple control variables and multiple manipulated inputs are present.

Obviously, the structure of the control and its variables, as well as the complexity of the process/system, are critical for the model selection, as will be illustrated in Section 3.5. Further, controls can be roughly categorized according to two main schemes:

- feed-back (or closed loop);
- feed-forward (or open loop).

In a feed-forward control scheme the controller respond to change in input variables (manipulated or disturbances), in a pre-defined way, while in feedback control the control variable is measured and compared with a target value (e.g. a set-point). The difference between the actual and the target value is called “error”. In general, feedback control manipulates inputs in order to minimize the error. Feedback control schemes are necessary for complex processes, involving dynamic effects. In buildings, for example, feed-forward controls are found in lighting system while feedback controls are found in thermal applications such as HVAC. Two basic schemes of feed-forward and feedback control are reported respectively in Figure 2.

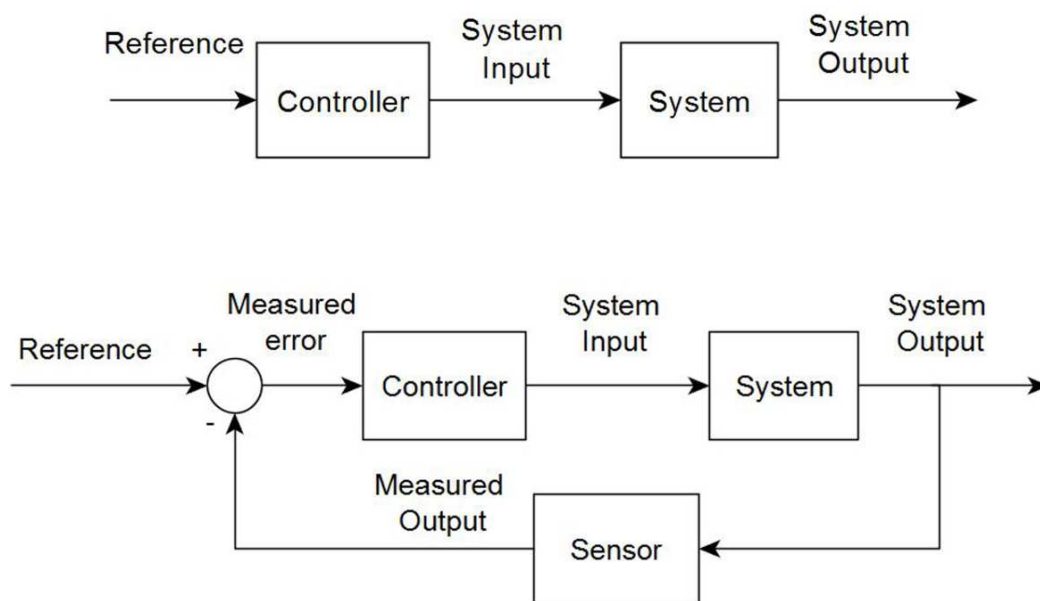


**Figure 2. Feed-forward (open loop) and feed-back (closed loop) control schemes.**

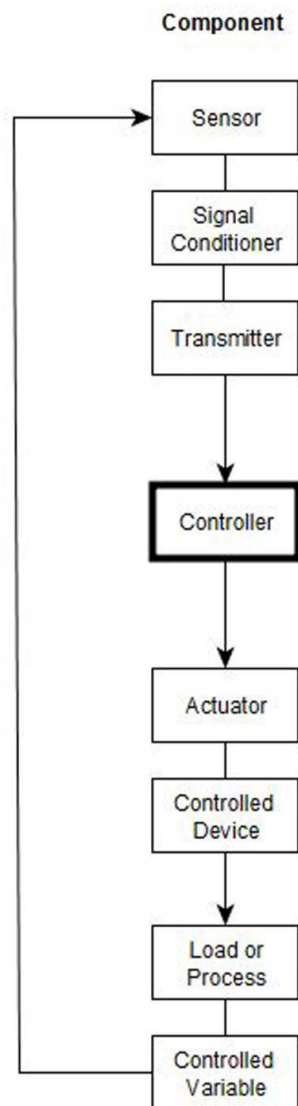


**Figure 3. Detailed control scheme, including sensor, controller and actuator.**

Finally, a more detailed scheme, involving a sensor and an actuator is reported in Figure 3. In the following sections, other fundamental elements constituting control systems are described, starting from physical elements such as components, devices and networks.

### **3.3. CONTROL DEVICES, NETWORKS AND SYSTEMS INTEGRATION**

A BACS generally comprises two major levels: the *basic control layer* and the *supervisory control layer* [10,11, 15-20]. Usually, the basic control layer is composed by Single Input - Single Output (SISO) controllers such as *sensors and actuators* [17,21]. These controllers are used, for example, for the set-point tracking in different building zones and subzones and at the level of individual technologies (e.g. terminal units, generators, etc.). The *supervisory control layer* instead can com-

prise either a human operator or an automated Energy Management System (EMS) and can be seen as a Multi Input/Multi Output (MIMO) system, such as *control models*.

Of course the enabling element is the communication infrastructure (network, protocols, etc.) connecting the different layers of the system. Generally, in simple BAC, just the basic control layer is present. In these systems, in fact, both the integration level and the complexity are lower. Advanced control systems, on the contrary, in addition to sensors and actuators, use a supervisory control layer [17,20,22], which can be governed by a set of rules (Rule Based Control) or by a model (Model Based Control), models for control are described in detail in Section 3.4.

These systems are used to optimize system operation adjusting the set points and operating schedules (settings in the basic control layer) in order to save energy and reduce running costs while ensuring appropriate comfort levels and services, considering variable conditions [19]. Generally, the variable conditions include weather, occupancy rates, operating schedules, time of the day, and energy tariffs [15,23]. Both basic and supervisory control layers are present in advanced building performance simulation tools, although research efforts are today concentrated on rationalizing and simplifying the tools aimed at designing Model Predictive Control (MPC) for buildings [24-26]. As stressed before, system integration is fundamental for performance optimization, an example of integration is represented by Integrated Room Automation (IRA) and it deals with the simultaneous control of HVAC as well as blind positioning and electric lighting of a building zone, maintaining the room temperature as well as CO<sub>2</sub> and luminance levels within a given comfort range [19,27-30]. A summarizing scheme is reported in Figure 4.

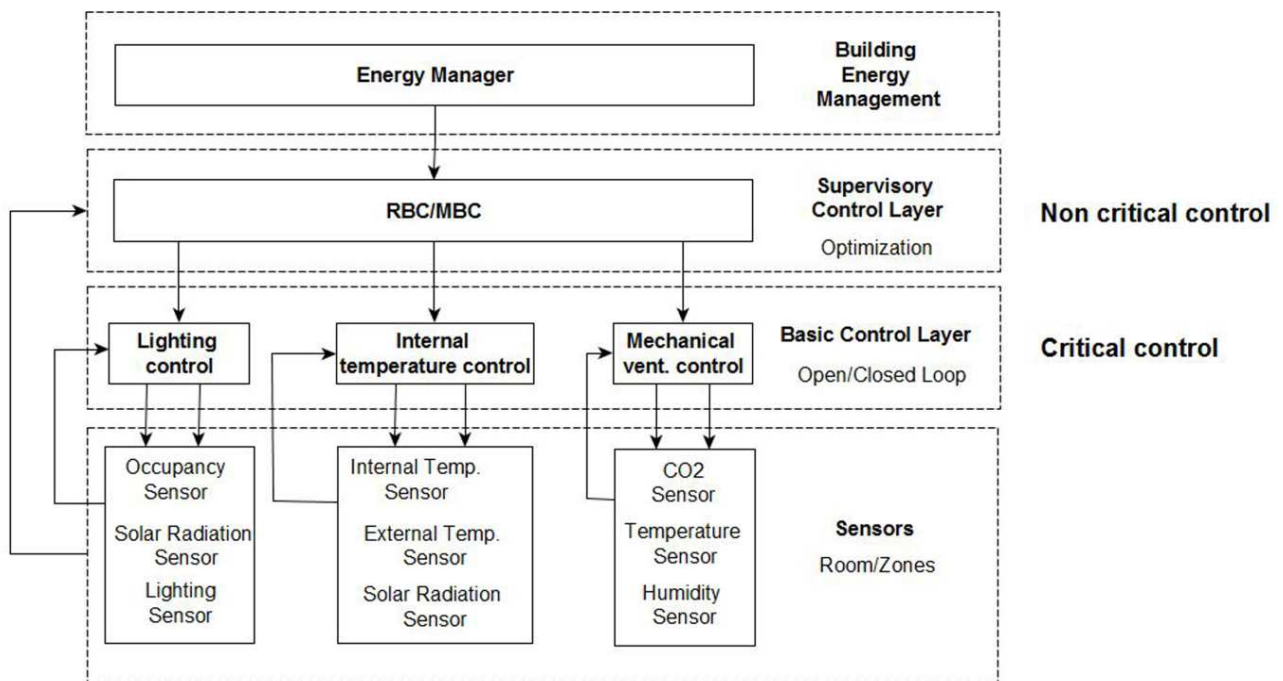


**Figure 4. Scheme of a Building Automation and Control System, including basic and supervisory control layer.**

Sensors are devices that measures physical quantities and convert them to a digital or analog signal. They are used, in control systems, together with actuators, which are control devices able to link the control signal to the controlled device, translating the signal from sensor into an action of the device. Actuators are used in a different way in basic or advanced control systems. In the first case, they

have to manage sensors information and directly actuate the control function. In the second case, the supervisory control layer (acquiring data from sensors) controls actuators and, therefore, they do not act in a direct way. An overview of typical sensors and actuators used is presented in [31]. In BACS it is useful to have several informative sensor that can map fundamental data useful for building model calibration. The design of appropriate control schemes (i.e. sensor types, placement, overall layout, etc.) for detailed inverse building modeling is itself an element of research, in the sense that it cannot be seen separately from the modeling strategy pursued and all the other relevant applications that will use the data. This research topic is particularly relevant at present if we think about the IoT paradigm, introduced before. Given the problem of “performance gap” in low energy buildings and the necessity of “occupants’ proofing” of design solutions for efficient buildings, it is useful to concentrate on two fundamental aspects that are related to real-time building operation and that affects several of the assumption made in energy modeling (summarized in Table 2):

- Occupancy detection (ventilation, internal gains, lighting,);
- Internal Environmental Quality (IEQ) control (temperature, humidity, air speed, IAQ, etc.).

The implications of these two fundamental aspects for sensors and actuators in BACS will be described in the two following sections.

### **3.3.1. OCCUPANCY DETECTION AND BEHAVIORAL MODELING**

Occupancy detection for modeling and optimization of technical system can be used to find a good compromise between internal comfort and energy savings [7,32], although, at present, occupancy detection is related just to ventilation and lighting control.

The most frequently used sensors in occupancy detection are the following:

- presence;
- movement;
- CO<sub>2</sub> concentration.

With respect to ventilation control, a fundamental issue is the modulation of Air Change Rate (ACR) to fulfill thermal loads and Indoor Air Quality (IAQ) requirements, depending on the specific typology of HVAC system. Technical standards and building regulations provide minimum ACR levels (considering outdoor fresh air) to maintain satisfactory IAQ based on occupancy profile and on the type of end-use of the building zones. However, in several cases the IAQ is lower than the recommended values at maximum occupancy and the ACR is higher than necessary in condition with low occupancy [8, 33,34], resulting in energy waste and/or inadequate conditions for occupants [35]. A control system that can predict occupancy intensities or automatically adapt the ACR (and in particular the outdoor fresh air rate fraction) to the actual occupancy level of the thermal zone can reduce energy waste for ventilation and air handling processes [8]. The term adopted for this type of systems is Demand-Controlled Ventilation (DCV). The potential in terms of energy saving is notable; for example, in [34] it is shown a potential saving of 40% from November to March (with outside temperatures of 11-28°C) through an optimized DCV that use CO<sub>2</sub> concentration data to detect number of occupants, while in [33] a 20% saving in electrical energy for cooling is found. As described before, outdoor fresh air rates and ventilation requirements are related to end-use and occu-

pancy: therefore, the amount of energy savings that can be obtained by DCV can largely vary depending on these two parameters.

Movement sensors are also used in heating, cooling and lighting control; the presence of a continuously updated occupancy model can help maintaining optimal comfort conditions in response to changing situations in the outdoor and indoor environment [36,37].

From the technical point of view, occupancy detection systems can be classified according to the presence or absence of a terminal device aimed at this scope and are therefore indicated as:

- terminal based detection systems;
- non-terminal based detection systems.

Examples of *terminal based detection systems* are mobile phones or Radio Frequency IDentification (RFID) tags inserted in objects carried by the occupants [38]. Generally, this type of occupancy detection systems are not well accepted for privacy concerns.

On the other hand, *non-terminal based detection systems* provide occupancy information in a less “intrusive” way. Example in this case are CO<sub>2</sub> sensors, Passive Infra-Red (PIR) sensors and image recording (camera) devices [38,39]. CO<sub>2</sub> sensors are able to measure the concentration of carbon dioxide (CO<sub>2</sub>) in a space, in parts-per-million (ppm) [40]. These sensors exploit the CO<sub>2</sub> concentrations due to people presence; a person, in fact, produces and exhales carbon dioxide as a consequence of normal metabolic processes. Therefore, the concentrations of CO<sub>2</sub> inside occupied buildings are higher than in unoccupied rooms or outdoor air [41].

PIR sensors are pyroelectric devices that detect motion by measuring changes in the infrared level emitted by surrounding objects [42]. Since all objects with a temperature above absolute zero, including, of course, humans, emit heat energy in the form of radiation [38], PIR sensors are able to detect occupancy [38,42], but the disadvantage is that they are simple movement sensors and often cannot determine precisely if the room is occupied or not [7]. Image recording devices, such as video cameras are often used in buildings for security purposes but their use has also been explored for occupancy measurement [36,38,43,44]. Vision-based technologies utilize visual attributes of the objects and use computer vision methods to extract the identification and location data.

A development of applications in this sense can be cost-effective, since it makes the implementation of an additional technology for occupancy sensing unnecessary [36].

Finally, wireless sensor networks technology can also be exploited, especially in the retrofit of existing buildings, where the introduction of new technological devices can be problematic. In general, non-terminal based detection systems require minimal maintenance and supervision [7,45], thus reducing running costs.

### **3.3.2. INDOOR ENVIRONMENTAL QUALITY CONTROL AND ANALYSIS**

As introduced before IAQ is related to occupancy and is a subset of Internal Environmental Quality (IEQ). With respect to thermal comfort, which is a relevant part of IEQ, temperature control is the fundamental element [31]. In HVAC systems, internal air temperature is typically the primary controlled variable and it is used as a parameter to address human well-being, using empirical comfort models [46]. Of course, other factors such as humidity, radiant temperature and air velocity also affect comfort [47], nevertheless temperature control remains the basic element to ensure thermal comfort.

At a technical level, *temperature sensors* measure indoor, duct, outdoor air temperature, but also water or refrigerant temperature. The typical accuracy is  $\pm 5^{\circ}\text{C}$ , or better, but it is normally sufficient for HVAC applications. They can be categorized by the effect used to generate the temperature-versus-signal response: bimetal, fluid expansion, electrical self-powered, electrical resistance. The temperature sensor measurement technologies used are Resistance Temperature Detector (RTD), thermistor, thermocouple and integrated circuit, but the most commonly used are the first two, and both quantify temperature based on the changing resistance of an element [31]. Humidity, instead, may be sensed as relative humidity, dew-point temperature, or wet-bulb temperature, but relative humidity is the most common quantity measured. The first humidity sensors used hygroscopic materials, which, absorbing water vapor from the air, change dimension in response to changes in humidity. These mechanical sensors are still commonly used in portable sensors, simple electric controls (humidistats) and enthalpy economizer controllers, but their accuracy can decrease with use due to variations in material quality and hysteresis effects [47]. In general, manufacturers recommend a maintenance (check and calibration) once a year, and once every six months if subjected to high temperature or humidity; for all these reasons they are typically more expensive than temperature sensors [31]. A detailed explanation about temperature and humidity sensors can be found in [47].

The most common actuator for thermal control is the thermostat, which gives simple ON/OFF signal to plants, according to scheduled programs. In recent years different types of “intelligent” thermostats have appeared on the market. The difference between a conventional thermostat and an “intelligent” one is that the first one uses a set of pre-defined rules (e.g. timer-based schedules), while the second has the ability to adapt its control strategy to the users’ preferences [48-50]. In any case, the thermal control is affected by the behavior of the user. An interesting research shown how people use thermostats at home, and is underlined that 56% of homeowners always program their thermostats, 32% sometimes program their thermostats, 9% never program their thermostats, and 3% do not know how to do that [51]. This means that control systems managed only by customers cannot ensure optimal operation and proper energy savings. Similar arguments are valid for another type of actuator used in hydronic heating systems with radiators, the thermostatic valve. In the last ten years, several research groups carried out surveys on the current thermal control strategies in buildings [10,52] and their studies show that, typically, room thermostats and/or thermostatic valves on radiators are used [52,53]. Thermostatic Valves located on individual Radiators (TVR) have the ability to maintain a set-point temperature according to users preferences [54]. Some studies revealed that in many cases occupants fail to use TVR in an optimal way, and the settings used result in overheating and, consequently, energy waste [51].

### **3.4. CONTROL MODES AND STRATEGIES**

As introduced before in the description of feedback controls, the controller acts to minimize the difference between the actual and the target value (error). The method used by the controller to correct the error is generally defined *control mode*. The most common control modes are:

- ON/OFF;

- Proportional (P);
- Proportional/Integral (PI);
- Proportional/Integral/Derivate (PID);
- Artificial Intelligence (AI) based modes.

One of the simplest and most commonly used control models is ON/OFF [10,55,56]. This mode can be applied to HVAC, lighting and shading systems within buildings. This mode refers to a single function or subsystem, laying in the first layer of the Intelligent Building Pyramid [9], reported in Figure 1, and corresponds to the *basic control layer* [45,57,58]. As shown by Wang [9], the individual functions or subsystems can be either considered as autonomous elements, groups or even completely integrated. In the first two cases, the overall performance may be not optimal, given the inability to obtain an overall description of building operation, while in the case of integrated control, a comprehensive and realistic description and analysis of energy and economic savings becomes feasible [2,30]. This topic will be illustrated more in detail later in Section 3.6, dedicated to data analysis and building performance tracking.

PI and PID controllers are widely used for thermal systems to improve set-point tracking. PID controllers are also used in ventilation systems control [34,35,59] e.g. to control variable frequency pumps to supply chilled water to the AHUs. Here, the PID controller allows maintaining a certain differential pressure between supply water and return water by moderating the frequency of the input power to the motor. In general, the advantage of using a PID control system is that the integrator can minimize the errors in tracking. However the trade-off is that it is a little more complex to implement than an ON/OFF controller [55]. Although these controllers may improve the control performance without a priori knowledge about the physical phenomena, they need to be tuned correctly, which is rarely made in practice [10] (less than 5% according to [53]). These controllers cannot guarantee by themselves the optimization of energy consumptions because they are aimed at this global objective but just as a single function (e.g. the control of the stability of internal temperature) [53,60]. In order to overcome these difficulties, self-tuning algorithms are studied to enhance energy efficiency [10,48,61-64], but, a supervisory control is preferable, to ensure a real overall optimization [10,53,55]. This type of control places itself in the third level of the pyramid in Figure 1, in which the individual functions are no longer independent, but operated by a single and comprehensive control system. An intermediate solution can be defined by the organization according to the multifunctional logic (the second layer of Figure 1). Depending on the level of aggregation of functions, control strategies can be subdivided into two categories: system level and subsystem level strategies. Typically they are organized in these ways:

- system level, integrated automation
  - optimum start/intermittent operation;
  - weather compensation;
  - RBC and MBC for a specific aggregation of function;
  - RBC and MBC for the overall building optimization
- subsystem level:
  - terminal units (e.g. fan-coil, radiant systems, etc.);
  - distribution systems (e.g. air loops, water loops, etc.);
  - generation systems (e.g. boiler, furnaces, heat pumps, chillers, etc.);
  - storage systems (e.g. hot/cold water storage tanks, etc.).

Indeed, there are elements whose mutual influence is particularly relevant in terms of energy performance and IEQ. As shown before, the control of occupancy, for example, can have an important

impact on ventilation systems operation, while weather forecasts are crucial for heating, cooling and shading systems control, i.e. to anticipate the building thermal dynamics.

In order to overcome the problems and to exploit effectively the potential outlined in Chapter 2, the implementation of advanced control policies, consequently, requires the development of integrated models to predict the behavior of the controlled environment and to learn optimal operational strategies from actual operating conditions. The evolution of integrated controls in buildings follows the rapid evolution of modeling and simulation tools, exploiting high performance computational techniques and software [65,66]. For the reasons illustrated before, an integrated control aimed at building performance optimization needs necessarily a Multi Input - Multi Output (MIMO) modeling strategy.

### 3.4.1. RULE BASED CONTROL (RBC) AND MODEL BASED CONTROL (MBC)

Each system can be controlled in a *direct way*, using sensors and actuators (without having a priori knowledge of the phenomena), or in an *indirect way*, using models that predict the system behavior (knowing the underlying physical phenomena). Normally, the term "building automation" refers to basic systems, which run individual plant components according to a *direct logic*. It usually works according to certain pre-set rules allowing to the scheme "if *initial condition*, then *action*" [28,67], where the initial conditions are controlled by sensors, while the actions by actuators, which act directly on the individual elements and functions. These systems are RBC and are the current control practice in simple Integrated Room Automation (IRA) [28,67,68]. RBC critically depends on correct choices in terms of rules and associated parameters [28].

A completely different approach is represented by an *indirect logic* which employs models to simulate the building behavior, in order to compare different control strategies and, then, choose the better one [49,69,70]. Therefore, the system does not depend on predetermined set of rules and is able to adapt to every situation, even those that are not contemplated by the rules themselves. This approach is a MBC and it is more complex compared to RBC, fundamentally because of the effort required in process modeling. Nonetheless, MBC approaches, for the reasons outlined in Chapter 2, are particularly interesting, because they are able to describe the relevant aspects of a certain process or system in terms of energy efficiency. Essentially, MBC strategies can capture complex dynamic interconnections among phenomena that RBC strategies cannot capture effectively [15,71], although there exist examples of RBC strategies derived by simulated MBC, by means of rules learning methods [72-74]. A basic scheme of a RBC/MBC model is reported in Figure 5.

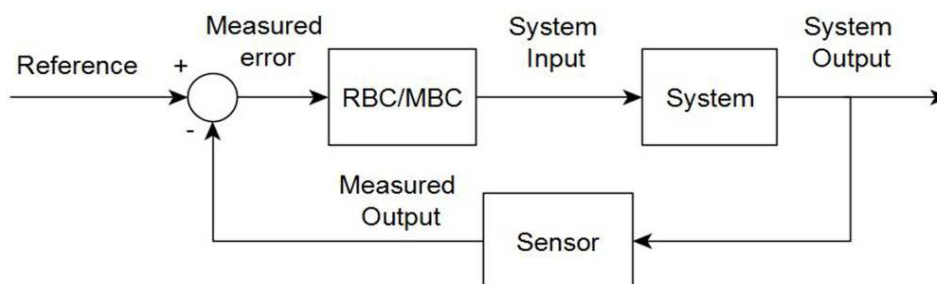


Figure 5. RBC/MBC control scheme.

In most of the cases however, advanced control strategies work with models and algorithms to implement saving strategies [22,49,75-77].

### **3.4.2. ADAPTIVE CONTROL AND LEARNING TECHNIQUES**

The term *adaptive* can be associated to both RBC and MBC strategies [78] and it is an attribute of all the systems that are able to learn on their own how to make decisions incrementally by means of data acquisition, or that are able to self-regulate and adapt to variable and evolving conditions [10]. These techniques generally mimic the human adaptive principle [79]: “if a change occurs, people react in ways which tend to restore their comfort”. Thus, the origin and development of the adaptive approach is due to the user comfort improvement by means of autonomous intelligence [64,79,80]. However, empirical evidence shows that conventional self-tuners can occasionally identify inappropriate parameters [48,57]. Adaptive approaches normally use *black-box models* (described in detail in the relative Paragraph 3.5.3 ) which progressively “learn” (by means of statistical and machine learning techniques) input/output relationships using the data measured by sensors and controllers during operation [78,80]. This ability brings some advantages, such as the decrease in the commissioning time and the possibility to optimize nonlinear systems, but brings also some disadvantages, when a clearly defined process model is not present. The major requirements of a self-learning model, according to [81], are the following ones:

- progressively “forget” the rather inaccurate initialization;
- keep enough “different” learning examples in order to avoid convergence problems;
- allow the model to improve as the knowledge of the system (e.g. the thermal characteristics of the building improves).

The data collected during operation, on which the learning strategy and the underlying *black-box models* rely, tend to reduce the prediction errors over time, incrementing progressively the accuracy of the forecast. However, if some data are misinterpreted, it is nonetheless possible to have an increase in the prediction errors [82]. For all these reasons, normally, the adaptive approach is combined with a predictive approach, in order to supplement self-learning capabilities with predictive ones. A predictive-adaptive control system, for example, is used in [59] to optimize the operation of a Variable Air Volume (VAV) air-conditioning system. This system uses a simplified physical model to predict the responses of the system with sufficient accuracy in a wide range. A *Genetic Algorithm* (GA) [83] is used to search the optimal settings of the variables of the process (i.e. AHU supply air temperature, outdoor airflow rate and chilled water temperature set-points, etc.) by minimizing the cost function (representing the operation of the system). The adaptability is determined by the ability of the GA optimizer to tune automatically the operational settings [4,84,85]. Combinations of statistical/machine learning techniques and MBC are also possible, as described in [15]. In this case the operational set-points of an HVAC systems are optimized by forecasting weather conditions and electricity prices through machine learning techniques, which are working with real-time data. In particular, the authors found that by using only *black-box models* (i.e. data driven models operating with real-time conditions), without having a building model and HVAC topology information, it is not possible to predict effectively building energy behavior, since the effect of one thermal zone on the overall energy balance would be difficult to assess. Further, authors observed that real-time occupancy data are rarely available on a fine granular level. These limitations can result in reduced control capabilities and energy savings. As a conclusion, an appropriate

combination of process knowledge (e.g. a physical model) and data driven model to predict future operating conditions (e.g. statistical/machine learning models) can potentially determine the optimal trade-off between ease of implementation and energy savings [15].

### **3.4.3. MODEL PREDICTIVE CONTROL**

As introduced in the previous section, the ability to predict internal and external conditions is crucial to implement energy saving strategies, in particular with respect to the operation of HVAC systems [10,27,54,71,76,77,86,87] and distributed generation technologies [88]. RBC control meets relevant limits in the prediction of building behavior because it is based on pre-defined rules that generally can't foresee all possible scenarios, although improvements can be made with respect both to the definition of parametric operation scenarios (simulated offline) and to rule learning methods [72-74]. Instead, MPC control, when supplemented with predictive capabilities, can generate and analyze multiple possible operating scenarios, identifying the optimal settings [89-91]. This type of control is called *Model Predictive Control* (MPC) and is one of the most promising methods of advanced control [15,20,22,27,28,56,60,67,68,76,91-99].

The main idea of MPC, instead, is correlated with a dynamic optimization logic and it is defined by the following steps:

- a model is used to compute the predicted process/system output variables, based on input variables (controlled and disturbances);
- an objective function is used to compute the performance of the system, according to relevant criteria;
- this objective function is minimized over a certain prediction horizon to determine future actions (i.e. controlled input variables);
- the first action is applied to the process/system and the process restarts from step 1.

MPC is also known as Receding Horizon Control (RHC) [17,28,54,56,87,93,97,99-104] and is not a single strategy but rather a class of control methods that use a model of the process to forecast the future conditions and disturbances, in order to obtain the best control action through the minimization of an objective function subject to some constraints [20,69,92,93,102]. MPC is therefore an optimization problem applied to a certain process in a dynamic way. Initially used in the late '70s in chemical and petrochemical industries, MPC became widely used in several other branches of industry [53,97,105]. In building control applications, MPC received an increasing attention in recent years [66], following the evolution of dynamic building performance simulation and optimization tools [106] and the evolution of computational tools and resources [53]. The application of MPC for optimized building operation, in fact, requires a dynamic model of the building itself [8,28,60] and one of the key elements for the quality of MPC is the correct identification of the process model [20,27,56,68,92,97,107]. System identification therefore comes into play, since the model should be directly constructed or calibrated with respect to observed data. The process models used in MPC can either maintain an underlying physical structure (i.e. white-box or grey-box models that will be illustrated in the related Section 3.5.), or simply exploit statistical or machine learning formulations (i.e. black box models) [56,92,97,108,109]. Further, weather prediction is a major issue in MPC for buildings; it is possible to use empirical models, e.g. Gaussian Process (GP) model and Artificial Neural Network, advanced Numerical Weather Prediction (NWP) models or weather data delivered by meteorological server [54,82,89,110-113]. Several research studies showed how a 24 h forecast-

ing horizon is generally appropriate [54,110,111] for predictive control strategies. A 24 h horizon is substantially compatible with the operational management of energy infrastructures, for example the day-ahead electricity market and so MPC can play an important role in improving the interaction between buildings and energy infrastructures.

Beyond outdoor air temperature [114,115], moreover solar radiation forecasting is crucial to improve the quality of building simulation models suitable for control [93]. The performance boundaries of MPC and the improvement over advanced RBC are difficult to assess extensively due to the inherent variability of operational patterns of real buildings, however it seems reasonable, based on recent comparative studies [22,53,89,92,93,98,104,116], to hypothesize an average improvement of approximately 30 %. The main advantage of MPC over the RBC currently used in BACS is determined by the possibility to anticipate weather, occupancy, thermal behavior and comfort [94,102,117].

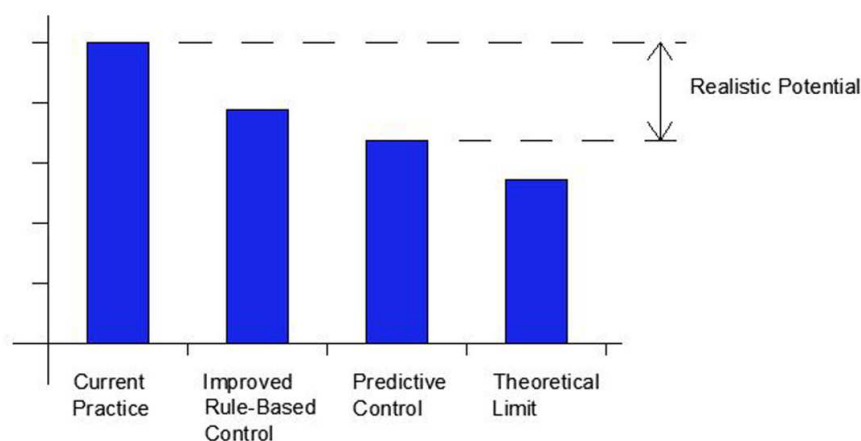


**Figure 6. Theoretical and realistic potential energy savings of Model Predictive Control compared to current practice.**

In Figure 6 the theoretical and realistic potential energy savings due to different control systems are represented, comparing current practice, improved non-predictive control, predictive control and performance bound. The last level is an ultimate threshold on the performance of any controller, and thus used as a theoretical limit for benchmark [28,67]. This benchmark corresponds to a controller that can perfectly forecast the future. The control system that is the closest to this performance bound is the real predictive control, characterized by a small error in the forecast [118].

### **3.5. BUILDINGS AND CONTROL MODELS**

For all the reasons described in the previous paragraphs, it has been shown that Model Based Control (MBC) with predictive capabilities, i.e. model predictive control (MPC) is the most promising approach for building control and energy management [53]. In fact thermal and electric load prediction, is essential for many building control strategies [60,68,119] However, despite the solid theoretical base of system modeling and identification the application during real-time building opera-

tion is challenging [60]. As introduced before, the discrepancy between the predicted and real building performance is a major issue [22,120-122] and BACS, for the reason outlined in Section 3.2, can give a contribution in this sense. The discrepancy is basically due to:

- assumption about the performance of components and features that can be different from “as built” conditions;
- uncertainty in the evolution of climate data patterns;
- uncertainty in the behavior of occupants;
- model type and accuracy.

Although building energy simulation (BES) has been traditionally concentrated in the building design phase, modeling strategies can be applied furthermore in the building operation phase [40, 109], by employing model reductions techniques [121]. A survey of building performance assessment tools is presented in [123]. However, several research studies highlight the fact that the detailed dynamic models, generally used for performance simulation (physics-based model), are not suitable for MPC [28,60,68,119,124,125]. The basic conditions that a model for MPC should satisfy are simplicity, stability and accuracy and precision in the estimation of system dynamics [22,53,68,91,100].

Detailed simulation models used in building sciences present several non-linearities. Linearity, convexity and the use of continuous variables are important to obtain easily solvable optimization problems [20,28,86,97]. Discrete variable can be handled as well in Mixed Integer Linear Programming (MILP) in a computationally efficient way. Different models used in MPC are illustrated in [68] while in [126] the difference between linear and non-linear formulation is explained. For all these reasons, in the last decades, the problems concerning the selection of models to be used in building control has been discussed [22,27,53,60,68,76,77,86,91,95-97,105,109,124,126-128].

The models used for building performance evaluation can be subdivided into three categories white-box, grey-box and black-box models [68,75,113,125,129] whose essential characteristics are synthesized in Table 4. In [75] a comparative study of various types of models is presented. The traditional approach in building design is to use a detailed bottom-up [130] knowledge driven approach, i.e. a white-box model. An alternative is to use a top-down [130] data driven approach, i.e. a black-box model [109,125,127,131].

**Tab. 4 - Different types of models for building performance simulation, control and analysis.**

Model type	Description	Advantages	Disadvantages
White-box	Detailed physics-based models (knowledge driven) employing algebraic and differential equations (ODE <sup>1</sup> , PDE <sup>2</sup> )	Accuracy and precision, detailed physical description of phenomena	Computational effort, difficult and error-prone modeling and implementation process
Grey-box	Simplified physics-based models with algebraic equations and first order ODE, whose parameters can be determined from measured data.	Easier implementation with respect to white-box models, simplified physical description of phenomena, computational efficiency	Not accurate and precise as white-box models, error-prone implementation process
Black-box	Empirical models (data driven) are based on little or no physical behavior of the system and rely	Computational efficiency and flexibility, simple implementation with respect	Absence of a physical representation, opaque to the user

<sup>1</sup> Ordinary Differential Equation

<sup>2</sup> Partial Differential Equation

	on the available data to identify the model structure. They are suitable for predicting future behavior under a similar set of conditions	to achievable accuracy	
--	---	------------------------	--

Generally, the models used in control are derived from empirical data through system identification techniques [25,132] and are appropriately simplified to overcome the limitations of white-box models (i.e. non-linearities, dimension, etc.). The parameters identified in data driven models in general don't have a direct physical interpretation and don't preserve a simplified physical structure, such as the one of grey-box models. By preserving a physical interpretation, grey-box models can provide potential insights on the performance of building components and technical system, differently from black-box models. On the other hand, black-box models can be used where there is no a priori knowledge of the input/output relationship, for example, in climate and occupancy patterns prediction [59]. In this case, however, due to absence of an underlying physical model data over a long period and a large variety of conditions are necessary for the training process [63,113]. Hybrid models (combination of various techniques), are also present [15,60,93,103,109,125].

The building model is generally simplified, for control purpose or calibration, using a lumped parameter formulation [60,71,76,87,91,133-137]. The parameters are estimated by using identification techniques or directly by model fitting (error minimization) [53,60,75,105,125,136,137]. In [138] an overview of simplified building simulation models is presented. As introduced before, grey-box models have the ability to combine predictive capabilities and computational efficiency while preserving physical structure and transparency in the modeling process. The possibility to determine the lumped parameters using real-time operation data (through statistical learning) opens up interesting possibilities, establishing a methodological continuity with white-box model calibration techniques [139-141]. In the following sections, the problems related to the different modeling strategies will be described in detail, showing the potential continuity among building performance simulation practices, model reduction for control and data analysis for performance tracking.

### 3.5.1. WHITE-BOX MODELS

As introduced before, white-box models are used for BES and are not in on-line MPC, although they can be used to evaluate optimized control strategies off-line, by means of optimization [70, 72]. In other words, simulation data from white box models can be used to train advanced RBC systems. White-box models, with respect to control applications, should be seen as a complementary tool [37,68,70,97,108,119,124,142]. Online models, in fact, should be able to use measured data, perform a computational process and apply actions in real-time [97,111,135]. Co-simulation is time consuming and thus not cost effective for industrial implementation and to promote large diffusion of MPC [95,113], due to the dimension of the optimization problem and the non-linearities determined by the detailed description of physical phenomena in building simulation [8,9,19,21,27,28,42,59,60,71,76,97,113,137,143,144]. Indeed validated software tools such as ESPr, TRNSYS and ENERGYPLUS [145] can be used to perform off-line computation and testing [72], although the model comparison and validation methodology presents inherent limitations [68,120].

### **3.5.2. GREY-BOX MODELS**

Grey-box models can be used both for BES and MPC. In fact, grey-box models provide an adequate accuracy level in the prediction of the dynamics [27,146-148], while maintaining a simple and computationally controllable formulation. Further, the model parameters can be easily identified from measured data preserving a certain level of transparency (simplified physical/modeling) of the model itself. Grey-box models, as introduced before represent a compromise between the bottom-up, design-oriented approach of white-box models and the flexibility in learning complex input/output relationships of black-box models. Thanks to the computational tractability and the dimension of linear/linearized models, they can be applied not only in a deterministic framework, but also in a stochastic framework [109,126,128,131], more appropriate for the control of real-time building operation. Clearly the definition of the model structure (for model reduction) constitutes an issue and, generally, depends on the specific use of the model [119]. The reduction of the dimension is particularly important for computational reasons [30,59,97,138], and most of the formulations are based on lumped parameters [99,102,117,135,136] and, particularly, on the resistance-capacity analogy for thermal processes [133,60,8,27,53,54,20,22,28,57,67,71,85,91,101,104,109,113,128,149]. Generally, a node represents a zone or a component and the nodes of the system are connected with resistance and capacities. The model is assembled by writing system of the governing differential equations [22,138], that can be then represented in a state-space form. A state-space model is a mathematical formulation which describes systems of linear differential equations in a compact way [92] and is commonly used for dynamic systems simulation and control purpose. This type of model formulation is used in some of the leading projects for aimed at connecting BES to MPC [27,68] and, in general, is quite common in building control applications [133,54,22,87,91,109,128,131,149].

A discrete (finite differences) linear state-space formulation of the building dynamic model [133,138] can be included in a Linear Programming (LP) model [150,151] for optimization. Discrete variables (ON/OFF states, discrete choices, etc.) can be handled as well by using MILP formulation, determining a “Hybrid System” formulation [152]. This type of formulations presents several advanced system in terms of computational efficiency, even for large-scale problems. Interior point methods are used as well for MPC [153,154].

### **3.5.3. BLACK-BOX MODELS**

As outlined before, an alternative to both detailed and simplified physical models is represented by data driven models. Building performance estimations can be based, in principles, on statistical data [19,103,155,156] and subspace identification methods are widely used in control systems [17,56,92,97,157]. The objective of system identification is to describe a process by means of a linear, time invariant and discrete time model [56,92,97,103,143]. More in general, statistical and machine learning techniques can help determining input/output relationships without detailed a priori knowledge of the phenomena themselves. A review on energy models obtained by data analysis can be found in [126,158].

In some cases, the efficiency of a decision can be directly assessed using techniques such as Data Envelopment Analysis (DEA) [159,160]. This kind of approach can be used to evaluate the effectiveness of measures without a detailed underlying physical model [159,160]. In general, hybrid techniques combining black-box models with white-box and grey-box models, as well as with other black-box models, are also possible. In [158], for example DEA with Index Decomposition Analysis (IDA) is combined with an Artificial Neural Network (ANN) [161]. The tight integration of these is aimed at joint historical data analysis prediction and optimization for energy management. IDA is a technique that enables the decomposition and ordering the elements that affect commodity consumption [21,58,162], while ANN is simply aimed at learning input/output relationships [138]. ANN have been widely used in BACS [18,57,63,78,81,163-165], because of their ability to learn complex patterns [82] and optimize non-linear systems [78].

A different technique with similar applications is Support Vector Machines (SVM) [161]. The main advantage of SVM over ANN is related to the fact that the statistical learning process is cast as a convex optimization problem [150].

Another machine learning technique is Gaussian Processes (GP) regression [166]. It has been used in the prediction of hourly data patterns, in particular, related to weather [110,167] and occupancy [44]. In contrast to ANN and SVM which are parametric techniques GP is a non-parametric technique, suitable to identify long term temporal and spatial trends [111]. Further one of its special features is the ability to predict not only numerical values, but also their uncertainty boundaries. Probabilistic methods such as Bayesian Networks and Markov Chain Monte Carlo (MCMC) are also widely used for the prediction of the likelihood of events. These methods can be used, for example, to simulate occupancy schedules [168] or to predict probabilistic weather and energy consumption patterns [77,95,169].

The online optimization of black-box models through heuristics [83], such as Genetic Algorithms (GA), can be used to find optimal dynamic settings within operation ranges allowed by RBC [4,59,85,86]. However, linear/linearized formulations of optimization models are preferable as they can be solved very efficiently by LP/MILP [53,28,67,87,170,171]. Linear dynamical systems can be conveniently represented as a state-space or as a transfer function[60], as introduced before.

Generally, system identification and regression techniques can be used to identify empirical models suitable for control [68,81,86,97,99,109,126,157,170], such as Auto-Regressive with Exogenous Inputs (ARX), Auto-Regressive with Moving Averages and Exogenous Inputs (ARMAX) or others. In parallel, regression techniques can be used to predict building energy performance as a function of relevant factors [155,159,160,172-174]. Linear regression and system identification, as described in the previous section, can be used to obtain simplified physical models, thus establishing a potential continuity between black-box and grey-box approaches, while ANN or SVM cannot be used for this purpose [170].

### **3.6. BACS AND BUILDING ENERGY MANAGEMENT**

As illustrated before, BACS and TBM are aimed at managing and optimizing the performance of heating, cooling, ventilation, DHW onsite power generation, etc. Given the complexity of the inter-

action among the factors that determine energy consumption several strategies can be implemented and exploited starting from the fundamental elements reported in Table 1.

Additionally, the evolution of design and operation practices towards the nZEB<sup>3</sup> paradigm requires an evolution in the BACS sector [13] whose essential functions will be:

- central integrated control for better coordination among subsystems and devices.
- monitoring and feedback, for the fast detection of malfunctioning and performance issues and for encouraging energy saving behaviors;
- optimization with respect to technical constraints and IEQ;
- load management, load shifting, and active/passive energy storage management.

The first three functions have been already introduced and are related to the evolution pathway of BACS and of the models for integrated building control. Considering the fourth function, this is closely connected to the dynamic conditions within the grid. While “active” storage systems (e.g. water storage tank, batteries, etc.) [175,176] can be operated according to optimal dynamic energy management strategies [171,177-179], “passive” thermal storage with the building fabric can be exploited by means of optimized strategies [172,180]. In the following sections the fundamental issues with respect to load management and performance monitoring will be described.

### **3.6.1. LOAD MANAGEMENT AND PERFORMANCE OPTIMIZATION**

The advantages determined by load management are not simply related to energy savings but to the reductions of cost of energy services [70,137]. In some cases, where dynamic tariffs are current, the moment of energy purchase can affect the cost by a factor ten [13]. A typical example of load management is building pre-heating/pre-cooling, whose effect is to shift the peak load. While adaptive algorithms can be used to find the optimal start and intermittent operation regime, more advanced forecasting capabilities are needed for a positive interaction with the grid, following a dispatch optimization strategies in a day-ahead market perspective. Predictive capabilities are needed to exploit thermal storage potential [16,20,181]. Clearly, an adequate understanding of the building dynamic behavior (e.g. by means of a model) enables the improvement of the adaptability of the building technical system to fluctuating pricing conditions within the electric grid [32,76,91,111,182], considering at the same time schedules, comfort and internal environmental quality constraints. By integrating a load (heating/cooling/electricity) forecasting module with an optimization module, it is possible to dispatch distributed energy resources and to optimally enhance the adaptability in grid interaction [170,171,183].

Several examples of the advantages of load management can be found in literature although they have to be evaluated related to the specific applications and end-uses. In [20] an MPC is used to control the pre-heating of the concrete ceiling system. It is shown that the beneficial side effect is a significant peak load reduction; the saving are more significant for the more insulated building block, 28%, compared to the less insulated block, 17%. In [22] it is shown that a MPC can reduce the peak input of 44% compared to a classical on-off control system. In [100] it is shown how a MPC can optimally manage chiller operation to store the thermal energy in the water tank, decreasing the costs by 25% compared to ON/OFF control.

---

<sup>3</sup> nearly Zero Energy Building

The combined use of both active and passive storage under optimal control is investigated for 24-hour deterministic simulation study in [181]. The experiment shows that the individual storage systems reduce the daily total operating cost of 16-17% respectively, while their combination leads to a saving of 26% compared to the conventional solution without storage. In addition, the use of adaptive systems with self-learning capability can increase the effectiveness of load management by learning, for example, the trend of usage profiles. In [15] it was shown that a predictive-adaptive control system, which proactively assesses climate forecasts and energy costs in order to automatically manage the loads, can result in an energy reduction of 20-30%. This study combines a Numerical Weather Prediction (NWP) model, which gives a five-day-ahead weather forecast, with a predictive dynamic model that uses statistical and machine learning techniques in order to create a low-cost and adaptive building model using available sensors data. In [81] the use of a predictive-adaptive system using ANNs (one to predict building model and two for climate forecasts) and an optimal control, allows an energy saving equal to 70%, during the intermediate seasons (compared to a standard commercial controller) and an annual reduction of 36%.

Standard thermal controllers provide the maximum heating power at the beginning of the operation period, while more advanced control types anticipate actions in order to shift peaks or distribute loads. The test shows a mid-season saving of 50% and a global reduction of 13% compared to a commercial controller. It has to be underlined that, theoretically, ANN and other machine learning techniques can progressively improve performance by learning over a long time span, but in order to transparently compare the results in terms of energy savings, consumption data have to be necessarily “normalized” with respect to weather, occupancy and operating schedules (period of operation).

Of course, in operational management we have to consider both the technical constraints, related to energy and cost, and the interaction with occupants (comfort indexes, IAQ, etc.). Typically, the objective of a supervisory control is to minimize a cost function while ensuring adequate comfort and satisfying technical constraints [10,27,53,54,17,22,28,56,58,76,84,93,111,116,137,149,183]. In fact, beyond accurate system modeling, an important aspect of MPC is the definition of an appropriate objective function for optimization, according to which the optimal operation strategy is determined, considering the dynamic evolution of weather conditions, loads and energy prices [16,59,76,77,86,111,183]. Global performance optimization should consider simultaneously multiple criteria, appropriately weighted in the objective function, or formulated as constraints. Optimization with multiple objective functions is possible as well [184], although single-objective formulations are preferable from the computational point of view [77,171]. The performance criteria considered have general sustainability implications, which are economic (running cost), environmental (CO<sub>2</sub> emissions, primary energy, etc.) and social (IAQ, comfort indexes, etc.), establishing, in principles, a link with general sustainability assessment schemes [185].

The implementation of advanced control policies, therefore, requires the development of integrated MIMO models [69,122,146]. Examples of these strategies are given by [98] and [132]. The first study compares a dedicated control of lighting system with an integrated one that uses weather condition, occupancy and HVAC operation data; the annual energy savings are 20% and 25% respectively. In [58], an integrated RBC is tested that it is able to save 30% of heating energy during the coldest month (January), by controlling in an integrated way lighting, shading and HVAC system.

Particularly interesting are the optimization strategies that join together heating, cooling and electricity demand [22,182], because they can be formulated effectively with similar techniques, such as LP/MILP [27].

When dealing with system modeling problems (e.g. an integrated room automation) generally non-linear phenomena can be encountered [27]. However, linear and linearized (e.g. piecewise linear) formulations are accurate enough for practical applications [22,53,143,171,186]. Iterative linearization techniques are also possible [22,27,53,67,86,87,116,170,171]. Further, parametric linear models can furthermore be used [138,170], maintaining a physical interpretation of the model parameters. As mentioned before, optimization model formulation and algorithms are the core of MPC [20,67,98,99,116,149]. Further, the results with respect to the different performance criteria can be relevant. For example in [104] a MPC which is able to reduce the electric consumption of the cooling system of 50% achieves a cost saving of 75%, while increasing the Coefficient Of Performance (COP) of system itself of only 1.5%. In [28,67] an extensive comparison is presented of the performance improvement of MPC over conventional RBC in terms of annual energy consumption, the average potential energy saving identified is 35%.

Finally, the report on *BIQ'S system* [15], describes a hybrid approach coupling MPC with machine learning models, showing an energy saving potential of 30% during colder days and 10% in hotter days. In this case, the objective function is the weighted sum of three competing criteria (running cost, CO<sub>2</sub> emission and comfort). The model is tunable based on the operation priorities. Further, it has been shown that, by relaxing the comfort index Predicted Percentage of Dissatisfied (PDD) [187] up to 10% during unoccupied times, energy savings can be up to 45% in days with temperature oscillations and up to 25% in days with narrow temperature oscillations. These evidences confirm, on the one hand, that the research activity on occupancy sensing and modeling is very important and, on the other hand, that the relaxation of comfort constraints should be considered as one of the key topics to increase savings and flexibility.

### **3.6.2. PERFORMANCE MONITORING, TRACKING AND DATA ANALYSIS**

Monitoring and data analysis is essential for appropriate commissioning and performance tracking [188,189] measuring performance and calibration as design and measured energy consumption can present a large gap [75,121]. Several research studies showed that the simple tuning of existing control systems can determine moderate energy savings. In [190] a potential saving of 15% is reported for temperature control tuning of a heating system. In [5] tabular values are given for the increase of energy consumption due to control malfunctioning, for heating, cooling, ventilation, DHW and lighting. As already discussed before, even detailed design phase simulations cannot ensure the energy efficiency in real-time operation unless a calibration and tuning process is performed on a continuous base [114,115]. It is now clear that, in order to reach consistent results in terms of energy efficiency at the EU scale [191], it is required to develop BACS applications where savings are transparently identified and shown by means of visual tools [29,75,121,170,171,182,192,193]. The systematic study of occupant's behavioral patterns [194,195] can result in a reduction from 5% to 40%, as shown in recent studies [7,8,30,33,34,44,45,80,196]. Further, adaptive and predictive control technologies should be necessarily fed by measured data [80,81,97] and therefore synergies with data analytics strategies should be encouraged. The transparent assessment of the advantage in terms of cost is another issue for promoting the development of advanced BACS applications [19]. TBM, if supplemented by data analytics can highly enhance its potential. As an example, [31] shows how data analytics added to TBM can help identifying 80% of faults and operational issues

with respect to the 20% of a conventional configuration. A scheme of the potential savings related to monitoring and advanced control over current practice [31] is presented in Figure 7.

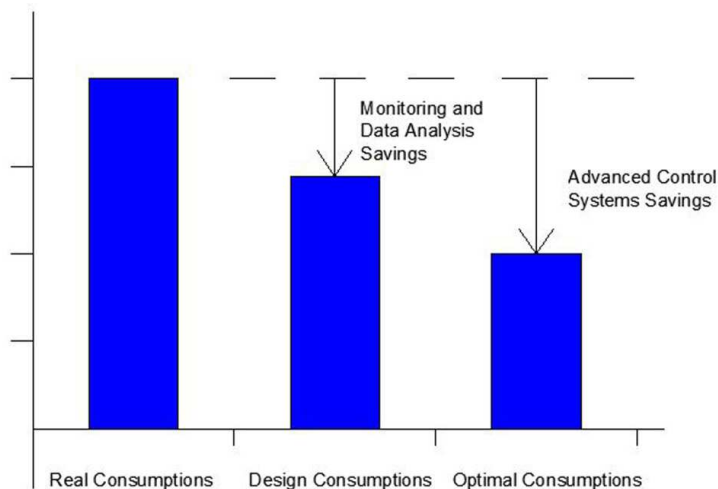


**Figure 7. Potential energy savings related to monitoring and advanced control with respect to practice.**

Data analytics can therefore contribute to TBM from a general standpoint, not merely related to performance optimization, but to the overall improvement of building management over the entire life cycle. Finally, data analytics strategies can be linked effectively moreover to building pathology detection [197], where data acquisition is necessary for diagnostics.

### 3.7. DISCUSSION

The chapter illustrates some of the most relevant topics with respect to BACS for performance optimization. The rapid development of new paradigms and practices in building energy design and operation is facing the problem, particularly relevant for low and nearly Zero Energy Buildings (nZEB), of a gap between predicted (design phase) and measured (operation phase) energy performance. Further, design and operation practices should evolve and consider the uncertainties related to the evolution of climate conditions (i.e. climate change proofing) and end-use (i.e. occupants proofing). A notable potential for energy saving is related to commissioning, performance tracking and advanced control strategies. These elements could benefit from a methodological integration of building performance simulation, control and data analytics (for performance tracking) disciplines and practices, which are not seamlessly integrated at present. A first step towards this methodological integration is connected to the analysis of various types of models used for energy efficiency practices, across the different phases of the building life cycle.

For these reasons, the analysis of the state of the art underlines a need to identify links among the different modeling strategies, from bottom-up, engineering oriented, detailed simulation tools to domain specific model reduction (e.g. control) to top-down, statistical approaches for building performance tracking. The links identified and highlighted should be considered as a starting point for further research aimed at improving the transparency of the performance evaluation across the dif-

ferent phases of the building life cycle, by means of common performance indicators (energy, emissions, cost, comfort, etc.) and data shared across the different phases. It has to be underlined the fact that, beyond tools, a new culture of data for the sustainability of the built environment has to be promoted.

The improved transparency of methods should foster performance benchmarking practices, including techno-economic optimization (cost optimal analysis) to promote a higher market responsiveness to efficient technologies and innovative practices.

Further, with respect to model reliability, the current schemes and standards for the verification and validation of dynamic building simulation models should evolve by including criteria for model calibration, considering uncertainty and sensitivity analysis criteria, which could be used furthermore as probabilistic criteria for design phase simulations. In fact, model calibration problem is already considered in measurement and verification protocols for building commissioning. Finally, all these elements should be supplemented by visualization strategies, as visual control are necessary to show quickly and clearly if the building is operating within standard conditions or outside them. In other words, the evolution of models and visualization techniques can play a key role for the reduction of the performance gap. Of course, BACS can act as an enabling technology to collect data on a continuous base and to enable adaptive and predictive control strategies. Innovative MBC strategies, as shown before, can be linked both with BES and with performance tracking in a more effective way with respect to current practices, by means of innovative applications on BACS.

## LIST OF REFERENCES

- [1] Quaranta GG. La domotica per l'efficienza energetica delle abitazioni, 2013.
- [2] Chwieduk D. Towards sustainable-energy buildings. *Applied Energy*. 2003;76:211-7
- [3] Pierucci A DG. Building Automation e sostenibilità in edilizia, 2013.
- [4] Hagrais H, Callaghan V, Colley M, Clarke G. A hierarchical fuzzy-genetic multi-agent architecture for intelligent buildings online learning, adaptation and control. *Information Sciences*. 2003;150:33-57
- [5] EN 15232:2012, Energy performance of buildings - Impact of Building Automation, Controls and Building Management
- [6] EN 15221:2006-1/6, Facility management
- [7] Nguyen TA, Aiello M. Energy intelligent buildings based on user activity: A survey. *Energy and Buildings*. 2013;56:244-57
- [8] Wang S. Dynamic simulation of building VAV air-conditioning system and evaluation of EMCS on-line control strategies. *Building and Environment*. 1999;34:681-705
- [9] Wang S. *Intelligent Buildings and Building Automation*, 2010
- [10] Dounis AI, Caraiscos C. Advanced control systems engineering for energy and comfort management in a building environment—A review. *Renewable and Sustainable Energy Reviews*. 2009;13:1246-61.
- [11] Dounis A, Caraiscos C. Intelligent technologies for energy efficiency and comfort in a building environment. *International conference of technology and automation*. Thessaloniki, Greece 2005. p. 91-5.
- [12] Hagrais H, Callaghan V, Colley M, Clarke G. A hierarchical fuzzy-genetic multi-agent architecture for intelligent buildings online learning, adaptation and control. *Information Sciences*. 2003;150:33-57
- [13] Ecofys for European Copper Institute, Role of Building Automation related to Renewable Energy in nZEB's. 2014
- [14] Brown DL, Burns JA, Collis S, Grosh J, Jacobson CA, Johansen H, et al. *Applied & Computational Mathematics - Challenges for The Design and Control of Dynamic Energy Systems*. 2011.
- [15] Zavala V, Skow D, Celinski T, Dickinson P. Techno-economic evaluation of a next-generation building energy management system. Technical Report ANL/MCS-TM-313, Argonne National Laboratory; 2011.
- [16] Zaheer-uddin M, Zheng GR. Optimal control of time-scheduled heating, ventilating and air conditioning processes in buildings. *Energy Conversion and Management*. 2000;41:49-60.
- [17] Castilla M, Álvarez JD, Berenguel M, Rodríguez F, Guzmán JL, Pérez M. A comparison of thermal comfort predictive control strategies. *Energy and Buildings*. 2011;43:2737-46.
- [18] Yamada F, Yonezawa K, Sugawara S, Nishimura N. Development of air-conditioning control algorithm for building energy saving. *Control Applications, 1999 Proceedings of the 1999 IEEE International Conference on*. Hawaii, USA 1999. p. 1579-84 vol. 2.
- [19] Marinakis V, Doukas H, Karakosta C, Psarras J. An integrated system for buildings' energy-efficient automation: Application in the tertiary sector. *Applied Energy*. 2013;101:6-14.
- [20] Široký J, Oldewurtel F, Cigler J, Průvara S. Experimental analysis of model predictive control for an energy efficient building heating system. *Applied Energy*. 2011;88:3079-87.
- [21] Kolokotsa D, Kalaitzakis K, Antonidakis E, Stavrakakis GS. Interconnecting smart card system with PLC controller in a local operating network to form a distributed energy management and control system for buildings. *Energy Conversion and Management*. 2002;43:119-34.
- [22] Maasoumy M, Sangiovanni-Vincentelli A. Total and peak energy consumption minimization of building HVAC systems using model predictive control. *IEEE Design & Test of Computers*. 2012;29
- [23] Katz RH, Culler DE, Sanders S, Alspaugh S, Chen Y, Dawson-Haggerty S, et al. An information-centric energy infrastructure: The Berkeley view. *Sustainable Computing: Informatics and Systems*. 2011;1:7-22.
- [24] Building Resistance-Capacitance Modeling (BRCM) Matlab Toolbox (<http://www.brcm.ethz.ch/doku.php>).

- [25] MLE+ Toolbox for energy-efficient building automation design, co-simulation and analysis (<http://mlab.seas.upenn.edu/mlep/>).
- [26] OpenBuild-An integrated simulation environment for building control (<http://sourceforge.net/projects/openbuild/>).
- [27] Lehmann B, Gyalistras D, Gwerder M, Wirth K, Carl S. Intermediate complexity model for Model Predictive Control of Integrated Room Automation. *Energy and Buildings*. 2013;58:250-62.
- [28] Oldewurtel F, Parisio A, Jones CN, Gyalistras D, Gwerder M, Stauch V, et al. Use of model predictive control and weather forecasts for energy efficient building climate control. *Energy and Buildings*. 2012;45:15-27.
- [29] Borean C, Ricci A, Merloni G. Energy@ home: A " user-centric" energy management system. *Metering International*. 2011;3:52.
- [30] Mathews EH, Arndt DC, Piani CB, van Heerden E. Developing cost efficient control strategies to ensure optimal energy use and sufficient indoor comfort. *Applied Energy*. 2000;66:135-59.
- [31] TIAX LLC, Energy Impact of Commercial Building Controls and Performance Diagnostics: Market Characterization, Energy Impact of Building Faults and Energy Savings Potential. 2005
- [32] Newsham GR, Birt BJ. Building-level occupancy data to improve ARIMA-based electricity use forecasts. *Proceedings of the 2nd ACM Workshop on Embedded Sensing Systems for Energy-Efficiency in Building*. Zurich, Switzerland: ACM; 2010. p. 13-8.
- [33] Brandemuehl MJ, Braun JE. The impact of demand-controlled and economizer ventilation strategies on energy use in buildings, 1999.
- [34] Wang S, Xu X. Optimal and robust control of outdoor ventilation airflow rate for improving energy efficiency and IAQ. *Building and Environment*. 2004;39:763-73.
- [35] Wang S, Xu X. A robust control strategy for combining DCV control with economizer control. *Energy Conversion and Management*. 2002;43:2569-88.
- [36] İçođlu O, Mahdavi A. VIOLAS: A vision-based sensing system for sentient building models. *Automation in Construction*. 2007;16:685-712.
- [37] Shen E, Hu J, Patel M. Energy and visual comfort analysis of lighting and daylight control strategies. *Building and Environment*. 2014;78:155-70.
- [38] Labeodan T, Zeiler W, Boxem G, Zhao Y. Occupancy measurement in commercial office buildings for demand-driven control applications—A survey and detection system evaluation. *Energy and Buildings*. 2015;93:303-14.
- [39] Cali D, Matthes P, Huchtemann K, Streblov R, Müller D. CO<sub>2</sub> based occupancy detection algorithm: Experimental analysis and validation for office and residential buildings. *Building and Environment*. 2015;86:39-49
- [40] Lewry A, Ortiz J, Nabil A, Schofield N, Vaid R, Hussain S, et al. Bridging the gap between operational and asset ratings – the UK experience and the green deal tool. 2014.
- [41] Fisk WJ. A pilot study of the accuracy of CO<sub>2</sub> sensors in commercial buildings. Lawrence Berkeley National Laboratory. 2008.
- [42] Anandan R, Karthik B, Kumar TVUK. Wireless Home and Industrial automation system using GSM. *Journal of Global research in Computer Science*. 2013;4:126-32.
- [43] Brooks RA. The Intelligent Room project. *Proceedings of the 2nd International Conference on Cognitive Technology (CT '97)*. Aizu, Japan: IEEE Computer Society; 1997. p. 271.
- [44] Erickson VL, Lin Y, Kamthe A, Brahme R, Surana A, Cerpa AE, et al. Energy efficient building environment control strategies using real-time occupancy measurements. *Proceedings of the First ACM Workshop on Embedded Sensing Systems for Energy-Efficiency in Buildings*. Berkeley, California, USA: ACM; 2009. p. 19-24.
- [45] Agarwal Y, Balaji B, Dutta S, Gupta RK, Weng T. Duty-cycling buildings aggressively: The next frontier in HVAC control. *Information Processing in Sensor Networks (IPSN), 2011 10th International Conference on*. Chicago, IL, USA2011. p. 246-57.
- [46] Cigler J, Prívvara S, Vána Z, Žáčková E, Ferkl L. Optimization of Predicted Mean Vote index within Model Predictive Control framework: Computationally tractable solution. *Energy and Buildings*. 2012;52:39-49.
- [47] Montgomery R, McDowall R. Chapter 4 - Sensors and Auxiliary Devices. In: by Trtfcwow, by RMc, McDowall R, editors. *Fundamentals of HVAC Control Systems*. Oxford: Elsevier; 2008. p. 106-59.

- [48] Nesler CG. Adaptive control of thermal processes in buildings. *Control Systems Magazine, IEEE*. 1986;6:9-13.
- [49] Mahdavi A. Simulation-based control of building systems operation. *Building and Environment*. 2001;36:789-96.
- [50] Kleiminger W, Mattern F, Santini S. Predicting household occupancy for smart heating control: A comparative performance analysis of state-of-the-art approaches. *Energy and Buildings*. 2014;85:493-505.
- [51] Peffer T, Pritoni M, Meier A, Aragon C, Perry D. How people use thermostats in homes: A review. *Building and Environment*. 2011;46:2529-41.
- [52] Peeters L, Van der Veken J, Hens H, Helsen L, D'haeseleer W. Control of heating systems in residential buildings: Current practice. *Energy and Buildings*. 2008;40:1446-55.
- [53] Hazyuk I, Ghiaus C, Penhouet D. Optimal temperature control of intermittently heated buildings using Model Predictive Control: Part II – Control algorithm. *Building and Environment*. 2012;51:388-94.
- [54] Kummert M, André P, Nicolas J. Optimal heating control in a passive solar commercial building. *Solar Energy*. 2001;69, Supplement 6:103-16.
- [55] Chinnakani K, Krishnamurthy A, Moyne J, Fangming G. Comparison of energy consumption in HVAC systems using simple ON-OFF, intelligent ON-OFF and optimal controllers. *Power and Energy Society General Meeting, 2011 IEEE*. San Diego, CA, USA2011. p. 1-6.
- [56] Prívvara S, Šíroký J, Ferkl L, Cigler J. Model predictive control of a building heating system: The first experience. *Energy and Buildings*. 2011;43:564-72.
- [57] Mozer M. The neural network house: An environment that adapts to its inhabitants. *Proc AAAI Spring Symp Intelligent Environments*. Madison, WI, USA1998. p. 110-4.
- [58] Béguery P, Kissavos A, Sahlin P, AB ES. A building control oriented simulation architecture. *13<sup>th</sup> Conf Intl Building Perf Simulation Ass*. Chambéry, France, 2013.
- [59] Wang S, Jin X. Model-based optimal control of VAV air-conditioning system using genetic algorithm. *Building and Environment*. 2000;35:471-87.
- [60] Hazyuk I, Ghiaus C, Penhouet D. Optimal temperature control of intermittently heated buildings using Model Predictive Control: Part I – Building modeling. *Building and Environment*. 2012;51:379-87.
- [61] Ardehali MM, Saboori M, Teshnelab M. Numerical simulation and analysis of fuzzy PID and PSD control methodologies as dynamic energy efficiency measures. *Energy Conversion and Management*. 2004;45:1981-92.
- [62] Bao-Gang H, Mann GKI, Gosine RG. A systematic study of fuzzy PID controllers-function-based evaluation approach. *Fuzzy Systems, IEEE Transactions on*. 2001;9:699-712.
- [63] Anderson CW, Hittle DC, Katz AD, Kretchmar RM. Synthesis of reinforcement learning, neural networks and PI control applied to a simulated heating coil. *Artificial Intelligence in Engineering*. 1997;11:421-9.
- [64] Calvino F, La Gennusa M, Rizzo G, Scaccianoce G. The control of indoor thermal comfort conditions: introducing a fuzzy adaptive controller. *Energy and Buildings*. 2004;36:97-102.
- [65] International Energy Agency (IEA - EBC), Annex 60: New Generation Computational Tools for Building & Community Energy Systems.
- [66] Henze GP. Model predictive control for buildings: a quantum leap? *Journal of Building Performance Simulation*. 2013;6:157-8.
- [67] Oldewurtel F, Parisio A, Jones CN, Morari M, Gyalistras D, Gwerder M, et al. Energy efficient building climate control using Stochastic Model Predictive Control and weather predictions. *American Control Conference (ACC)*, 2010. Baltimore, MD, USA2010. p. 5100-5.
- [68] Prívvara S, Cigler J, Váňa Z, Oldewurtel F, Sagerschnig C, Žáčková E. Building modeling as a crucial part for building predictive control. *Energy and Buildings*. 2013;56:8-22.
- [69] Kummert M, André P. Simulation of a model-based optimal controller for heating systems under realistic hypothesis. *9<sup>th</sup> International IBPSA Conference*. Montréal, Canada2005.
- [70] Karlsson JF, Moshfegh B. Energy demand and indoor climate in a low energy building—changed control strategies and boundary conditions. *Energy and Buildings*. 2006;38:315-26.
- [71] Fouquier A, Brun A, Faggianelli GA, Suard F. Effect of wall merging on a simplified building energy model: accuracy vs number equations. *13<sup>th</sup> Conf Intl Building Perf Simulation Ass*. Chambéry, France2013.

- [72] Coffey B, Haghghat F, Morofsky E, Kutrowski E. A software framework for model predictive control with GenOpt. *Energy and Buildings*. 2010;42:1084-92.
- [73] May-Ostendorp P, Henze GP, Corbin CD, Rajagopalan B, Felsmann C. Model-predictive control of mixed-mode buildings with rule extraction. *Building and Environment*. 2011;46:428-37.
- [74] Corbin CD, Henze GP, May-Ostendorp P. A model predictive control optimization environment for real-time commercial building application. *Journal of Building Performance Simulation*. 2012;6:159-74.
- [75] European Commission, Programme IEE (Intelligent Energy Europe), Building EQ - The EPBD and Continuous Commissioning - Tools and methods for linking EPDB and continuous commissioning. 2007.
- [76] Zavala VM. Real-Time Optimization Strategies for Building Systems. *Industrial & Engineering Chemistry Research*. 2012;52:3137-50.
- [77] Giretti A, Lemma M, Larghetti R, Ansuini R. Environmental modeling for the optimal energy control of subway stations. *Gerontechnology*. 2012;11:168.
- [78] Kanarachos A, Geramanis K. Multivariable control of single zone hydronic heating systems with neural networks. *Energy Conversion and Management*. 1998;39:1317-36.
- [79] Nicol JF, Humphreys MA. Adaptive thermal comfort and sustainable thermal standards for buildings. *Energy and Buildings*. 2002;34:563-72.
- [80] Dalamagkidis K, Kolokotsa D, Kalaitzakis K, Stavrakakis GS. Reinforcement learning for energy conservation and comfort in buildings. *Building and Environment*. 2007;42:2686-98.
- [81] Morel N, Bauer M, El-Khoury M, Krauss J. Neurobat, a Predictive and Adaptive Heating Control System Using Artificial Neural Networks. *Solar Energy Journal*. 2001;21:161-201.
- [82] Beccali M, Cellura M, Lo Brano V, Marvuglia A. Forecasting daily urban electric load profiles using artificial neural networks. *Energy Conversion and Management*. 2004;45:2879-900.
- [83] Boithias F, El Mankibi M, Michel P. Genetic algorithms based optimization of artificial neural network architecture for buildings' indoor discomfort and energy consumption prediction. *Build Simul*. 2012;5:95-106.
- [84] Yan Y, Zhou J, Lin Y, Yang W, Wang P, Zhang G. Adaptive optimal control model for building cooling and heating sources. *Energy and Buildings*. 2008;40:1394-401.
- [85] Alcalá R, Benítez JM, Casillas J, Cerdón O, Pérez R. Fuzzy control of HVAC systems optimized by genetic algorithms. *Applied Intelligence*. 2003;18:155-77.
- [86] Lute P, van Paassen D. Optimal indoor temperature control using a predictor. *Control Systems, IEEE*. 1995;15:4-10.
- [87] Gwerder M, Tödli J. Predictive control for integrated room automation. 8<sup>th</sup> REHVA World Congress Clima. Lausanne, Switzerland, 2005.
- [88] Borbely AM, Kreider JF. *Distributed Generation: The Power Paradigm for the New Millennium*: Taylor & Francis; 2001.
- [89] Cho SH, Zaheer-uddin M. Predictive control of intermittently operated radiant floor heating systems. *Energy Conversion and Management*. 2003;44:1333-42.
- [90] Mahdavi A, Pröglhöf C. A model-based approach to natural ventilation. *Building and Environment*. 2008;43:620-7.
- [91] Candanedo JA, Dehkordi VR, Lopez P. A control-oriented simplified building modelling strategy. 13<sup>th</sup> Conf Intl Building Perf Simulation Ass. Chambéry, France, 2013.
- [92] Cigler J, Privara S. Subspace identification and model predictive control for buildings. *Control Automation Robotics & Vision (ICARCV)*, 2010 11th International Conference on. Singapore, 2010. p. 750-5.
- [93] Zacekova E, Privara S. Control relevant identification and predictive control of a building. *Control and Decision Conference (CCDC)*, 2012 24th Chinese. Taiyuan, China, 2012. p. 246-51.
- [94] Zavala V, Thomas C, Zimmerman M, Ott A. Next-generation building energy management systems and implications for electricity markets. *Argonne National Laboratory (ANL)*; 2011.
- [95] Ansuini R, Vaccarini M, Giretti A, Ruffini S. Model for the real-time control of subway stations. 13<sup>th</sup> Conference of International Building Performance Simulation Association. Chambéry, France 2013.
- [96] Lee JH, Morari M, Garcia CE. State-space interpretation of model predictive control. *Automatica*. 1994;30:707-17.

- [97] Morari M, H. Lee J. Model predictive control: past, present and future. *Computers & Chemical Engineering*. 1999;23:667-82.
- [98] Li P, Li D, Vrabie D, Bengea S, Mijanovic S. Experimental Demonstration of Model Predictive Control in a Medium-Sized Commercial Building. 2014.
- [99] Freire RZ, Oliveira GH, Mendes N. Development of single-zone predictive equations using linear regression for advanced controllers synthesis. Proc of the Nineth Building Simulation Conference (IBPSA'05). Montréal, Canada, 2005.
- [100] Yudong M, Borrelli F, Hancey B, Packard A, Bortoff S. Model Predictive Control of thermal energy storage in building cooling systems. Decision and Control, 2009 held jointly with the 2009 28<sup>th</sup> Chinese Control Conference CDC/CCC 2009 Proceedings of the 48<sup>th</sup> IEEE Conference on. Shanghai, P.R. China, 2009. p. 392-7.
- [101] Ghiaus C, Hazyuk I. Calculation of optimal thermal load of intermittently heated buildings. *Energy and Buildings*. 2010;42:1248-58.
- [102] Freire RZ, Oliveira GHC, Mendes N. Predictive controllers for thermal comfort optimization and energy savings. *Energy and Buildings*. 2008;40:1353-65.
- [103] Ferkl L, J. S, Privara S. Model predictive control of buildings: The efficient way of heating. Control Applications (CCA), 2010 IEEE International Conference on. Yokohama, Japan, 2010. p. 1922-6.
- [104] Yudong M, Borrelli F, Hancey B, Coffey B, Bengea S, Haves P. Model Predictive Control for the Operation of Building Cooling Systems. *Control Systems Technology, IEEE Transactions*. 2012;20:796-803.
- [105] Froisy JB. Model predictive control—Building a bridge between theory and practice. *Computers & Chemical Engineering*. 2006;30:1426-35.
- [106] Nguyen A-T, Reiter S, Rigo P. A review on simulation-based optimization methods applied to building performance analysis. *Applied Energy*. 2014;113:1043-58.
- [107] Huang B, Malhotra A, C. Tamayo E. Model predictive control relevant identification and validation. *Chemical Engineering Science*. 2003;58:2389-401.
- [108] Privara S, Vana Z, Cigler J, Ferkl L. Predictive control oriented subspace identification based on building energy simulation tools. Control & Automation (MED), 2012 20th Mediterranean Conference on. Barcelona, Spain, 2012. p. 1290-5.
- [109] Madsen H, Holst J. Estimation of continuous-time models for the heat dynamics of a building. *Energy and Buildings*. 1995;22:67-79.
- [110] Zavala VM, Constantinescu EM, Anitescu M. Economic impacts of advanced weather forecasting on energy system operations. Innovative Smart Grid Technologies (ISGT), 2010. Gaithersburg, MD, USA2010. p. 1-7.
- [111] Zavala VM, Constantinescu EM, Krause T, Anitescu M. Weather forecast-based optimization of integrated energy systems. Technical report, Argonne National Laboratory; 2009.
- [112] Grünenfelder W, Tödli J. The use of weather predictions and dynamic programming in the control of solar domestic hot water systems. 3<sup>rd</sup> Mediterranean Electrotechnical Conference (Melecon). Madrid, Spain, 1985.
- [113] Zhou Q, Wang S, Xu X, Xiao F. A grey-box model of next-day building thermal load production for energy-efficient control. *International Journal of Energy Research*. 2008;32:1418-31.
- [114] Bynum JD, Claridge DE, Curtin JM. Development and testing of an Automated Building Commissioning Analysis Tool (ABCAT). *Energy and Buildings*. 2012;55:607-17.
- [115] Lin G, Claridge DE. A temperature-based approach to detect abnormal building energy consumption. *Energy and Buildings*. 2015;93:110-8.
- [116] Sturzenegger D, Gyalistras D, Gwerder M, Sagerschnig C, Morari M, Smith R. Model Predictive Control of a Swiss Office Building. Clima 2013 - 11<sup>th</sup> RHEVA World Congress. Prague, Czech Republic, 2013.
- [117] Karlsson H, Hagetoft C-E. Application of model based predictive control for water-based floor heating in low energy residential buildings. *Building and Environment*. 2011;46:556-69.
- [118] ETH Zurich, Use of weather and occupancy forecasts for optimal building climate control (OptiControl): Two years progress report. 2009.

- [119] Gao T, Schumacher B, Hegetschweiler W, Gwerder M, Tschanz M, Walti M. Multizone building with VAV Air-Conditioning System simulation for evaluation and test of control systems. Bi-annual IBPSA Building Simulation Conference. Beijing, China, 2007.
- [120] de Wilde P. The gap between predicted and measured energy performance of buildings: A framework for investigation. *Automation in Construction*. 2014;41:40-9.
- [121] International Energy Agency (IEA - EBC), Annex 58: Reliable Building Energy Performance Characterization based on full scale dynamic measurement.
- [122] Performer Blog, Intrinsic & in-use Building Energy Simulation, July 2 2014 <http://performer-project.eu/intrinsic-use-building-energy-simulation/>.
- [123] Markovic D, Cvetkovic D, Masic B. Survey of software tools for energy efficiency in a community. *Renewable and Sustainable Energy Reviews*. 2011;15:4897-903.
- [124] Trčka M, Hensen JLM, Wetter M. Co-simulation for performance prediction of integrated building and HVAC systems – An analysis of solution characteristics using a two-body system. *Simulation Modelling Practice and Theory*. 2010;18:957-70.
- [125] Afram A, Janabi-Sharifi F. Gray-box modeling and validation of residential HVAC system for control system design. *Applied Energy*. 2015;137:134-50.
- [126] Jiménez MJ, Madsen H. Models for describing the thermal characteristics of building components. *Building and Environment*. 2008;43:152-62.
- [127] Scacchi W. Experience with software process simulation and modeling. *Journal of Systems and Software*. 1999;46:183-92.
- [128] Bacher P, Madsen H. Identifying suitable models for the heat dynamics of buildings. *Energy and Buildings*. 2011;43:1511-22.
- [129] Reddy TA. *Applied Data Analysis and Modeling for Energy Engineers and Scientists*: Springer US; 2011.
- [130] EN 16212:2012, Energy Efficiency and Savings Calculation, Top-down and Bottom-up Methods.
- [131] Andersen KK, Madsen H, Hansen LH. Modelling the heat dynamics of a building using stochastic differential equations. *Energy and Buildings*. 2000;31:13-24.
- [132] Bernal W, Behl M, Nghiem TX, Mangharam R. MLE+: A Tool for Integrated Design and Deployment of Energy Efficient Building Controls 4<sup>th</sup> ACM Workshop On Embedded Sensing Systems For Energy-Efficiency In Buildings, BuildSys 2012.
- [133] Kramer R, van Schijndel J, Schellen H. Inverse modeling of simplified hygrothermal building models to predict and characterize indoor climates. *Building and Environment*. 2013;68:87-99.
- [134] Calleja Rodríguez G, Carrillo Andrés A, Domínguez Muñoz F, Cejudo López JM, Zhang Y. Uncertainties and sensitivity analysis in building energy simulation using macroparameters. *Energy and Buildings*. 2013;67:79-87.
- [135] Wen J, Smith TF. Development and validation of online models with parameter estimation for a building zone with VAV system. *Energy and Buildings*. 2007;39:13-22.
- [136] Mendes N, Oliveira R. Energy efficiency and thermal comfort analysis using the powerdomus hygrothermal simulation tool. 9<sup>th</sup> International IBPSA Conference. Montréal, Canada 2005.
- [137] Braun JE. Reducing energy costs and peak electrical demand through optimal control of building thermal storage 1990.
- [138] Kramer R, van Schijndel J, Schellen H. Simplified thermal and hygric building models: A literature review. *Frontiers of Architectural Research*. 2012;1:318-25.
- [139] Raftery P, Keane M, O'Donnell J. Calibrating whole building energy models: An evidence-based methodology. *Energy and Buildings*. 2011;43:2356-64.
- [140] Manfren M, Aste N, Moshksar R. Calibration and uncertainty analysis for computer models – A meta-model based approach for integrated building energy simulation. *Applied Energy*. 2013;103:627-41.
- [141] Coakley D, Raftery P, Keane M. A review of methods to match building energy simulation models to measured data. *Renewable and Sustainable Energy Reviews*. 2014;37:123-41.
- [142] Clarke JA, Cockroft J, Conner S, Hand JW, Kelly NJ, Moore R, et al. Simulation-assisted control in building energy management systems. *Energy and Buildings*. 2002;34:933-40.

- [143] Oldewurtel F, Jones CN, Morari M. A tractable approximation of chance constrained stochastic MPC based on affine disturbance feedback. *Decision and Control, 2008 CDC 2008 47<sup>th</sup> IEEE Conference on. Cancun2008.* p. 4731-6.
- [144] de Wilde P, Martinez-Ortiz C, Pearson D, Beynon I, Beck M, Barlow N. Building simulation approaches for the training of automated data analysis tools in building energy management. *Advanced Engineering Informatics.* 2013;27:457-65.
- [145] Crawley DB, Hand JW, Kummert M, Griffith BT. Contrasting the capabilities of building energy performance simulation programs. *Building and Environment.* 2008;43:661-73.
- [146] De Coninck R. Grey-Box Based Optimal Control for Thermal Systems in Buildings - Unlocking Energy Efficiency and Flexibility, PhD Thesis, KU Leuven. 2015.
- [147] De Coninck R, Magnusson F, Åkesson J, Helsen L. Toolbox for development and validation of grey-box building models for forecasting and control. *Journal of Building Performance Simulation.* 2015:1-16.
- [148] Berthou T. Developpement de modeles de batiment pour la prevision de charge de climatisation et l'elaboration de strategies d'optimisation energetique et d'efficacement, PhD Thesis, Mines Tech Paris. 2014.
- [149] Lara B, Patron O, Cigler J, Oldewurtel F, Barroto M. Model Predictive Control for a Tropical Island Hotel. *Clima 2013 - 11<sup>th</sup> RHEVA World Congress.* Prague, Czech Republic, 2013.
- [150] Boyd SP, Vandenberghe L. *Convex Optimization:* Cambridge University Press; 2004.
- [151] Vanderbei RJ. *Linear Programming: Foundations and Extensions:* Springer; 2013.
- [152] Control of Constrained Hybrid Systems (<http://control.ee.ethz.ch/~cohysys/modeling.php>).
- [153] Touretzky CR, Baldea M. Integrating scheduling and control for economic MPC of buildings with energy storage. *Journal of Process Control.* 2014;24:1292-300.
- [154] Touretzky CR, Baldea M. Nonlinear model reduction and model predictive control of residential buildings with energy recovery. *Journal of Process Control.* 2014;24:723-39.
- [155] Jaffal I, Inard C, Ghiaus C. Fast method to predict building heating demand based on the design of experiments. *Energy and Buildings.* 2009;41:669-77.
- [156] Ghiaus C. Experimental estimation of building energy performance by robust regression. *Energy and Buildings.* 2006;38:582-7.
- [157] Ferkl L, Jan Š. Ceiling radiant cooling: Comparison of ARMAX and subspace identification modelling methods. *Building and Environment.* 2010;45:205-12.
- [158] Olanrewaju OA, Jimoh AA. Review of energy models to the development of an efficient industrial energy model. *Renewable and Sustainable Energy Reviews.* 2014;30:661-71.
- [159] Lee W-S, Lee K-P. Benchmarking the performance of building energy management using data envelopment analysis. *Applied Thermal Engineering.* 2009;29:3269-73.
- [160] Lee W-S. Benchmarking the energy efficiency of government buildings with data envelopment analysis. *Energy and Buildings.* 2008;40:891-5.
- [161] Witten IH, Frank E, Hall MA. *Data Mining: Practical Machine Learning Tools and Techniques: Practical Machine Learning Tools and Techniques:* Elsevier Science; 2011.
- [162] Ang BW, Zhang FQ. A survey of index decomposition analysis in energy and environmental studies. *Energy.* 2000;25:1149-76.
- [163] Asakawa K, Takagi H. Neural networks in Japan. *Commun ACM.* 1994;37:106-12.
- [164] Teeter J, Mo-Yuen C. Application of functional link neural network to HVAC thermal dynamic system identification. *Industrial Electronics, IEEE Transactions on.* 1998;45:170-6.
- [165] Jian L, Ruxu D. Thermal comfort control based on neural network for HVAC application. *Control Applications, 2005 CCA 2005 Proceedings of 2005 IEEE Conference on2005.* p. 819-24.
- [166] Rasmussen CE, Williams CKI. *Gaussian Processes for Machine Learning (Adaptive Computation and Machine Learning):* The MIT Press; 2005.
- [167] Heo Y, Graziano D, Zavala VM, Dickinson P, Kamrath M, Kirshenbaum M. Cost-effective Measurement and Verification Method for Determining Energy Savings under Uncertainty. *ASHRAE Annual Conference.* Denver, CO, USA, 2013.

- [168] Aerts D, Minnen J, Glorieux I, Wouters I, Descamps F. A method for the identification and modelling of realistic domestic occupancy sequences for building energy demand simulations and peer comparison. *Building and Environment*. 2014;75:67-78.
- [169] Choudhary R, Initiative EEC. A Probabilistic Model for Assessing Energy Consumption of the Non-Domestic Building Stock. *proc of: Building Simulation*. Sydney, Australia 2011.
- [170] Wille-Hausmann B, Erge T, Wittwer C. Decentralised optimisation of cogeneration in virtual power plants. *Solar Energy*. 2010;84:604-11.
- [171] Manfren M. Multi-commodity network flow models for dynamic energy management – Mathematical formulation. *Energy Procedia*. 2012;14:1380-5.
- [172] Ghiaus C. Equivalence between the load curve and the free-running temperature in energy estimating methods. *Energy and Buildings*. 2006;38:429-35.
- [173] Tian W, Song J, Li Z, de Wilde P. Bootstrap techniques for sensitivity analysis and model selection in building thermal performance analysis. *Applied Energy*. 2014;135:320-8.
- [174] Castillo L, Enríquez R, Jiménez MJ, Heras MR. Dynamic integrated method based on regression and averages, applied to estimate the thermal parameters of a room in an occupied office building in Madrid. *Energy and Buildings*. 2014;81:337-62.
- [175] Nkwetta DN, Vouillamoz P-E, Haghghat F, El-Mankibi M, Moreau A, Daoud A. Impact of phase change materials types and positioning on hot water tank thermal performance: Using measured water demand profile. *Applied Thermal Engineering*. 2014;67:460-8.
- [176] Steen D, Stadler M, Cardoso G, Groissböck M, DeForest N, Marnay C. Modeling of thermal storage systems in MILP distributed energy resource models. *Applied Energy*. 2015;137:782-92.
- [177] Adhikari RS, Aste N, Manfren M. Multi-commodity network flow models for dynamic energy management – Smart Grid applications. *Energy Procedia*. 2012;14:1374-9.
- [178] Adhikari RS, Aste N, Manfren M. Optimization concepts in district energy design and management – A case study. *Energy Procedia*. 2012;14:1386-91.
- [179] Kraning M, Chu E, Lavaei J, Boyd S. Dynamic Network Energy Management via Proximal Message Passing. *Found Trends Optim*. 2014;1:73-126.
- [180] Aste N, Leonforte F, Manfren M, Mazzon M. Thermal inertia and energy efficiency – Parametric simulation assessment on a calibrated case study. *Applied Energy*. 2015;145:111-23.
- [181] Henze GP, Felsmann C, Knabe G. Evaluation of optimal control for active and passive building thermal storage. *International Journal of Thermal Sciences*. 2004;43:173-83.
- [182] Adhikari RS, Aste N, Manfren M. Multi-commodity network flow models for dynamic energy management – Smart Grid applications. *Energy Procedia*. 2012;14:1374-9.
- [183] Mařík K, Schindler Z, Stluka P. Decision support tools for advanced energy management. *Energy*. 2008;33:858-73.
- [184] Magnier L, Haghghat F. Multiobjective optimization of building design using TRNSYS simulations, genetic algorithm, and Artificial Neural Network. *Building and Environment*. 2010;45:739-46.
- [185] CESBA - Common European Sustainable Building Assessment ([http://wiki.cesba.eu/wiki/Main\\_Page](http://wiki.cesba.eu/wiki/Main_Page)).
- [186] Mayne DQ, Seron MM, Raković SV. Robust model predictive control of constrained linear systems with bounded disturbances. *Automatica*. 2005;41:219-24.
- [187] ISO 7730:2008, Ergonomics of the thermal environment - Analytical determination and interpretation of thermal comfort using calculation of the PMV and PPD indices and local thermal comfort criteria.
- [188] The Building Performance Tracking Handbook - Continuous improvement for every building. California Energy Commission. 2011.
- [189] Energy information handbook - Applications for Energy Efficient Building Operations. Lawrence Berkeley National Laboratory. 2011.
- [190] ABITCOOP, Società cooperativa edilizia di abitazioni, Modena, [www.abitcoop.it](http://www.abitcoop.it).
- [191] Energy Efficiency Directive, 2012/27/EU.

- [192] Maile T, Bazjanac V, Fischer M. A method to compare simulated and measured data to assess building energy performance. *Building and Environment*. 2012;56:241-51.
- [193] Active demand: the future of electricity, The Address - 1<sup>st</sup> International Workshop, Clamart, Paris, France, June 9, 2010.
- [194] International Energy Agency (IEA - EBC), Annex 66: Definition and Simulation of Occupant Behavior in Buildings.
- [195] Yu Z, Fung BCM, Haghghat F, Yoshino H, Morofsky E. A systematic procedure to study the influence of occupant behavior on building energy consumption. *Energy and Buildings*. 2011;43:1409-17.
- [196] Lawrence Berkeley National Laboratory, A Meta-Analysis of Energy Savings from Lighting Controls in Commercial Buildings, 2011.
- [197] Watt D. *Building Pathology: Principles and Practice*: Wiley; 2009.

## 4. REDUCED ORDER BUILDING ENERGY MODELS

In the previous chapters has been shown that dynamic models generally used to simulate the building behavior (physics-based models), in control systems present several limitation [1-6] in terms of computational tractability and efficiency.

The basic conditions that a model for control and diagnostics should satisfy, in fact, are reasonable simplicity, enough accuracy in the estimation of system dynamics, usability for prediction in real time operation [7-11].

On the one hand, physics-based models, generally, need detailed information and result in non-linear problem while the linearity (more in general convexity) is important to obtain easily solvable optimization problems [2,12-14].

On the other hand, black box models, thus, have been widely used in optimal control applications because they can deal with the problem of non-linearity [15]. However, these kind of models are obtained by means of statistical/machine learning algorithms and, consequently, the identified parameters don't have a physical interpretation, losing part of the useful information that can be extracted by measured data [1,6,16-19] and which is necessary in an integrated modeling process.

In order to overcome these issues, hybrid models, mixing knowledge-based (physics-based) and statistical approaches, are introduced (generally called grey-box models) [6,17,18,20-24]. In hybrid models, the building energy dynamics is generally described by the reduced the size of the model using lumped parameters [1,9,25-31]. The structure of the model (i.e. the reduction strategy) is found by applying basic physical principles and the parameters are estimated by using identification techniques [1,6,10,29,31-33]. In this way, it is possible to envision a path to bridge the research in:

1. automatic control (Model Predictive Control)
2. diagnostics (Fault Detection and Diagnosis, Performance Monitoring)
3. energy efficiency (Optimized Energy Management)
4. construction (innovation in design practices by reducing the performance gap).

The feasibility of an integrated approach is confirmed by different international studies on model predictive control [34] and on building performance characterization based on full-scale dynamic measurement [35].

In all these research initiatives, building energy models have been formulated using reduced-order modeling strategies, suitable for real-time operation and for inverse modeling. These models obtained an accuracy comparable to more detailed models, which, however, would be unusable for control purposes and diagnostics, as described before. In order to be able to create an integrated workflow of analysis, all the models used are cast as optimization problems. In order to describe all the relevant elements in modeling, the chapter concentrate on the following aspects:

1. fundamental definitions in modeling;
2. building energy dynamics;
3. optimization models formulation;
4. dynamic models validation;
5. analysis of operation data (inverse modeling);
6. model predictive control;
7. visualization of model output data.

The ability to predict energy demand as well as the comfort conditions in buildings, allows not only to distribute the load during the most convenient moments of the day (pre-heating and/or pre-cooling strategies), but also to manage the energy produced by renewable sources or the storage capacity (active or passive). Further, diagnostic capabilities can actively contribute to the reduction of the performance gap, by clearly identifying the most relevant performance issues. As a conclusion, the possibility of using different types models, structured in a coherent way, across the building life cycle is a necessary step to be able to optimize performance at all stages, considering energy, economy and environment related criteria.

#### **4.1. FUNDAMENTAL DEFINITIONS IN MODELING**

Before entering into the detail description of the models it can be useful to give some definitions and clarifications about model types and properties. The most relevant elements considered are:

1. linear and non-linear models;
2. time variant and time invariant models;
3. discrete and continuous time models;
4. direct and inverse models.

All these elements contribute to the possibility of defining a unified modeling workflow, suitable for multiple tasks, as introduced before.

##### **4.1.1. LINEAR AND NON-LINEAR MODELS**

As already underlined, nonlinearity is a common issue when examining cause-effect relations and it can be defined as a relationship that cannot be explained as a linear combination of its variable inputs. Simple linear model, for example, relates two variables “x” and “y” with a straight line:

$$y = mx + b$$

while nonlinear regression must generate a line (typically a curve) as if every value of “y” was a random variable. Nonlinear models are more complicated than linear models to develop because the function is created through a series of approximations (iterations) that may stem from trial-and-error. It is easily understandable that, all complex models that intend to describe the building dynamics are not linear, but may be simplified and/or treated so as to make linear the relationship between the variables analyzed.

Linear relationship is a statistical term used to describe the relationship between a variable and a constant. Linear relationships can be expressed in a graphical format where the variable and the constant are connected via a straight line or in a mathematical format where the independent variable is multiplied by the slope coefficient, added by a constant, which determines the dependent variable.

In conclusion a problem can be described both in a non linear or linear way, depending on the approximation and the final objectives.

#### **4.1.2. TIME VARIANT AND TIME INVARIANT MODELS**

A time invariant system (TIV) is a system whose output does not depend on time, and on the contrary, a time varying system output has an explicit correlation upon time. In other words, the time invariance of a system is demonstrated by the fact that the output given by an input applied in different moments will be identical except for a time delay.

The combination between the time dependency and the linearity of a model can identify the complexity of the problem, especially for optimization problem. A linear time invariant (LTI) system can be defined as the easier to be solved and analyzed and, in fact, is a very well known field, also called LTI system theory, which has direct applications in control theory.

#### **4.1.3. DISCRETE AND CONTINUOUS TIME MODELS**

Finally, a system can be described and/or analyzed in discrete or continuous time; the first refers to a determinate sample of time between two discrete variables, while, in the second one there are an infinite number of points between two variables.

Discrete time is often used, for example, in case of indirect model using empirical measurements that can be seen as separated points in time. Non linear models, instead, are generally described in continuous time; a complex description of physical phenomena, in fact, generally uses a continuous function time dependent.

Depending on all these considerations, different kind of equations are used in order to solve different models. The main two types of equations used are just related to a discrete or continuous time context; the difference equation are used in the first case while differential equations for the second one.

The process to transform a continuous function (or model) in a discrete one is called discretization and it permits to obtain a discrete difference equation from a continuous differential one and, thus, to have a set of equations suitable for a numerical computing. Further, a difference equation can be written in three forms: forward, backward and central differences and, each form can be solved with a different method. In this research the third form is used, solved with the Crank-Nicolson method.

#### **4.1.4. DIRECT AND INVERSE MODELS**

Mathematical models are frequently used in both technical and non-technical areas; in this research inverse models are used in order to analyze real measurements to obtain building thermal characteristics. The aim of inverse problem, in fact, is to reconstruct the model from a set of measurements [36]. As defined by Bertero and Boccaccio in [37], "*one can say that a direct problem is a problem oriented along a cause-effect sequence [...] then the corresponding inverse problem is associated with the reversal of the*

*cause-effect sequence and consist of finding the unknown causes of known consequences*". Normally, direct problems are considered more fundamental and, for that reason, are also much more investigated [38]. Nowadays, however, the large amount of available tools for the acquisition and storage of data, allows to exploit the indirect systems. This is useful also because the greater the complexity of the systems that we want to analyze (in this case the building-plant system, but also district), the larger the uncertainty that characterizes them; the only formulation of direct problems then becomes ineffective and creates the performance gap. In such a situation, therefore, the inverse models have a great potential; in the next figure, in fact, it is shown that a direct formulation start with a (physical) model in which are introduced the "inputs" providing "outputs", on the contrary, the inverse model start with the "output" to provide information about the model. For this reason, inverse models are also defined as parameter identification techniques; thanks to the correlation between data, in fact, it is possible to find parameters that characterize the model.

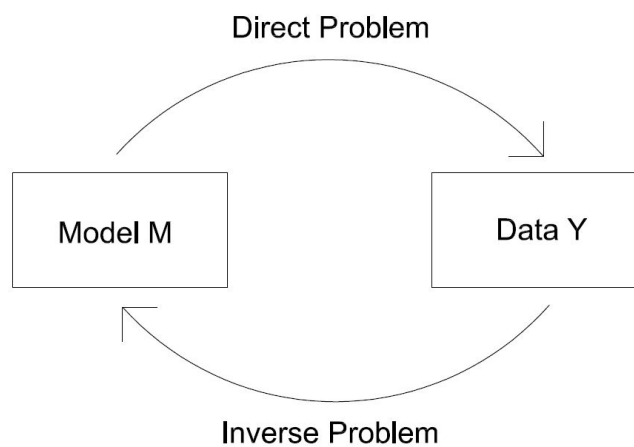


**Figure 8. Direct and Indirect Logic.**

The next scheme shows, on the left, the flow of direct formulation, which starts from the inputs  $x$ , inserted in a model  $M$ , adding an error  $u$  (generally due to model simplification or measurement errors) you can get the output  $y$ . Proceeding to the formulation of the "inverse process" (scheme on the right), it is now easy to see that the new input data  $y$  is corrupted by hardly classifiable errors  $u$  before to enter on the inverse model  $M^{-1}$ .

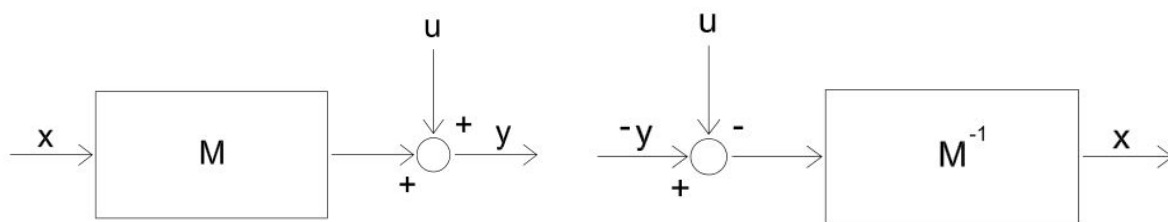


**Figure 9. Direct and Indirect Schemes.**

Further, an inverse model can easily generates more than one output  $x$ ; for example the direct problem "2+2" has just one solution (4), but if you have just the number "4" and you want to find two numbers which the sum gives you "4" as a result, you can have infinite solutions. In other cases is possible to have no solutions, for example when you have a data corrupted by errors. In some case, in fact, different accuracies due to instruments of measurements can pose a "unreal" problem, as:

$$\begin{cases} x + y = 2 \\ 2x + 2y = 4.01 \end{cases}$$

In conclusion, by its nature, two important characteristics of inverse problems are that (i) often they have many solutions and (ii) are always affected by errors due to uncertainties of measurements and model simplifications [36]. Thus, inverse models can be very helpful but the use of correct estimation methods and uncertainty analysis is fundamental.

## 4.2. BUILDING ENERGY DYNAMICS

The building energy dynamics is formulated following the indications given in the standards UNI EN ISO 13790 [39], UNI EN ISO 13791 [40], UNI EN ISO 13792 [41], UNI EN 15255 [42] and ISO 52000 [43]. The model is a lumped parameters model for dynamic hourly simulation and optimization.

The lumped parameter modeling is based on the *Resistance-Capacitance approach* (RC), exploiting the electrical analogy. The essential elements of the model are nodes (i.e. temperatures), resistors (i.e. thermal resistances) and capacitors (i.e. thermal capacities). A graphical representation of the model is reported hereafter.

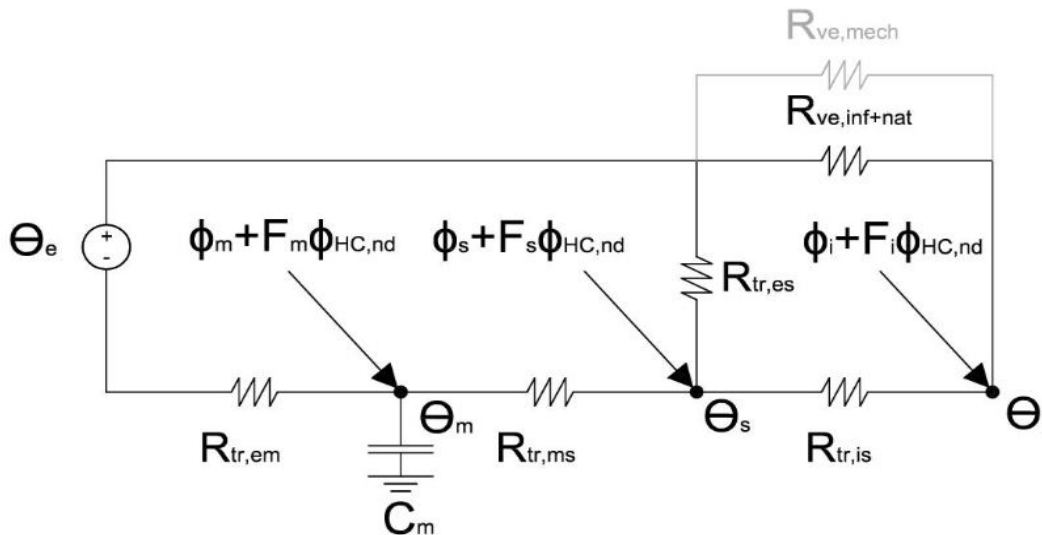


Figure 10. RC network (6R1C).

where:

- the nodes are:
  - the external air temperature  $\theta_e$ ;
  - the internal air temperature  $\theta_i$ ;
  - the surface temperature  $\theta_s$ ;
  - the mass temperature  $\theta_m$ .

- the resistances are:
  - the mechanical ventilation  $R_{ve,mech}$ ;
  - the natural ventilation and infiltration  $R_{ve,nat}$ ;
  - the transmission due to no inertia elements  $R_{tr,es}$ ;
  - the transmission due to massive elements  $R_{tr,em}$  and  $R_{tr,ms}$ ;
  - the transmission due to heat exchange between internal air and the internal surface  $R_{tr,is}$ .
- the capacity is:
  - the global thermal capacity  $C_m$
- the heat fluxes are:
  - the solar and internal gains fraction on the internal air node  $\Phi_i$
  - the solar and internal gains fraction on the surface node  $\Phi_s$
  - the solar and internal gains fraction on the mass node  $\Phi_m$
  - the heat flow fraction due to heating/cooling system on the internal air node  $F_i\Phi_{HC,nd}$
  - the heat flow fraction due to heating/cooling system on the surface node  $F_s\Phi_{HC,nd}$
  - the heat flow fraction due to heating/cooling system on the mass node  $F_m\Phi_{HC,nd}$

The main resistors of the network are due to the heat exchange for ventilation  $H_{ve}$  and for transmission  $H_{tr}$ . The first one is directly connected to the internal air node  $\theta_i$  and can be divided into the heat transfer coefficient for mechanical and natural ventilation depending on the temperature of the starting node (external air  $\theta_e$  or pretreated air  $\theta_{sup}$ , for example, in the case of heat recovery system) while the second one can be divided into two major parts depending on the envelope elements. Generally windows elements are considered with no mass and the related heat transfer coefficient  $H_{tr,es}$  connects directly the external node  $\theta_e$  to the surface node  $\theta_s$ . The heat transmission through the massive elements is divided in three steps, describing respectively  $H_{tr,em}$ ,  $H_{tr,ms}$  and  $H_{tr,is}$ : (i) from the external node  $\theta_e$  to the mass node  $\theta_m$ , (ii) from the mass node  $\theta_m$  to the surface node  $\theta_s$ , (iii) from the surface node  $\theta_s$  to the internal air node  $\theta_i$ .

The main capacitor of the network instead is the thermal mass of the building that is represented by a global thermal capacity  $C_m$  and an effective mass area  $A_m$  that will influence the whole system.

The total solar  $\Phi_{sol}$  and internal  $\Phi_{int}$  gains are distributed on the internal air node  $\theta_i$ , surfaces node  $\theta_s$  and mass node  $\theta_m$  using conductive and radiative coefficients; the conductive part will be assigned to the internal air node  $\theta_i$  while the radiative one to the surface  $\theta_s$  and mass  $\theta_m$  nodes.

Similarly, the heat flow due to heating and cooling plant  $\Phi_{HC,nd}$  is split in a conductive part applied to the internal air node  $\theta_i$  and a radiative part divided to the surface  $\theta_s$  and mass nodes  $\theta_m$  according to other factors that are respectively called  $F_i$ ,  $F_s$  and  $F_m$  as suggested by the Standards UNI EN ISO 13792:2012 [41] and UNI EN 15255 [42].

The calculation of the *incident solar radiation* on differently oriented vertical surfaces is one of the main problems dealt with; this is due to the fact that usually the climate file simply provides the global (direct and diffuse) solar radiation, on horizontal surface. Thus, it was introduced a calculation method [44,45] that automatically splits this value on each vertical surface in the model. Finally, using some hourly coefficients it is also possible to use a daily or monthly average temperature and split it into hourly values [39]. It is important to note that this procedure is used in order to vali-

date and check the model in the worse situations (without usable hourly data) but the possibility to have a real time connection to the weather station and, so, to hourly data is preferable. The specifications about solar radiation and external temperature calculations are in the “climate data analysis”.

All the specifications about the building energy calculation are given in the next sections.

#### 4.2.1. INPUT AND OUTPUT DATA OF MODEL

The required **input** for the RC model are in the following Tables, divided in different areas:

- building location and orientation;
- building control, operation and activities;
- building zone geometry;
- building zone envelope.

**Tab. 5 - Main input data required by the RC model.**

Area	Symbol	Quantity	Unit
Building Location and Orientation	-	Latitude (North positive)	[deg]
	-	Longitude (East positive)	[deg]
	-	GMT zone (East positive)	[h]
	$\theta_{e,av}$	Daily Mean External Air Temperature	[°C]
	$\theta_{e,max}$	Daily Maximum External Air Temperature	[°C]
	$G_h$	Daily Radiation	[kJ/m <sup>2</sup> ]
	-	Rotation (counterclockwise positive) [-45;+45]	[deg]
	-	Albedo	[-]
Building Control, Operation and Activities	$\theta_{i,H}$	Heating set-point temperature zone	[°C]
	$\theta_{i,sb,H}$	Heating set-back temperature zone	[°C]
	$\theta_{i,C}$	Cooling set-point temperature zone	[°C]
	$\theta_{i,sb,C}$	Cooling set-back temperature zone	[°C]
	$ACR_{nat}$	Air change rate natural ventilation/infiltration	[1/h]
	$ACR_{mech}$	Air change rate mechanical ventilation (IAQ)	[1/h]
	$ACR_{min}$	Minimum air change rate infiltration	[1/h]
	$\eta_{HR}$	Heat recovery efficiency mechanical ventilation	[%]
	$\Phi_L$	Internal gains for artificial lighting	[W/m <sup>2</sup> ]
	$\Phi_A$	Internal gains for appliances	[W/m <sup>2</sup> ]
	$\Phi_{oc}$	Internal gains for people occupancy	[W/m <sup>2</sup> ]
	$f_{c,\phi int}$	Convective part of internal gain	[-]
	$f_{r,\phi int}$	Radiative part of internal gain	[-]
	$f_{c,sys,H}$	Technical system convective fraction for Heating	[-]
	$f_{c,sys,C}$	Technical system convective fraction for Cooling	[-]
	-	Heating schedule	[-]
-	Cooling schedule	[-]	

	-	Natural ventilation/infiltration Schedule	[-]
	-	Mechanical ventilation (IAQ) Schedule	[-]
	-	Heat recovery Schedule	[-]
	-	Artificial lighting Schedule	[-]
	-	Occupancy Schedule	[-]
	-	Appliance Schedule	[-]
	f	Fraction of Operation Period (Number of days in a week)	[%]
	$\eta_{sys}$	Conversion factor for Heating/Cooling system (for primary energy)	[-]
Building Zone Geometry	$A_{w,n}$	Total exterior surfaces (North)	[m <sup>2</sup> ]
	$A_{w,e}$	Total exterior surfaces (East)	[m <sup>2</sup> ]
	$A_{w,s}$	Total exterior surfaces (South)	[m <sup>2</sup> ]
	$A_{w,w}$	Total exterior surfaces (West)	[m <sup>2</sup> ]
	$A_{w,r}$	Total exterior surfaces (Roof)	[m <sup>2</sup> ]
	$\eta_{w,n}$	Ratio between transparent and total exterior surfaces (North)	[%]
	$\eta_{w,e}$	Ratio between transparent and total exterior surfaces (East)	[%]
	$\eta_{w,s}$	Ratio between transparent and total exterior surfaces (South)	[%]
	$\eta_{w,w}$	Ratio between transparent and total exterior surfaces (West)	[%]
	$\eta_{w,r}$	Ratio between transparent and total exterior surfaces (Roof)	[%]
	$A_G$	Ground surface	[m <sup>2</sup> ]
	NFA	Net Floor Area	[m <sup>2</sup> ]
	GFA	Gross Floor Area	[m <sup>3</sup> ]
	NV	Net Volume	[m <sup>2</sup> ]
GV	Gross Volume	[m <sup>3</sup> ]	
Building Zone Envelope	$U_W$	Exterior Wall Transmittance	[W/m <sup>2</sup> k]
	$U_T$	Exterior Transparent Element Transmittance	[W/m <sup>2</sup> k]
	$U_R$	Exterior Roof Transmittance	[W/m <sup>2</sup> k]
	$U_G$	Exterior Ground Floor Transmittance	[W/m <sup>2</sup> k]
	$F_F$	Frame fraction coefficient for Transparent Surfaces	[%]
	$g_{gl,n}$	Solar gain coefficient for Transparent Surfaces with perpendicular radiation	[%]
	$\alpha_W$	Opaque surfaces absorbance External Walls Surface	[-]
	$\alpha_R$	Opaque surfaces absorbance External Roof Surface	[-]
	$\alpha_F$	Opaque surfaces absorbance External Frame Surface	[-]
	$f_{Cm}$	Specific Global Thermal Capacity	[J/km <sup>2</sup> ]
	$f_{Am}$	Multiplier of surface for effective mass area	[-]
	$A_{at}$	Multiplier of internal surface area	[-]

Similarly, the main **output** provided are divided into the following areas:

- heat losses and heat gains;
- reduced-order hourly model parameters;
- hourly data in tables and graphs;
- summary of yearly results.

**Tab. 6 - Main output data provided by the RC model.**

Area	Symbol	Quantity	Unit
Heat Losses and Heat Gains	$H_W$	Heat Transfer Coefficient for Transmission from Exterior wall	[W/K]
	$H_R$	Heat Transfer Coefficient for Transmission from Roof	[W/K]
	$H_G$	Heat Transfer Coefficient for Transmission from Ground	[W/K]
	$H_{tr}$	Total Heat Transfer Coefficient for Transmission from Opaque Component	[W/K]
	$H_{tr,w}$	Total Heat Transfer Coefficient for Transmission from Transparent Surfaces	[W/K]
	$ACR_{nat}$	Air Change Rate for natural ventilation/infiltration	[m <sup>3</sup> /h]
	$ACR_{mech}$	Air Change Rate for mechanical ventilation	[m <sup>3</sup> /h]
	$H_{ve,nat}$	Heat Transfer Coefficient for Natural ventilation/infiltration	[W/K]
	$H_{ve,mech}$	Heat Transfer Coefficient for Mechanical ventilation	[W/K]
	$H$	Global Heat Transfer Coefficient (for Transmission and Ventilation)	[W/K]
	$\Phi_L$	Total Internal gains for artificial lighting	[W]
	$\Phi_A$	Total Internal gains for appliances	[W]
	$\Phi_{OC}$	Total Internal gains for occupancy	[W]
Reduced-Order Hourly Model Parameters	$A_{tot}$	Total Area of surfaces facing the building zone	[m <sup>2</sup> ]
	$H_{tr,is}$	Heat Transfer Coefficient between Internal Air and Surface	[W/K]
	$H_{tr,ms}$	Heat Transfer Coefficient between Surface and Mass	[W/K]
	$H_{tr,em}$	Heat Transfer Coefficient between Mass and External Air	[W/K]
	$C_m$	Global Thermal Capacity	[J/m <sup>2</sup> K]
Hourly Data in Tables and Graphs	$\theta_e$	External Air Temperature	[°C]
	$I_{solH}$	Horizontal solar radiation	[W/m <sup>2</sup> ]
	$\Phi_L$	Artificial lighting Gains	[kWh]
	$\Phi_A$	Appliances Gains	[kWh]
	$\Phi_{OC}$	Occupancy Gains	[kWh]
	$\Phi_H$	Heating load (Energy Needs)	[kWh]
	$\Phi_C$	Cooling load (Energy Needs)	[kWh]
	$\theta_{i,sp}$	Heating and Cooling set-point/set-back Temperature	[°C]
	$ACR_{nat}$	Air Change Rate for Natural ventilation	[1/h]
	$ACR_{mech}$	Air Change Rate for Mechanical ventilation	[1/h]
	$\theta_{i,UN}$	Internal air temperature	[°C]
$\theta_{i,FF}$	Free floating air temperature	[°C]	
Summary of Yearly Results	$\Phi_{H,nd}$	Heating Yearly Energy Demand	[kWh]
	$\Phi_{C,nd}$	Cooling Yearly Energy Demand	[kWh]
	$\Phi_{H,nd,Y,sp}$	Specific Heating Yearly Energy Demand	[kWh/m <sup>2</sup> ]
	$\Phi_{C,nd,Y,sp}$	Specific Cooling Yearly Energy Demand	[kWh/m <sup>2</sup> ]
	$\Phi_{H,sys,Y,p}$	Primary Heating Yearly Energy Demand	[kWh]
	$\Phi_{C,sys,Y,p}$	Primary Cooling Yearly Energy Demand	[kWh]
	$\Phi_{H,sys,Y,sp}$	Specific Primary Heating Yearly Energy Demand	[kWh/m <sup>2</sup> ]
	$\Phi_{C,sys,Y,sp}$	Specific Primary Cooling Yearly Energy Demand	[kWh/m <sup>2</sup> ]
	$\Phi_{H,nd,Y,max}$	Peak Heating Power	[kW]
$\Phi_{C,nd,Y,max}$	Peak Cooling Power	[kW]	

	$\Phi_{H,nd,Y,max,sp}$	Specific Peak Heating Power	[kW/m <sup>2</sup> ]
	$\Phi_{C,nd,Y,max,sp}$	Specific Peak Cooling Power	[kW/m <sup>2</sup> ]
	$\theta_{i,max}$	Minimum Annual Hourly Zone Temperature	[°C]
	$\theta_{i,av}$	Average Annual Hourly Zone Temperature	[°C]
	$\theta_{i,min}$	Minimum Annual Hourly Zone Temperature	[°C]

#### 4.2.2. ENERGY BALANCE OF NODES

As already explain the non-linearities determined by the detailed description of physical phenomena is a problem in control systems and linear/linearized formulations of optimization models are preferable. Thus, starting from the Lumped Parameter Model (RC) already described, a Linear Time-Varying Model is built.

The model is a Differential Algebraic Equation (DAE) discretized with a Crank-Nicolson scheme (considering a time step of one hour) as in the simplified hourly model of ISO 13790 [39]. The mass node temperature  $\theta_m$  is determined with a differential equation while the surface  $\theta_s$  and air  $\theta_i$  nodes are determined by means of two algebraic equations using the average mass temperature in the time step considered in the differential equation.

$$\theta_{m,i-1} - \theta_{m,i} + \frac{H_{tr,em}}{c_m \Delta\tau} (\theta_e - \bar{\theta}_m) + \frac{H_{tr,ms}}{c_m \Delta\tau} (\theta_s - \bar{\theta}_m) + \frac{\phi_m}{c_m} + \frac{F_{mH}\Phi_{H,nd} - F_{mC}\Phi_{C,nd}}{c_m \Delta\tau} = 0 \quad \text{Eq. (1)}$$

$$H_{tr,es}(\theta_e - \theta_s) + H_{tr,ms}(\bar{\theta}_m - \theta_s) + H_{tr,is}(\theta_i - \theta_s) + \phi_s + F_{sH}\Phi_{H,nd} - F_{sC}\Phi_{C,nd} = 0 \quad \text{Eq. (2)}$$

$$H_{ve,inf+nat}(\theta_e - \theta_i) + H_{tr,is}(\theta_s - \theta_i) + \phi_i + F_{iH}\Phi_{H,nd} - F_{iC}\Phi_{C,nd} = 0 \quad \text{Eq. (3)}$$

$$\bar{\theta}_m = \frac{\theta_{m,i} - \theta_{m,i-1}}{2} \quad \text{Eq. (4)}$$

#### 4.2.3. TEMPERATURE OF NODES

For each steps, in order to obtain the internal temperatures and, consequently, to be able to determine the energy needs (in the case of the Non Linear Time Varying model), the following quantities are calculated.

**Tab. 7 - Main quantities calculated by the RC model.**

Symbol	Quantity	Eq.	Unit
$\theta_i$	Internal Air temperature for the considered period	Eq.(5)	[°C]
$\theta_s$	Surfaces Temperature for the considered period <sup>4</sup>	Eq.(6)	[°C]
$\theta_{m,t}$	Mass Temperature for a given time step at the end of the period	Eq.(7)	[°C]

<sup>4</sup>The value of  $\theta_s$  is a mix between air and mean radiant temperature.

$\Phi_{m,tot}$	Overall heat flow on the Mass Node	Eq.(8)	[W]
$\theta_m$	Mass Temperature for the considered period	$\frac{(\theta_{m,t} + \theta_{m,t-1})}{2}$	[°C]
$\theta_{op}$	Operative Temperature	$(f_{op} \times \theta_i) + [(1 - f_{op}) \times \theta_s]$	[°C]

It is important to note that, using a dynamic calculation, it is necessary to calculate the mass temperature at the first moment of the considered period (t-1) and the mass temperature on the final moment of the considered period (t). In our case, in fact, the time-step for the calculation is the hour ( $\Delta\tau = 3600s$ ).

The main equation used to calculate the internal temperature is:

$$\theta_i = \frac{(H_{tr, is} \times \theta_s) + (H_{ve} \times \theta_e) + \Phi_i + F_{iH} \Phi_H - F_{iC} \Phi_C}{[H_{tr, is} + H_{ve}]} \quad \text{Eq. (5)}$$

The main equations used to calculate the surface and mass temperatures are:

$$\theta_s = \frac{(H_{tr, ms} \times \theta_m) + (H_{tr, es} \times \theta_e) + \Phi_s + F_{sH} \Phi_H - F_{sC} \Phi_C + H_{tr, 1} \left[ \theta_e + \frac{\Phi_i + F_{iH} \Phi_H - F_{iC} \Phi_C}{H_{ve}} \right]}{[H_{tr, ms} + H_{tr, es} + H_{tr, 1}]} \quad \text{Eq. (6)}$$

$$\theta_{m,t} = \frac{\theta_{m,t-1} \times \left[ \frac{C_m}{\Delta\tau} - 0,5 \times (H_{tr, 3} + H_{tr, em}) \right] + \Phi_{mtot}}{\left[ \frac{C_m}{\Delta\tau} + 0,5 \times (H_{tr, 3} + H_{tr, em}) \right]} \quad \text{Eq. (7)}$$

Finally, the overall heat flow on the mass node is calculated as:

$$\Phi_{m,tot} = \Phi_m + F_{mH} \Phi_H - F_{mC} \Phi_C + (H_{tr, em} \times \theta_e) + \frac{H_{tr, 3} \left[ \Phi_s + F_{sH} \Phi_H - F_{sC} \Phi_C + (H_{tr, es} \times \theta_e) + H_{tr, 1} \left( \theta_e + \frac{\Phi_i + F_{iH} \Phi_H - F_{iC} \Phi_C}{H_{ve}} \right) \right]}{H_{tr, 2}} \quad \text{Eq. (8)}$$

Note that for all the steps the formula will change; in the case of  $\theta_{i, FF}$ , for example, the internal gains  $\Phi_i$  and the heat flow  $\Phi_{HC}$  are zero and, in the case of  $\theta_{i, 0}$  instead the internal gains are used but the heat flow is zero.

#### 4.2.4. INTERNAL AND SOLAR GAINS

The hourly internal gains  $\Phi_{int}$  are calculated just multiplying the total specific value from input to the net floor area (Eq.9), while the hourly solar gains  $\Phi_{sol}$  are calculated separately for each orientation (north, south, east, west and horizontal) as the sum of the hourly solar gains reached through the transparent and opaque elements  $\Phi_{sol, T}$  and  $\Phi_{sol, op}$  and the hourly losses through the sky  $\Phi_{sol, sky}$  (Eq.10-13).

$$\Phi_{int} = \sum(\Phi_A + \Phi_L + \Phi_{OC}) \times NFA \quad \text{Eq. (9)}$$

$$\Phi_{sol} = \sum \Phi_{sol,T} + \sum \Phi_{sol,Op} - \sum \Phi_{sol,sky} \quad \text{Eq. (10)}$$

with:

$$\Phi_{sol,T} = F_{sh,ob} \times F_{sh,gl} \times G_{\beta} \times (1 - F_F) \times (g_{gl} \times F_w) \times A_T \quad \text{Eq. (11)}$$

$$\Phi_{sol,Op} = (G_{\beta} \times R_{se} \times \alpha_w \times A_w \times U_w) + (F_{sh,ob} \times G_{\beta} \times R_{se} \times \alpha_F \times A_T \times F_F \times U_T) \quad \text{Eq. (12)}$$

$$\Phi_{sol,sky} = (R_{se} \times h_r \times A_w \times V_F \times U_w \times \Delta\theta_{er}) + (R_{se} \times h_r \times A_T \times F_F \times V_F \times U_T \times \Delta\theta_{er}) \quad \text{Eq. (13)}$$

where:

- $\Phi_A, \Phi_L, \Phi_{OC}$  are respectively the specific internal gains due to appliances, artificial lighting and occupancy;
- NFA is the Net Floor Area;
- $F_{sh,ob}$  and  $F_{sh,gl}$  are respectively the shading factor due to fixed or mobile devices;
- $G_{\beta}$  is the solar radiation on a specific surface;
- $F_F$  is the frame fraction of the transparent element;
- $g_{gl}$  is the solar gain factor;
- $F_w$  is the correction factor for solar energy transmittance of glazed elements;
- $A_T$  and  $A_w$  are respectively the transparent element and the wall area;
- $U_T$  and  $U_w$  are respectively the transparent element and the wall transmittance;
- $R_{se}$  and  $h_r$  are respectively the external surface heat resistance and the radiative heat transfer coefficient;
- $\alpha_w$  and  $\alpha_F$  are the wall and frame surfaces absorbance;
- $V_F$  is the view factor to the sky;
- $\Delta\theta_{er}$  is the average difference between external air temperature and sky temperature.

The required **input factors** for the simulation model are given below. In the Table are also given the default values assumed by the standard UNI EN ISO 13790:2008 [39] and the related chapter in which they are described them.

**Tab. 8 - Input Factors and Default Values provided by UNI EN ISO 13790.**

Symbol	Quantity	Unit	Default value	UNI EN ISO 13790
$\Delta\theta_{er}$	Average difference between external air temperature and sky temperature	[K]	11 <sup>5</sup>	11.3.5
$R_{se}$	External surface heat resistance	[m <sup>2</sup> K/W]	0,04	11.3.5
$F_w$	Correction factor for solar energy transmittance of glazed elements	[-]	0,9	11.4.2
$V_{Fv}$	View factor to the sky for vertical surfaces	[-]	0,5	11.4.6
$V_{Fh}$	View factor to the sky for horizontal surfaces	[-]	1	11.4.6

<sup>5</sup> The default values are dependent on the zone: 9 in sub-polar areas, 13 in the tropics and 11 in intermediate zone

$\varepsilon$	Emissivity of external surface	[-]	0,9	11.4.6
$h_r$	Radiative heat transfer coefficient	[W/m <sup>2</sup> K]	4,5 <sup>6</sup>	11.4.6

#### 4.2.5. HEAT TRANSFER IN BUILDING

The relevant quantities used for model assembly, concerning the calculation of Heat Transfer and Heat Capacity of the building/zone, are included in the following table, together with references to the parts of UNI EN ISO 13790:2008 [39].

**Tab. 9 - Simplified equations provided by UNI EN ISO 13790.**

Symbol	Quantity	Unit	Equations	Ref
$H_{tr, is}$	Coupling conductance between nodes $i$ (internal air) and $s$ (surfaces)	[W/K]	$h_{is} \times A_{tot}$	7.2.2.2
$A_{tot}$	Total Area of surfaces facing the building zone	[m <sup>2</sup> ]	$NFA \times A_{at}$	7.2.2.2
$H_{tr, op}$	Overall Heat transfer coefficient by transmission for external opaque elements (wall, roof and ground surfaces)	[W/K]	$\sum_{i=1}^n (A_i \times U_i)$	8.3
$H_{tr, w}$	Heat transfer coefficient by transmission for external “no mass” elements (windows)	[W/K]	$\sum_{i=1}^n (A_i \times U_i)$	8.3.1
$H_{ve, nat}$	Heat transmission coefficient by natural ventilation	[W/K]	$\eta_{nat} \times NFA \times 0,34$	9.3.1
$H_{ve, mech}$	Heat transmission coefficient by mechanical ventilation with heat recovery	[W/K]	$\eta_{mech} \times NFA \times 0,34 \times (1 - \eta_{HR})$	9.3.3.8
$H_{tr, em}$	Coupling conductance between nodes $e$ (external air) and $m$ (mass)	[W/K]	$\frac{1}{\frac{1}{H_{tr, op}} - \frac{1}{H_{tr, ms}}}$	12.2.2
$H_{tr, ms}$	Coupling conductance between nodes $m$ (mass) and $s$ (surfaces)	[W/K]	$h_{ms} \times A_m$	12.2.2
$A_m$	Effective Mass Area	[m <sup>2</sup> ]	$f_{Am}^7 \times NFA$	12.3.1.2
$C_m$	Global Heat Capacity	[J/K]	$f_{Cm}^8 \times NFA$	12.3.1.2
$f_m$	Heat gain factor on mass node $m$	[-]	$\frac{A_m}{A_{tot}}$	C.2

<sup>6</sup>  $h_r$  is given by equation  $4 \cdot \varepsilon \cdot (5,67 \cdot 10^{-8}) \cdot (\theta_{ss} + 273)^3$  but to a first approximation can be taken equal to  $5 \cdot \varepsilon$  which corresponds to an average temperature of 10°C

<sup>7</sup> Default Values for dynamic parameters

<sup>8</sup> Default Values for dynamic parameters

$f_s$	Heat gain factor on surfaces node $s$	[-]	$1 - \frac{A_m}{A_{tot}} - \frac{H_{tr,w}}{h_s \times A_{tot}}$	C.2
$\Phi_i$	Heat flow from heat gain on air node	[W]	$f_{c\Phi_{INT}} \times \Phi_{INT}$	C.2
$\Phi_m$	Heat flow from heat gain on mass node	[W]	$f_m \times (\Phi_i + \Phi_{sol})$	C.2
$\Phi_s$	Heat flow from heat gain on surface node	[W]	$f_s \times (\Phi_i + \Phi_{sol})$	C.2
$H_{tr,1}$	Overall Heat flow factor	[W/K]	$\frac{1}{\frac{1}{H_{ve}} - \frac{1}{H_{tr,is}}}$	C.3
$H_{tr,2}$	Overall Heat flow factor	[W/K]	$H_{tr,1} + H_{tr,w}$	C.3
$H_{tr,3}$	Overall Heat flow factor	[W/K]	$\frac{1}{\frac{1}{H_{tr,2}} - \frac{1}{H_{tr,ms}}}$	C.3

According to note 5, the internal heat capacity of the building zones  $C_m$  and the effective mass area  $A_m$  are calculated with the default value for dynamic parameters suggested by the UNI EN 13790 [39] in section 12.3.1.2 (Table 12). Anyway, they can be also calculated starting from the actual internal heat capacities of construction components  $k$  multiplied and their surface  $A$ :

$$C_m = \sum_j (\kappa_j \cdot A_j) \quad \text{Eq. (14)}$$

$$A_m = \frac{C_m^2}{\sum_j (A_j \cdot k_j^2)} \quad \text{Eq. (15)}$$

Finally, the required **input factors** for the simulation model are given below. In the Table are also given the default values assumed by the standard UNI EN ISO 13790:2008 [39] and the related chapter in which they are described them.

**Tab. 10 - Input Factors and Default Values provided by UNI EN ISO 13790.**

Symbol	Quantity	Unit	Default value	UNI EN ISO 13790
$A_{at}$	Conversion factor for internal surfaces	[-]	4,5	7.2.2.2
$h_{is}$	Heat transfer coefficient between nodes a (internal air) and s (surfaces)	[W/m <sup>2</sup> K]	3,45	7.2.2.2
$f_{c,\Phi_{int}}$	Convective fraction of internal gain	[-]	0,5	C.2
$f_{r,\Phi_{int}}$	Radiative fraction of internal gain	[-]	0,5	C.2
$h_{ms}$	Heat transfer coefficient between nodes m (mass) and s(surfaces)	[W/m <sup>2</sup> K]	9,1	12.2.2
$f_{op}$	Correction factor for operative temperature $\theta_{op}$	[%]	0,3	C.3

#### 4.2.6. FACTORS FOR NODAL ENERGY GAINS OF TECHNICAL SYSTEMS

In order to calculate the heat flow fractions due to heating and cooling system on air, surface and mass nodes, the following coefficients are considered, according to [41,42].

**Tab. 11– Heat Flow Fractions coefficient due to Heating and Cooling System.**

Symbol	Quantity	Unit	Equations
$F_{iH}$	Convective fraction due to heating system on the internal air node	[-]	$f_{c,sys,H}$
$F_{iC}$	Convective fraction due to cooling system on the internal air node	[-]	$f_{c,sys,C}$
$F_{sH}$	Radiative fraction due to heating system on the surface node	[-]	$f_s(1-f_{c,sys,H})$
$F_{sC}$	Radiative fraction due to cooling system on the surface node	[-]	$f_s(1-f_{c,sys,C})$
$F_{mH}$	Radiative fraction due to heating system on the mass node	[-]	$f_m(1-f_{c,sys,H})$
$F_{mC}$	Radiative fraction due to cooling system on the mass node	[-]	$f_m(1-f_{c,sys,C})$

The next table indicates some convective factors  $f_{c,sys}$  for heat flow due to different technical system; as shown in the previous table, the radiative part  $f_{r,sys}$  is calculated as 1 minus the convective fraction  $f_{c,sys}$ .

**Tab. 12–Convective fraction of internal gains due to different technical system.**

Technical System	Heating	Cooling
	$f_{c,sys,H}$	$f_{c,sys,C}$
Air system	1,0	1,0
Radiant floor	0,5	0,1
Radiant ceiling	0,1	0,5
Radiant vertical surface	0,5	0,1
Fan-coil/radiators	0,8	0,8

#### 4.2.7. CLIMATE DATA ANALYSIS

As introduced in the previous section, the model can be used both when detailed weather data are present or when only limited data are present, by employing techniques for data reconstruction, generally used in forecasting. With respect to the hourly temperature, it is sufficient to have the minimum and maximum daily value (or one of the two and the amplitude of oscillation) to reconstruct a profile, using appropriate coefficients [46]. In the case of a simulation of representative days for each month, the profile is calculated as follows, starting from monthly average data  $\theta_{e,av}$ , and averaging the value for the time-step, following the discretization rule explained before:

$$\theta_e = \frac{(\theta_{e,av}+(\alpha \times C_i)) + (\theta_{e,av}+(\alpha \times C_{i+1}))}{2} \quad \text{Eq. (16)}$$

**Tab. 13 - Data used for Hourly External Temperature calculation.**

Symbol	Quantity	Unit	Equations
$\theta_{e,av}$	Mean Monthly External Temperature	[°C]	From Climate Data
$\alpha$	Monthly Amplitude of Temperature oscillation	[°C]	$\theta_{e,max} - \theta_e$
$\theta_{e,max}$	Maximum Monthly External Temperature	[°C]	From Climate Data
$C_i$	Hourly coefficient $i$	[-]	From Settings
$C_{i+1}$	Hourly coefficient $i+1$	[-]	From Settings

With respect to the reconstruction of solar radiation profiles on every surface of the building the method starts from global daily radiation of horizontal surface and then splits the value into direct and diffuse hourly components, in such a way that solar geometry algorithms can be used to project them in energy in every surface. The method employed in the model is described in [44,45].

#### 4.2.8. INTERMITTENT OPERATION ACCOUNTING

A main issue when simulating representative load profiles (i.e. with daily schedules for a representative day for each month) is related to the accounting of energy in the case of intermittent operation. Initially, the energy needs in the case of intermittent operation was calculated just using the percentage of the ON period (energy consumption proportional to operation time). For example if the energy needs of a day is 1 kWh, the month has 31 days and the system is ON for the 70% of the month, the monthly energy needs is  $1 * 31 * 0.7 = 21.7$  kWh. In this way, however, is not considered that, in case of light construction and extended OFF period (e.g. when the system is OFF for all the weekend, or rather more than 48 hours), the energy need to bring-back the building into a heated/cooled state will need more energy than in a normal situation (e.g. when the plant is OFF just for some hour).

Therefore, it has been introduced some equations to calculate more accurately the energy spent at the starting point of the period in order to cover the energy loss during the OFF period. This kind of energy is called *Free Running Energy* ( $FRE_{HC}$ ) [47].

The output from model simulations required are the average Free-Floating temperatures of the considered period (both during ON and OFF period), the main thermal characteristics of the buildings, or rather the Total Heat Transfer Coefficient for transmission (due to both opaque and transparent components) and the Global Thermal Capacity of the building, the average heat transfer coefficient due to the ventilation just for the OFF period and the external air temperature of the whole considered period.

**Tab. 14 - Data used for Free Running Energy calculation.**

Symbol	Quantity	Unit
$\theta_{i,FF,av}$	Average Free-Floating Temperature	°C
$H_{tr,tot}$	Total Heat Transfer Coefficient for transmission	W/K

$H_{ve,av}$	Average Ventilation Rate (during OFF period) <sup>9</sup>	W/K
$C_m$	Global Thermal Capacity	W/K
$\theta_e$	Average External Air Temperature	°C

Firstly, the number of hours (time) that the thermal zone needs to lose the energy incorporated in the mass can be calculated as:

$$Time = \frac{C_m}{H_{tr,tot} + H_{ve,av}} \times \ln \frac{\theta_{i,FF,av,OFF} - \theta_e}{\theta_{i,FF,av,ON} - \theta_e} \quad \text{Eq. (17)}$$

In the case that the *time* is lower than the number of hours of OFF period<sup>10</sup>, the Free Running Energy needed to bring-back the thermal zone into a heated/cooled state is calculated as:

$$FRE_{HC} = (\theta_{i,FF,av,ON} - \theta_{i,FF,av,OFF}) \times (H_{tr,tot} + H_{ve,av}) \times f \times N \times t \quad \text{Eq. (18)}$$

where

- *f* is normally equal to 2 due to the charge/discharge effect<sup>11</sup>;
- *N* is the number of week during the considered period calculated as the number of monthly days divided by the number of weekly days;
- *t* is normally equal to 24 and are the number of hour in a day.

Finally, the **Energy Demand** will result as:

$$\Phi_{HC,nd,Y} = \frac{\Phi_{HC,nd,Y,ONperiod} \times \%ONperiod}{100\%} + FRE_{HC} \quad \text{Eq. (19)}$$

### 4.3. OPTIMIZATION MODEL FORMULATION

For the reasons described before, the building performance model is described as an optimization problem, defined according to the following elements.

1. Objective function:
  - a. Energy demand.
2. Variables:
  - a. Power demand (continuous).
3. Constraints:
  - a. Power demand (always positive);
  - b. Temperature bounds (set-points);
  - c. Power limits (maximum power dependent on system sizing);
  - d. Boundary conditions (initial-final temperature of nodes).

<sup>9</sup> Where  $H_{ve,tot} = H_{ve,nat} + H_{ve,mech}$  and if  $H_{ve,tot} = 0$  the minimum ventilation for infiltration is set as  $H_{ve,min} = 0,0001$ .

<sup>10</sup> in the case that the *time* is higher, the Free Running Energy is considered proportionally.

<sup>11</sup> the energy is counted double because the building during the OFF period lose the energy incorporated in the mass and, thus, when the system re-start has to give two times the energy.

Depending on the formulation of the objective function, the variables and the parameters used for calculation. The possibilities considered are the following:

1. non linear time variant model objective function;
2. linear time-variant model objective function;
3. linear time invariant model (2 states, 1 hidden state) objective function;
4. linear time invariant model (1 state, 2 hidden states) objective function.

The specific formulations are described in the following section of the chapter. For all the models the energy demand is calculated for each representative day  $\Phi_{HC,d}$  and then summed up to obtain monthly energy demand  $\Phi_{HC,M}$  (multiplying by the number of the monthly days  $n$ ) and annual energy demand  $\Phi_{HC,Y}$ . It is important to remember that this model is built with a predictive control system logic, thus, with the objective to predict the next day energy needs (24 hour ahead forecast). The same for the peak power for heating and cooling.

$$\Phi_{HC,Y} = \sum \Phi_{HC,M} \quad \text{Eq. (20)}$$

$$\Phi_{HC,M} = \Phi_{HC,d} \times n \quad \text{Eq. (21)}$$

$$\Phi_{HC,d} = \sum \Phi_{HC,h} \quad \text{Eq. (22)}$$

$$\Phi_{HC,Y,max} = \Phi_{HC,M,max} \quad \text{Eq. (23)}$$

$$\Phi_{HC,M,max} = \Phi_{HC,d,max} \quad \text{Eq. (24)}$$

#### 4.3.1. NON LINEAR TIME VARIANT MODEL OBJECTIVE FUNCTION

The main **output** calculated is the *hourly energy demand* and it is determined by calculating the *energy required for heating or cooling*  $\Phi_{HC}$ , that is necessary to provide or extract from the node  $\theta_i$  in order to maintain the required temperature. The approach is to start calculating the internal temperature in a free-floating condition and, then, to apply a certain heat flow ( $\Phi_{HC,0}$  and  $\Phi_{HC,10}$  that respectively stand for 0 and 10 W/m<sup>2</sup>) in order to increase or decrease the air temperature until achieve the set-point temperature with a necessary heat flow  $\Phi_{HC,un}$ . The **main calculation steps** are summarized below.

**Tab. 15 - Main calculation steps provided by the RC model.**

Symbol	Quantity
FF	Free Floating conditions
$\Phi_{HC,0}$	No power applied but internal gains and ventilation normal condition
$\Phi_{HC,10}$	10 W/m <sup>2</sup> applied and internal gains and ventilation normal condition
$\Phi_{HC,UN}$	Unrestricted power and internal gains and ventilation normal condition

The equation used to calculate the unrestricted hourly energy needs  $\Phi_{HC,un}$  is:

$$\Phi_{HC,un} = \frac{\Phi_{HC,10} \times (\theta_{i,setpoint} + \theta_{i,0})}{(\theta_{i,10} + \theta_{i,0})} \quad \text{Eq. (25)}$$

At this point, the only problem remaining is how to find the starting mass temperature for the first hour of each day  $\theta_{m,HCun,t-1,x}$ . It is solved by means of a nonlinear optimization technique (generalized reduced gradient) imposing the convergence of mass temperature. This criterion is acceptable as described in ISO 13792 and EN 15255 for the dynamic simulation of single days [41,42]:

$$\min \sum_{i=1}^n (\theta_{m,FF,t-1,x} - \theta_{m,FF,t,y}) + \sum_{i=1}^n (\theta_{m,HCun,t-1,x} - \theta_{m,HCun,t,y}) \quad \text{Eq. (26)}$$

$$\text{s.t.} \quad \forall_i (\theta_{m,FF,t-1,x} - \theta_{m,FF,t,y}) = 0$$

$$\forall_i (\theta_{m,HCun,t-1,x} - \theta_{m,HCun,t,y}) = 0$$

$$\text{variables:} \quad \theta_{m,FF,t-1,x,i}, \theta_{m,HCun,t-1,x,i}$$

where

- $i$  is the number of the days or months considered;
- $x$  is the first hour of the  $i$  considered (0.00 am);
- $y$  is the final hour of the  $i$  considered (24.00 pm);
- $t$  is the time step considered (hour);
- $\theta_{m,FF}$  is the mass temperature in Free-Floating condition;
- $\theta_{m,HCun}$  is the mass temperature in Unrestricted power condition.

It has to be remembered that, using a dynamic calculation, it is necessary to calculate the mass temperature at the first moment of the considered period ( $t-1$ ) and the mass temperature on the final moment of the considered period ( $t$ ), with  $\Delta t = 3600s$ .

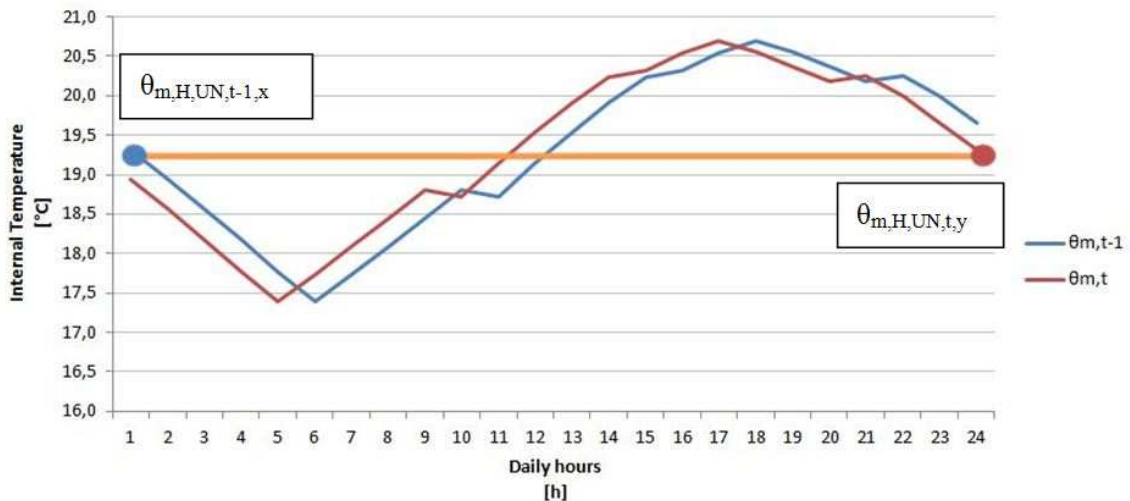


Figure 11. Mass temperatures at time  $t$  and  $t-1$  for a day  $i$ , in Unrestricted Power Condition.

#### 4.3.2. LINEAR TIME-VARIANT MODEL OBJECTIVE FUNCTION

The model is solved with a Linear Programming (LP), or rather it is not solved with the convergence method previously described (Eq.26) but using linear objective function and constraints (Eq.27). Thus, the full (time variant) linear programming formulation is:

$$\begin{aligned} \min \quad & \sum \Phi_{H,j} + \sum \Phi_{C,j} && \text{Eq. (27)} \\ \text{s.t.:} \quad & \forall_j \theta_{i,H,j} \geq \theta_{sp,H} \\ & \forall_j \theta_{i,C,j} \leq \theta_{sp,C} \\ & \forall_j \Phi_{H,j} \leq \Phi_{H,max} \\ & \forall_j \Phi_{C,j} \leq \Phi_{C,max} \\ & \sum \Phi_H + \sum \Phi_C \geq 0 \\ & \text{Eq.(1)} \\ & \text{Eq.(2)} \\ & \text{Eq.(3)} \\ \text{variables:} \quad & \Phi_H, \Phi_C, \theta_i, \theta_s, \theta_m \end{aligned}$$

where:

- $j$  is the hourly value;
- $\Phi_H$  is the calculated hourly energy needs for heating period;
- $\Phi_C$  is the calculated hourly energy needs for cooling period;
- $\theta_{i,H}$  is the calculated hourly internal air temperature for heating period;
- $\theta_{i,C}$  is the calculated hourly internal air temperature for cooling period;
- $\theta_{sp,H}$  is the required hourly set point temperature for heating period;
- $\theta_{sp,C}$  is the required hourly set point temperature for cooling period;
- $\Phi_{H,max}$  is the maximum power available during the heating period;
- $\Phi_{C,max}$  is the maximum power available during cooling period.

#### 4.3.3. LINEAR TIME INVARIANT MODEL (2 STATES, 1 HIDDEN STATE) OBJECTIVE FUNCTION

The linear time invariant model can be used in an inverse way for identification, by minimizing the following objective function.

$$\begin{aligned} & \min \quad \sum(\theta_{i,\text{sim},j} - \theta_{i,\text{meas},j})^2 + \sum(\theta_{s,\text{sim},j} - \theta_{s,\text{meas},j})^2 & \text{Eq. (28)} \\ \text{s.t.} \quad & \forall_i (\theta_{m,\text{FF},t-1,x} - \theta_{m,\text{FF},t,y}) = 0 \\ & \forall_i (\theta_{m,\text{HCun},t-1,x} - \theta_{m,\text{HCun},t,y}) = 0 \\ & \text{ACR}_{\text{LB}} \leq \text{ACR}_{\text{id}} \leq \text{ACR}_{\text{UB}} \\ & \Phi_{\text{int,LB}} \leq \Phi_{\text{int,id}} \leq \Phi_{\text{int,UB}} \\ & U_{\text{W,LB}} \leq U_{\text{W,id}} \leq U_{\text{W,UB}} \\ & U_{\text{T,LB}} \leq U_{\text{T,id}} \leq U_{\text{T,UB}} \\ & U_{\text{R,LB}} \leq U_{\text{R,id}} \leq U_{\text{R,UB}} \\ & U_{\text{G,LB}} \leq U_{\text{G,id}} \leq U_{\text{G,UB}} \\ & C_{\text{m,LB}} \leq C_{\text{m,id}} \leq C_{\text{m,UB}} \\ & A_{\text{m,LB}} \leq A_{\text{m,id}} \leq A_{\text{m,UB}} \\ & A_{\text{at,LB}} \leq A_{\text{at,id}} \leq A_{\text{at,UB}} \\ & f_{\text{c,sys,H,LB}} \leq f_{\text{c,sys,H,id}} \leq f_{\text{c,sys,H,UB}} \\ & f_{\text{c,sys,C,LB}} \leq f_{\text{c,sys,C,id}} \leq f_{\text{c,sys,C,UB}} \\ & h_{\text{ms,LB}} \leq h_{\text{ms,id}} \leq h_{\text{ms,UB}} \\ & h_{\text{is,LB}} \leq h_{\text{is,id}} \leq h_{\text{is,UB}} \\ & f_{\text{c},\Phi_{\text{int,LB}}} \leq f_{\text{c},\Phi_{\text{int,id}}} \leq f_{\text{c},\Phi_{\text{int,UB}}} \\ \text{variables:} \quad & \theta_{m,\text{FF},t-1,x}, \theta_{m,\text{HCun},t-1,x}, \text{ACR}_{\text{id}}, \Phi_{\text{int,id}}, U_{\text{W,id}}, U_{\text{T,id}}, U_{\text{R,id}}, U_{\text{G,id}}, C_{\text{m,id}}, \\ & A_{\text{m,id}}, A_{\text{at,id}}, f_{\text{c,sys,H,id}}, f_{\text{c,sys,C,id}}, h_{\text{ms,id}}, h_{\text{is,id}}, f_{\text{c},\Phi_{\text{int id}}} \end{aligned}$$

where

- $i$  is the number of the days or months considered;
- $x$  is the first hour of the  $i$  considered (0.00 am);
- $y$  is the final hour of the  $i$  considered (24.00 pm);
- $t$  is the time step considered (hour);
- $\text{sim}$  is the calculated value;
- $\text{meas}$  is the measured value;
- $\text{LB}$  is the Lower Bound imposed;
- $\text{UB}$  is the Upper Bound imposed;
- $\text{id}$  is the identified parameter;
- $\theta_i$  is the internal air temperature in Unrestricted power condition;
- $\theta_s$  is the surface temperature in Unrestricted power condition;
- $\theta_{m,\text{FF}}$  is the mass temperature in Free-Floating condition;
- $\theta_{m,\text{HCun}}$  is the mass temperature in Unrestricted power condition;

- ACR is the Air Change Rate value [1/h];
- $\Phi_{int}$  is the internal gains value [W/m<sup>2</sup>];
- $U_W$  is wall transmittance [W/m<sup>2</sup>K];
- $U_T$  is transparent component transmittance [W/m<sup>2</sup>K];
- $U_R$  is roof transmittance [W/m<sup>2</sup>K];
- $U_G$  is ground floor transmittance [W/m<sup>2</sup>K];
- $C_m$  is the global thermal capacity [J/kgm<sup>2</sup>];
- $A_m$  is the multiplier of surface for effective mass area [-];
- $A_{at}$  is the conversion factor for internal surface [-];
- $f_{c,sys,H}$  is the technical system convective fraction for heating season [-];
- $f_{c,sys,C}$  is the technical system convective fraction for cooling season [-];
- $h_{ms}$  is the heat transfer coefficient between the mass and surface nodes [W/m<sup>2</sup>K];
- $h_{is}$  is the heat transfer coefficient between the internal air and surface nodes [W/m<sup>2</sup>K];
- $f_{c,\Phi_{int}}$  the internal gain convective fraction [-].

As before, it has to be remembered that, using a dynamic calculation, it is necessary to calculate the mass temperature at the first moment of the considered period (t-1) and the mass temperature on the final moment of the considered period (t), with  $\Delta t = 3600s$ .

The two states that are considered to be measurable are the air temperature  $\theta_i$  and average surface temperature  $\theta_s$  (measurable with sensors). The temperature of the mass nodes  $\theta_m$  is considered as a hidden state, which is not directly measured. In a direct use, the model is solved in an analogous way to the one with the linear time-variant objective function, with the only difference that parameters are time invariant.

#### 4.3.4. LINEAR TIME INVARIANT MODEL (1 STATE, 2 HIDDEN STATES) OBJECTIVE FUNCTION

The linear time invariant model can be used in an inverse way for identification, by minimizing the following objective function.

$$\begin{aligned} \min \quad & \sum (\theta_{i,sim,j} - \theta_{i,meas,j})^2 && \text{Eq. (29)} \\ \text{s.t.} \quad & && \text{as for Eq. (28)} \\ \text{variables:} \quad & && \text{as for Eq. (28)} \end{aligned}$$

The single state that is considered to be measurable is the air temperature  $\theta_i$ . The average surface temperature  $\theta_s$  and the temperature of the mass nodes  $\theta_m$  are considered as hidden states, which are not directly measured. In a direct use, the model is solved in an analogous way to the one with the linear time-variant objective function, with the only difference that parameters are time invariant.

#### 4.4. DYNAMIC MODEL VALIDATION

The *simplified hourly method* described by the standard UNI EN ISO 13790 [39] is not automatically validated, so the RC model was validated in two steps. First, *best test* provided by ASHRAE Standard 140 [48] have been used. This Standard provide 18 test cases specially designed for validation of building energy simulation model: "*they can be used for identifying and diagnosing predictive differences from whole building energy simulation software that may possibly be caused by algorithmic differences, modeling limitations, input differences, or coding errors*".

The ASHRAE *best-test* tested are the following:

- Case 600 – The **Base Case Low Mass Building** is a rectangular single zone, thus, all the components are external. The internal load are continuous 200 W (60% radiative, 40% convective, 100% sensible). The infiltration rate is 0,5 air change per hour continuous. The mechanical system is a 100% convective air system, 100% efficient with no duct losses and no capacity limitation, no latent heat extraction, non-proportional-type dual set point thermostat with dead band, heating systems starts with internal temperature lower than 20°C and cooling systems starts with internal temperature greater than 27°C;
- Case 620 – *East/West Window Orientation Test* for Low Mass Building, as 600 except for windows orientation;
- Case 640 – *Thermostat Setback Test* for Low Mass Building. From 23:00 to 07:00 heat ON if zone temperature is lower than 10°C, from 07:00 to 23:00 heat ON if zone temperature is greater than 20°C, all hours cool ON if zone temperature is greater than 27°C, otherwise mechanical equipment is OFF;
- Case 650 – *Night Ventilation Test* for Low Mass Building. From 18:00 to 07:00 vent fan is ON, from 07:00 to 1800 vent fan is OFF, heating is always OFF, from 07:00 to 18:00 cool is ON if zone temperature is lower than 27°C, otherwise cool is OFF, from 18:00 to 07:00 cool is OFF, vent fan capacity is 1703.16 m<sup>3</sup>/h in addition to specified infiltration rate, and there is no waste heat from fan;
- Case 600FF – *Free Floating Temperature Test* for Low Mass Building, as 600 except that there is no mechanical heating or cooling system;
- Case 650FF – *Free Floating Temperature Test* for Low Mass Building with *Night Ventilation*, as Case 650 except that there is no mechanical heating or cooling system;
- Case 900 – The **Base Case High Mass Building** is the same building model of 600 except for heavier mass wall and floor;
- Case 920 – *East/West Window Orientation Test* for High Mass Building, as 620 except for heavier mass wall and floor;
- Case 940 – *Thermostat Setback Test* for High Mass Building, as 640 except for heavier mass wall and floor;
- Case 950 – *Night Ventilation Test* for High Mass Building, as 650 except for heavier mass wall and floor;

- Case 900FF – Free Floating Temperature Test for High Mass Building, as 900 except that there is no mechanical heating or cooling system;
- Case 950FF – Free Floating Temperature Test for High Mass Building with *Night Ventilation*, as 950 except that there is no mechanical heating or cooling system.

The results of tested cases are reported in the following tables.

**Tab. 16 -Annual Heating Energy Needs Results for ASHRAE BEST TEST and RC model**

ASHRAE Case Number	BESTEST		RC model	Validation Status
	Lower Bound	Upper Bound		
	[MWh]	[MWh]	[MWh]	
600	4,30	5,71	5,18	Yes
620	4,61	5,94	5,08	Yes
640	2,75	3,80	2,46	No
650	0,00	0,00	0,00	Yes
900	1,17	2,04	2,08	No
920	3,26	4,30	3,64	Yes
940	0,79	1,41	1,07	Yes
950	0,00	0,01	0,00	Yes

**Tab. 17 -Annual Cooling Energy Needs Results for ASHRAE BEST TEST and RC model**

ASHRAE Case Number	BESTEST		RC model	Validation Status
	Lower Bound	Upper Bound		
	[MWh]	[MWh]	[MWh]	
600	6,14	8,45	6,52	Yes
620	3,42	5,48	4,56	Yes
640	5,95	8,10	6,25	Yes
650	4,82	7,06	5,23	Yes
900	2,13	3,67	2,79	Yes
920	1,84	3,31	2,94	Yes
940	2,08	3,55	2,61	Yes
950	0,39	0,92	0,78	Yes

**Tab. 18 -Annual Maximum Temperature Results for ASHRAE BEST TEST and RC model**

ASHRAE Case Number	BESTEST		RC model	Validation Status
	Lower Bound	Upper Bound		
	[°C]	[°C]	[°C]	
600FF	64,9	75,1	55,91	No
650FF	63,2	73,5	55,18	No
900FF	41,8	46,4	44,69	Yes
950FF	35,5	38,5	37,41	Yes

**Tab. 19 -Annual Minimum Temperature Results for ASHRAE BEST TEST and RC model**

ASHRAE Case Number	BESTEST		RC model	Validation Status
	Lower Bound	Upper Bound		

	[°C]	[°C]	[°C]	
600FF	-18,8	-15,6	-13,0	No
650FF	-23,0	-21,0	-18,8	No
900FF	-6,4	-1,6	-1,6	Yes
950FF	-20,2	-17,8	-16,3	Yes

Secondary, the model was validated through the European Standard UNI EN 15265 [49] that provide 12 validation tests. European Standards, in fact, does not impose any specific numerical technique for the calculation of the energy requirements for room heating or cooling and the internal temperatures. Accordingly, "*for the validation of any existing or new numerical solution to the assumptions and the procedures defined, the procedures included in this clause shall be satisfied, and the results shall be within the range indicated for each test*".

The UNI EN 15265 *validation cases* are the following:

- 1 – The **Reference case** have external opaque wall and shaded glazing system only on west facade, adiabatic internal vertical wall, adiabatic ceiling and adiabatic floor. The internal gains are 20 W/m<sup>2</sup> (100% convective) from 8:00 to 18:00, only during weekdays. The ventilation rate is 1 ACH from 08:00 to 18:00, only during weekdays, and there are no infiltration. The heating system have a continuous operation all days of the week with a set point for heating of 20°C with no dead band and a set point for cooling of 26°C with no dead band;
- 2 – As test 1 + *change inertia* of ceiling and floor components;
- 3 – As test 1 + *no internal gains*;
- 4 – As test 1 + *no solar protection*;
- 5 – As test 1 + *intermittent heating and cooling* with unlimited power: heating and cooling are used only from 08:00 to 18:00 during weekdays;
- 6 – As test 2 + *intermittent heating and cooling* as for test 5;
- 7 – As test 3 + *intermittent heating and cooling* as for test 5;
- 8 – As test 4 + *intermittent heating and cooling* as for test 5;
- 9 – As test 5 + *external roof*;
- 10 – As test 6 + *external roof*;
- 11 – As test 7 + *external roof*;
- 12 – As test 8 + *external roof*;

The Energy needs results are compared to reference values, as recommended by the Standard, with the following formulation:

$$rQ_{HC} = \left| \frac{(Q_{HC} - Q_{HC,ref})}{Q_{tot,ref}} \right| \quad \text{Eq. (30)}$$

where:

$Q_{HC}$  is the seasonal Energy Needs (separately for Heating and for Cooling) calculated by the RC model;  
 $Q_{HC,ref}$  is the seasonal Energy Needs (separately for Heating and for Cooling) provided by the Standard;  
 $Q_{tot,ref}$  is the yearly Energy Needs (the sum of Heating and Cooling demand) provided by the Standard;  
 $rQ_{HC}$  is the accuracy of the model used.

The model is validated if the resulting  $rQ_{HC}$  is lower than 0.15 and there are three levels of accuracy:

- A if  $rQ_{HC} \leq 0,05$ ;
- B if  $rQ_{HC} \leq 0,10$ ;

- C if  $rQ_{H,C} \leq 0,15$ .

The results of tested cases is reported in the following tables.

**Tab. 20 -Annual Heating and Cooling Results for UNI EN 15256 validation cases.**

Case Number	Heating $rQ_H$	Cooling $rQ_C$	Heating Validation Level	Cooling Validation Level
1	-0,01	0,06	A	B
2	-0,01	0,05	A	B
3	-0,05	0,00	B	A
4	0,02	0,13	A	C
5	-0,05	0,07	B	B
6	-0,10	0,06	C	B
7	-0,21	-0,01	No	A
8	-0,03	0,01	A	A
9	-0,05	0,04	A	A
10	-0,03	0,06	A	B
11	-0,19	0,00	No	A
12	-0,05	0,00	B	A

#### 4.5. OPERATION DATA ANALYSIS

In this research two main inverse models are used; **linear regression** and **ARX model**. The first one is the simplest approach to estimate the line that represents the data collected and, hence, it is able to estimate better linear or nearly linear processes. The ARX model, instead, is an AutoRegressive model with an eXogenous input; it is a regression but correlates the output data in time and, for that reason, it is one of the most used models for estimating dynamical systems [50]. This kind of model (ARX) is also used to estimate the parameters used by the Model Predictive Control described in Section 4.6.

As explained in the previous chapters, a detailed energy simulation, which is normally done during the design phase, is important in order to understand the indicative energy needs of a building, but, during the operation phase of it, the real energy consumptions are often very different with the ones predicted (performance gap problem). Normally the gap is due to different kind of errors and uncertainties occurred during design, construction and operation phases but it can be analyzed and correct using inverse models and parameter identification techniques able to control and monitoring the energy consumptions both online and offline. The inverse modeling techniques, in fact, are able to analyze real data in order to identify and verify some basic parameters of the building operation [35,51,52]; this makes possible to monitor and detect any malfunctions of the building-plant system, but also to calibrate optimization models and predictive control tools [53].

For example, a *linear regression* permits to get a *Global Coefficient of Dispersion* from the analysis of Monthly Energy Consumptions (*energy signature*). Is important to underline that, the heat balance of a building, from which result the energy consumptions, is mainly influenced by the losses and the main parameter that influence the losses is the Global Coefficient of Dispersion that is a sum of the Heat Transfer

Coefficients for Dispersion and Ventilation. This two values, during the design phase are difficult to achieve, the first one because the thermal characteristics of the materials attested by the producers can greatly vary after the installation [54,55], while the second one because it is difficult to predict.

Then, another key feature that affects the thermal balance is the Heat Capacity and, for example, an *ARX model* allows to obtain the *Time Constant* of the building which is the ratio between the Global Capacity and the Global Coefficient of Dispersion, analyzing the Hourly Free-Floating Temperatures.

As already mentioned, however, these inverse models can be used not only for monitoring (off-line), but also for control and optimization techniques (thus on-line). Further, in energy management fields, in fact, it is spreading more and more the use of machine learning techniques which provide to learn, and then to predict and to adapt the systems to different situations, using data analysis.

In conclusion, considering the current developments and recommendation [56], the most effective approach (in terms of cost and benefit ratio) seems to be the following:

- daily and monthly data analysis for static parameters identification;
- hourly data analysis with limited sampling of time intervals (2-3 days) for dynamic parameters identification.

In the next sections will be presented, firstly, the method used to estimate the parameter and solve the inverse models, some comments on the uncertainty analysis and the statistical indices used to evaluate the estimated parameters. Then the inverse models built will be described in order of complexity: starting from the two ARX models used to identify the parameters for the optimization model and then the linear regression used to monitoring the global building dispersion coefficient (H).

#### 4.5.1. PARAMETERS ESTIMATION PROCEDURE AND UNCERTAINTY ANALYSIS

In general, a linear regression has an equation of the form:

$$y_j = \alpha_0 + \alpha_1 x + u_j \quad \text{Eq. (31)}$$

where:

- $j$  is equal to the number of observations,  $j = 1, \dots, n$ ;
- $y_j$  is the dependent variable;
- $x$  is the independent variable;
- $\alpha_0 + \alpha_1 x$  is the regression line;
- $\alpha_0$  is the intercept (the value of  $y$  when  $x = 0$ );
- $\alpha_1$  is the slope of the regression line;
- $u_j$  is the statistical error.

The most common method for estimating the unknown parameters  $x$  in a linear regression model is the method of least-squares (LS). This method calculates the best-fitting line for the observed data by minimizing the differences between the observed data and the regression line, or rather, by minimizing the sum of the squares of the vertical deviations (SSR) from each data point to the line:

$$\min \sum_{j=1}^n (y_j - \hat{y}_j)^2 \quad \text{Eq. (32)}$$

where

- $y_j$  are the observed data;
- $\hat{y}_j$  are the estimated data.

The minimization did for the research is computed in Matlab with the generic LS matrix formulation:

$$X = (A^T A)^{-1} A^T y \quad \text{Eq. (33)}$$

where

- $X$  is the estimated parameters matrix;
- $A$  is the design matrix that contains the independent variables;
- $y$  is the vector of observed data.

As said before, an important consideration is about the accuracy of the estimated parameters and the uncertainty of the data. These can be addressed with two main kind of analysis: *analytical* or *probabilistic*.

The first one is calculated with the *variance-covariance matrix*  $R_x$  that depends, in general, on the "noise corruption" of the observed data expresses with the covariance matrix  $R_y$  [57]. The covariance matrix  $R_y$  usually depends on how the observed data  $y$  are generate and, in the case of uncorrelated errors it is a diagonal matrix with the squared errors of the observed data ( $u_j^2$ ) in the diagonal. It has to be noted that the fully formulation of the LS method is:

$$X = (A^T R_y^{-1} A)^{-1} A^T R_y^{-1} y \quad \text{Eq. (34)}$$

where the covariance matrix  $R_y$  can be eliminated just in case of equally accurate data.

In other cases the whole formulation expressed in Eq. (34) has to be used in order to consider the errors of the observed data  $y$ , while the uncertainty of the estimated parameters is calculated with the *variance-covariance matrix*  $R_x$  as:

$$R_x = A^\dagger R_y (A^\dagger)^T \quad \text{Eq. (35)}$$

with  $A^\dagger = (A^T R_y^{-1} A)^{-1} A^T R_y^{-1}$

In case of *Models 1*, for example, the observed data  $y$  are the monthly energy needs  $Q$ , that can be affected on instrument errors which cause equally accurate errors and, thus, Eq.(33) can be used. However the energy needs can be convert, for example in the daily average power  $q$  [ $W/m^3$ ] in order to directly correlate global coefficient of dispersion  $H$  in a more convenient unit, with the following equation:

$$q = \frac{Q}{\Delta T \cdot V} \quad \text{Eq. (36)}$$

where

- $q$  the daily average power [ $W/m^3$ ];
- $Q$  the monthly energy needs [ $kWh$ ];
- $\Delta T$  are the number of hours of the month [ $h$ ];
- $V$  is the volume of the heated/cooled space [ $m^3$ ].

The uncertainty of observed data, in this case, is due to three errors:

- $u_{(Q)}$  which depends on instrument errors [58];
- $u_{(\Delta T)}$  which depends on the accuracy of the moment in which the monthly energy need is recorded (i.e. if it is recorded the same day and the same hour every month);
- $u_{(V)}$  which depends on the accuracy of the measurement of the heated/cooled volume.

Thus, it is calculated as:

$$u_{(q)}^2 = \left( \frac{1}{\Delta t \cdot V} \right)^2 u_{(Q)}^2 + \left( -\frac{Q}{\Delta t^2 \cdot V} \right)^2 u_{(\Delta T)}^2 + \left( -\frac{Q}{\Delta t \cdot V^2} \right)^2 u_{(V)}^2 \quad \text{Eq. (37)}$$

Having different numbers of hours for each month, the final errors in  $R_y$  are non equally accurate, thus, the Eq.(34) has to be used. This is important to underline that inverse models are very delicate and we must be very careful managing the data.

The probabilistic approach, instead, can be based on the bootstrapping method [59]. The latter is founded on the fact that, having a certain amount of observed data  $y$ , it is possible to see the variation of the estimated parameters  $x$ , varying more times the sample of observed data. Basically, the objective is to estimate the parameters many times, each time using a different part of the observed data, so as to obtain a probabilistic distribution of the parameters.

Finally some statistical indices about the regression can be calculated. One of the most used is the coefficient of determination R-squared ( $R^2$ ) that represent an indicator of the goodness of the regression model, evaluating how the data fit the estimated values. The  $R^2$  can assume values from 0 to 1, where 1 means that the data fitting is perfect and the formula is:

$$R^2 = 1 - \frac{\sum_{j=1}^n (y_j - \hat{y}_j)^2}{\sum_{j=1}^n (y_j - \bar{y})^2} \quad \text{Eq. (38)}$$

where

- $n$  is the number of observed data;
- $y_j$  are the observed data;
- $\hat{y}_j$  are the estimated data;
- $\bar{y}$  is the average of observed data;
- the numerator is also called Sum of Square Residual (SSR);
- the denominator is also called Total Sum of Square (TSS).

Other two statistical indices are calculated in order to evaluate the estimation; the Nominal Mean Base Error (NMBE) and the Coefficient of Variation (CV) Root Mean Square Error (RMSE) [60]. The first measures the bias between estimated and observed data but, due to a compensation effect it is assessed together with the CV(RMSE) which is calculated as the RMSE normalized to the mean of the observed values [61]. These indices are defined as:

$$NMBE = \frac{1}{\bar{y}} \frac{\sum_{j=1}^n (y_j - \hat{y}_j)}{n-1} \cdot 100\% \quad \text{Eq. (39)}$$

$$CV(RMSE) = \frac{1}{\bar{y}} \sqrt{\frac{\sum_{j=1}^n (y_i - \hat{y}_i)^2}{n-1}} \cdot 100\% \quad \text{Eq. (40)}$$

where

- $n$  is the number of observed data;
- $y_j$  are the observed data;
- $\hat{y}_j$  are the estimated data;
- $\bar{y}$  is the average of observed data.

Finally, a simple regression can be used in order to calibrate and analyze some static and monthly data. In order to develop the linear regression and to explore the total heat transfer coefficient of the building, the first direct problem that is considered is a simplified steady state thermal balance.

#### 4.5.2. SIMPLIFIED DIRECT MODEL

In general, the building thermal load can be expressed, for heating and cooling season, as the sum of gains and losses, or rather the difference between the outgoing and the incoming loads:

$$\Delta Q_h = Q_{out} - f_h Q_{in} \quad \text{Eq. (41)}$$

$$\Delta Q_c = Q_{in} - f_c Q_{out} \quad \text{Eq. (42)}$$

where  $Q_{in}$  and  $Q_{out}$  are respectively the incoming and outgoing loads and  $f_h$  and  $f_c$  are monthly heat gains and heat losses utilization factors [39].

In a simplified way the incoming and the outgoing loads can be expressed as:

$$Q_{in} = Q_{sol} + Q_{int} \quad \text{Eq. (43)}$$

$$Q_{out} = Q_{ve} + Q_{tr} \quad \text{Eq. (44)}$$

where:

- $Q_{sol}$  is the heat loads from solar radiation;
- $Q_{int}$  is the heat loads from internal source (occupancy, electrical equipment, lighting ecc.);
- $Q_{ve}$  is the heat loads due to air exchange (infiltration and natural and mechanical ventilation);
- $Q_{tr}$  is the heat loads due to envelope transmission.

The *Heat Loads* are expressed, in a simplified **steady state** models, as:

$$Q_{sol} = I_{sol} \quad \text{Eq. (45)}$$

$$Q_{int} = \sum q_{int} \quad \text{Eq. (46)}$$

$$Q_{ve} = mc(\theta_i - \theta_e) = H_{ve}(\theta_i - \theta_e) \quad \text{Eq. (47)}$$

$$Q_{tr} = \sum UA(\theta_i - \theta_e) = H_{tr}(\theta_i - \theta_e) \quad \text{Eq. (48)}$$

where:

- $I_{sol}$  is the solar radiation [ $\text{W}/\text{m}^2$ ];
- $q_{int}$  are the internal gains [ $\text{W}/\text{m}^2$ ];
- $m$  is the ventilation rate [ $\text{kg}/\text{s}$ ];
- $c$  is the specific heat of air [ $\text{kJ}/\text{kgK}$ ];
- $\theta_i$  and  $\theta_e$  are the internal and external temperatures [ $^{\circ}\text{C}$ ];
- $U$  is the thermal transmittance [ $\text{W}/\text{m}^2\text{K}$ ];
- $A$  is the area [ $\text{m}^2$ ];
- $H_{ve}$  is the global Heat transfer coefficient for ventilation [ $\text{W}/\text{K}$ ];
- $H_{tr}$  is the global Heat transfer coefficient for Transmission [ $\text{W}/\text{K}$ ].

Based on these assumptions, the building thermal load during the heating and cooling period are defined as:

$$\begin{aligned} \Delta Q_h &= (Q_{ve} + Q_{tr}) - f_h(Q_{sol} + Q_{int}) \\ &= H_{ve}(\theta_i - \theta_e) + H_{tr}(\theta_i - \theta_e) - f_h(I_{sol} + \sum q_{int}) \\ &= H(\theta_i - \theta_e) - f_h(I_{sol} + \sum q_{int}) \end{aligned} \quad \text{Eq. (49)}$$

$$\begin{aligned} \Delta Q_c &= (Q_{sol} + Q_{int}) - f_c(Q_{ve} + Q_{tr}) \\ &= I_{sol} + \sum q_{int} - f_c H_{ve}(\theta_i - \theta_e) + f_c H_{tr}(\theta_i - \theta_e) \\ &= I_{sol} + \sum q_{int} - f_c H(\theta_i - \theta_e) \end{aligned} \quad \text{Eq. (50)}$$

Where  $H$  is the sum of the heat transfer coefficient for transmission  $H_{tr}$  and ventilation  $H_{ve}$  [62,63].

Then, in order to explore also the global capacitance of the building, a **dynamic** expression of heat exchange is needed. The building capacitance  $C$  can be assumed as the ratio between the hourly thermal balance and the internal temperatures variations during the same hour in a free-floating condition:

$$\begin{aligned} C &= \frac{\Delta Q d\tau}{d\theta_i} = \frac{H(\theta_{i,t} - \theta_{e,t}) + Q_{sol}}{(\theta_{i,t+1} - \theta_{i,t})} \\ (\theta_{i,t+1} - \theta_{i,t}) &= \frac{H}{C}\theta_{i,t} + \frac{H}{C}\theta_{e,t} + \frac{Q_{sol}}{C} \\ \theta_{i,t+1} &= (1 - \frac{H}{C})\theta_{i,t} + \frac{H}{C}\theta_{e,t} + \frac{f}{C}I_{sol} \end{aligned} \quad \text{Eq. (51)}$$

where:

- $C$  is the global thermal capacity of the building [ $J/m^2K$ ];
- $\Delta Q d\tau$  is the energy variation during time  $t$ ;
- $d\theta_i$  is the internal air temperature variation during time  $t$ .

Based on Eq. (49), (50) and (51) the inverse models have been formulated, as described in the following paragraphs.

#### 4.5.3. SIMPLIFIED INVERSE MODEL

Starting from Eq. (49) and (50) the regression *Model 1* (Table 21) is created to derive physical parameters as in *energy signature* methodology [64]: correlating external temperature  $\theta_e$  and the average daily thermal power  $q$  it is possible to obtain the global heat transfer coefficient  $H$ .

**Tab. 21 - Model formulation for linear regression.**

	Inverse Model	Regression Coefficient
<b>Model 1</b>	$q_h = \alpha_0 + \alpha_1 \theta_e + u$	$\alpha_0 \cong H\theta_i + f_h I_{sol} + \sum q_{int}$
		$\alpha_1 \cong -H$
	$q_c = \beta_0 + \beta_1 \theta_e + u$	$\beta_0 \cong I_{sol} + \sum q_{int} - f_c H\theta_i$
		$\beta_1 \cong f_c H$

It has to be noted that, with the heating data regression, the  $H$  is directly obtained while, with summer consumptions, the estimated parameter contains also the  $f_c$  factor, thus, it is not the pure  $H$  value.

Further, with the estimated parameters also the Balance Point Temperature  $\theta_{bp}$  can be derived as shown in Table 22.

**Tab. 22 - Estimated Parameters from linear regression (Model 1).**

Element			Regression Parameter	Uncertainty
H	Heat Transfer Coefficient	[W/K]	$\alpha_1$	$\Delta \alpha_1$
$\theta_{bp}$	Balance Point Temperature	[°C]	$-\alpha_0/\alpha_1$	$(\alpha_0/\alpha_1) \sqrt{[(\Delta\alpha_0/\alpha_0)^2 + (\Delta\alpha_1/\alpha_1)^2]}$

The latter refers to the outdoor temperature for which the heating rate flux is zero or rather the set-point temperature is reached without energy needs; it also permits to derive the average free-running temperature  $\theta_{fr}$  [63] as:

$$\theta_{fr} = \theta_i + \theta_e - \theta_{bp} \quad \text{Eq. (52)}$$

The free-running temperature  $\theta_{fr}$  represents the average internal temperature in free-floating condition and it can be helpful in order to estimate the possibility to use free-cooling and ventilation during the middle season (spring and autumn) [63]. Using the graphical view (Fig. 12) it is possible to see that: (i)

the heating system will be turn ON when the free-running temperature is lower than the heating set-point temperature, (ii) the *ventilation* can be used when the free-running temperature is higher than the heating set-point temperature and the external temperature is lower than the cooling set point temperature, (iii) the *free-cooling* will be usable when the free-running temperature is higher than the cooling set-point temperature and the external temperature is lower than the cooling set-point temperature, (iv) the cooling system will be turn ON when the external temperature is higher than the cooling set-point temperature [63]. Further, with the graphical view it is possible to see directly the Balance Point temperatures for heating and cooling seasons which, in this case, are respectively around 11 and 26 °C. It means that the heating system will be turned ON when the external temperature will be under 11°C, the cooling system if upper than 26 °C while the ventilation and free-cooling between 11 and 26 °C.

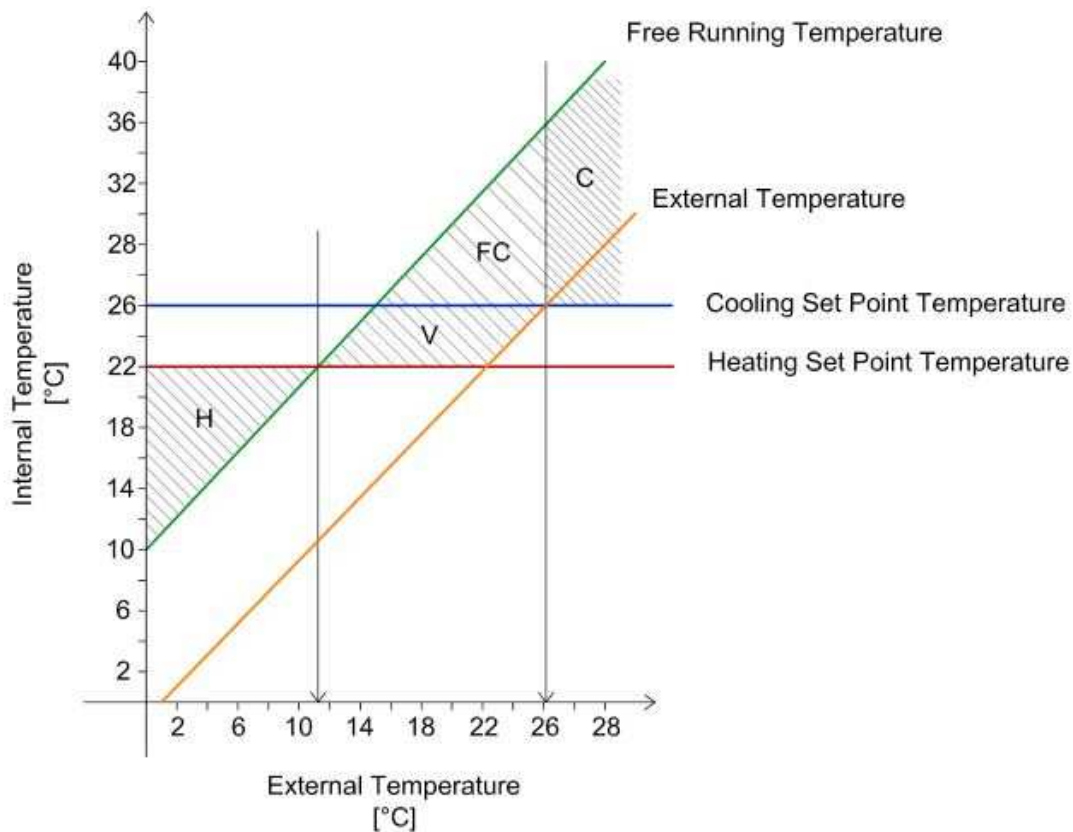


**Figure 12.** Graphical view of internal conditions during the year respect the external temperature; H is the heating period, V is the ventilation period, FC is the free-cooling period and C is the cooling period.

It has to be noted that, this graph and the corresponding free-running temperature can be used in a "static" way (using the linear regression with monthly energy needs) in order to give a general idea of the internal conditions compared to the external temperature during the whole year, but it can be more useful, in case of an online calculation and a continuous calibration of the free running temperature, considering also hourly data of internal gains and solar radiation. Further, the Balance Point Temperature and the consequent Free Running temperature has to be calculated with both heating and cooling energy needs linear regressions; for simplicity here just one graph is reported but in the following chapter more details will be presented.

Based on Eq.(51) instead, the ARX model is formulated.

**Tab. 23 -Model formulation for ARX Model.**

	Inverse Model	Regression Coefficient
<b>Model 2</b>	$\theta_{i,t+1} = \gamma_0 + \gamma_1\theta_{i,t} + \gamma_2\theta_{e,t} + u$	$\gamma_0 \cong \frac{f}{C} I_{sol} + u$
		$\gamma_1 \cong (1 - \frac{H}{C})$
		$\gamma_2 \cong \frac{H}{C}$

In this case, the ARX model permits to evaluate the *time constant*  $\tau$  of the building using hourly data of internal free-floating temperature ( $\theta_i$ ) and outdoor temperature ( $\theta_e$ ). The time constant  $\tau$  is calculated as the ratio between the heat capacity C and the global heat loss coefficient H and measures how rapidly the internal temperature changes according to external inputs [65]. It should be underlined that, the time constant is a dynamic parameter and, in fact, is derived by hourly data.

**Tab. 24 - Estimated Parameters from ARX Model (Model 2).**

Element		Regression Parameter	Uncertainty
$\tau$	Time Constant [h]	$1/\gamma_2$	$\Delta \gamma_2 / (\gamma_2)^2$

Considering both the insulation and the inertia, the time constant is able to express the building dynamic better than the heat loss coefficient; buildings, in fact, do not respond instantaneously to the external or internal heat sources and, also during the winter, the influence of the mass can be high. Further, the time constant has a direct effect on the evaluation of (i) comfort, because influences also the surface temperature and thus the operative temperature, and (ii) energy savings, because it explains the possibility to store energy and, thus, the intermittent heating managing.

#### 4.6. MODEL PREDICTIVE CONTROL

As anticipated, in recent years, a fast development of technical and control tools for energy optimization is ongoing. The main characteristic that are needed to enable this development are:

- Ability to predict energy needs and relevant quantities for modeling comfort;
- Usability in real time (online) operation.

A Model Predictive Control (MPC) consists of an optimization model able to run online and suitable to determine control actions with an optimized logic. Therefore, MPC is itself an optimization model, which follows the general structure described in Section 4.3.

In general, the following data are used in modeling:

- Objective function:
  - Energy demand;
  - Cost of energy services;
  - CO<sub>2</sub> emission.

- Variables:
  - Power demand (continuous);
  - Violations of set-point temperature (continuous) [34];
  - Technical system activation (binary, switch among two comfort model [66-68]).
- Constraints:
  - Power (always positive);
  - Temperature bounds (considering violations);
  - Power limits (maximum power dependent on system sizing);
  - Boundary conditions (initial-final temperature);
  - Comfort bounds (identify violations of bounds with respect to comfort categories, in a graphical or numerical way).

The first goal, in this research, is to reduce the energy demand (and consequently the related use of energy carriers for building services), keeping the internal temperatures within a certain comfort band, determined based on comfort models. Thus, first the model of thermal building dynamics has to be described in order to obtain the internal temperatures. After that, the comfort model has to be considered to formulate constraints (predicted internal temperatures will have to remain within boundaries). In conclusion in the following paragraph these two essential elements will be shown:

- Model Predictive Control formulation (optimization model used for control purpose);
- Fanger Comfort Model reduction [66-68] suitable for the implementation in MPC.

#### 4.6.1. OPTIMIZATION MODEL FOR MPC

The optimization model for MPC is formulated in order to find the minimum energy needs that satisfies the constraints with a limited possibility to violate them, or rather with a certain flexibility on the set-point temperatures [34]. In general, the objective function can incorporate economic (operation cost) and environmental (CO<sub>2</sub> emission) criteria, but in this case the priority is given to the quantification of the energy savings. The optimization model is formulated as follows:

$$\begin{aligned}
 & \min \sum \Phi_{H,j} + \sum \Phi_{C,j} && \text{Eq. (53)} \\
 \text{s.t.} & \quad \forall_j \Phi_{H,j} \leq \Phi_{H,\max} \\
 & \quad \forall_j \Phi_{C,j} \leq \Phi_{C,\max} \\
 & \quad \forall_i \sum_{j=1}^n (\theta_{sp,H,j} - \theta_{red,H,j}) \leq \theta_{red,limit,i} \\
 & \quad \forall_i \sum_{j=1}^n (\theta_{red,C,j} - \theta_{sp,C,j}) \leq \theta_{red,limit,i} \\
 & \quad \forall_j (\theta_{sp,H,j} - \theta_{red,H,j}) \leq \theta_{red,limit,j} \\
 & \quad \forall_j (\theta_{red,C,j} - \theta_{sp,C,j}) \leq \theta_{red,limit,j} \\
 & \quad \forall_j (\theta_{red,H,j} \times \sigma_{H,j}) \geq (\theta_{sp,H,j} \times \sigma_{H,j}) \\
 & \quad \forall_j (\theta_{red,C} \times \sigma_{C,j}) \leq (\theta_{sp,C} \times \sigma_{C,j})
 \end{aligned}$$

variables<sup>12</sup>:  $\Phi_H$ ,  $\Phi_C$ ,  $\theta_{red,H}$ ,  $\theta_{red,C}$

where

- $j$  is the hourly value;
- $i$  is the daily value;
- $\Phi_H$  is the calculated hourly energy needs for heating period;
- $\Phi_C$  is the calculated hourly energy needs for cooling period;
- $\Phi_{H,max}$  is the maximum power available during the heating period;
- $\Phi_{C,max}$  is the maximum power available during the cooling period;
- $\theta_{red,H}$  are the degree-hours violated during the heating period calculated by the MPC;
- $\theta_{red,C}$  are the degree-hours violated during the cooling period calculated by the MPC;
- $\theta_{red,limit}$  are the maximum degree-hours/day of violation required;
- $\theta_{sp,H}$  is the hourly set point temperature for heating period;
- $\theta_{sp,C}$  is the hourly set point temperature for cooling period.
- $\sigma_H$  is the hourly mode of heating system (ON or OFF);
- $\sigma_C$  is the hourly mode of cooling system (ON or OFF);

#### 4.6.2. COMFORT MODEL

As explained before, once obtained the prediction of internal temperatures based on the actual ones, a comfort model has to be added and it is derived from Fanger Theory [66-68].

The premise of the environmental well-being is due to a set of physical variables and the HVAC systems have just the purpose of controlling appropriately the values of some of these quantities within the built environment.

The main parameters from which the thermal comfort depends are *temperature*, *humidity* and *air velocity*, but also the *radiant temperature* and the *air quality* can be evaluated. As mentioned, the MPC presented in this research will control two main variables that are the *indoor air temperature*  $\theta_{i,t+1}$  and the *surface temperature*  $\theta_{s,t+1}$  (which represents the radiant temperature). Finally the *operative temperature*  $\theta_{op,t+1}$  is derived in a simplified way from the previous two temperatures as:

$$\theta_{op,t+1} = (f_{op} \times \theta_{i,t+1}) + [(1 - f_{op}) \times \theta_{s,t+1}] \quad \text{Eq. (54)}$$

where  $f_{op}$  is a percentage that can be chosen<sup>13</sup>.

Further the human thermal sensation is tied to the human body thermal energy balance which is influenced by physical activity (metabolic rate) and from clothing. The *metabolic rate*  $M$  expresses the energy produced by the body in a range of time, that is partially converted in work  $L$  and partially in heat load  $Q$ ; the unit is the MET that represents the metabolic rate in a quite condition and is equal to  $58 \text{ W/m}^2$  where the area is referred to the human body and is set equal to an average of  $1,8 \text{ m}^2$ . The next table reassumes the main values of  $M$  that can be referred to the residential and tertiary uses [66,67].

<sup>12</sup> All the variables have to be positive

<sup>13</sup>The same equation is used in the RC model (sections 4.2.3 and 4.2.5, Tables 7 and 10) as suggested by the Standard 13790:2008 with a  $\gamma$  equal to 0.3.

**Tab. 25 -Metabolic Rates due to different kind of Activity.**

Activity	Metabolic rate (M)	
	W/m <sub>2</sub>	MET
Lying	46	0.8
Sitting	58	1.0
Sedentary	70	1.2
Light standing	93	1.6
Average Standing	116	2.0
Walking (2-5 km/h)	110-200	1.9-3.4

The *clothing* variable is calculated with its resistance  $I_{cl}$  and the unit is the CLO (0,155 m<sup>2</sup>K/W) that corresponds on an average resistance of a "European cloth used in a medium season". The next table reassumes the main values of clothing that can be referred to the residential and tertiary uses in temperate weather [66].

**Tab. 26 –Clothes Resistances due to different kind of clothes.**

Clothes	Clothes Resistance (I <sub>cl</sub> )	
	m <sup>2</sup> K/W	CLO
Naked	0	0
Summer Clothing	0.05	0.3
Medium Clothing for Internal use	0.11	0.7
Winter Clothing for Internal use	0.16	1
Winter Clothing for External use	0.23	1.5

The human body thermal balance, in conclusion, can be assumed as:

$$Q = M - E - B - (R + C) \quad \text{Eq. (55)}$$

where

- Q is the thermal power emits or absorbed by the human body;
- M is the metabolic rate;
- E is the thermal power dispersed for evaporation;
- B is the sensible heat dispersed with breathing;
- R is the thermal power dispersed for radiation;
- C is the thermal power dispersed for convection.

In order to have a comfort model, thus, is important to evaluate the well-being condition that is reached with a condition of "thermal equilibrium" or rather when Q is equal to zero [66-68].

Then, Professor Fanger presents a theory based on a statistical global index of the well-being condition called PMV (Predicted Mean Vote). The PMV expresses a numerical vote of the thermal feeling between 7 different conditions.

**Tab. 27 -PMV from Fanger Theory**

PMV	Thermal Feeling
+ 3	Too Hot
+ 2	Hot
+ 1	Warm
0	Neutral
- 1	Cool
- 2	Cold
- 3	Too Cold

A simplified expression of the PMV formulation [69] can be used when the Metabolic rate is between 1 and 2 MET, the air velocity is lower than 0.1 m/s and the clothes resistance is higher than 0.5 CLO. The reduced model has an acceptable accuracy also outside these boundaries, for example with air velocity up to 0.2 m/s and clothes resistance of 0.4 CLO. It is easy to see that, for a generic tertiary and residential uses, this conditions are satisfied and the equation is:

$$PMV = (0.092 - 0.03M) \left[ \frac{43.61M + 40.12MI_{Cl} + 14.61I_{Cl} + 4.44(\theta_i + \theta_{mr}) - 305}{1 + 1.38I_{Cl}} \right] \quad \text{Eq. (56)}$$

where

- M is the metabolic range;
- $I_{Cl}$  is the clothes resistance;
- $\theta_i$  is the internal air temperature;
- $\theta_{mr}$  is the mean radiant temperature that is set equal to the surface temperature  $\theta_s$ .

In conclusion, using Eq.(56) it is possible to verify if the predicted temperatures  $\theta_{i,t+1}$  and  $\theta_{s,t+1}$  lead to an acceptable PMV, otherwise the action variables  $u$  on the state space model will be changed. The limits of acceptable PMV is considered an input.

#### **4.7. MODEL OUTPUT AND VISUALIZATION OF RELEVANT QUANTITIES**

Finally, it is possible to summarize the relevant quantities that are obtained as model output and are suitable for visualization. The objective of the research is proposing an integrated direct and inverse modeling approach to be used across building life cycle phases, able to support multiple tasks such as performance monitoring, energy management, predictive control, etc.

Visualization is necessary in all tasks that are, of course, automated but require, at the same time, a supervision by practitioners. The relevant quantities are subdivided according to thermal zone and system levels and to the dynamic and stationary models and reported in the following table.

**Tab. 28 - Static and Dynamic Data for Zone and System level.**

<b>ZONE LEVEL</b>	<b>DYNAMIC</b>	Internal air temperature, surface temperature (mean radiant), operative temperature, verify set-point/set-back temperature
		Violation of set-point heating/cooling
		External air temperature
		PMV – PDD
		Adaptive comfort boundary
		Load profile (heating/cooling)
		Part-load operation of technical systems
		Occupancy patterns Vs Technical system operation patterns
	<b>STATIONARY</b>	Building balance (monthly)
		Energy signatures
Free running temperature		
Bin data method		
<b>SYSTEM LEVEL</b>	<b>DYNAMIC</b>	Cost function (electricity tariffs)
		Cost (dynamic)
		Load matching (buy/sell to grid)
		Load matching (production/demand) (eventually integration with other MILP strategies for optimization of whole-site energy management, including storage)
		Part load operation of technical systems
		Virtual storage, dispatch flexibility
	<b>STATIONARY</b>	Building balance at the meter level (buy/sell to grid)
		Building balance at the meter level (production/demand)

In this way, it is possible to identify all the relevant elements that are necessary with respect to the multiple tasks reported before, both at the whole-building level (system level) and at single zone level. The subdivision according to dynamic and stationary models depends on the granularity of data available, for dynamic models hourly/sub-hourly data are available, for stationary models daily/monthly data are available.

## LIST OF REFERENCES

- [1] Hazyuk I, Ghiaus C, Penhouet D. Optimal temperature control of intermittently heated buildings using Model Predictive Control: Part I – Building modeling. *Building and Environment*. 2012;51:379-87.
- [2] Oldewurtel F, Parisio A, Jones CN, Gyalistras D, Gwerder M, Stauch V, et al. Use of model predictive control and weather forecasts for energy efficient building climate control. *Energy and Buildings*. 2012;45:15-27
- [3] Privara S, Cigler J, Váňa Z, Oldewurtel F, Sagerschnig C, Žáčková E. Building modeling as a crucial part for building predictive control. *Energy and Buildings*. 2013;56:8-22.
- [4] Gao T, Schumacher B, Hegetschweiler W, Gwerder M, Tschanz M, Walti M. Multizone building with VAV Air-Conditioning System simulation for evaluation and test of control systems. *Bi-annual IBPSA Building Simulation Conference*. Beijing, China2007
- [5] Trčka M, Hensen JLM, Wetter M. Co-simulation for performance prediction of integrated building and HVAC systems – An analysis of solution characteristics using a two-body system. *Simulation Modeling Practice and Theory*. 2010;18:957-70.
- [6] Afram A, Janabi-Sharifi F. Gray-box modeling and validation of residential HVAC system for control system design. *Applied Energy*. 2015;137:134-50
- [7] Privara S, Cigler J, Váňa Z, Oldewurtel F, Sagerschnig C, Žáčková E. Building modeling as a crucial part for building predictive control. *Energy and Buildings*. 2013;56:8-22.
- [8] Maasoumy M, Sangiovanni-Vincentelli A. Total and peak energy consumption minimization of building hvac systems using model predictive control. *IEEE Design & Test of Computers*. 2012;29.
- [9] Candanedo JA, Dehkordi VR, Lopez P. A control-oriented simplified building modeling strategy. *13thConf Intl Building Perf Simulation Ass*. Chambéry, France2013.
- [10] Hazyuk I, Ghiaus C, Penhouet D. Optimal temperature control of intermittently heated buildings using Model Predictive Control: Part II – Control algorithm. *Building and Environment*. 2012;51:388-94.
- [11] Yudong M, Borrelli F, Hancey B, Packard A, Bortoff S. Model Predictive Control of thermal energy storage in building cooling systems. *Decision and Control, 2009 held jointly with the 2009 28th Chinese Control Conference CDC/CCC 2009 Proceedings of the 48th IEEE Conference on*. Shanghai, P.R. China2009. p. 392-7.
- [12] Lute P, van Paassen D. Optimal indoor temperature control using a predictor. *Control Systems, IEEE*. 1995;15:4-10.
- [13] Morari M, H. Lee J. Model predictive control: past, present and future. *Computers & Chemical Engineering*. 1999;23:667-82.
- [14] Široký J, Oldewurtel F, Cigler J, Privara S. Experimental analysis of model predictive control for an energy efficient building heating system. *Applied Energy*. 2011;88:3079-87.
- [15] Wang S, Jin X. Model-based optimal control of VAV air-conditioning system using genetic algorithm. *Building and Environment*. 2000;35:471-87.
- [16] Zavala V, Skow D, Celinski T, Dickinson P. Techno-economic evaluation of a next-generation building energy management system. *Technical Report ANL/MCS-TM-313*, Argonne National Laboratory; 2011.
- [17] Zacekova E, Privara S. Control relevant identification and predictive control of a building. *Control and Decision Conference (CCDC), 2012 24th Chinese*. Taiyuan, China2012. p. 246-51.
- [18] Madsen H, Holst J. Estimation of continuous-time models for the heat dynamics of a building. *Energy and Buildings*. 1995;22:67-79.
- [19] Ferkl L, J. S, Privara S. Model predictive control of buildings: The efficient way of heating. *Control Applications (CCA), 2010 IEEE International Conference on*. Yokohama, Japan2010. p. 1922-6.
- [20] Mahdavi A. Simulation-based control of building systems operation. *Building and Environment*. 2001;36:789-96.
- [21] Giretti A, Lemma M, Larghetti R, Ansuini R. Environmental modeling for the optimal energy control of subway stations. *Gerontechnology*. 2012;11:168.

- [22] Jiménez MJ, Madsen H. Models for describing the thermal characteristics of building components. *Building and Environment*. 2008;43:152-62.
- [23] Scacchi W. Experience with software process simulation and modeling. *Journal of Systems and Software*. 1999;46:183-92.
- [24] Bacher P, Madsen H. Identifying suitable models for the heat dynamics of buildings. *Energy and Buildings*. 2011;43:1511-22.
- [25] Fouquier A, Brun A, Faggianelli GA, Suard F. Effect of wall merging on a simplified building energy model: accuracy vs number equations. 13thConf Intl Building Perf Simulation Ass. Chambéry, France2013.
- [26] Zavala VM. Real-Time Optimization Strategies for Building Systems†. *Industrial & Engineering Chemistry Research*. 2012;52:3137-50.
- [27] Gwerder M, Tödtli J. Predictive control for integrated room automation. 8th REHVA World Congress Clima. Lausanne, Switzerland2005.
- [28] Wen J, Smith TF. Development and validation of online models with parameter estimation for a building zone with VAV system. *Energy and Buildings*. 2007;39:13-22.
- [29] Mendes N, Oliveira R. Energy efficiency and thermal comfort analysis using the powerdomushydrothermal simulation tool. 9th International IBPSA Conference. Montréal, Canada2005.
- [30] Kramer R, van Schijndel J, Schellen H. Inverse modeling of simplified hygrothermal building models to predict and characterize indoor climates. *Building and Environment*. 2013;68:87-99.
- [31] Braun JE. Reducing energy costs and peak electrical demand through optimal control of building thermal storage1990.
- [32] European Commission, Programme IEE (Intelligent Energy Europe), Building EQ - The EPBD and Continuous Commissioning - Tools and methods for linking EPDB and continuous commissioning. 2007.
- [33] Froisy JB. Model predictive control—Building a bridge between theory and practice. *Computers & Chemical Engineering*. 2006;30:1426-35.
- [34] Gwerder M, Gyalistras D, Sagerschnig C, Smith RS, Sturzenegger D, Final Report: Use of weather and occupancy forecast for optimal building climate control (Opticontrol), Automatic Control Laboratory, ETH Zurich, Switzerland, 2013.
- [35] International Energy Agency (IEA - EBC), Annex 58: Reliable Building Energy Performance Characterization based on full scale dynamic measurement.
- [36] R. Snieder, J. Trampert, *Inverse Problems in Geophysics*, Samizdat Press, 1999, [http://samizdat.mines.edu/snieder\\_trampert/](http://samizdat.mines.edu/snieder_trampert/)
- [37] M. Bertero, P. Boccaccio, *Introduction to Inverse Problems in Imaging*, IOP Publishing, Bristol 1998
- [38] J. B. Keller, *Inverse Problems*, *The American Mathematical Monthly* (Mathematical Association of America), Vol. 83, No. 2 (Feb., 1976), pp. 107-118, <http://www.jstor.org/stable/2976988>
- [39] UNI EN ISO 13790:2008, Energy performance of buildings, Calculation of energy use for space heating and cooling.
- [40] UNI EN ISO 13791:2012 Thermal performance of buildings - Calculation of internal temperatures of a room in summer without mechanical cooling - General criteria and validation procedures.
- [41] UNI EN ISO 13792:2012 Thermal performance of buildings Calculation of internal temperatures of a room in summer without mechanical cooling - Simplified methods.
- [42] UNI EN 15255:2008, Energy performance of buildings - Sensible room cooling load calculation - General criteria and validation procedures.
- [43] ISO 52000:2014, Energy performance of buildings - Overarching EPB assessment
- [44] Gueymard C. (2000) Prediction and performance assessment of mean hourly global radiation, *Solar Energy* 68.
- [45] Belli L, Irraggiamento solare superficiale: messa a punto di un metodo di calcolo e validazione, Tesi di laurea, 2013.
- [46] ASHRAE Handbook 2009 - Fundamentals.
- [47] Krarti M, *Weatherization and Energy Efficiency Improvement for Existing Homes: An Engineering Approach*, CRC Press, 2012.

- [48] ANSI/ASHRAE Standard 140-2011, Standard Method of Test for the Evaluation of Building Energy Analysis Computer Programs.
- [49] EN 15265:2007, Energy performance of buildings. Calculation of energy needs for space heating and cooling using dynamic methods. General criteria and validation procedures.
- [50] B. Carlsson, Linear regression Systems and Control, Department of Information Technology, Uppsala University, August 31, 2011
- [51] H. Masuda, D. E. Claridge, Estimation of Building Parameters Using Simplified Energy Balance Model and Metered Whole Building Energy Use, Proceedings of the Twelfth International Conference for Enhanced Building Operations, Energy Systems Laboratory, Manchester, UK, October 24–25 (2012)
- [52] O. Mejri – B. Peuportier – A. Guiavarch: “Comparison of different method for estimating the building envelope thermal characteristics”, 13th Conference of building performance simulation association, Chambéry 2013
- [53] V.S.K.V. Harish, A. Kumar, Reduced order modeling and parameter identification of a building energy system model through an optimization routine, Applied Energy, Vol. 162, pp. 1010-1023, 2016.
- [54] F. Asdrubali, F. D’Alessandro, G. Baldinelli, F. Bianchi, Evaluating in situ thermal transmittance of green buildings masonries—A case study, Case Studies in Construction Materials, Vol. 1, pp. 53–59, 2014.
- [55] UNI 10351:1994, Building materials - Thermal conductivities and vapour permeabilities.
- [56] ASHRAE RP-1404 - Measurement, modeling, analysis and reporting protocols for short-term M&V of whole building energy performance, 2014.
- [57] B. Carlsson, Linear regression Systems and Control, Department of Information Technology, Uppsala University, August 31, 2011
- [58] ENEA, M. Dell’Isola, P. Vigo, G. Ficco, L. Celenza, Analisi e caratterizzazione metrologica dei sistemi di misura delle reti termiche distribuite, 2014
- [59] Singh K, Xie M, Bootstrap: A Statistical Method, Rutgers University, USA. Retrieved from <http://www.stat.rutgers.edu/home/mxie/RCPapers/bootstrap.pdf> (2008).
- [60] ASHRAE Guideline 14-2002, Measurement of Energy and Demand Savings
- [61] E. Fabrizio, V. Monetti, Methodologies and Advancements in the Calibration of Building Energy Models, Energies, Vol. 8, pp. 2548-2574, 2015
- [62] L. Tronchin, M. Manfren, L.C. Tagliabue, Multi-scale analysis and optimization of building energy performance—Lessons learned from case studies, Sustainable Cities and Society, 2015.
- [63] C. Ghiaus, Equivalence between the load curve and the free-running temperature in energy estimating methods, Energy and Buildings, 38 (2006), pp. 429–435
- [64] ISO EN 16346:2013, Energy performance of buildings — Assessment of overall energy performance
- [65] J. Karlsson, Possibilities of Using Thermal Mass in Buildings to Save Energy Cut Power Consumption Peaks and Increase the Thermal Comfort, Lund Institute of Technology, Lund University, 2012
- [66] UNI EN ISO 7730:2006, Ergonomia degli ambienti termici - Determinazione analitica e interpretazione del benessere termico mediante il calcolo degli indici PMV e PPD e dei criteri di benessere termico locale.
- [67] EN 15251:2007, Indoor environmental input parameters for design and assessment of energy performance of buildings addressing indoor air quality, thermal environment, lighting and acoustics.
- [68] ANSI/ASHRAE Standard 55:2013 Thermal Environmental Conditions for Human Occupancy.
- [69] Energy management - UNI CEI 11339:2009, Master Training Documents.

## 5. APPLICATIONS

Following the general structure of chapter 3.6. on BACS and Building Energy Management and the reduced order Building Energy Models described in chapter 4., a case study is used in order to analyze the overall methodology presented in the thesis. Starting from a phase of Operation Data Analysis (see chapter. 4.5.), in fact, the Model Predictive Control (see chapter. 4.6.) was used to optimize the energy consumptions and evaluate the internal comfort.

In detail, the following steps are described in this chapter:

- comparison between detailed and simplified energy simulation models;
- direct model calibration by means of data analysis;
- parameter identification with inverse models;
- optimization and energy management.

It should be recalled that the research goal is to obtain a procedure that can analyze and verify different moments (e.g. seasons, week and weekend, hours of the day etc.) and, thus, operation typology (e.g. heating, cooling, ventilation etc.) required to control and monitoring the energy needs, aimed at optimizing and, therefore, reducing the consumptions ensuring the desired comfort.

As already explained in Chapter 3, often, the actual data needed to run an optimization algorithm are not available, then it is possible to use a building simulation model and identification technique in order to get them. Anyway, to do this, the model has to be easily calibrated with some real data. To calibrate a detailed energy simulation software, such as EnergyPlus (EP) or Trnsys, it's very complicated because of the high number of input data needed. Hence, the lumped parameters model (RC) is investigated and used here.

Firstly, a comparison between models is presented in order to verify that the calculated energy from the simplified model (RC) corresponds to what is calculated using the detailed one (EP), then, through data analytics the optimization phase will be shown. Starting from monthly actual data the main lumped parameter (heat transfer coefficient  $H$  and global capacity  $C$ ) will be analyzed to calibrate the model and then, with hourly data simulated with the calibrated model, the identification phase will be tested. It has to be underlined that, in case of available data concerning hourly thermal energy demand, internal air and surface temperatures, the identification phase can be done directly with them.

Finally the optimization algorithm (MPC) is used in order to show the possible energy saving comparing with the comfort category.

### 5.1. CASE STUDY DESCRIPTION

The case study is a residential complex located in Rodano, province of Milan (latitude  $45^{\circ}28'N$ , longitude  $9^{\circ}21'E$  and altitude 112 meters a.s.l). The total area is about  $10'800\text{ m}^2$  and the built area is approximately  $14'800\text{ m}^2$  ( $7'500\text{ m}^2$  above ground and  $7'300\text{ m}^2$  underground). The property in-

cludes three buildings arranged around a courtyard and composed of a basement, two floors and an attic floor with a total of 59 housing units. The buildings are directly connected to each other through the basement where all the service areas, technical rooms, garages and direct accesses to the staircases are located. In the central courtyard, finally, two separate buildings designed for specific activities have been planned (i.e. gym and common room).

**Tab. 29 - Apartments distribution on the case study.**

Building	Number of Apartments	Gross Floor Area (above ground) [m <sup>2</sup> ]
1	16	2'137
2	13	1'441
3	30	3'976
Tot	59	7'554

The building design followed some simple sustainable rules as window shading and natural ventilation strategies. Regarding the shading analysis, the area is free from external buildings that obstruct the solar radiation, while the complex is configured such as to avoid as much as possible the self-shading. Every single building, however, has deep overhangs on the worst orientation achieving, in summer, to stop the incident solar radiation. Then, natural ventilation has been favored in almost all units by a double facing layout, allowing an effective cross ventilation that can be used as a passive cooling system and for air quality improvement.



**Figure 13. Case Study: Ground Floor Plan.**

The orientation is basically imposed by the presence of the internal court, towards the bigger openings over look; Buildings 1 and Buildings 3 are mainly oriented along the North-South axis while Building 2, the smallest one, is oriented on the East-West axis. Thus, Buildings 1 has the main view on West, Building 2 on South and Building 3 on East; an exception is made for the apartments on the southern part of Buildings 1 and Buildings 3 that have this facade more widely opened.

Finally, the building structure consists of pillars and slabs and special care has been taken on the thermal characteristics of the external components (e.g. windows, wall, roof and basement) that have been designed to have a low transmittance value (the average transmittance of opaque components is  $0.2 \text{ W/m}^2\text{K}$  while for the windows is  $1.35 \text{ W/m}^2\text{K}$ ) and a high global thermal capacity in order to assure a time lag of more than 14 hours.

**Tab. 30 - Main characteristics of opaque components in design phase**

<b>Component</b>	<b>Thickness</b> [m]	<b>Transmittance</b> [ $\text{W/m}^2\text{K}$ ]	<b>Time lag Module</b> [h]
External Wall of Apartments	0.49	0.19	23
External Wall of Cellars	0.48	0.22	23
External Wall of Attic	0.25	0.19	9
Wall between Staircase and Apartments	0.39	0.34	11
Wall between Apartments	0.32	0.38	12
Wall between Apartments and Hollow Spaces	0.26	0.32	7
Wall between Garage	0.15	1.47	3
Wall between Garage and Hollow Spaces	0.48	0.21	20
Wall of Hollow Spaces	0.40	2.64	10
Wall between Hollow Spaces	0.24	0.20	7
Floor of Garage (on ground)	0.68	1.50	18
Floor of Staircase (on ground)	0.83	0.30	2
Floor of Cellars (on ground)	0.89	0.24	21
Floor of Hollow Space (on ground)	0.50	2.12	13
External Floor of Apartments	0.57	0.21	21
Floor of Apartment (on staircase)	0.55	0.23	19
Floor of Apartment (on hollow spaces)	0.58	0.20	22
Roof of Apartment	0.21	0.17	4
External Ceiling of Apartment	0.62	0.21	21
Roof of Garage, Staircases and Cellars_1	0.43	0.23	14
Roof of Garage, Staircases and Cellars_2	0.45	0.23	14
Ceiling of Apartment (on hollow space)	0.39	0.27	13
Internal Floor of Apartments	0.50	0.38	18

**Tab. 31 - Main characteristics of transparent components in design phase**

<b>Transparent Component</b>	<b>Dimensions</b> [m]	<b>Transmittance</b> [ $\text{W/m}^2\text{K}$ ]	<b>Solar Heat Gain Factor</b> [-]
TC_1	1.4 x 0.9	1.37	0.57
TC_2	1.6 x 2.7	1.35	0.54
TC_3	0.7 x 2.7	1.37	0.57
TC_4	1.5 x 2.4	1.35	0.54
TC_5	1.4 x 2.4	1.35	0.54
TC_6	0.7 x 1.5	1.36	0.57
TC_7	1.6 x 2.4	1.35	0.54
TC_8	1.4 x 1.5	1.35	0.54

TC_9	2.4 x 2.7	1.35	0.54
TC_10	0.8 x 0.8	1.8	0.57
TC_11	0.8 x 2.1	1.35	0.54
TC_12	1.4 x 2.1	1.35	0.54
TC_13	0.7 x 1.2	1.8	0.57
TC_14	0.6 x 0.8	1.8	0.57
TC_15	0.6 x 1.0	1.8	0.57
TC_16	1.6 x 1.5	1.35	0.54
TC_17	1.4 x 1.4	1.36	0.57
TC_18	2.6 x 2.7	1.35	0.54
TC_19	1.0 x 2.4	1.35	0.54
TC_20	0.7 x 2.4	1.35	0.54
TC_21	0.7 x 2.1	1.36	0.54
TC_22	1.0 x 1.0	1.36	0.57

Furthermore, the HVAC systems were chosen with the aim to improve the energy performances of the buildings, reducing the consumption and integrating renewable energy sources. The heating system is a geothermal Heat Pump (HP) using water from the heat exchanger installed into the foundation slab, and, alternately with groundwater pumped through a bore. The main technical details of the HP are: nominal peak power of 240 kW, COP equal to 4.6 with an inlet temperature of 35°C and the EER equal to 6.4 with an inlet temperature of 22°C. The delivery system consists of radiant floor panels (used both in heating and cooling period). Specially in heating operation, using a lower water circulation temperature (35-45 °C), and this solution is able to increase the efficiency of the system with respect to a traditional system with radiators. In summer, instead, the water temperature has to be controlled in order to avoid condensations on the floor surface. This is guaranteed both by the presence of relative humidity probes and by the Air Handling Units (AHUs). Finally, the renewable energy is produced by a photovoltaic system composed by two main parts; the first is dedicated to the common areas and is composed by 416 modules (620 m<sup>2</sup>) facing south and installed on the northern part of the garden with a peak capacity of about 87 kW<sub>p</sub>. The second is dedicated to the private consumptions and occupies a total area of about 480 m<sup>2</sup> with 215 panels located on the roofs and oriented on East and West with a total peak power of 19.46 kW<sub>p</sub>.

Then, a home automation system permits to monitor and control different areas:

- the internal conditions of each thermal zone (temperature and humidity values);
- the systems configurations (the operational state of the plants, the water temperatures on the distribution systems, the power used by the HP, etc.);
- the external consumptions as emergency lighting, emergency power supply and irrigation of green areas.

## 5.2. BUILDING ENERGY SIMULATIONS

The case study was used, in a first step, in order to evaluate the simplified model explained in Chapter 4. First of all a comprehensive energy simulation models based on EnergyPlus (EP) [1] that

is a detailed building energy simulation software including all relevant building physical processes, is presented. The detailed simulation is useful to compare the results obtained with the lumped parameter model (RC) in order to demonstrate that the latter is accurate enough although for the analysis of more complex building than the *best tests* rooms used for the validation [2,3].

The building used for this first step simulation phase is Building 1 as it can be considered a mean between Building 3 that is the biggest and most used and the Building 2 that is almost empty. This is important to be stressed because the unsold apartments have a negative influence on the consumptions increasing the global heat transfer coefficient of the building.

**Tab. 32 - Unsold Apartments in the Case Study buildings**

	Total number of apartments	Unsold apartments 2014-2015		Unsold apartments 2015-2016	
		Count	Percentage	Count	Percentage
Building 1	16	4	25%	4	25%
Building 2	13	9	70%	7	54%
Building 3	30	10	37%	4	13%

### 5.2.1. DETAILED SIMULATION

In order to run the detailed simulation with EnergyPlus, the building has been divided in different zones; in particular the 16 apartments have been divided into 28 thermal zones and the other common spaces in 19 non-heated zones, or rather 3 staircase blocks, 4 garage areas, 2 big hollow spaces in the basement and 10 little hollow spaces in the attic floor.

**Tab. 33 - Thermal Zones Division of Apartments**

Apartment Number	Staircase	Floor	Thermal Zone Code	Heated Floor Area[m <sup>2</sup> ]
1	A	Ground Floor	1_E1_GF	62
2	A	Ground Floor	2_E1_GF	107
3	A	Ground Floor	3_E1_GF	79
4	A	First Floor	4_E1_FF	84
	A	Attic	4_E1_A	66
5	A	First Floor	5_E1_FF	75
	A	Attic	5_E1_A	53
6	A	First Floor	6_E1_FF	71
	A	Attic	6_E1_A	75
7	A	First Floor	7_E1_FF	75
	A	Attic	7_E1_A	68
8	B	Basement	8_E1_B	46
	B	Ground Floor	8_E1_GF	82
9	B	Basement	9_E1_B	46
	B	Ground Floor	9_E1_GF	81
10	B	First Floor	10_E1_FF	82

	B	Attic	10_E1_A	64
11	B	First Floor	11_E1_FF	81
	B	Attic	11_E1_A	63
12	C	Basement	12_E1_B	46
	C	Ground Floor	12_E1_GF	67
13	C	Ground Floor	13_E1_GF	99
14	C	First Floor	14_E1_FF	67
	C	Attic	14_E1_A	49
15	C	First Floor	15_E1_FF	42
	C	Attic	15_E1_A	33
15_bis	C	First Floor	15bis_E1_FF	57
	C	Attic	15bis_E1_A	46

**Tab. 34 - Non-Heated Zones of Building 1.**

Staircase	Floor	Thermal Zone Code	Floor Area [m <sup>2</sup> ]
Staircase_A	Basement to First Floor	A_E1	135
Staircase_B	Basement to First Floor	B_E1	81
Staircase_C	Basement to First Floor	C_E1	81
Garage_A	Basement	A_E1_B	37
Garage_B	Basement	B_E1_B	142
Garage_C	Basement	C_E1_B	120
Garage_D	Basement	D_E1_B	45
HollowSpace_A	Basement	INT_A_E1_B	367
HollowSpace_B	Basement	INT_B_E1_B	157
HollowSpace_Apt4	Attic	INT_4_E1_A	5
HollowSpace_Apt5	Attic	INT_5_E1_A	19
HollowSpace_Apt6	Attic	INT_6_E1_A	7
HollowSpace_Apt7	Attic	INT_7_E1_A	8
HollowSpace_Apt10	Attic	INT_10_E1_A	3
HollowSpace_Apt11	Attic	INT_11_E1_A	3
HollowSpace_Apt10-11	Attic	INT_10-11_E1_A	4
HollowSpace_Apt14	Attic	INT_14_E1_A	3
HollowSpace_Apt14-15	Attic	INT_14-15_E1_A	9
HollowSpace_Apt15bis	Attic	INT_15bis_E1_A	3

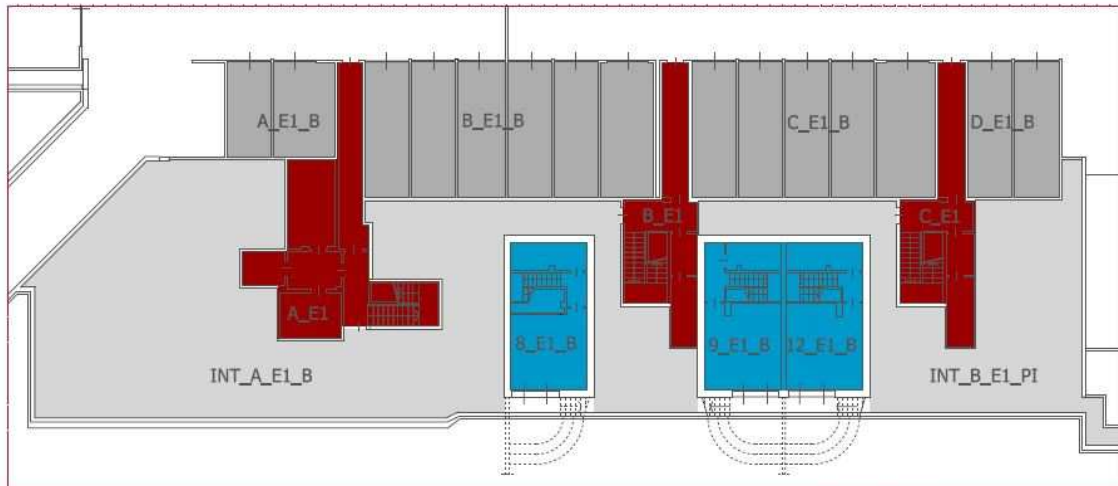


**Figure 14. Basement Plan of Building 1.**

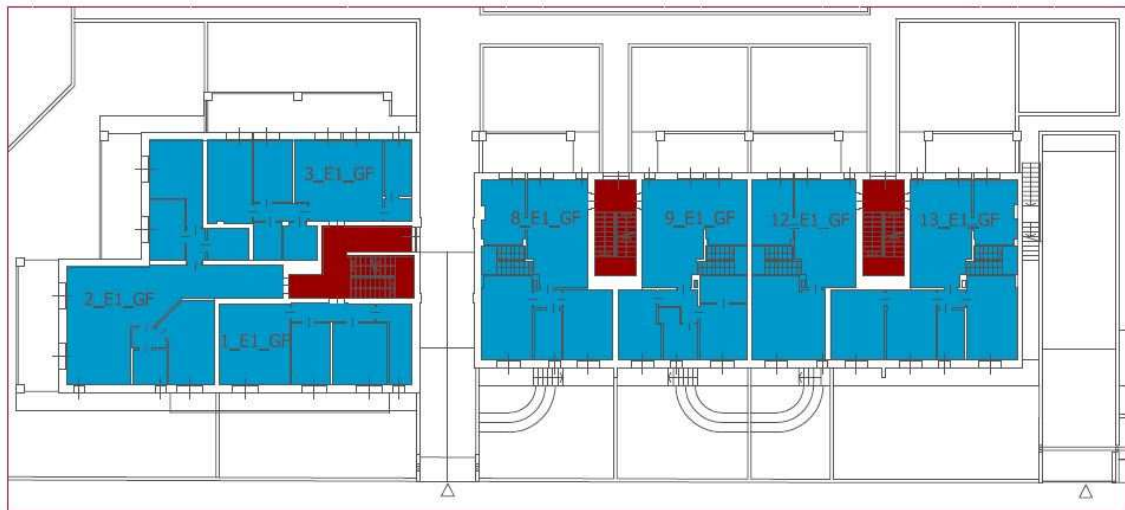


**Figure 15. Ground Floor Plan of Building 1.**

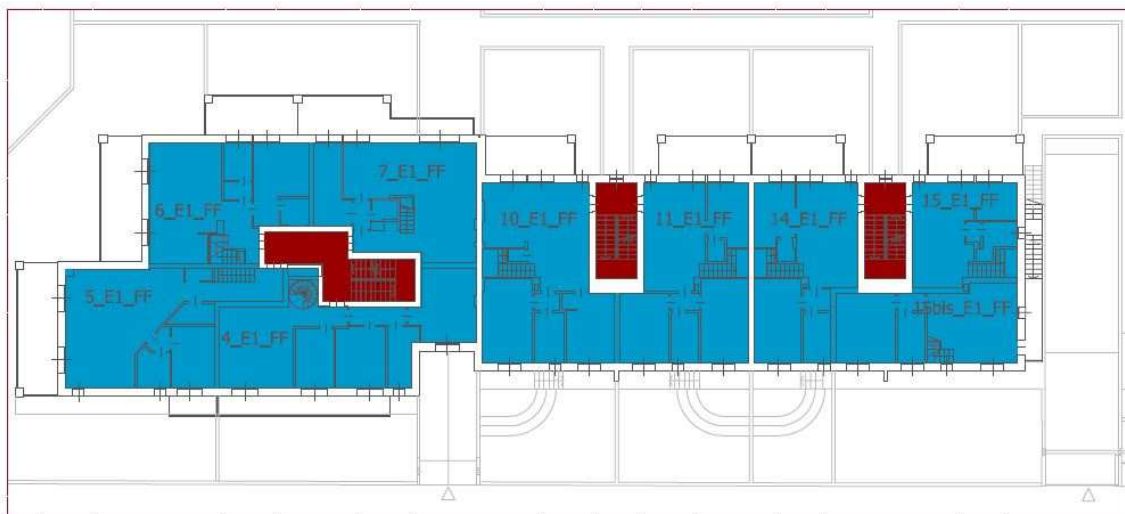


**Figure 16. First Floor Plan of Building 1.**

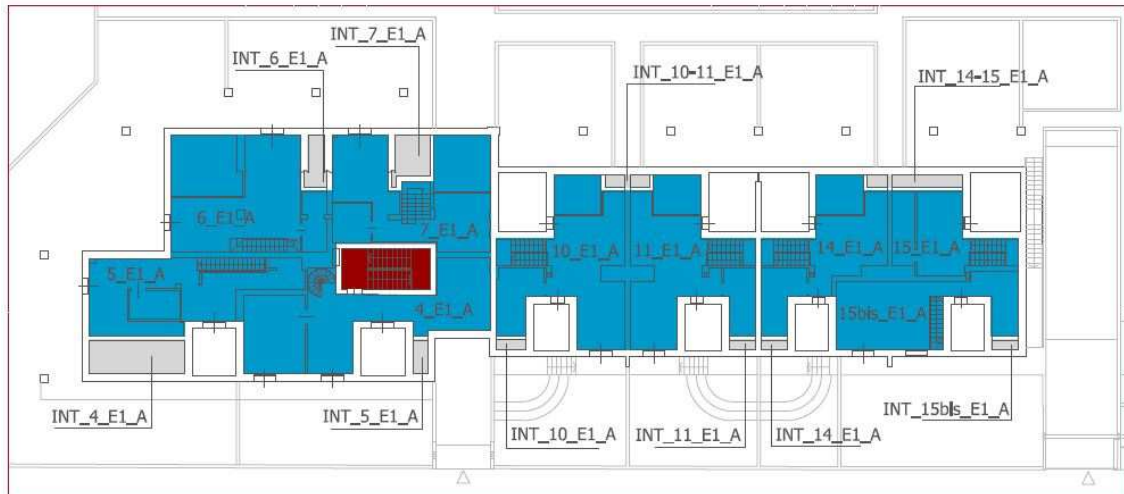


**Figure 17. Attic Floor Plan of Building 1.**

Then, for each thermal zone, all the opaque and transparent components have to be assigned; the materials and the relative thermal characteristics are listed on the next table. In detail, 23 opaque components with 31 different materials (of which more 11 are insulation layers) and 22 transparent components (Tab. 31 - Main characteristics of transparent components in design phase1) are used. It has to be note that all the data come from technical sheets and drawings given by the builders.

**Tab. 35 - Materials used for the detailed simulation**

<b>Name of Single Layer Material</b>	<b>Thickness [m]</b>	<b>Conductivity [W/mK]</b>	<b>Density [kg/m<sup>3</sup>]</b>	<b>Specific heat [J/kgK]</b>
Brick High Resistance 1	0.120	0.251	600	840
Brick High Resistance 2	0.080	0.231	700	840
Brick High Resistance 3	0.120	0.190	930	840
Brick Vela Alveolater 1	0.150	0.201	800	1000
Brick Vela Alveolater 2	0.200	0.220	800	1000
Brick Vela Alveolater 3	0.380	0.140	725	1000
Ceramic Tile	0.020	1.163	2000	840
Concrete	0.20	1.909	2400	1000
Expanded Polystyrene (EPS)	0.080	0.036	30	1340
Fir 1	0.080	0.150	450	1700
Fir 2	0.025	0.120	450	1700
Hollow-core Concrete Slab	0.250	0.740	1800	840
Lightweight Screed with EPS	Variable	0.088	350	1000
Mortar	Variable	0.900	1800	1000
Radiant Floor Panels	0.025	0.037	125	1030
Reinforced Concrete	Variable	1.910	2500	850
Reinforced Concrete Slab	0.200	1.910	2500	850
Rock Wool Panel Airrock	0.060	0.035	70	1030
Rock Wool Panel Durock 1	0.080	0.033	170	1030
Rock Wool Panel Durock 2	0.120	0.038	170	1030

Rock Wool Panel Frontrock 1	Variable	0.036	90	1030
Rock Wool Panel Hardrock	0.160	0.040	190	1030
Rock Wool Panel Superrock	0.080	0.035	35	1030
Rock Wool Rigid Panels 1	0.050	0.040	150	1030
Rock Wool Rigid Panels 2	0.100	0.035	150	1030
Screed (sand and cement)	Variable	0.930	1800	840
Sound Dampening Panels	0.005	0.033	100	920
Vapor Barrier	0.002	0.187	30	900
Waterproof Barrier	0.008	0.230	1700	900
Wood Fibers Panels	0.020	0.067	300	1500
Wood Panels OSB	0.019	0.140	620	1700

Finally, schedules have been created in order to describe the operation of the building and users' profiles. In detail, as shown in Tables 36-37, a *continuous profile* considers, for used apartments (*heated zones*), continuous internal gains (IG), natural ventilation air changes (NV), heating and cooling operation set-points (H,C) while an *intermittent profile* considers, for used apartments, continuous internal gains and natural ventilation but the heating system is ON 10 hours for 183 days (from 15<sup>th</sup> of October to 15<sup>th</sup> of April) and the cooling system is ON 10 hours for 182 days (from 16<sup>th</sup> of April to 14<sup>th</sup> of October). The H/C schedule is really used in the case study and, thus, it will be used for all the other simulations in this chapter as the "actual" H/C schedule.

For *non-heated zone* as non-sold apartments, garages, staircases and hollow spaces other values are assigned and, in detail, non-sold apartments and hollow spaces are considered with no internal gains and a minimum air change rate due to infiltrations while garages and staircases are considered with higher natural ventilation and low internal gains due to lighting (see Table 38).

**Tab. 36 - General Schedules for Heated Zones**

	Unit	Continuous Operation	Intermittent Operation
<b>Internal Gain (IG)</b>	[W/m <sup>2</sup> ]	4	4
	[h/day]	24	24
	[day/year]	365	365
<b>Natural Ventilation (NV)</b>	[1/h]	0,3	0,3
	[h/day]	24	24
	[day/year]	365	365
<b>Heating System (H)</b>	[°C]	22	Variable
	[h/day]	24	10
	[day/year]	183	183
<b>Cooling System (C)</b>	[°C]	26	Variable
	[h/day]	24	10
	[day/year]	182	182

**Tab. 37 - Hourly Schedules for Heated Zones**

Hours	Continuous Operation				Intermittent Operation			
	IG	NV	H	C	IG	NV	H	C
	[W/m <sup>2</sup> ]	[1/h]	[°C]	[°C]	[W/m <sup>2</sup> ]	[1/h]	[°C]	[°C]

1	4	0.3	22	26	4	0.3	19	30
2	4	0.3	22	26	4	0.3	19	30
3	4	0.3	22	26	4	0.3	19	30
4	4	0.3	22	26	4	0.3	19	30
5	4	0.3	22	26	4	0.3	19	30
6	4	0.3	22	26	4	0.3	19	30
7	4	0.3	22	26	4	0.3	22	26
8	4	0.3	22	26	4	0.3	22	26
9	4	0.3	22	26	4	0.3	22	26
10	4	0.3	22	26	4	0.3	19	30
11	4	0.3	22	26	4	0.3	22	26
12	4	0.3	22	26	4	0.3	22	26
13	4	0.3	22	26	4	0.3	22	26
14	4	0.3	22	26	4	0.3	22	26
15	4	0.3	22	26	4	0.3	19	30
16	4	0.3	22	26	4	0.3	22	26
17	4	0.3	22	26	4	0.3	22	26
18	4	0.3	22	26	4	0.3	19	30
19	4	0.3	22	26	4	0.3	19	30
20	4	0.3	22	26	4	0.3	19	30
21	4	0.3	22	26	4	0.3	22	26
22	4	0.3	22	26	4	0.3	19	30
23	4	0.3	22	26	4	0.3	19	30
24	4	0.3	22	26	4	0.3	19	30

**Tab. 38 - Schedule for Non-heated zones**

Non-Heated Zone	Unit	Garage and Stair Case	Hollow Space and unsold Apartments
<b>Internal Gain (IG)</b>	[W/m <sup>2</sup> ]	2	0
	[h/day]	24	24
	[day/year]	365	365
<b>Natural Ventilation (NV)</b>	[1/h]	0,5	0,1
	[h/day]	24	24
	[day/year]	365	365

The climate data used are real measurements of external temperature and solar radiation in Rodano during the years 2014 and 2015 from Arpa Lombardia [4].

By comparing the data collected with other available climate files it is possible to note that both the outdoor temperature and the global solar radiation are higher than the average values. It has to be underlined, finally, that the data from January to September are referred to the year 2015 while data from October to December are referred the 2014; this is because the analyses have been focused on the real energy consumptions from heating season 2014-2015 and, consequently, data from October 2014 to April 2015 have been needed. In the next figures the monthly averages of the main climate data are shown.

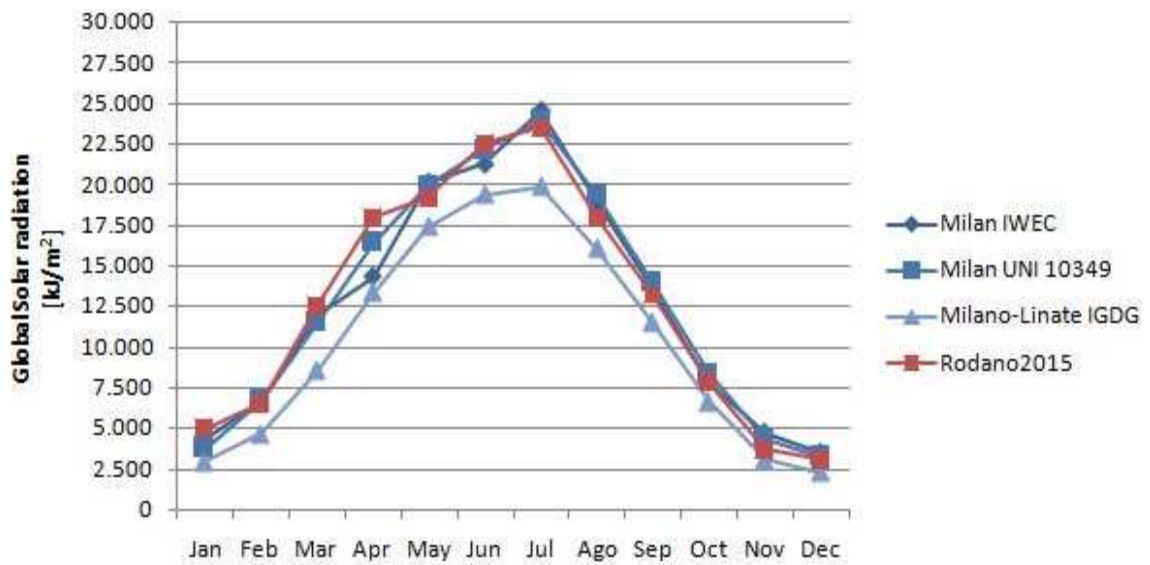


Figure 18. Horizontal Solar Radiation distribution from different Weather Files.



Figure 19. External Temperature distribution from different Weather Files.

In conclusion the results are presented, in the next table and graph are listed both monthly and seasonal energy needs calculated with the detailed simulation of the case study model, in continuous and intermittent operations as explained in Tables 36-38.

Tab. 39 - Energy Needs simulated with EnergyPlus for Building 1.

	Heating Energy Needs		Cooling Energy Needs	
	Continuous Operation	Intermittent Operation	Continuous Operation	Intermittent Operation
	[kWh]	[kWh]	[kWh]	[kWh]
January	9673	8577	0	0
February	8218	7265	0	0

March	3396	2897	0	0
April	193	144	222	151
May	0	0	3171	2518
June	0	0	7625	6341
July	0	0	12149	10662
August	0	0	7811	6688
September	0	0	2694	2370
October	214	117	91	77
November	4186	3290	0	0
December	8989	7782	0	0
Year	34868	30070	33763	28807

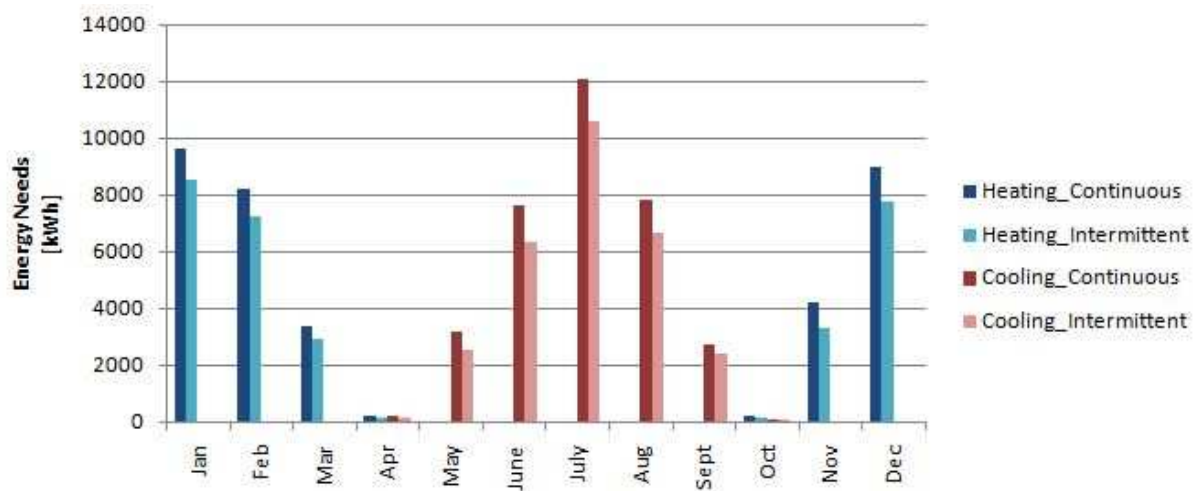


**Figure 20. Monthly Energy Demand simulated with EnergyPlus.**

Although the actual operation mode is the "intermittent" one, both the operations are simulated in order to have more configuration to compare with the simplified models. The goal, here, in fact, is to verify that the energy requirements calculated with the detailed model is equal to that calculated from the simplified model, and it will be presented in the following sections.

### 5.2.2. SIMPLIFIED SIMULATION

In order to run the simplified simulation with the RC model presented in Chapter 4. the following input data have been collected. In detail, the model allows to analyze a thermal zone for a time; having more apartments you can choose to simulate each zone separately or, as here performed, to consider the building as an equivalent thermal zone. The surfaces in contact with non-heated spaces are considered *exterior*. Further, it has to be underlined that both the linear (LP) and non-linear (NLP) model formulations were run obtaining the same results. All the results and data as from "RC" model are concerning both the direct models.

**Tab. 40 - Geometrical Input for RC model**

Geometrical Item	Unit	Value
Total exterior surface N	[m <sup>2</sup> ]	376
Total exterior surface E	[m <sup>2</sup> ]	526
Total exterior surface S	[m <sup>2</sup> ]	399
Total exterior surface W	[m <sup>2</sup> ]	471
Total surface roof	[m <sup>2</sup> ]	608
Ratio between transparent and total surface N	[-]	0.01
Ratio between transparent and total surface E	[-]	0.12
Ratio between transparent and total surface S	[-]	0.10
Ratio between transparent and total surface W	[-]	0.23
Ratio between transparent and total surface roof	[-]	0.02
Ground surface	[m <sup>2</sup> ]	535
Gross floor area	[m <sup>2</sup> ]	1610
Net floor area	[m <sup>2</sup> ]	1369
Gross volume	[m <sup>3</sup> ]	4833
Net volume	[m <sup>3</sup> ]	3697

Then, the main characteristics of the considered components are listed, as the transmittance of opaque and transparent external surfaces, windows, walls, basement and roof and the overall thermal capacity. The shading factor can be indicated with a single value through the solar gain factor or with hourly coefficients that may vary for all the hours of the year. To ease the simulation it is initially introduced a solar gain factor equal to 0.30 calculated starting from the geometric designs of the building. The thermal capacity, finally, has been defined according to the values provided by the UNI EN ISO 13790 [5] for *heavy* construction components.

**Tab. 41 - Default values for dynamic parameters provided by UNI EN ISO 13790 [5]**

Class	Monthly and seasonal method	Simple hourly method	
	C <sub>m</sub> [J/k]	A <sub>m</sub> [m <sup>2</sup> ]	C <sub>m</sub> [J/K]
Very light	80 000 x A <sub>f</sub>	2.5 x A <sub>f</sub>	80 000 x A <sub>f</sub>
Light	110 000 x A <sub>f</sub>	2.5 x A <sub>f</sub>	110 000 x A <sub>f</sub>
Medium	165 000 x A <sub>f</sub>	2.5 x A <sub>f</sub>	165 000 x A <sub>f</sub>
<b>Heavy</b>	<b>260 000 x A<sub>f</sub></b>	<b>3.0 x A<sub>f</sub></b>	<b>260 000 x A<sub>f</sub></b>
Very heavy	370 000 x A <sub>f</sub>	3.5 x A <sub>f</sub>	370 000 x A <sub>f</sub>

**Tab. 42 - Physical characteristic of building component used for RC simulation**

Building Component Item	Unit	Value
Exterior wall transmittance	[W/m <sup>2</sup> K]	0.19
Roof transmittance	[W/m <sup>2</sup> K]	0.17
Ground (ISO 13370 methodology for energy analysis) transmittance	[W/m <sup>2</sup> K]	0.20
Transparent surfaces transmittance	[W/m <sup>2</sup> K]	1.35
Frame fraction coefficient for transparent surfaces	[-]	0.2
Solar gain coefficients for transparent surfaces with perpendicular radiation	[-]	0.3

Opaque surfaces absorbance external walls	[-]	0.3
Opaque surfaces absorbance roof	[-]	0.6
Opaque frame absorbance transparent surfaces	[-]	0.6
Global thermal capacity per m <sup>2</sup> of floor area	[J/m <sup>2</sup> K]	260000
Multiplier of surface for effective mass area	[-]	3.00

The building operation data are the same as the ones used by the detailed model, or rather for the used apartments because no schedules are required for non-heated zones.

**Tab. 43 - Building Operation Data used for RC simulation**

Heating set-point temperature zone	$\theta_{int,H,set-point}$	[°C]	22.0
Cooling set-point temperature zone	$\theta_{int,C,set-point}$	[°C]	26.0
Heating set-back temperature zone	$\theta_{int,H,set-back}$	[°C]	19.0
Cooling set-back temperature zone	$\theta_{int,C,set-back}$	[°C]	30.0
Heating/Cooling schedule		[-]	Variable <sup>14</sup>
Air change rate natural ventilation/infiltration		[1/h]	0.3
Natural ventilation/infiltration schedule		[-]	00:00-23:00
Internal gains		[W/m <sup>2</sup> ]	4.00
Internal gains schedule		[-]	00:00-23:00

The weather file is derived from Arpa hourly data used for the detailed simulation but, as explained in section 4.2.7, the RC model uses daily average data and hourly coefficients in order to reconstruct the daily profiles.

**Tab. 44 - Daily climate data used for RC simulation**

	External Temperature	Global Solar Radiation
	[°C]	[kJ/m <sup>2</sup> ]
January	4.1	5009
February	4.4	6577
March	10.0	12573
April	14.4	18023
May	19.2	19215
June	23.5	22549
July	28.1	23540
August	24.2	18028
September	19.0	13237
October	15.7	7840
November	10.6	3689
December	5.3	3076

Below, the figures are showing the profiles of each representative day of the month reconstructed from the RC model, concerning both the outdoor temperature that the horizontal solar radiation.

<sup>14</sup> As reported in Tables 36 and 37

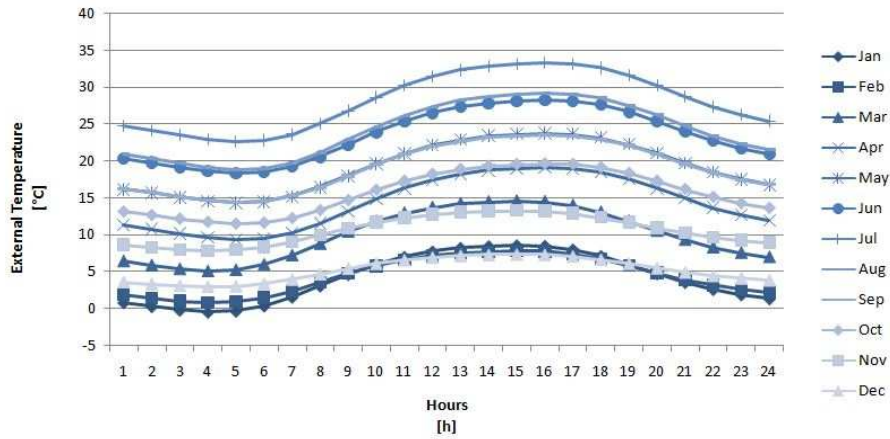


**Figure 21. Daily Profiles of External Temperature used by the RC model.**

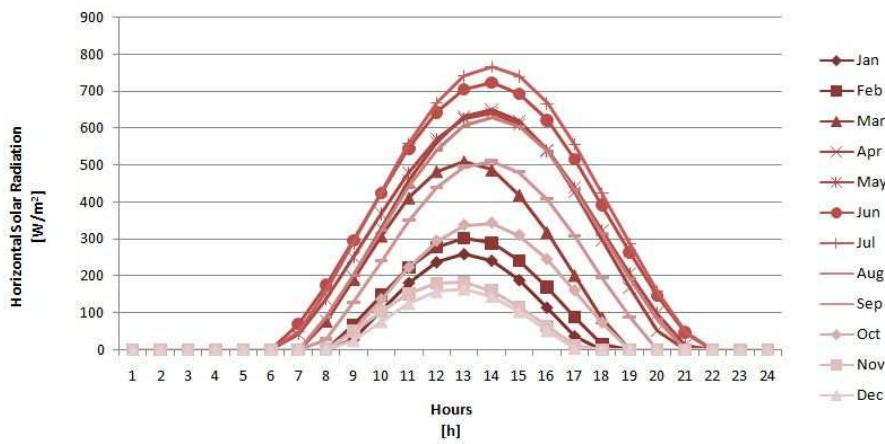


**Figure 22. Daily Profiles of Horizontal Solar Radiation used by the RC model.**

### 5.2.3. COMPARISONS

The results from RC model are presented and compared with monthly energy needs obtained with the detailed simulation (EP). Although the seasonal results are almost identical, considering the monthly requirements you can make a distinction; major differences are concerning the intermediate seasons.

**Tab. 45 - Comparison between Monthly Energy Needs with *Continuous* and *Intermittent Operations* calculated with EnergyPlus and RC models**

	Continuous Operation				Intermittent Operation			
	Heating Energy Needs		Cooling Energy Needs		Heating Energy Needs		Cooling Energy Needs	
	EP	RC	EP	RC	EP	RC	EP	RC
	[kWh]	[kWh]	[kWh]	[kWh]	[kWh]	[kWh]	[kWh]	[kWh]
January	9673	9511	0	0	8577	8445	0	0

February	8218	8128	0	0	7265	7216	0	0
March	3396	2496	0	0	2897	2107	0	0
April	193	0	222	0	144	0	151	0
May	0	0	3171	3547	0	0	2518	3100
June	0	0	7625	7615	0	0	6341	6778
July	0	0	12149	12305	0	0	10662	10951
August	0	0	7811	7428	0	0	6688	6602
September	0	0	2694	2089	0	0	2370	1769
October	214	0	91	0	117	0	77	0
November	4186	4619	0	0	3290	4084	0	0
December	8989	9507	0	0	7782	8447	0	0
Year	34868	34260	33763	32985	30070	30299	28807	29200

Firstly, the energy needs of October and April, for both the operation modes, are null for the RC model but not for the EP one; the reason is concerning the fact that, with the RC model they are simulated using average monthly climate data, thus, just “half of the month” has to be taken into account. At the same time it should be noted that this comparisons only aid to verify that the validation presented in Section 4.4. is correspondingly proper for the case study; the model, in fact, is designed for a predictive control purpose and it calculates the daily energy needs, therefore the reported monthly energy is a daily quantity multiplied by the number of monthly days. Further, for this reason, the day is calculated on average climatic conditions of each month. In conclusion, using the correct hourly data, it will calculates the correct energy needs, as done for the other months.

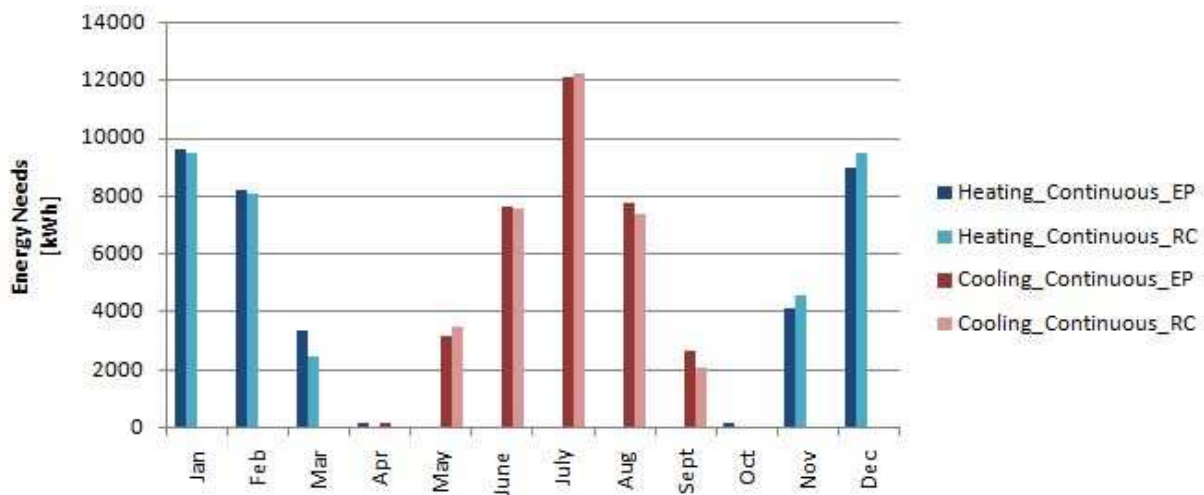


**Figure 23.** Comparison between Monthly Energy Needs with *Continuous Operation* calculated with EP and RC models.

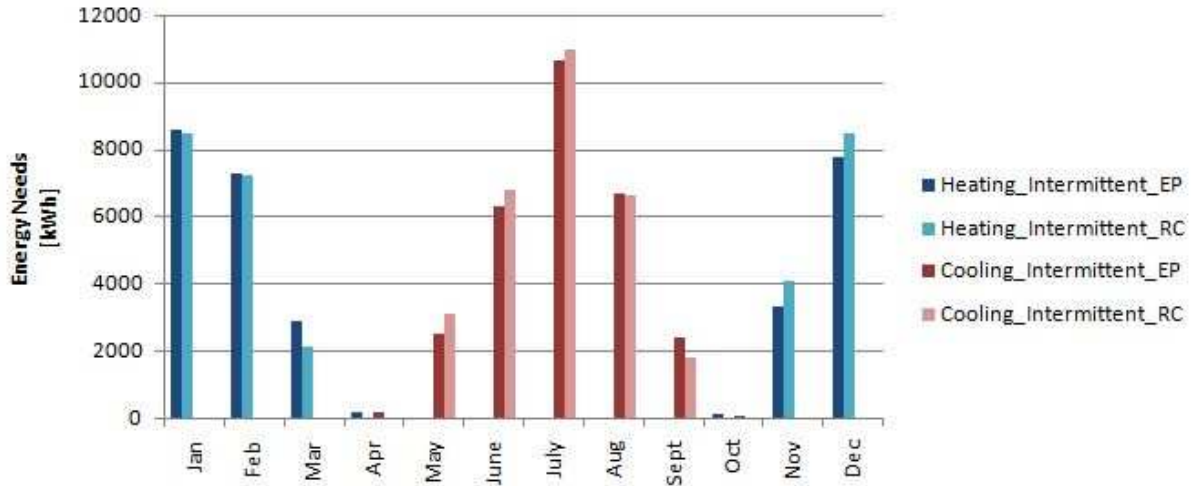


**Figure 24. Comparison between Monthly Energy Needs with *Intermittent Operation* calculated with EP and RC models.**

In any case, it is possible to note easily in the graphs, that the differences, both monthly and yearly, for continuous and intermittent operation, are quite low, especially taking into account the fact that the shading factor has been used constant throughout the year. The obtained results, in fact, can be considered sufficiently accurate since it is normally acceptable a  $\pm 15\%$  deviation while in this case is around  $\pm 2\%$ .

**Tab. 46 - Comparison between Seasonal Energy Needs calculated with EP and RC models**

Yearly Energy Needs	Heating Energy Needs		Cooling Energy Needs	
	Continuous Operation	Intermittent Operation	Continuous Operation	Intermittent Operation
	[kWh]	[kWh]	[kWh]	[kWh]
Energy Plus	34868	30070	33763	28807
RC Model	34260	30299	32958	29200
Difference (RC/EP)	- 2%	+ 1%	- 2%	+ 1%

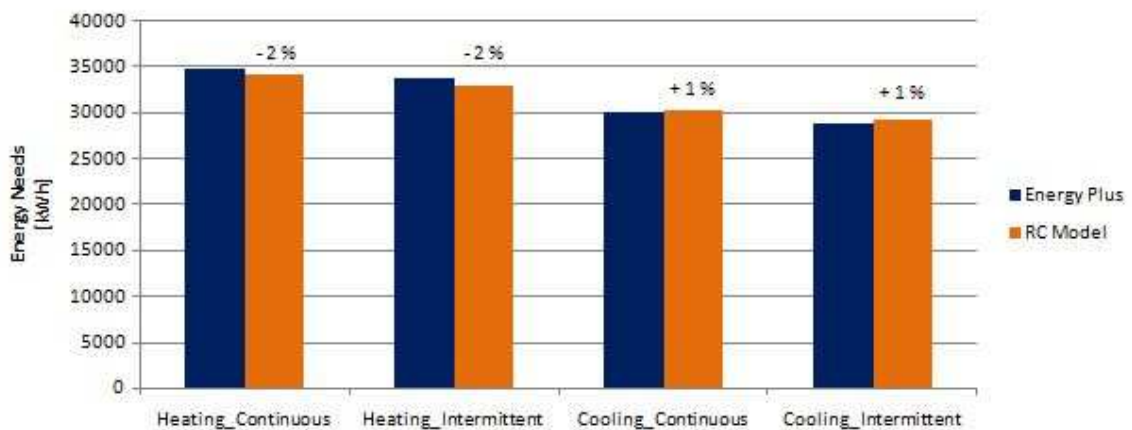


**Figure 25. Comparison between Seasonal Energy Needs calculated with EP and RC models.**

### 5.3. PERFORMANCE MONITORING, TRACKING AND DATA ANALYSIS

After showing that the RC model is able to simulate the energy needs of a real building with enough accuracy, it is possible to continue with the main purpose of the research: the monitoring and optimal management of buildings energy needs in operational phase. As explained in section 3.6.2., monitoring and data analysis, in fact, are essential for appropriate commissioning in order to reduce the performance gap between design and measured energy consumptions. Only after the monitoring phase, or rather the verification and calibration of the model will be possible to start with the optimization phase.

Before to use the Model Predictive Control, in fact, is fundamental to be sure that the building model used by the optimization algorithm is calibrated, or rather that the input data entered (from the design phase) actually correspond to the real ones. The calibration phase, therefore, starts by the main data analysis (in this case the main input data that has to be checked are resistance and capacity of the building because the model used by the MPC is a RC model) in order to verify that the actual consumptions coincide to the simulated ones and, thus, verify that the model is calibrated.

In other words, considering that in this phase the main problem is concerning the performance gap, the first step has to analyze the operation data in order to check if the design conditions are changed.

This will be done through three main steps:

- Heat Transfer Coefficient investigation through the monthly energy needs analysis;
- On-site measurements and experimental analysis;
- Global Capacity investigation through the hourly Free-Floating Temperature analysis.

#### 5.3.1. MONTHLY ENERGY NEEDS ANALYSIS – HEAT TRANSFER COEFFICIENT INVESTIGATION

Below are listed the energy consumptions for heating season 2014-2015 measured by heat meters placed in the technical rooms of case study. Although the heat meters measure the consumption of each individual apartment, at first, the monthly consumption for each building are shown. It has to be noted, in fact, that the actual consumptions are very far from those estimated in the previous paragraph.

**Tab. 47 - Real Energy Needs during heating season 2014-2015**

	Building 1	Building 2	Building 3	Tot
	[kWh]	[kWh]	[kWh]	[kWh]
October	1730	227	2263	4220
November	6341	1814	11308	19463
December	12248	3438	21268	36954
January	15540	3659	25846	45045

February	14024	3675	23501	41200
March	9387	2532	14294	26213
April	2730	881	3369	6980
HeatingSeason	62000	16226	101849	180075

**Tab. 48 - Real Energy Needs during cooling season 2015**

	Building 1	Building 2	Building 3	Tot
	[kWh]	[kWh]	[kWh]	[kWh]
May	685	22	804	1511
June	4858	569	8298	13725
July	9094	1682	16174	26950
August	6096	1378	9172	16646
September	1417	360	2100	3877
Cooling Season	22150	4011	36548	62709

The next Figures are showing both the simulated and measured energy needs. As shown in the first Figure, the actual energy needs for heating are almost double compared to the predicted values; this can be considered an example of *performance gap*.

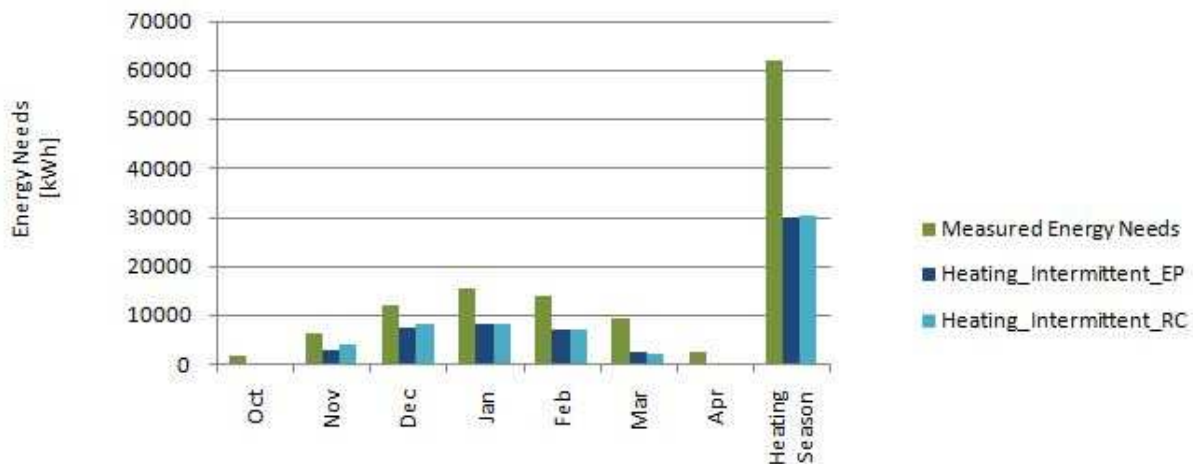


**Figure 26. Comparison between Energy Needs Measured and Estimated - Building 1 Heating Season.**

Regarding the cooling season, instead, the energy consumptions are lower than the calculated ones, but the differences are more slight, and above all, it has to be underlined that generally the cooling needs are more difficult to assess precisely because of the more variation of the internal gains and ventilation data respect to the winter season, specially for residential uses.

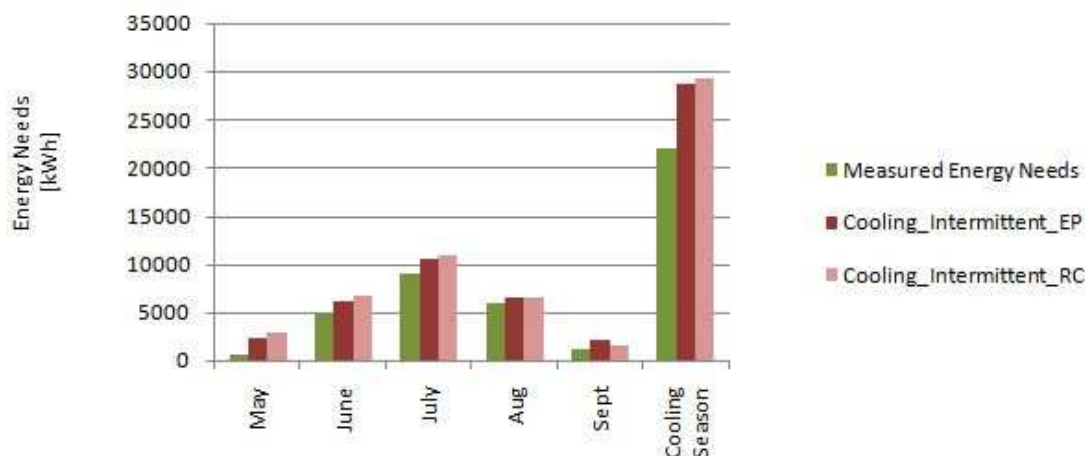


**Figure 27. Comparison between Energy Needs Measured and Estimated - Building 1 Cooling Season.**

Consequently, the next step is to use the inverse models, already explained in Section 4.5., in order to verify if the main coefficients used by the RC model (the global heat loss coefficient  $H$  and the thermal capacity  $C$ ) are correct, otherwise the model needs to be calibrated.

Initially, the global dispersion coefficient  $H$  of the entire *building 1* was analyzed, using the linear regression *Model 1* (Paragraph 4.5.3., Table 21) with the total energy needs transformed in the average specific daily power and the external temperature. As explained in Paragraph 4.5.1, in fact, the monthly energy needs [kWh] can be converted in the daily average power  $q$  [ $W/m^3$ ] (Eq.36) in order to achieve the global coefficient of dispersion  $H$  in a more convenient unit [ $W/m^3K$ ].

**Tab. 49 - Daily Power and External Temperature measured during heating season for Building 1**

		October	November	December	January	February	March	April
<b>Daily Power</b> [ $W/m^3$ ]	2014-2015	0.63	2.38	4.45	5.65	5.65	3.41	1.03
	2015-2016	0.56	2.46	4.66	5.69	4.72	3.29	0.38
<b>External Temp.</b> [ $^{\circ}C$ ]	2014-2015	15,65	10,57	5,25	4,14	4,42	9,97	14,39
	2015-2016	13,21	8,44	4,71	3,61	6,59	9,47	15,03

**Tab. 50 - Daily Power and External Temperature measured during cooling season for Building 11**

		May	June	July	August	September
<b>Daily Power</b> [ $W/m^3$ ]	2015	0.25	1.83	3.31	2.22	0.53
<b>External Temp.</b> [ $^{\circ}C$ ]	2015	19.15	23.46	28.12	24.15	19.05

From the data above the linear regression lines and related coefficients have been obtained. As already explained, in fact, it is possible to derive the global dispersion coefficient by the slope of the regression line, or rather the coefficient  $\alpha_1$  (for more details see Section 4.5).

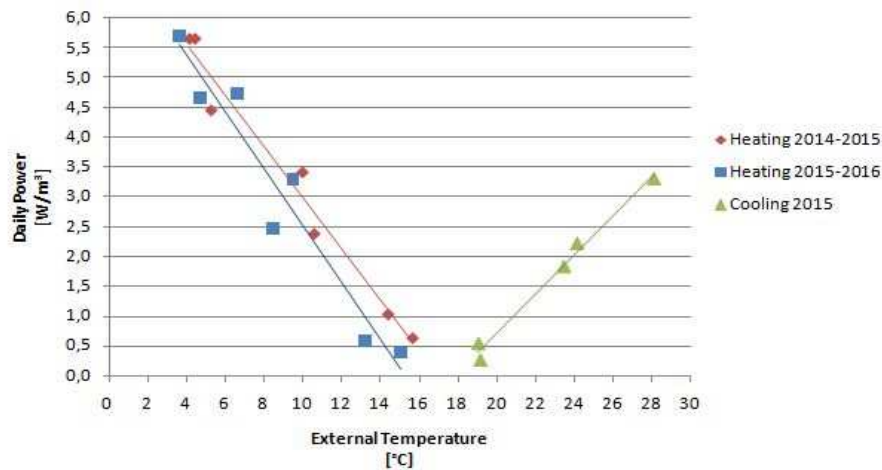


**Figure 28. Regression Line of Measured Daily Power - Building 1.**

According to the chart in Figure 28, the slopes regarding the two heating season regression lines are quite similar, and, thus, it is likely that the total heat transfer coefficient is constant in time. Further, also the summer regression slope seems to be similar. For a more detailed comparison the estimated parameters are analyzed below.

**Tab. 51 - Estimated Parameter with Linear regression (Model 1) - Building 1.**

	Intercept	Slope
	$\alpha_0$	$\alpha_1$
Heating 2014-2015	7.26	-0.43
Heating 2015-2016	7.27	-0.48
Cooling 2015	-5.88	0.33

Comparing the estimated parameters  $\alpha_1$  (H) with the heat transfer coefficient calculated at the design stage (0.25) is clear that the first one is much higher. The next table, in fact, shows the calculations according to which, assumed the transmittance values of main components and Air Change Rate of 0.3 volumes/hour as recommended by the standard, we get a global transmission coefficient of 0.25 W/m<sup>3</sup>K.

**Tab. 52 - Heat transfer Coefficients from Design Phase calculation - Building 1**

Design Phase	Transmittance	Area	Heat Transfer Coefficient	Specific Global Heat Transfer Coefficient
	[W/m <sup>2</sup> K]	[m <sup>2</sup> ]	[W/K]	[W/m <sup>3</sup> K]
H <sub>tr,wall</sub>	0.19	1557	296	
H <sub>tr,roof</sub>	0.17	596	101	
H <sub>tr,ground</sub>	0.20	535	107	
H <sub>tr,windows</sub>	1.35	227	307	

<b>H<sub>tr</sub></b>	-	-	811	0.17 <sup>15</sup>
<b>H<sub>ve</sub></b>	-	-	377 <sup>16</sup>	0.08
<b>H</b>	-	-	1188 <sup>17</sup>	<b>0.25</b>

At this point, it can be separately analyzed the energy consumptions of each apartment and check all the regression parameters obtained in order to verify that the global coefficient H is higher than the predicted one. As before, the measured consumptions are converted into daily average power.

**Tab. 53 - Daily Power measured during heating season 2014-2015**

	October	November	December	January	February	March	April
Apartment	[W/m <sup>3</sup> ]	[W/m <sup>3</sup> ]	[W/m <sup>3</sup> ]	[W/m <sup>3</sup> ]	[W/m <sup>3</sup> ]	[W/m <sup>3</sup> ]	[W/m <sup>3</sup> ]
1	1.28	5.66	8.70	11.36	11.17	6.66	1.40
2	0.44	2.24	4.94	5.52	5.60	3.95	1.36
3	0.11	2.16	3.41	4.79	4.67	2.51	0.63
5	0.29	2.02	4.45	5.23	5.02	2.89	0.71
6	0.27	1.81	3.02	3.15	3.55	1.58	0.37
7	0.69	2.23	3.90	4.66	4.10	1.90	0.46
8	0.28	2.20	4.46	5.86	6.19	3.91	1.56
9	1.36	1.51	3.79	5.59	5.38	2.76	0.93
10	0.81	3.78	5.51	6.65	6.54	4.13	1.32
12	0.91	1.34	4.37	5.52	5.78	3.87	1.63
14	0.32	1.85	3.79	5.02	5.39	4.17	0.86
15	1.12	3.57	5.34	8.38	8.18	5.24	1.56

**Tab. 54 - Daily Power measured during heating season 2015-2016**

	October	November	December	January	February	March	April
Apartment	[W/m <sup>3</sup> ]	[W/m <sup>3</sup> ]	[W/m <sup>3</sup> ]	[W/m <sup>3</sup> ]	[W/m <sup>3</sup> ]	[W/m <sup>3</sup> ]	[W/m <sup>3</sup> ]
1	1.28	3.63	7.03	9.69	9.79	6.09	0.42
2	0.19	2.12	4.64	5.44	4.57	3.39	0.39
3	1.00	1.88	4.71	6.78	5.03	4.09	0.49
5	0.61	2.16	4.57	5.15	4.22	3.15	0.21
6	0.17	1.35	2.84	3.05	2.02	0.90	0.00
7	0.37	1.89	3.43	4.43	3.11	1.54	0.00
8	0.49	2.52	4.53	5.91	4.74	3.51	0.61
9	0.00	1.40	3.97	4.37	3.49	2.26	0.00
10	1.04	3.70	5.66	6.77	5.69	4.34	0.74
12	0.96	3.42	4.65	5.53	4.97	3.74	0.75
14	0.43	2.01	5.06	6.27	5.54	3.87	0.44
15	0.82	4.83	7.54	9.15	7.99	6.01	0.87

<sup>15</sup>The Gross Volume is 4833 m<sup>3</sup>

<sup>16</sup> The Heat Loss Coefficient for Ventilation is calculated as 0.34\*0.3\*3697 where 0.34 [W/K] is cp, 0.3 is the ACR [1/h] and 3697 is the Net Volume [m<sup>3</sup>].

<sup>17</sup>The Global Heat Loss Coefficient H is the sum of H<sub>tr</sub> and H<sub>ve</sub>.

**Tab. 55 - Daily Power measured during cooling season 2015**

	May	June	July	August	September
Apartment	[W/m <sup>3</sup> ]	[W/m <sup>3</sup> ]	[W/m <sup>3</sup> ]	[W/m <sup>3</sup> ]	[W/m <sup>3</sup> ]
1	0.52	2.85	4.13	2.00	0.00
2	0.47	1.89	3.42	1.23	0.25
3	0.10	0.33	2.72	2.52	0.72
5	0.27	2.61	4.29	2.98	0.95
6	0.47	2.76	3.62	2.19	0.73
7	0.26	2.70	4.09	1.95	0.65
8	0.03	1.09	2.89	2.35	0.47
9	0.23	1.90	3.23	2.64	0.45
10	0.29	1.86	3.59	1.73	0.36
12	0.00	1.59	2.48	1.68	0.17
14	0.30	1.20	1.28	2.46	0.67
15	0.00	0.00	3.94	3.14	0.74

With the same linear regression *Model 1* (Paragraph 4.5.3., Table 21) the following parameters are estimated.

**Tab. 56 - Estimated Parameters with Linear regression (Model 1)**

Apartment	Heat Transfer Coefficient			Balance Point Temperature		
	Heating 2014-2015	Heating 2015-2016	Cooling 2015	Heating 2014-2015	Heating 2015-2016	Cooling 2015
	$-\alpha_1$	$-\alpha_1$	$-\alpha_1$	$-\alpha_0/\alpha_1$	$-\alpha_0/\alpha_1$	$-\alpha_0/\alpha_1$
1	0.86	0.81	0.40	16.8	15.4	17.7
2	0.43	0.47	0.32	17.2	15.0	18.3
3	0.38	0.50	0.26	16.1	15.5	17.9
5	0.43	0.45	0.42	16.1	15.2	17.5
6	0.28	0.32	0.34	16.3	13.1	17.0
7	0.35	0.41	0.40	16.5	13.6	17.9
8	0.45	0.47	0.30	16.9	15.5	18.3
9	0.38	0.46	0.34	17.2	13.4	17.8
10	0.49	0.54	0.35	17.6	16.1	18.3
12	0.40	0.43	0.26	17.6	16.6	17.9
14	0.40	0.53	0.13	16.9	15.1	13.5
15	0.58	0.76	0.36	17.4	15.7	16.5

Considering more seasons, it is also possible to compare the global dispersion coefficient during time. It has to be noted that the global dispersion coefficient is a sum of the heat coefficient for transmission plus the one for ventilation, therefore, it can change accordingly to different internal uses of the spaces (e.g. Air Change Rate). For that reason, generally, the differences are higher between the heating and cooling seasons, as is it possible to see in the following graph. Further, in case of large difference during the same season (for example between heating season 2014-2015

and 2015-2016), it may be due to a problem with the insulation layer, to a changing in the boundary condition of the apartments or, as already said, to a different uses of the space.

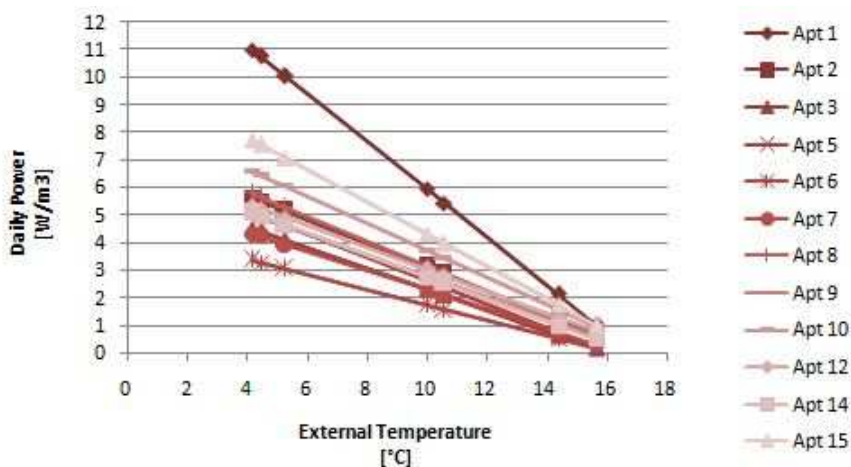


Figure 29. Graphical view of Linear Regression for heating season 2014-2015.

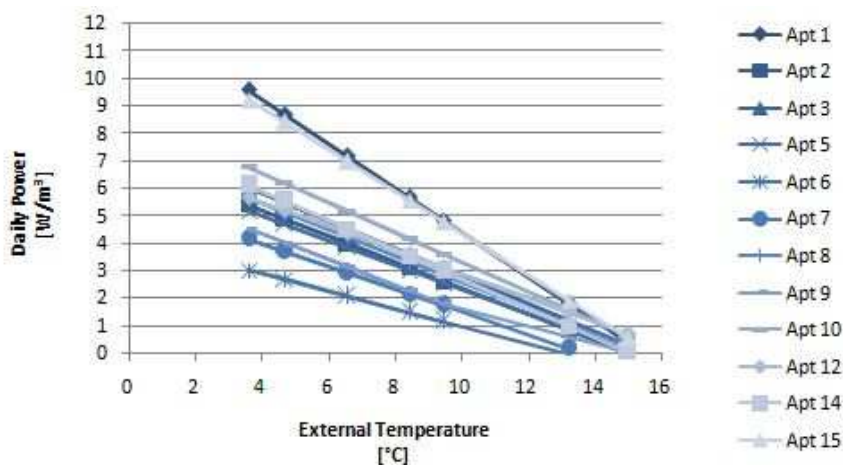


Figure 30. Graphical view of Linear Regression for heating season 2015-2016.

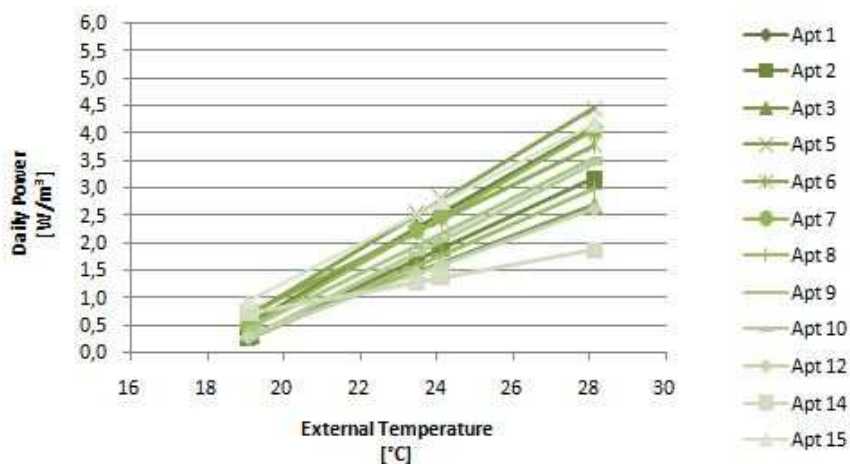
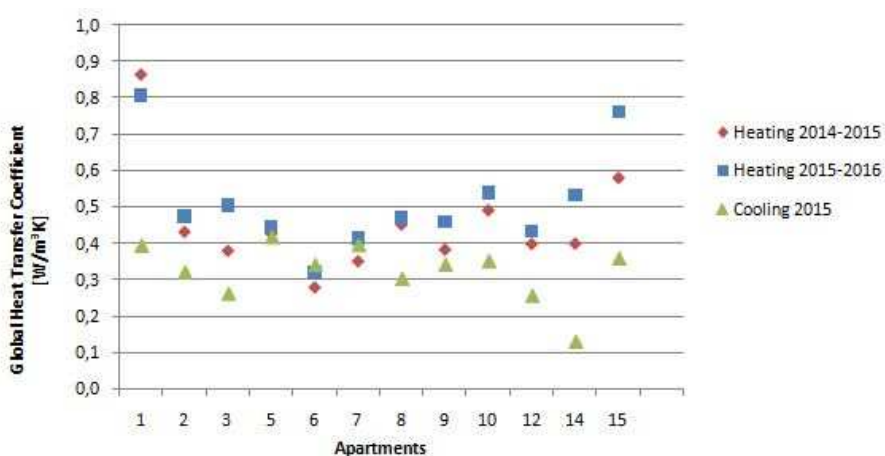


Figure 31. Graphical view of Linear Regression for cooling season 2015.

Then, considering the results, easily observable in the chart, it is clear that the dispersion of two flats (Apt.1 and 15), during both the winter seasons, is higher than the average. In detail, during the 2015-2016 winter season, the dispersion of Apt.1 slightly falls while the one of Apt.15 increase. Minimum dispersion instead regards the Apt.6 for both winter seasons, while in summer it is slightly above average. Analyzing the position of these flats you may notice that, accordingly to the results, the Apt. 6 is oriented to South-West and, thus, receives more solar gains, while the Apt. 1 and 15 are oriented to North-East. Further, both Apt. 1 and 15 border with a non-used apartment, thus, have more dispersion. In addition the Apt.1 has a different function (nursery) and have a different user profile (probably a higher ACR).

The following Figure shows a comparison between the estimated coefficient H for each apartment and for every season in order to see the changes over time.



**Figure 32. Global Dispersion Coefficients comparison during time.**

As can be seen from the graph, the maximum variation between the winter seasons are concerning the Apt. 3, 14 and 15, while, between different seasons, the Apt. 1, 14 and 15. All these analysis can be useful to do Fault Detection, analyzing where the dispersion is higher and where the differences are constant in time or not.

In conclusion it is even more evident that the average dispersion coefficient H in operation phase is higher than the one predicted. In order to better understand the variation, the following graph shows the distribution of the H coefficients estimated. It is possible to see that the most probable value (the peak in the graph) is in the range between 0.35 (green line which corresponds to the cooling season) to 0.40 (blue line which corresponds to the heating season 2015-2016). The different distribution between the cooling and winter season estimated parameters is simply due to the fact that in the first case the most likely value of H is also the highest one, while in winter cases the most probable value is the "average" coefficient; namely in the first case the distribution is not Gaussian as in the second one.

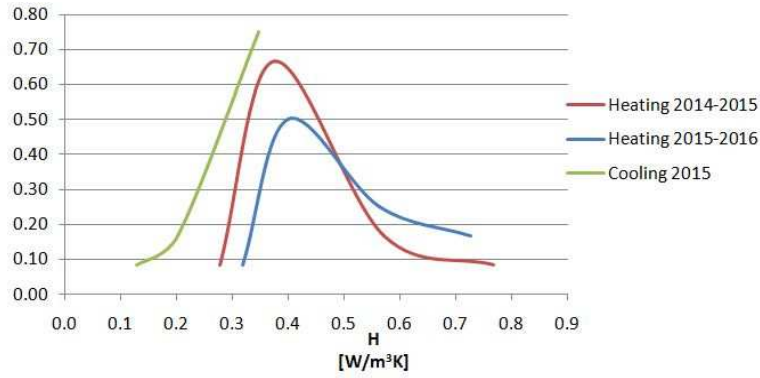


**Figure 33. Distribution of regression parameters H obtained with the linear regression Model 1.**

Calculating the simple average with all the estimated parameters, instead, the result is 0.43 while neglecting the three higher coefficients (Apartments 1 and 15) is 0.39.

**Tab. 57–Statistic values of Global Dispersion Coefficient estimated - Building 1**

	Average ( $\alpha_1$ )	Most Probable ( $\alpha_1$ )
Heating 2014-2015	0.45	0.37
Heating 2015-2016	0.51	0.40
Cooling 2015	0.32	0.35

Then, it is possible to calculate the daily power with the regression parameters and appreciate the difference between measured data and estimated ones and the relative statistical indices (Tab. 58) described in Paragraph 4.5.1.

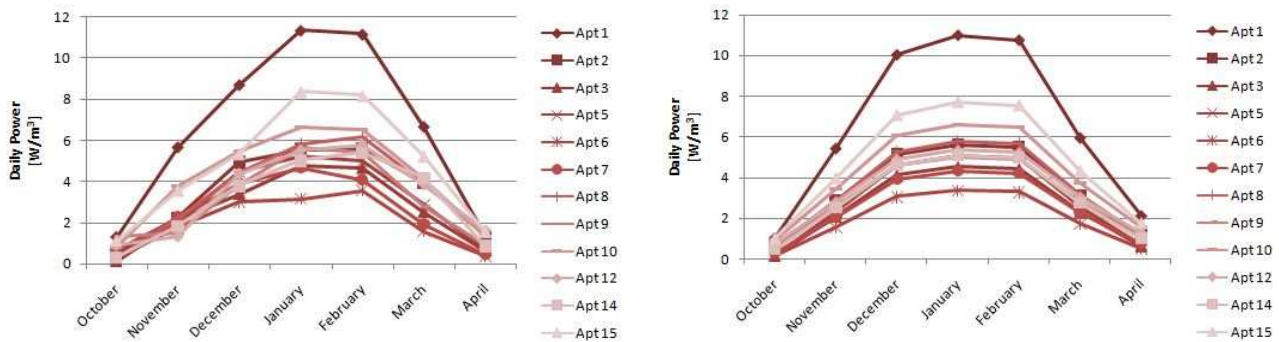


**Figure 34. Comparison between Daily Powers Measured and Estimated with Linear Regression Parameters – Heating Season 2014-2015.**

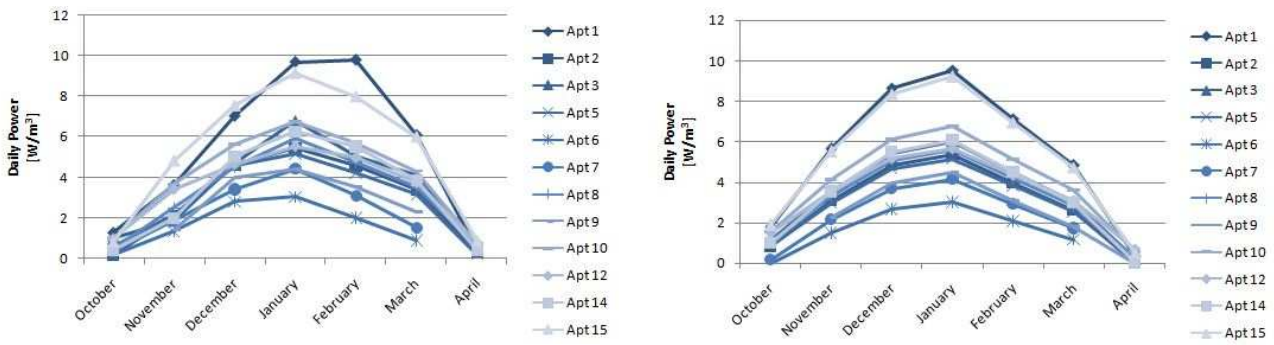


**Figure 35. Comparison between Daily Powers Measured and Estimated with Linear Regression Parameters – Heating Season 2015-2016.**

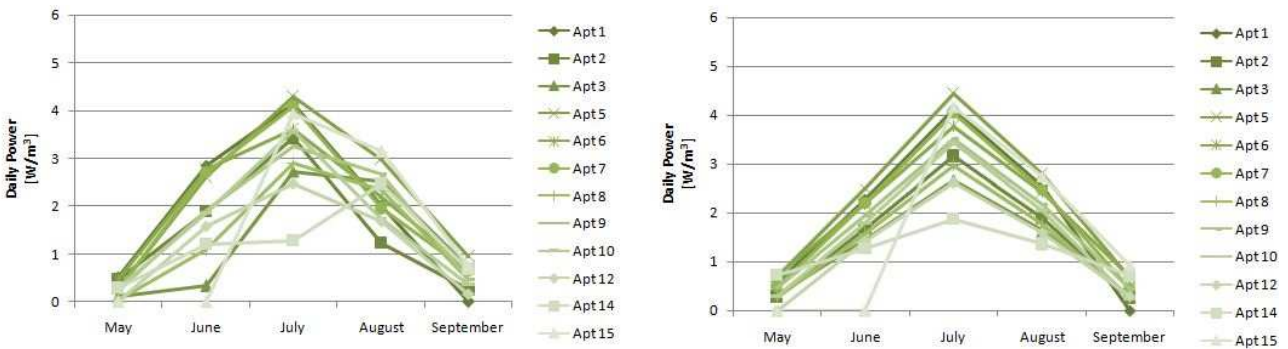


**Figure 36. Comparison between Daily Powers Measured and Estimated with Linear Regression Parameters – Cooling Season 2015.**

Concerning the statistical indices, it has to be underlined that the Nominal Mean Base Error (NMBE) results to be 0 for all the cases, thus, it is not reported. The Standard Error (SE) of each coefficient H estimated, instead, is listed in order to evaluate the accuracy of it. The Standard Error is directly calculated in Matlab as the squared root of the corresponding diagonal element of the coefficient covariance matrix.

**Tab. 58 - Statistical Indices of Linear regression (Model 1) - Building**

	Heating Season 2014-2015			Heating Season 2015-2016			Cooling Season 2015		
	R2	SE	CV <sub>(RMSE)</sub>	R2	SE	CV <sub>(RMSE)</sub>	R2	SE	CV <sub>(RMSE)</sub>
	[-]	[-]	[%]	[-]	[-]	[%]	[-]	[-]	[%]
<b>1</b>	0.97	± 0.07	11.11	0.82	± 0.17	29.81	0.92	± 0.09	24.18
<b>2</b>	0.95	± 0.04	13.09	0.90	± 0.07	22.07	0.91	± 0.06	26.32
<b>3</b>	0.97	± 0.03	12.71	0.83	± 0.10	27.82	0.63	± 0.11	59.04
<b>5</b>	0.99	± 0.02	6.93	0.94	± 0.05	16.44	0.97	± 0.04	13.20
<b>6</b>	0.98	± 0.02	9.96	0.98	± 0.03	10.30	0.93	± 0.05	17.54
<b>7</b>	0.97	± 0.03	11.63	0.97	± 0.04	10.36	0.94	± 0.06	20.38
<b>8</b>	0.92	± 0.06	17.57	0.91	± 0.07	19.39	0.89	± 0.06	30.08
<b>9</b>	0.87	± 0.07	22.70	0.82	± 0.13	17.08	0.95	± 0.05	17.76
<b>10</b>	0.98	± 0.03	8.03	0.95	± 0.05	12.99	0.98	± 0.03	11.80
<b>12</b>	0.86	± 0.07	23.06	0.94	± 0.05	13.87	0.98	± 0.03	12.73
<b>14</b>	0.86	± 0.07	24.59	0.86	± 0.10	26.72	0.35	± 0.10	55.78

<b>15</b>	0.90	± 0.08	18.90	0.92	± 0.10	17.47	0.97	± 0.08	22.12
<b>Tot</b>	0.97	± 0.03	10.54	0.94	± 0.06	16.88	0.99	± 0.02	8.50

Finally the Balance Point Temperature is used in order to calculate the Free Running Temperature ( $\theta_{fr}$ ) as described in Paragraph 4.5.3. (Eq.52). As you can see in Figure 37, three main  $\theta_{fr}$  are shown, one for each season, corresponding to the  $\theta_{fr}$  calculated for the whole building.

From the graphical view it is possible to see that:

- the heating system can be turn OFF with an external temperature that ranges between 16-17°C;
- ventilation can be used when the external temperature ranges between 16-17 and 26°C;
- free cooling can be used when the internal temperature is higher than 26°C and the external temperature ranges between 18°C and 26°C;
- the cooling system has to be turn ON with an external temperature higher than 26°C.

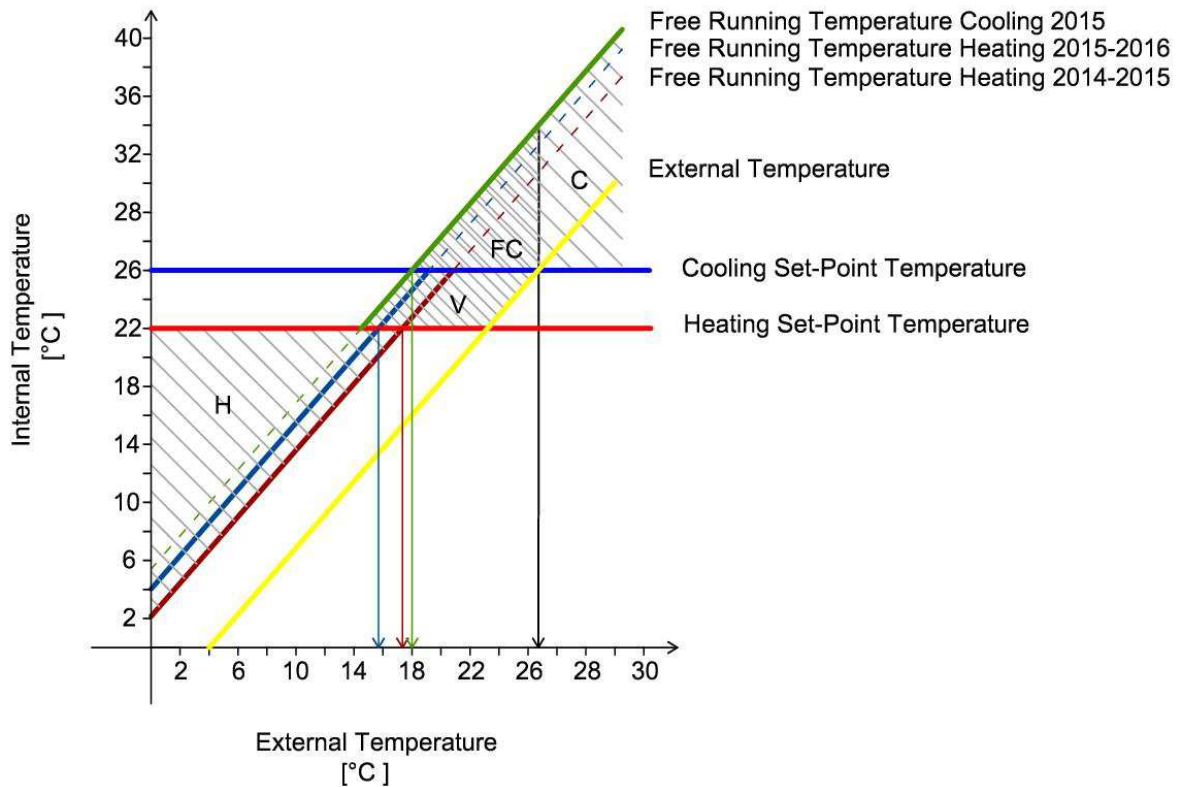


**Figure 37. Graphical view of system operations respect to internal and external temperature profiles.**

In conclusion, it is shown that, analyzing the monthly energy consumption, it is possible to monitor the global dispersion coefficient  $H$ . In detail it is possible to say that, the greater consumption of the case study, with respect to what expected during the design phase, are probably due to greater dispersions.

**5.3.2. ON SITE MEASUREMENTS - EXPERIMENTAL ANALYSIS**

In order to understand if the greater dispersion is due to the transmission or ventilation factor, the transmittance of the main components have been analyzed with a heat flow meter. The measurement in situ has shown, in fact, that the external wall transmittance is much higher than expected; using the thermal characteristics declared by the producers the transmittance was around 0,19 W/m<sup>2</sup>K while the heat flow meter measures an average transmittance of 0,35W/m<sup>2</sup>K. The measurement was conducted on two different wall portions, both facing north and with a time-step greater than 3 days (the minimum period generally required). In the following tables are described the main characteristics of the measurements done while, with the graphs, the trends of heat flux and external and internal temperatures recorded by the heat flow meter during the two measurements are shown.

**Tab. 59 - General data about External Wall Transmittance measurements**

	Units	29 February - 6 March	12-22 March
<b>Measurements Hours</b>	[h]	144	240
<b>Average Flux</b>	[W/m <sup>2</sup> ]	5.21	3.96
<b>Average External Temperature</b>	[°C]	7.06	9.73
<b>Average Internal Temperature</b>	[°C]	20.35	20.48
<b>Average Δθ (θi-θe)</b>	[K]	13.29	10.75
<b>Final U value</b>	[W/m <sup>2</sup> K]	0.36	0.35

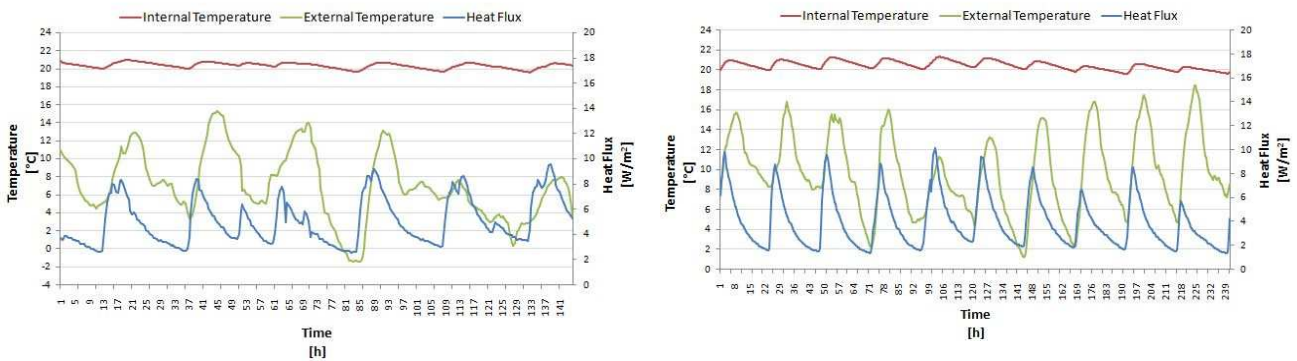


**Figure 38. Trend of Heat Flux, Internal and External Temperature during the two measurement sessions.**

To analyze the stability of the measured conditions it is advisable to analyze the relative progressive average; the next figures show it and it can be seen that they are stable enough during at least the last three days of measurement.

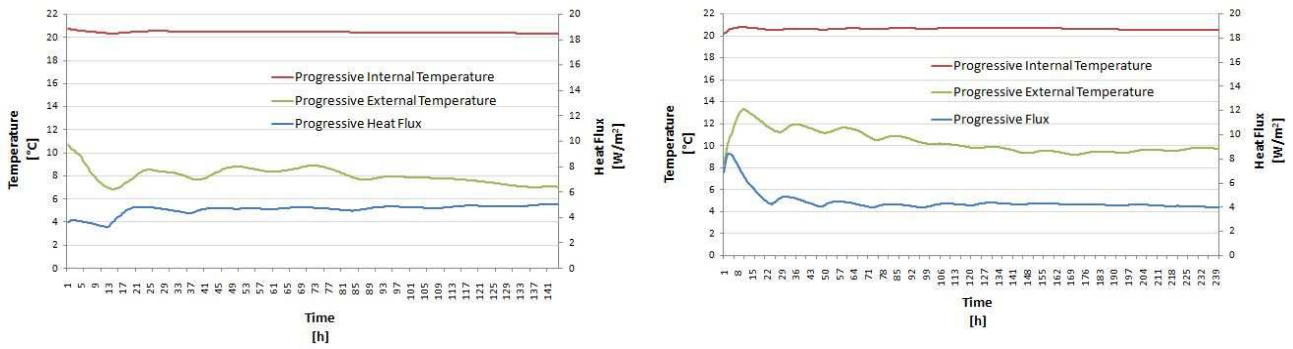


**Figure 39. Progressive Trend of Heat Flux, Internal and External Temperature during the two measurement sessions**

Finally, it has to be underlined that, the calculation method used to evaluate the transmittance is the average method, as recommended by the ISO 9869 [6], and, in detail:

$$U = \frac{1}{\left(R_i + \left(\frac{1}{\lambda}\right) + R_e\right)} \quad \text{Eq. (57)}$$

$$\lambda = \frac{\sum q}{\sum \theta_i - \sum \theta_e} \quad \text{Eq. (58)}$$

Where:

- U is the final transmittance of the element [W/m<sup>2</sup>K] considering also the surface resistances;
- R<sub>i</sub> and R<sub>e</sub> are the surface resistances considered as 0,13 and 0,04 [m<sup>2</sup>K/W];
- λ is the conductance of the element [W/m<sup>2</sup>K];
- q is the flux through the element [W/m<sup>2</sup>];
- θ<sub>i</sub> and θ<sub>e</sub> are the internal and external temperatures [°C].

The conductance and transmittance trends during the whole period of the measurement sessions are shown in the figures below. It is also possible to appreciate that, during the last three days the fluctuation was slight, as recommended by the regulation [6].

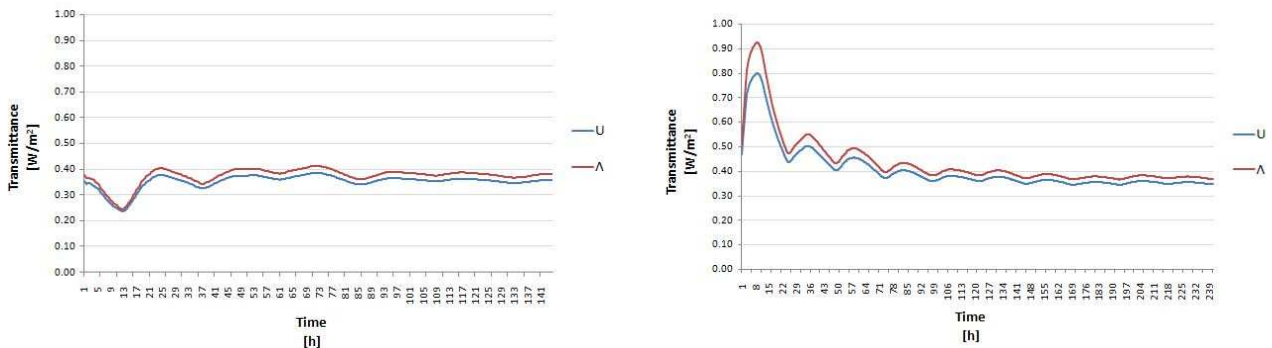


**Figure 40. Trend of conductance λ and transmittance U values during the two measurement sessions.**

The same was done for the basement wall in contact with hollow space. Analyzing the different linear regressions, in fact, it could be noted that the apartments with cellar had the higher losses.

**Tab. 60 - General data about Basement Wall Transmittance Measurement**

	Units	25-31 March
<b>Measurements Hours</b>	[h]	144
<b>Average Flux</b>	[W/m <sup>2</sup> ]	3.13
<b>Average External Temperature</b>	[°C]	16.81
<b>Average Internal Temperature</b>	[°C]	21.34
<b>Average <math>\Delta\theta</math> (<math>\theta_i - \theta_e</math>)</b>	[K]	5.16
<b>Final U value</b>	[W/m <sup>2</sup> K]	0.55

The measurements conditions were not optimal because the hollow spaces remained always at a temperature close to the internal conditions (thus is almost impossible to obtain a  $\Delta\theta$  of 10°C as recommended by the regulation [6]). In any case, the transmittance value definitely indicates an actual U value higher than the design one (0.25 W/m<sup>2</sup>K).

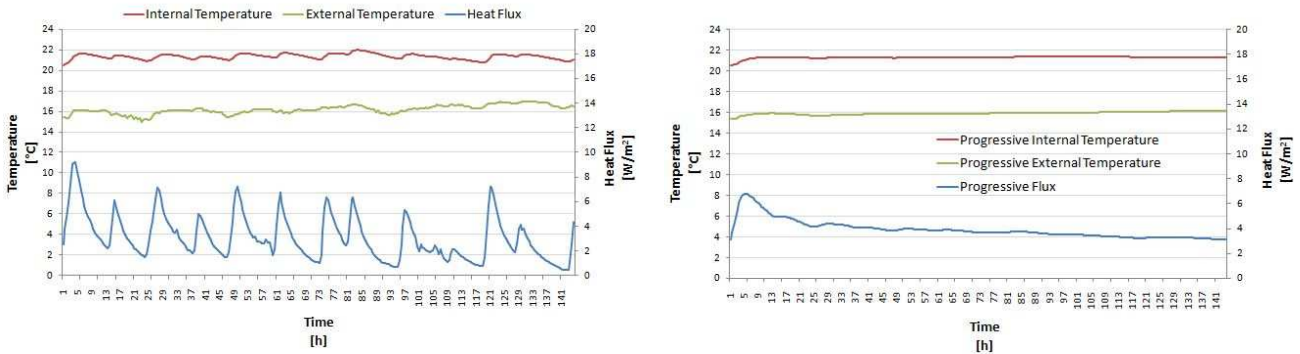


**Figure 41. Normal and Progressive Trend of Heat Flux, Internal and External Temperature during the third measurement session**

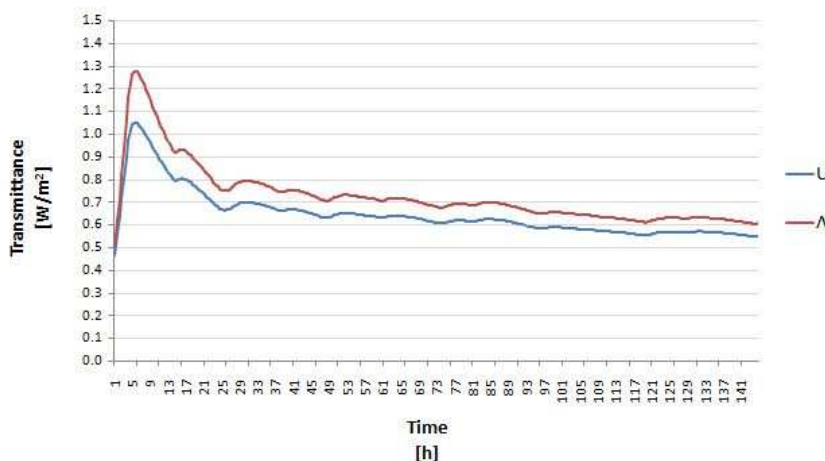


**Figure 42. Trend of conductance  $\lambda$  and transmittance U values during the third measurement session.**

**5.3.3. FREE FLOATING TEMPERATURE ANALYSIS – THERMAL CAPACITY INVESTIGATION**

The next step was to analyze the *time constant* of the building in order to check the ratio between the H coefficient and the global capacity C. Thus, for the reasons expressed in Paragraph 4.5.3., the free-floating temperature is measured considering an unsold apartment (Apt.13) in two sessions.

**Tab. 61 - General data about Free-Floating Temperature measurements.**

	Units	24-29 February	9-17 March
<b>Measurements Hours</b>	[h]	120	192
<b>Average External Temperature</b>	[°C]	6.40	9.21
<b>Average FF Temperature Measured</b>	[°C]	13.90	14.14
<b>Average FF Temperature Estimated</b>	[°C]	13.90	14.13

As first, in the following figures it is possible to see that, considering the external temperature fluctuation (in red), the free-floating temperature is highly constant; it means that the building has a massive envelope.

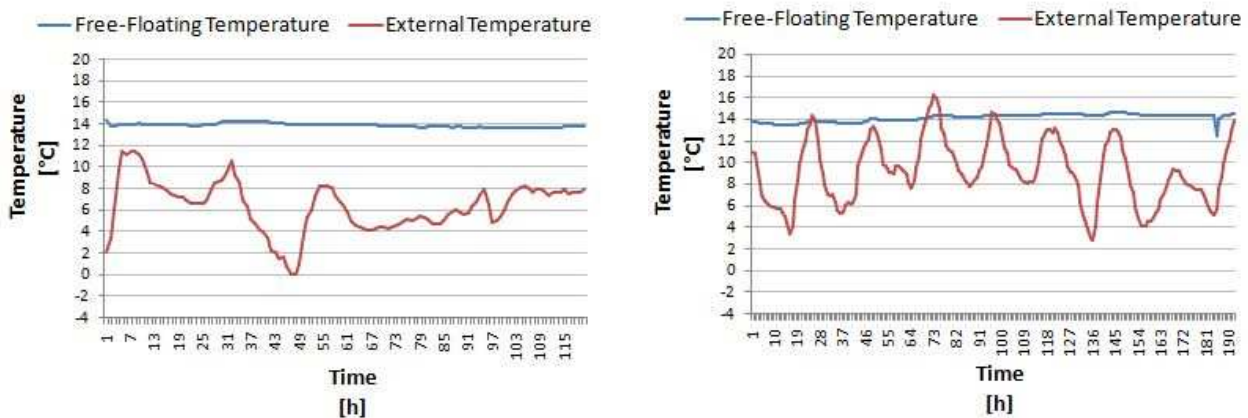


**Figure 43. Free-Floating Temperatures measured in Apartment 13 during the two measurement sessions.**

Then, with the ARX Model 2 (Paragraph 4.5.3., Table 23) the following estimated parameters are identified.

**Tab. 62 - Estimated Parameter with ARX model (Model 2) and relative Statistical Indices.**

Apt.13	Intercept	$\theta_i$ coefficient	$\theta_e$ coefficient	R2	NMBE	CV <sub>(RMSE)</sub>
	$\beta_0$	$\beta_1$	$\beta_2$	[-]	[%]	[%]
<b>24-29 February</b>	1.55	0.88	0.01	0.98	0.02	0.16
<b>9-17 March</b>	2.08	0.85	0.01	0.98	0.16	0.26

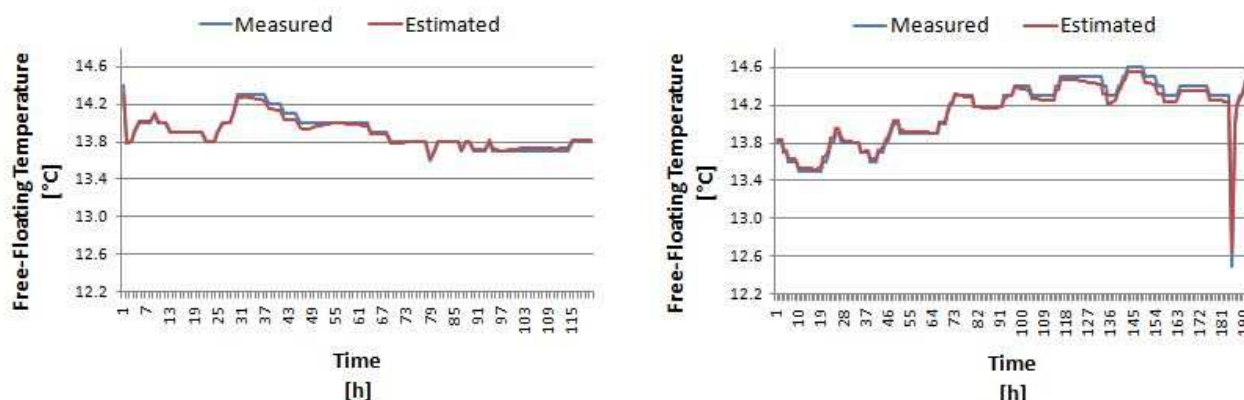


**Figure 44. Comparison between measured and estimated Free-Floating Temperatures with the ARX model 2.**

As explained in Section 4.5., from the estimated parameters of ARX model it is possible to analyze the *Time Constant* of the building ( $\tau$ ). The following table shows the comparison between the calculated and the estimated Time Constant.

**Tab. 63 - Comparison between Calculated and Estimates Parameters.**

	Unit	Design Phase Data (C/H)	Estimated Data ( $1/\beta_2$ )
$\tau$	[h]	481	140

Starting from the estimated time constant, also the global Capacity  $C_m$  is decreased (from 260000 to 165000 J/m<sup>2</sup>K) and the RC model is calibrated. In the following Paragraph the model calibration procedure is presented.

### 5.3.4. MODEL CALIBRATION

In order to obtain the H coefficient equal to 0.37 W/m<sup>3</sup>K, and in line with the transmittance values measured with the heat flow meters (see Tables 59-60), the transmittance of external walls and roof components have been changed from 0.19 and 0.17 W/m<sup>2</sup>K to 0.35 and 0.30 W/m<sup>2</sup>K respectively, while the  $H_{tr,ground}$  one from 0.20 to 0.55 W/m<sup>2</sup>K. The details are listed in the following table.

**Tab. 64 - Heat transfer Coefficients during Operation Phase - Building 1.**

Operation Phase	Transmittance	Area	Heat Transfer Coefficient	Specific Global Heat Transfer Coefficient
	[W/m <sup>2</sup> K]	[m <sup>2</sup> ]	[W/K]	[W/m <sup>3</sup> K]
$H_{tr,wall}$	0.35	1557	545	-
$H_{tr,roof}$	0.30	596	179	-
$H_{tr,ground}$	0.55	535	294	-

$H_{tr, windows}$	1.35	227	307	-
$H_{tr}$	-	-	1325	0.27
$H_{ve}$	-	-	363 <sup>18</sup>	0.10
$H$	-	-	1807	<b>0.37</b>

Concerning the natural ventilation and internal gains, different schedules have been created, maintaining the average values suggested by the regulation [5]. In fact, thanks to some interviews with residents, it was possible to know that normally the windows are opened just two-three times at days for about an hour. Correspondingly the internal gains are changed with the information obtained by the interviews. Thus, we supposed an operation regime as explained in Table 65.

**Tab. 65 - Hourly Schedules used for Model Calibration.**

Hours	Intermittent Operation				Actual Operation			
	Internal Gain	Air Change Rate	Heating	Cooling	Internal Gain	Air Change Rate	Heating	Cooling
	[W/m <sup>2</sup> ]	[1/h]	[°C]	[°C]	[W/m <sup>2</sup> ]	[1/h]	[°C]	[°C]
1	4	0.3	19	30	1	0.01	19	30
2	4	0.3	19	30	1	0.01	19	30
3	4	0.3	19	30	1	0.01	19	30
4	4	0.3	19	30	1	0.01	19	30
5	4	0.3	19	30	1	0.01	19	30
6	4	0.3	19	30	1	0.01	19	30
7	4	0.3	22	26	6	0.01	22	26
8	4	0.3	22	26	8	0.01	22	26
9	4	0.3	22	26	8	2.3	22	26
10	4	0.3	19	30	1	0.01	19	30
11	4	0.3	22	26	1	0.01	22	26
12	4	0.3	22	26	1	0.01	22	26
13	4	0.3	22	26	8	0.01	22	26
14	4	0.3	22	26	10	2.3	22	26
15	4	0.3	19	30	1	0.01	19	30
16	4	0.3	22	26	8	0.01	22	26
17	4	0.3	22	26	8	0.01	22	26
18	4	0.3	19	30	1	0.01	19	30
19	4	0.3	19	30	1	0.01	19	30
20	4	0.3	19	30	8	0.01	19	30
21	4	0.3	22	26	10	2.3	22	26
22	4	0.3	19	30	8	0.01	19	30
23	4	0.3	19	30	1	0.01	19	30
24	4	0.3	19	30	1	0.01	19	30
<b>Average</b>	4	0.3	-	-	4	0.3	-	-

<sup>18</sup>It is the daily average heat loss coefficient for ventilation  $H_{ve}$  where 0,01 ACR is equal to 1,26 W/K and 2,3 ACR is equal to 2891,05 W/K.

Changing just these parameters, the energy needs calculated with the calibrated RC model result very near to the real ones. In the following table and graph are listed both the results obtained using a continuous schedule for internal gains and natural ventilation (*Intermittent Operation*) and the *Actual Operation* achieved with the interviews.

**Tab. 66 - Comparison between Energy Needs Measured and Simulated with the Calibrated RC model – Heating Season.**

Monthly Energy Needs	Heating Season		
	Measured	Calibrated RC Model ( Intermittent Operation)	Calibrated RC Model (Actual Operation)
	[kWh]	[kWh]	[kWh]
<b>October</b>	1730	1670	1577
<b>November</b>	6341	7866	8216
<b>December</b>	12248	14513	14967
<b>January</b>	15540	14904	15159
<b>February</b>	14024	12892	13216
<b>March</b>	9387	5957	6336
<b>April</b>	2730	871	892
<b>Heating Season</b>	62000	58673	60362

**Tab. 67 - Comparison between Energy Needs Measured and Simulated with the Calibrated RC model – Cooling Season.**

Monthly Energy Needs	Cooling Season		
	Measured	Calibrated RC Model (Intermittent Operation)	Calibrated RC Model (Actual Operation)
	[kWh]	[kWh]	[kWh]
<b>May</b>	685	1921	2241
<b>June</b>	4858	7160	7691
<b>July</b>	9094	13396	14305
<b>August</b>	6096	7087	7684
<b>September</b>	1417	488	1041
<b>Cooling Season</b>	22150	30052	32961

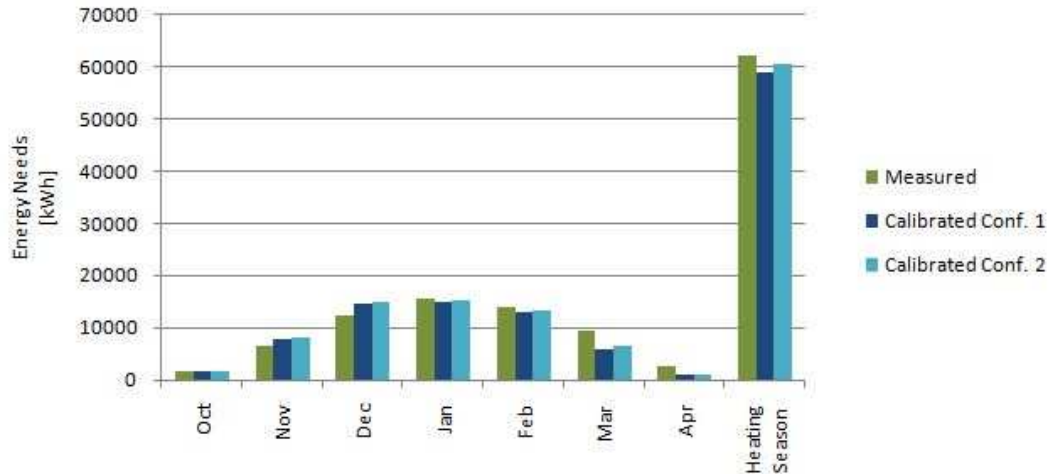


**Figure 45. Comparison between Energy Needs Measured and Simulated with the Calibrated RC model – Heating Season.**

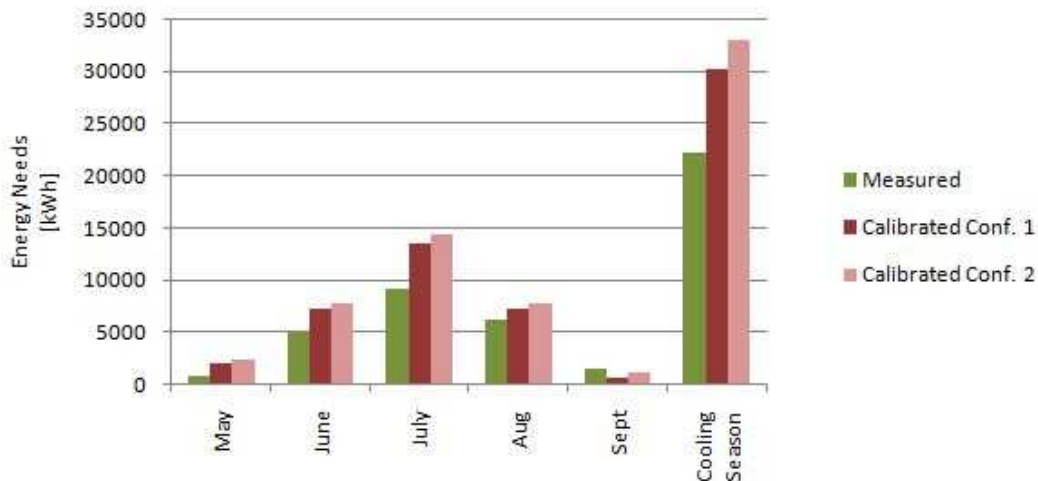


**Figure 46. Comparison between Energy Needs Measured and Simulated with the Calibrated RC model – Cooling Season.**

The above results show that the monthly consumptions analysis have well-calibrated the model for the heating season, while the summer consumptions are still higher from measured value. Probably the internal gains and the natural ventilation rate have to be reduced, but it should be also noted, again, that the calibration of the model through monthly consumptions is just a first step, and, further, a static evaluation is more problematic for a correct estimation of cooling needs because the consumption is much more sensitive to hourly changes. Therefore it is necessary to analyze hourly data.

### 5.3.5. PARAMETER IDENTIFICATION WITH INVERSE MODELS

In order to test the Linear Time Invariant (LTI) models presented in Section 4.3. different configurations of the case study are used. The actual hourly data needed to run the LTI models, for the case study, are not available, and hence, the direct RC model is used to simulate it. As explained in the aforesaid section, the data needed are: (i) hourly energy demand, (ii) hourly air temperature and (iii) hourly surface temperature. The first two are needed for both the LTI models while the surface temperature just for the 2 *States* model.

In detail six different configurations of the case study have been considered, the first three concerning the designed building envelope and the other three for the calibrated one:

- Designed Envelope
  - Configuration 1: Continuous Operation;
  - Configuration 2: Mixed Operation;
  - Configuration 3: Actual Operation;
- Calibrated Envelope
  - Configuration 4: Continuous Operation;
  - Configuration 5: Mixed Operation;
  - Configuration 6: Actual Operation.

All the specifications about the *Configurations* are listed in Table 68. It is possible to note that the table is referring just to the input data that are variable between different configurations; all the other inputs, for example the geometrical data, are the same as the listed in Paragraph 5.2.2. (Tables 40-44). The difference between designed and calibrated model, therefore, depends just on the transmittance values of exterior wall, roof and ground floor and thermal capacity.

Table 69 is showing in detail the hourly schedules. As anticipated, in fact, different types are used and, in detail, three main combinations:

- Continuous Operation (Configuration 1 and 4);
  - Continuous (24 hr/day) Heating and Cooling Operation
  - Continuous (24 hr/day) Ventilation
  - Continuous (24 hr/day) Internal Gains
- Mixed Operation (Configuration 2 and 5);
  - Actual (10 hr/day) or Intermittent (16 hr/day) Heating and Cooling Operation
  - Continuous (24 hr/day) or Actual (3 hr/day) Ventilation
  - Continuous (24 hr/day) or Actual (10 hr/day) Internal Gains
- Actual Operation (Configuration 3 and 6);
  - Actual (10 hr/day) Heating and Cooling Operation
  - Actual (3 hr/day) Ventilation
  - Actual (10 hr/day) Internal Gains

Note that the *Actual* schedules are referring to the real use of the building as showed in the previous Table 65, while the *Intermittent* one is a new schedule where the Heating and Cooling System is turn ON 16 hours per day (from 6.00 to 22.00).

**Tab. 68 – Variable Input Data for different case study simulation configurations**

Variable Input Data		Designed Model			Calibrated Model			
		Conf. 1	Conf. 2	Conf. 3	Conf. 4	Conf. 5	Conf. 6	
Heating Set-Point Temperature	[°C]	20	22	22	22	22	22	
Heating and Cooling Schedules	[-]	Cont.	Act.	Act.	Cont.	Int.	Act.	
Air Change Rate	[1/h]	0.3	0.3	2.3	0.3	2.3	2.3	
Ventilation Schedule	[-]	Cont.	Cont.	Act.	Cont.	Act.	Act.	
Internal Gains	[W/m <sup>2</sup> ]	4	4	10	4	10	10	
Internal Gains Schedule	[-]	Cont.	Cont.	Act.	Cont.	Act.	Act.	
Average Transmittance	Exterior Wall	[W/m <sup>2</sup> K]	0.19	0.19	0.19	0.35	0.35	0.35
	Roof	[W/m <sup>2</sup> K]	0.17	0.17	0.17	0.30	0.30	0.30
	Ground floor	[W/m <sup>2</sup> K]	0.20	0.20	0.20	0.55	0.55	0.55
Thermal Capacity	Global Thermal Capacity	[kJ/m <sup>2</sup> K]	260	260	260	165	165	165
	Multiplier of surface for effective Mass Area	[-]	3.00	3.00	3.00	2.50	2.50	2.50

**Tab. 69 - Hourly Schedules used for Identification Analysis**

Hours	Internal Gain		Ventilation		Heating and Cooling System		
	[W/m <sup>2</sup> ]		[1/h]		[°C]		
	Cont.	Act.	Cont.	Act.	Cont.	Int.	Act.
1	4	1	0.3	0.01	20/22/26	19/30	19/30
2	4	1	0.3	0.01	20/22/26	19/30	19/30
3	4	1	0.3	0.01	20/22/26	19/30	19/30
4	4	1	0.3	0.01	20/22/26	19/30	19/30
5	4	1	0.3	0.01	20/22/26	19/30	19/30
6	4	1	0.3	0.01	20/22/26	19/30	19/30
7	4	6	0.3	0.01	20/22/26	22/26	22/26
8	4	8	0.3	0.01	20/22/26	22/26	22/26
9	4	8	0.3	2.3	20/22/26	22/26	22/26
10	4	1	0.3	0.01	20/22/26	22/26	19/30
11	4	1	0.3	0.01	20/22/26	22/26	22/26
12	4	1	0.3	0.01	20/22/26	22/26	22/26
13	4	8	0.3	0.01	20/22/26	22/26	22/26
14	4	10	0.3	2.3	20/22/26	22/26	22/26
15	4	1	0.3	0.01	20/22/26	22/26	19/30
16	4	8	0.3	0.01	20/22/26	22/26	22/26
17	4	8	0.3	0.01	20/22/26	22/26	22/26
18	4	1	0.3	0.01	20/22/26	22/26	19/30
19	4	1	0.3	0.01	20/22/26	22/26	19/30
20	4	8	0.3	0.01	20/22/26	22/26	19/30
21	4	10	0.3	2.3	20/22/26	22/26	22/26
22	4	8	0.3	0.01	20/22/26	22/26	19/30
23	4	1	0.3	0.01	20/22/26	19/30	19/30

24	4	1	0.3	0.01	20/22/26	19/30	19/30
----	---	---	-----	------	----------	-------	-------

The schedules variability is needed to check if the models are able to identify exactly a variable data in time. The inverse models, in fact, are built in order to find the corresponding values that reconstruct the required hourly internal air (and surface) temperature and energy demand following an indicated schedule. Thus, in case of unknown schedule it is possible to obtain an average value, but, using the actual schedule it is possible to identify the real hourly values.

In Table 70 are listed the estimated parameters with the 2 *State* inverse model (Paragraph 4.3.3), starting from the hourly data simulated with the RC model. It should be stressed that the following parameters are identified with no more than two simulations; the optimization method used to run the LTI models, in fact, is iterative and, thus, the optimal value can be obtained with more than one simulation. For this reason, the tests are used furthermore to check how many simulations are needed in order to obtain an almost “perfect” value, where "perfect" stands for the same value put as an input in the direct simulation.

**Tab. 70–Identified Parameters with the ARX model - 2 States.**

Identified Parameters			Designed Model			Calibrated Model		
			Conf. 1	Conf. 2	Conf. 3	Conf. 4	Conf. 5	Conf. 6
<b>Air Change Rate</b>		[1/h]	0.300	0.300	2.300	0.300	2.299	2.300
<b>Internal Gains</b>		[W/m <sup>2</sup> ]	3.999	4.000	10.000	4.000	9.985	9.985
<b>Average Transmittance</b>	Exterior wall	[W/m <sup>2</sup> K]	0.188	0.190	0.190	0.350	0.336	0.337
	Transparent components	[W/m <sup>2</sup> K]	1.350	1.349	1.348	1.349	1.360	1.360
	Roof	[W/m <sup>2</sup> K]	0.171	0.170	0.170	0.300	0.309	0.308
	Ground floor	[W/m <sup>2</sup> K]	0.204	0.200	0.201	0.550	0.575	0.575
<b>Thermal Capacity</b>	Global Thermal Capacity	[kJ/m <sup>2</sup> K]	259.970	260.001	260.001	164.998	164.926	164.919
	Multiplier of surface for effective mass area	[-]	3.000	3.000	3.000	2.500	2.500	2.500
	Multiplier of internal surface area	[-]	4.501	4.500	4.500	4.500	4.499	4.500

Table 71, instead, is showing the estimated parameters with the 1 *State* inverse model (Paragraph 4.3.4). Similarly in this case no more than two simulations have been run in order to get the listed values.

**Tab. 71 – Identified Parameters with the ARX model - 1 State.**

Identified Parameters			Designed Model			Calibrated Model		
			Conf. 1	Conf. 2	Conf. 3	Conf. 4	Conf. 5	Conf. 6
<b>Air Change Rate</b>		[1/h]	0.301	0.301	2.303	0.299	2.300	2.300
<b>Internal Gains</b>		[W/m <sup>2</sup> ]	4.000	4.000	10.000	3.999	10.000	10.000
<b>Average Transmittance</b>	Exterior wall	[W/m <sup>2</sup> K]	0.191	0.191	0.190	0.349	0.350	0.350
	Transparent components	[W/m <sup>2</sup> K]	1.339	1.339	1.329	1.371	1.333	1.333
	Roof	[W/m <sup>2</sup> K]	0.170	0.170	0.170	0.300	0.301	0.301
	Ground floor	[W/m <sup>2</sup> K]	0.201	0.201	0.205	0.549	0.556	0.556

<b>Thermal Capacity</b>	Global Thermal Capacity	[kJ/m <sup>2</sup> K]	260.000	260.000	260.000	164.990	164.987	164.991
	Multiplier of surface for effective mass area	[-]	3.000	3.000	2.997	2.500	2.500	2.500
	Multiplier of internal surface area	[-]	4.499	4.499	4.507	4.504	4.500	4.500

From the results presented it is possible to verify the correct operation of both LTI models. The values, in fact, are specially reported with an accuracy equal to the third digit after the decimal point; normally the values to which refer, instead, are used with an accuracy not exceeding the second digit after the decimal point. This means that, at that level of accuracy the value is perfectly identified. Concerning the *2 States* LTI model the only exceptions are about the transmittance values for the 5<sup>th</sup> and 6<sup>th</sup> configuration where, the external wall transmittance results to be 0.34 W/m<sup>2</sup>K (instead of 0.35 W/m<sup>2</sup>K), the transparent components transmittance results to be 1.36 W/m<sup>2</sup>K (instead of 1.35 W/m<sup>2</sup>K), the roof transmittance 0.31W/m<sup>2</sup>K (instead of 0.30W/m<sup>2</sup>K) and the ground floor transmittance 0.58W/m<sup>2</sup>K (instead of 0.55W/m<sup>2</sup>K). Concerning the *1 State* LTI model, instead, the only exceptions are about the transparent components transmittances that result to be between 1.34 W/m<sup>2</sup>K and 1.37 W/m<sup>2</sup>K (while the input value is 1.35 W/m<sup>2</sup>K), the ground floor transmittance which results, in one out of three cases 0.21 W/m<sup>2</sup>K (instead of 0.20 W/m<sup>2</sup>K) and in two out of three cases 0.56 W/m<sup>2</sup>K (instead of 0.55 W/m<sup>2</sup>K).

It is almost clear that, in any case, these differences are very slight and, in conclusion, the estimation is more than acceptable.

#### **5.4. LOAD MANAGEMENT AND PERFORMANCE OPTIMIZATION**

As previously mentioned, once verified that the building model used by the Model Predictive Control is calibrated, the optimization phase can start. Considering what has been said in chapter 3.6.1., in fact, a predictive control allows, in general, to (i) estimate the energy consumptions and (ii) manage them optimally with respect to an objective function previously chosen. This objective function can be designed to minimize the energy required by the system but also the costs. As explained in Section 4.6., the optimization algorithm in this research is formulated in order to find the minimum energy needs that satisfies the constraints with a certain flexibility on the set-point temperatures. Further, the comfort analysis is achievable through the Fanger model. This can be considered the most simple objective function because the costs are not considered and therefore it is possible to have a minimum savings related only to an internal temperature reduction that allows at the same time to have a suitable internal comfort level. It must be stressed, therefore, that the savings potential of the predictive control could be higher using also the costs variation and, thus, applying the load management as explained in section 3.6.1.

### 5.4.1. GENERAL STATEMENTS

In this section, therefore, as the previous models, also the optimization algorithm (MPC) is tested with the case study. According to the optimization algorithm described in Paragraph 4.6.1. (Eq.53), six different *optimization cases* are been simulated for each building configurations presented for the identification analysis (Tables 68-69). The different optimization cases (Table 72) are related to the violation limits used by the MPC in order to save energy.

**Tab. 72 - Optimization Cases.**

Optimization Cases	Maximum Hourly Violation	Maximum Daily Violation
	[°C]	[°C]
<b>A</b>	0	0
<b>B</b>	0.5	5
<b>C</b>	0.5	10
<b>D</b>	1	5
<b>E</b>	1	10
<b>F</b>	1	15

Before showing the results it should be noted that the relationship between the maximum hourly and daily violation also depend on the number of heating/cooling hours per day provided by its schedule. It has to be noted, in fact, that, for example, as regards the *Actual* schedule, which sets 10 hours of heating/cooling per day, the cases C and F are equivalent to the cases B and D, respectively. This is because, counting a maximum of 0.5°C/hour for 10 hours per day, the daily violation cannot exceed 5°C/day and similarly considering 1°C/hour for 10 hours per day, the daily violation cannot exceed 10°C/day; therefore cases C and F result to be “null”.

Further, it must be underlined that the case A, i.e. the one which considers a maximum of 0 degrees both for the hourly and daily violations, will be the case of comparison for all the respective other 5 cases, for each configuration. In conclusion, it can be said that the case A is "not optimized" because does not violate the set-point temperature, while the case F will be the one that requires a greater violation.

The following tables, instead, are referring to the main conditions set for the calculation of PMV and comfort category. The input data required for the PMV calculation (Section 4.6.2, Eq.56), in fact, are related to the clothes resistance and the metabolic rate. The first is set according to the external temperature as shown in Figure 48, while the metabolic rate is fixed as 1.2 met that correspond to a sedentary activity which is desirable in a residential building. Further, the air velocity is set according to the Balance Point Temperature  $\theta_{bp}$  calculated (Paragraph 5.3.1. Table 56), or rather, it is set at 0.1 m/s during the cold months while is assumed a possible increase to 0.2 m/s during the warmer period, which is determined with a monthly average outdoor temperature higher than 16-17 °C.

**Tab. 73–Comfort input data used for Optimization.**

	<b>External Temperature</b>	<b>Air Velocity</b>	<b>Clothes Resistance</b>	<b>Metabolic Rate</b>
	[°C]	[m/s]	[CLO]	[met]
Jan	4,1	0,1	1,1	1,2
Feb	4,4	0,1	1,1	1,2
Mar	10,0	0,1	0,9	1,2
Apr	14,4	0,1	0,8	1,2
May	19,2	0,2	0,6	1,2
Jun	23,5	0,2	0,5	1,2
Jul	28,1	0,2	0,4	1,2
Ago	24,2	0,2	0,5	1,2
Sep	19,0	0,2	0,6	1,2
Oct	15,7	0,1	0,7	1,2
Nov	10,6	0,1	0,9	1,2
Dec	5,3	0,1	1,1	1,2

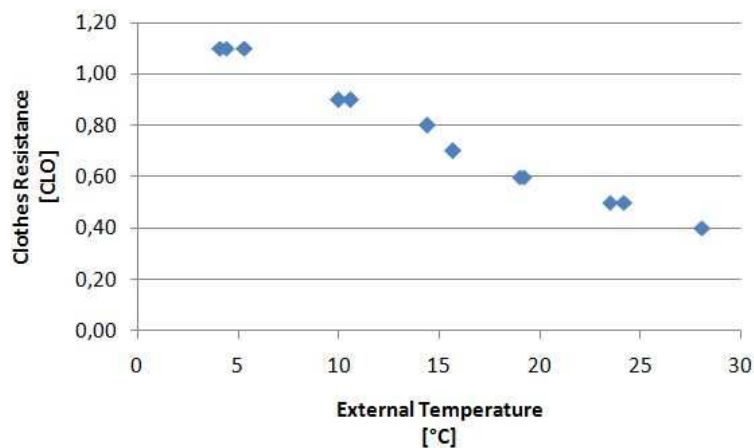


**Figure 47. Monthly Clothes Resistance values according to External Temperature.**

As already said, the previous figure shows the linear relationship between the external temperature and the value of clothes resistance. This is important because the resistance values are usually given according to a generic season (Section 4.6.2, Table 26); in this way, instead, it is possible to identify a suitable resistance for each defined temperature.

#### **5.4.2. SEASONAL ENERGY SAVING**

Considering the previous notes, below are shown the savings percentages calculated for each combination of different case study configurations and optimization cases.

**Tab. 74– Possible Energy Savings during Heating and Cooling Seasons with different optimization case**

Optimization Cases	Heating Season						Cooling Season					
	Designed Model			Calibrated Model			Designed Model			Calibrated Model		
	Conf. 1	Conf. 2	Conf. 3	Conf. 4	Conf. 5	Conf. 6	Conf. 1	Conf. 2	Conf. 3	Conf. 4	Conf. 5	Conf. 6
<b>A</b>	-	-	-	-	-	-	-	-	-	-	-	-
<b>B</b>	4%	6%	6%	3%	5%	5%	5%	7%	6%	7%	8%	9%
<b>C</b>	6%	6%	6%	5%	6%	5%	7%	7%	6%	9%	9%	9%
<b>D</b>	4%	7%	10%	4%	7%	8%	5%	11%	10%	8%	13%	15%
<b>E</b>	7%	11%	12%	6%	10%	11%	8%	14%	13%	12%	16%	17%
<b>F</b>	10%	11%	12%	9%	11%	11%	11%	14%	13%	15%	17%	17%

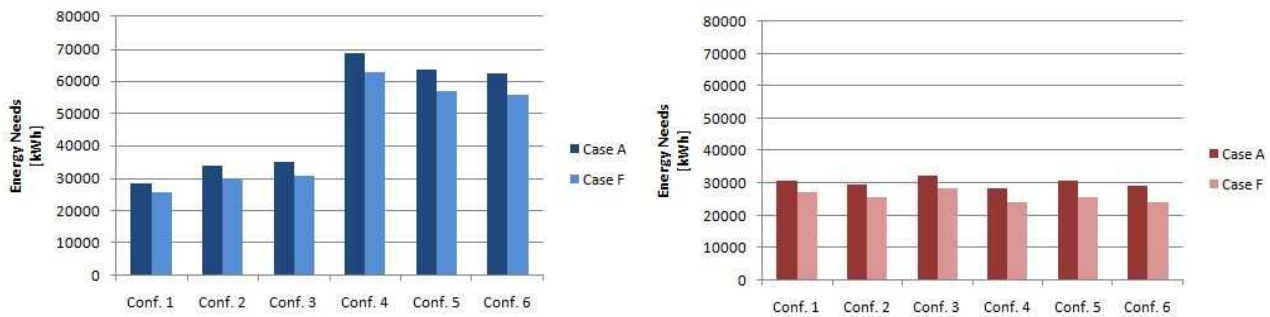


**Figure 48. Comparison – Possible Energy Savings during Heating and Cooling Season.**

Considering the variation between optimization cases (or rather vertically with respect to the values in the Tables 74-75), the energy saving is greater, correctly, as the degree of freedom of the internal temperature rises (optimization case F). Further, it is possible to see that the optimization case D (that consider a violation of 1°C/hour for a maximum of 5°C/day), in case of a configurations 1 and 4 (where the heating/cooling schedule is *continuous*), bring to a lower energy saving respect to the cases C (that consider a violation of 0,5°C/hour for a maximum of 10°C/day). It shows that, as previously said, it must be calculated the daily maximum violable temperature considering the heating/cooling hours of operation in order to get the maximum energy savings.

**Tab. 75– Possible Yearly Energy Savings with different optimization case.**

Optimization Cases	Designed Model			Calibrated Model		
	Conf. 1	Conf. 2	Conf. 3	Conf. 4	Conf. 5	Conf. 6
<b>A</b>	-	-	-	-	-	-
<b>B</b>	4%	6%	6%	4%	6%	7%
<b>C</b>	7%	6%	6%	6%	7%	7%
<b>D</b>	4%	9%	10%	5%	9%	10%
<b>E</b>	8%	13%	12%	8%	12%	13%
<b>F</b>	11%	13%	12%	10%	13%	13%

Considering the variation between configuration cases (or rather horizontally with respect to the values in the Tables 74-75), it is possible to note that both the partial and total savings rates are quite similar despite different conditions chosen for the different configurations, but the lower the required heating/cooling energy, i.e. the lower the operation hours per day, the greater the possible savings, especially for optimization cases D and E where the degrees of freedom are equal to 1°C/hour with a maximum of 5 and 10 °C/day respectively. As for the cases C and F, the difference is minimal. As a consequence, in fact, even if a direct correlation between maximum savings and a kind of configuration is not achievable, the highest percentages refer to configurations characterized by "Actual" operation schedules (Configurations 3 and 6).

In conclusion, the yearly energy savings, considering the assumptions about building configurations and optimization cases, can range from a minimum of about 6% (Case B - maximum violation of 0.5 °C/hour) to a maximum of about 12% (Case F - maximum violation of 1 °C/hour).

### 5.4.3. SEASONAL COMFORT ANALYSIS

The next step, therefore, is to verify the comfort conditions for each case and understand if the violated temperature is acceptable or not. As for the calculations in detail, see Section 4.6.2.

It should also be considered that the PMV is calculated according to the internal temperature and, hence, in the next tables and graphs a comparison between the daily average air temperature  $\theta_i$  and the relative PMV is provided.

**Tab. 76–Comparison between daily average internal temperature and PMV for different Optimization Cases – Heating Season.**

Optimization Cases	Heating Season											
	Conf.1		Conf.2		Conf.3		Conf.4		Conf.5		Conf.6	
	$\theta_i$	PMV	$\theta_i$	PMV	$\theta_i$	PMV	$\theta_i$	PMV	$\theta_i$	PMV	$\theta_i$	PMV
	[°C]	[-]	[°C]	[-]	[°C]	[-]	[°C]	[-]	[°C]	[-]	[°C]	[-]
<b>A</b>	20.5	-0.3	21.6	0.0	22.2	0.1	22.1	0.1	21.6	0.0	21.4	-0.1
<b>B</b>	20.3	-0.3	21.2	-0.1	21.8	0.0	21.8	0.0	21.3	-0.1	21.0	-0.2
<b>C</b>	20.1	-0.3	21.2	-0.1	21.8	0.0	21.6	0.0	21.2	-0.1	21.0	-0.2
<b>D</b>	20.3	-0.3	21.1	-0.1	21.6	0.0	21.8	0.0	21.2	-0.1	20.9	-0.2
<b>E</b>	20.1	-0.3	20.8	-0.2	21.4	-0.1	21.6	-0.1	20.9	-0.2	20.6	-0.3
<b>F</b>	19.9	-0.4	20.8	-0.2	21.4	-0.1	21.4	-0.1	20.8	-0.2	20.6	-0.3

**Tab. 77–Comparison between daily average internal temperature and PMV for different Optimization Cases – Cooling Season.**

Optimization Cases	Cooling Season											
	Conf.1		Conf.2		Conf.3		Conf.4		Conf.5		Conf.6	
	$\theta_i$	PMV	$\theta_i$	PMV	$\theta_i$	PMV	$\theta_i$	PMV	$\theta_i$	PMV	$\theta_i$	PMV
	[°C]	[-]	[°C]	[-]	[°C]	[-]	[°C]	[-]	[°C]	[-]	[°C]	[-]
<b>A</b>	25.9	0.3	26.1	0.4	26.0	0.3	25.6	0.2	25.5	0.2	25.8	0.3
<b>B</b>	26.2	0.4	26.5	0.5	26.5	0.5	25.8	0.3	25.9	0.3	26.2	0.4

<b>C</b>	26.3	0.4	26.5	0.5	26.5	0.5	25.9	0.3	25.9	0.3	26.2	0.4
<b>D</b>	26.2	0.4	26.8	0.6	26.7	0.6	25.9	0.3	26.1	0.4	26.4	0.5
<b>E</b>	26.4	0.5	27.0	0.6	26.9	0.6	26.1	0.4	26.2	0.4	26.6	0.5
<b>F</b>	26.6	0.5	27.0	0.6	26.9	0.6	26.2	0.4	26.3	0.4	26.6	0.5

Firstly, it is interesting to look at the internal temperature obtained in Case A with an heating/cooling continuous schedule (Configurations 1 and 4); here, in fact, compared with a fixed set-point temperature at 20/22 and 26°C there is an higher (in winter) or lower (in summer) average internal temperature. This means that, at certain times of the day, there will be a waste of energy. Looking at the Configurations 1 and 4, for example, the optimization case B brings at an average internal temperature very close to the set-point required ensuring an annual energy saving of 4% and a PMV equal to the value obtained without energy savings (Case A). Then, considering the Configuration 3, it has an "actual" schedule for internal gains (which has a high peak of gains during specific hours) and a very low transmittance values, thus, also in this configuration a waste of energy is ascribed the base case (optimization case A). Configurations 5 and 6, in fact, having a higher transmittance values, have higher losses and, consequently, the internal air doesn't exceed the set-point.

Concerning the PMV is evident that, during the winter season it ranges between 0 and -0.3 while in summer between 0.2 and 0.6. The configurations with an average PMV nearest to zero are, in winter, the 3<sup>rd</sup> and 4<sup>th</sup> and, for summer, the 4<sup>th</sup> and 5<sup>th</sup>. In any case, it should be emphasized that the scale defined for the PMV considers around zero a neutral feeling, starting from  $\pm 1$  a sensation of cool/warm, up to  $\pm 2$  hot/cold and  $\pm 3$  too hot/cold. Accordingly, every configuration allow to stay within the ideal comfort range.

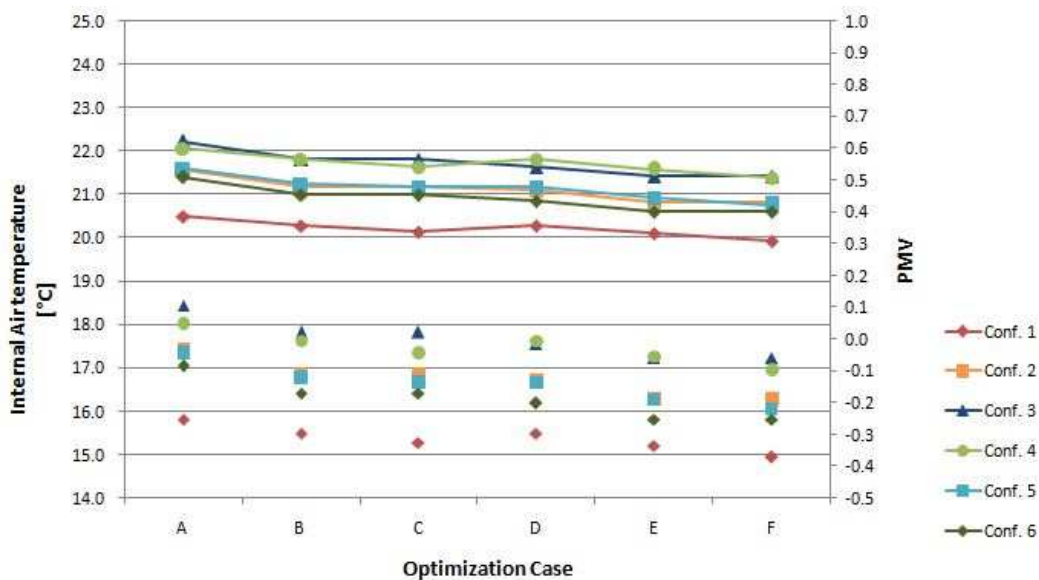


**Figure 49. Comparison between daily average internal temperature and PMV for different Optimization Cases – Heating Season.**

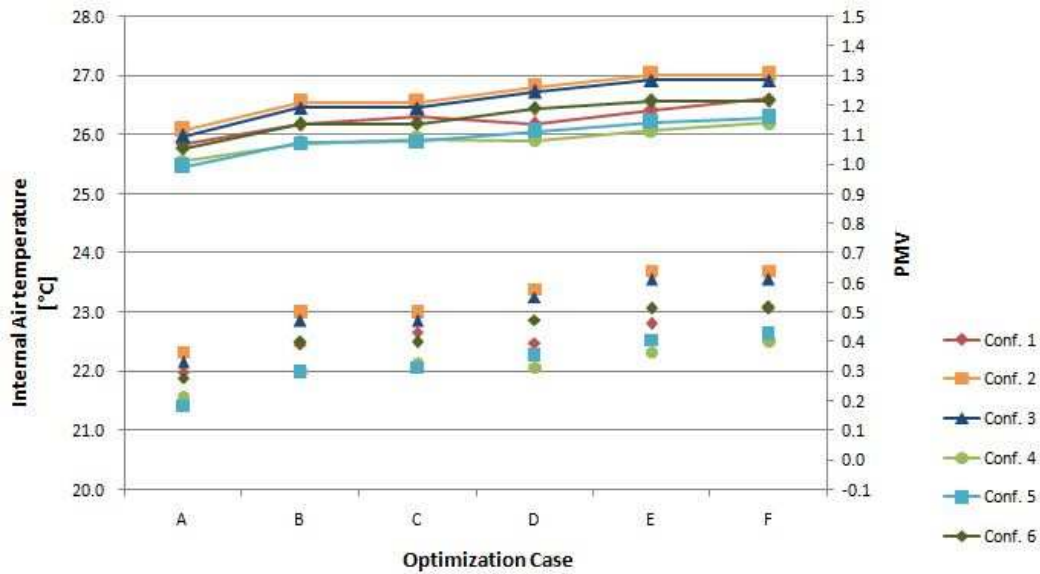


**Figure 50. Comparison between daily average internal temperature and PMV for different Optimization Cases – Cooling Season.**

The graphs show how the temperature differences between the base case (A) and the optimization case with more degrees of freedom (F) is slightly different between winter and summer seasons (not counting the Config.1 with a different set-point temperature). During the winter, in fact, the average difference considered in all the configurations is slightly less than  $-0.75^{\circ}\text{C}$ , while during the summer season it slightly exceeds  $+0.80^{\circ}\text{C}$ . The predicted mean vote (PMV), similarly, has an average variation of about  $-0.15$  during the winter and  $+0.24$  in summer.

In general, therefore, considering furthermore the energy savings, the summer season is slightly more favorable to a changing of the internal and comfort conditions, leading to a greater savings compared to winter.

Once you verified the average PMV it is also possible to calculate the achieved comfort category. This is defined according to the PMV boundaries described in Table 78.

It should be remembered that the values reported above refer to a seasonal average calculated from hourly values, thus, you can analyze the daily profile and the hourly peaks, both of the temperature and the PMV.

**Tab. 78–Comfort Category Limits.**

Comfort category	PMV Lower Bound	PMV Upper Bound
	[-]	[-]
<b>1</b>	-0.2	+ 0.2
<b>2</b>	-0.5	+ 0.5
<b>3</b>	-0.7	+ 0.7
<b>4</b>	$\leq 0.7$	$\geq 0.7$

Hence, on the basis of the described limits, it was possible to calculate, for each configuration, the average comfort category and the number of hours belonging to each category in order to compare the different optimization cases.

The next graphs show, for each configuration, the hourly trend of the PMV calculated; it is worthy to remember that, for each month, an average representative day is considered. Thus, the total amount of hours, is 288, or rather 24h per 12 days.

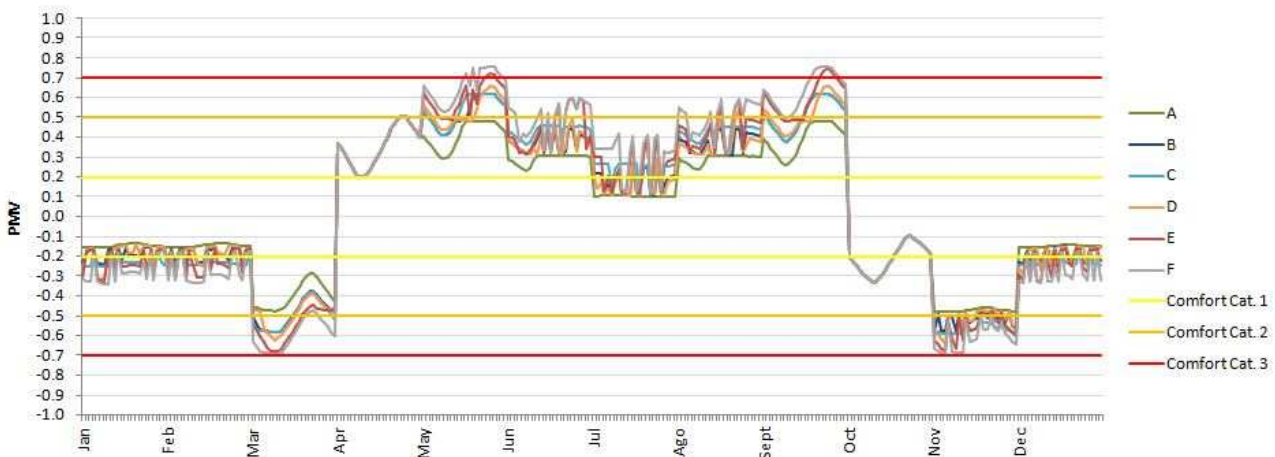
In addition to the hourly PMV profiles, the boundaries of the comfort categories are marked:

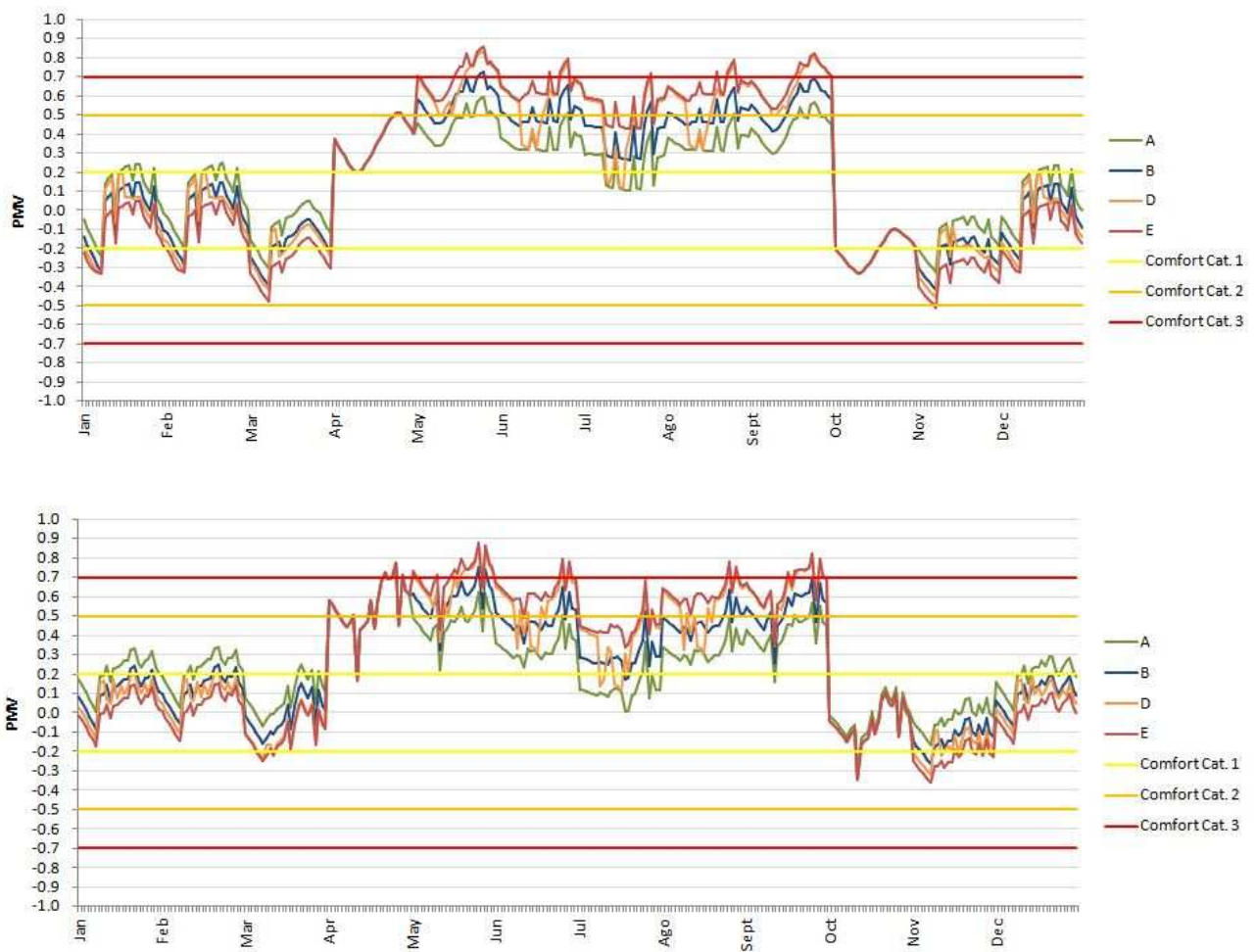
- the yellow lines mark the limits of Category 1;
- the orange lines mark the limits of Category 2;
- in the red lines mark the limits of Category 3.

Finally, it has to be remembered that, for configurations 2, 3 and 6 that are using *Actual* schedule for heating and cooling operation, the PMV profiles about optimization cases 3 and 6 are “null”, as previously explained.

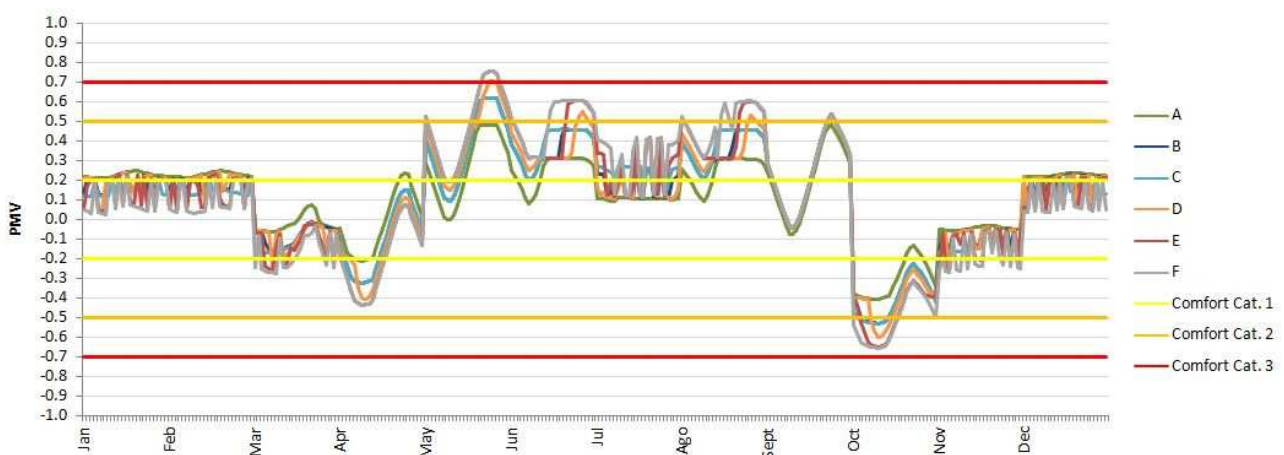
From the graphs it is immediately evident the different trend of the optimization cases and then assess their suitability, in terms of comfort. The base case (A), in fact, is generally the lower line and it is almost always included between the first and the second category, while the maximum violation case (E/F) is the higher and external line in the graph and for some hours it goes beyond the third category limits. Concerning the middle months (April and October), instead, the curves are generally the same for each optimization case because no energy is needed, thus, the internal air temperature and the relative PMV are the same for each simulation.

The analysis goes further calculating the amount of hours belonging to each category and the percentage variation of these from the base case (A) to the maximum violation case (E/F).





**Figure 51. Hourly PMV trend for different Designed Model Configurations (1-3).**



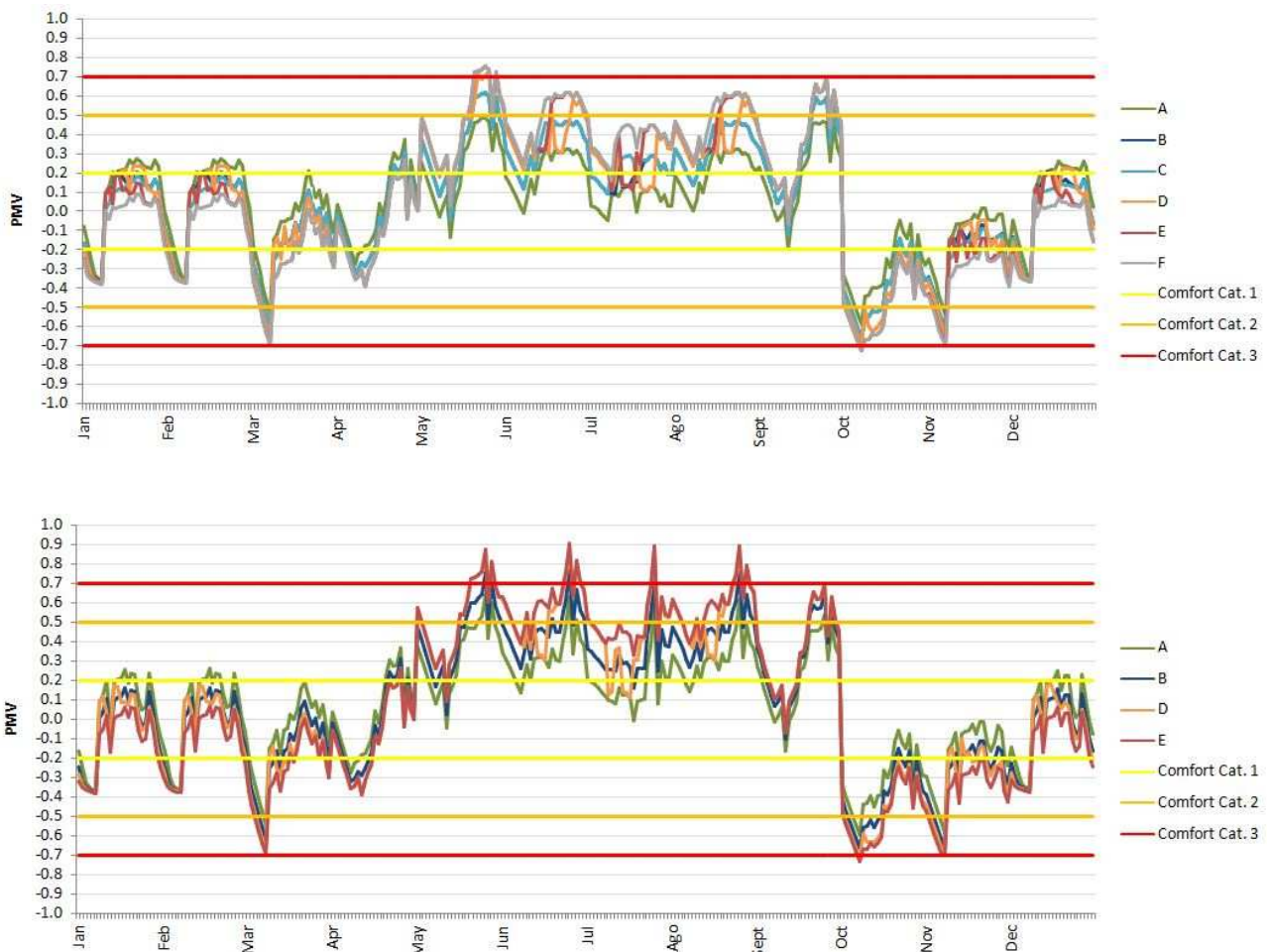


**Figure 52. Hourly PMV trend for different Calibrated Model Configuration (4-6).**

Looking at the graphs, it is possible to see that, within the same configuration, the PMV trend of different optimization cases follows the trend of the base case, widening it, while, comparing different configurations it is possible to note a marked difference in the overall trend. For example, looking at the configurations 1 and 4, with the continuous heating/cooling schedule, the PMV trend is, of course, more constant while, with the intermittent schedule (for all the other configurations), the hourly PMV varies between day and night in accordance with the changes defined by the schedule; as a consequence, the PMV is nearest to the centre of the graph, or rather the "neutral" feeling during the day and farther during the night. Additionally, the trend concerning the winter months is more regular than in summer.

Finally, some considerations about the monthly trends can be added; the profiles achieved in the colder months (January, February and December) are generally very similar whereas during the hottest months different trends occur. Moreover, the minimum and maximum peaks are concerning the middle season months: March, April, October and November for the minimum and May and September for the maximum.

Below, a graph for each configuration show the distribution of hours per year belonging to each comfort category, for each optimization case. The graphs are the results of a data post-processing of presented in the previous charts. In this way it is possible to directly see the time amount belonging

to each comfort category and its variation for each optimization case. For example, by placing an hour/year limit for the category 4, it is immediately possible to decide which case of optimization it is feasible or not.

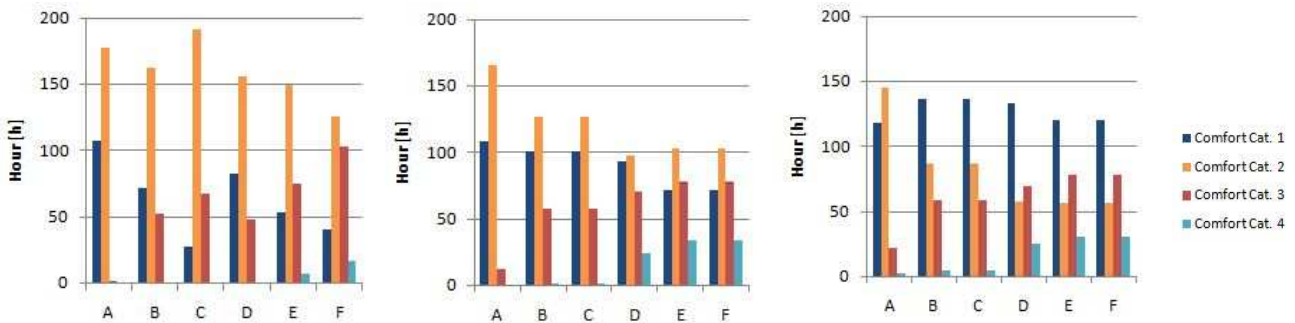


**Figure 53. Comparison between Comfort Category Hours obtained with the optimization cases for different Designed Model Configuration (1-3).**

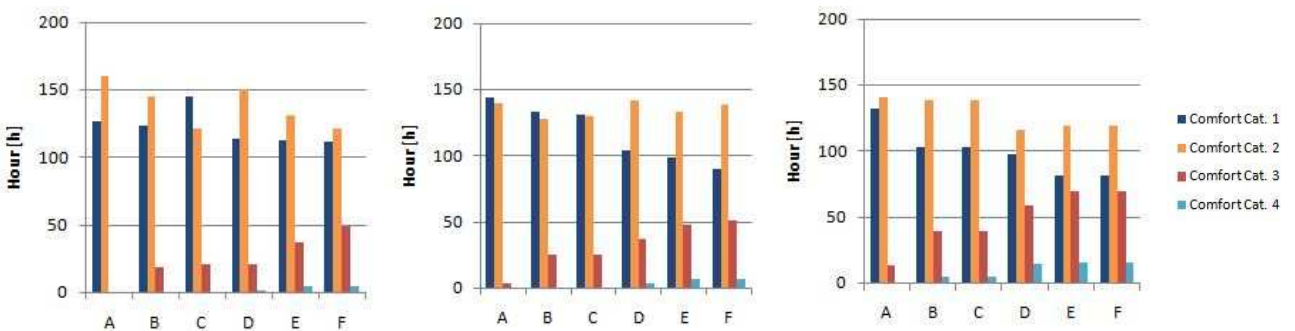


**Figure 54. Comparison between Comfort Category Hours obtained with the optimization cases for different Calibrated Model Configuration (4-6).**

Below the percentages of hours/year relative to each comfort category of base case (A) and the maximum violation case (F) are listed.

**Tab. 79– Yearly Comfort Categories Percentages variation from Optimization Case 1 and 6.**

Comfort Category	Config.1		Config.2		Config.3		Config.4		Config.5		Config.6	
	Case A	Case F	Case A	Case F	Case A	Case F	Case A	Case F	Case A	Case F	Case A	Case F
1	38%	14%	38%	25%	41%	42%	44%	39%	50%	32%	46%	28%
2	62%	44%	57%	36%	50%	20%	56%	42%	49%	48%	49%	42%
3	1%	36%	5%	27%	8%	27%	0%	17%	1%	18%	5%	24%
4	0%	6%	0%	12%	1%	11%	0%	2%	0%	2%	0%	6%

From the results it is evident that most of the hours belongs to the categories 1 and 2, especially as it regards the calibrated model configurations. In general, in fact, the average of hours ascribable to

these two comfort categories are respectively about 75% for the configurations of designed model and 86% for the calibrated model. Then, concerning the designed model configurations, the 21% of hours fits into the 3<sup>rd</sup> comfort category and the 4% to the 4<sup>th</sup>, while for the calibrated model configurations the percentages are, respectively, the 12% and the 2%.

The objective of these graphs, however, is the evaluation of the comfort variations between the base case of optimization (A) and the others; the reduction of the internal temperature, case by case, can bring to a substantial comfort variation and comparing the variation of the hour for each comfort category permits to understand, case by case, when the degree of freedom provided by the optimization algorithm is too high. From the graphs, for example, it is evident that the 4<sup>th</sup> category is increasing slightly (less than 4%, apart from the configurations 2 and 3 that reach 12 and 10%) while the 3<sup>rd</sup> category it grows on average, between the case A and the case F of the 26% for the designed configurations, and 18% for the calibrated ones.

In conclusion, using the comfort categories analysis it is possible to evaluate the maximum limit of degrees/hour or degrees/day of violation used in the optimization algorithm.

#### 5.4.4. DAILY AND HOURLY ANALYSIS

After the investigation about different building configurations, the *Actual* configuration (6) will be analyzed in deep in this section. As already said, the optimization cases C and F are “null”, due to the number of hours of heating/cooling system operation.

The next graphs and tables show the relationship between the internal temperature variation (the lines) and the daily specific energy reduction (the bars). As is seen, to a maximum variation of 1 °C/hour corresponds a reduction of about 10 Wh/m<sup>3</sup>. Considering the representative days, a monthly and seasonal comparison is also possible: during the summer season in fact, with a major temperature variation there is an increased energy demand reduction, on the contrary, the minor saving characterizes the intermediate months, i.e. April and September, where also the temperature variation is lower.

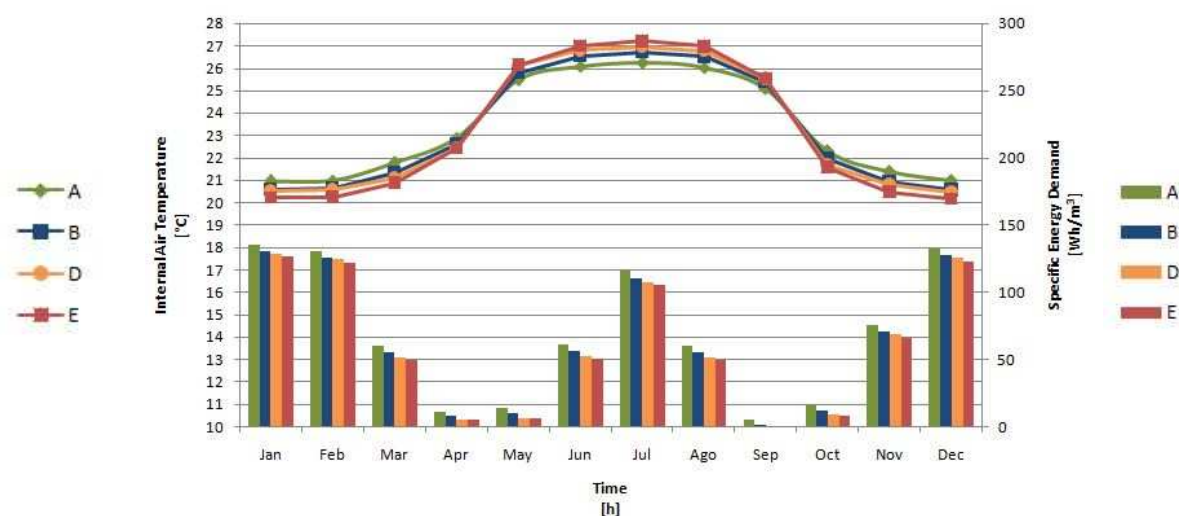


Figure 55. Comparison between Daily Temperature variation and Specific Energy reduction in Configuration 6.

Next Table 80 shows the daily average variation of internal temperature and energy needs for each representative day of the month. Note that each variation is calculated with respect to the base case A. Further the seasonal variation is added.

**Tab. 80 –Daily Temperature variation and Specific Energy reduction in Configuration 6.**

	Internal Air Temperature variation			Specific Energy reduction		
	[°C]			[Wh/m <sup>3</sup> ]		
	Case B	Case D	Case E	Case B	Case D	Case E
<b>Jan</b>	-0.4	-0.4	-0.7	4.4	6.2	8.7
<b>Feb</b>	-0.4	-0.5	-0.7	4.5	6.3	8.8
<b>Mar</b>	-0.4	-0.7	-0.9	5.0	8.3	9.9
<b>Apr</b>	-0.3	-0.5	-0.5	3.0	5.4	5.4
<b>May</b>	+0.3	+0.7	+0.7	3.7	7.3	7.3
<b>Jun</b>	+0.5	+0.7	+0.9	5.3	8.7	10.6
<b>Jul</b>	+0.5	+0.7	+1.0	5.6	8.7	11.1
<b>Ago</b>	+0.5	+0.7	+0.9	5.2	8.7	10.5
<b>Sep</b>	+0.3	+0.5	+0.5	3.3	4.9	4.9
<b>Oct</b>	-0.4	-0.6	-0.7	4.0	7.0	7.9
<b>Nov</b>	-0.4	-0.6	-0.9	5.0	7.3	10.0
<b>Dec</b>	-0.4	-0.5	-0.8	4.6	6.4	9.0
<b>Average Heating Season</b>	-0.4	-0.5	-0.7	4.4	6.7	8.5
<b>Average Cooling Season</b>	+0.4	+0.7	+0.8	4.6	7.7	8.9

Finally, it is possible to see the hourly variations and in the graph below, to ease the understanding, only the January and July representative days are shown: here it is even more evident the temperature variation of 0.5 or 1°C/hour set as a limit by the optimization cases (the lines) and, at the same time, the reduction of the hourly energy calculated in order to obtain the required temperature (the points). The hourly energy visualization (on the secondary axis) makes it clear that, predicted the internal and solar gains, the indoor temperature is reached in order to fully exploit the gains and, thus, minimize the energy needed. As a consequence, in winter, the energy is concentrated during the early morning because of the solar radiation is higher during the afternoon. It should also be noted that the peak of temperature in July is caused by the internal gains value of the relative assumed schedule: at 20 pm, in fact, are provided 8 W/m<sup>2</sup> caused by cooking (see Table 69). It can be considered reasonable in winter season but perhaps too high in summer. As previously mentioned, in fact, the ventilation and internal gains hourly values should be provided through the parameter identification technique starting from actual data.

Then, the temperature profiles show that the set-back temperature is not violated in any case, because the temperature variation is imposed only on the set-point temperature.

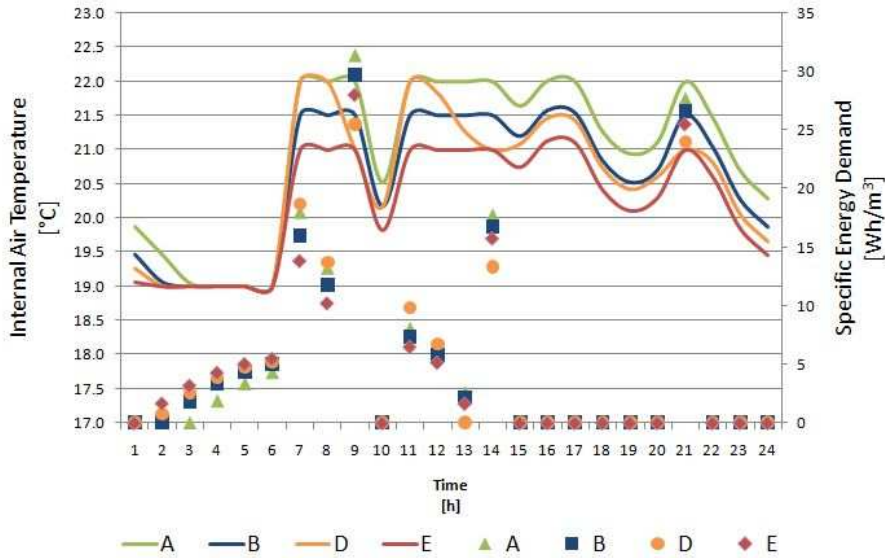


**Figure 56. Hourly Air Temperature and Specific Energy Demand trends for the representative days of January.**

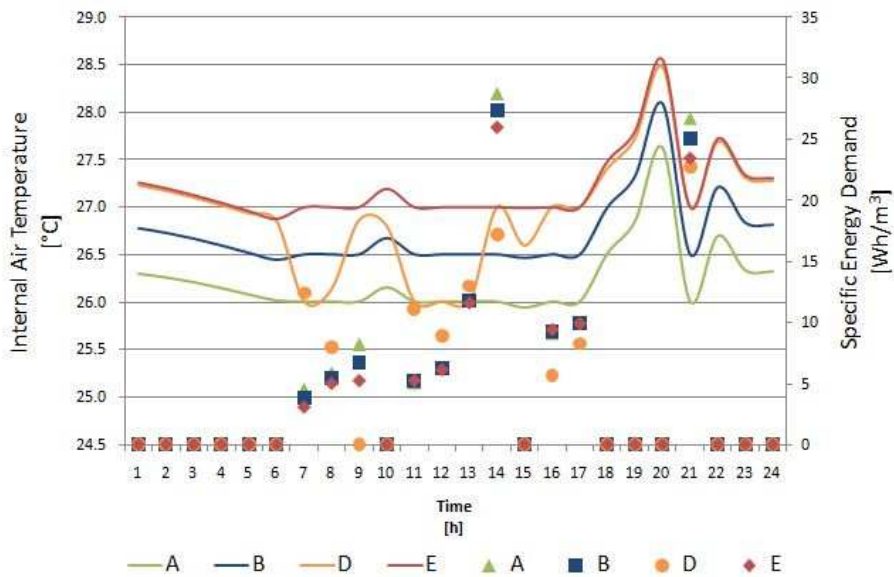


**Figure 57. Hourly Air Temperature and Specific Energy Demand trends for the representative days of July.**

Further, it is evident that the trend of the optimization case D (orange) differs from the cases B and E; in both months the temperature trend has a different profile however, above all, as regards the energy in the month of July, the hourly distribution is completely different. This demonstrates that the optimization algorithm, case by case, finds the optimal solution with respect to the various limits imposed.

Then, a daily comparison of saved energy (the bars) and obtained PMV (the lines) is proposed. The graph aims to show the relationship between the thermal energy reduction with respect to the variation of the PMV. As for the graph in the Figure 55, to a greater variation corresponds a greater reduction and vice versa but, the ultimate goal is to see and evaluate the amount of the variations.



**Figure 58. Comparison between Daily Average PMV variation and Thermal Energy reduction in Configuration 6 compared to Case A.**

Firstly, it should be noted that, concerning the secondary axe indicating the energy saved compared to the base case (A), the latter is void. Secondly, it is possible to see that, in contrast with the average seasonal PMV showed in Figures 49-50, the daily peaks are slightly higher; the maximum variation is concerning the July representative day (+0,32 in Case E) for summer and both November and March representative days (-0,19 in Case E) for winter. Therefore, comparing the optimization cases B and E, for example, to a PMV variation lower than 0.2 it is possible to double the energy saved. In any case, to deeply evaluate the peaks, the hourly trend must be checked. This graph is helpful to compare the PMV variation to the energy savings in order to be able to ensure that the comfort "reduction" has a real benefit during the whole year.

Like above, the next Table 81 shows the daily average variation of PMV and energy saved for each representative day of the month and each variation is calculated with respect to the base case A. Further the seasonal variation is added.

**Tab. 81 – Daily PMV variation and Thermal Energy reduction in Configuration 6 compared to Case A.**

	Daily PMV Variation			Daily Thermal Energy Saved		
	[-]			[kWh]		
	Case B	Case D	Case E	Case B	Case D	Case E
<b>Jan</b>	-0.02	-0.04	-0.09	16.4	22.8	32.2
<b>Feb</b>	-0.01	-0.02	-0.08	16.7	23.2	32.6
<b>Mar</b>	-0.10	-0.15	-0.19	18.4	30.6	36.7
<b>Apr</b>	-0.03	-0.08	-0.08	11.1	20.0	20.0
<b>May</b>	+0.09	+0.19	+0.19	13.6	27.1	27.1

<b>Jun</b>	+0.14	+0.22	+0.28	19.8	32.2	39.2
<b>Jul</b>	+0.16	+0.23	+0.32	20.6	32.3	41.2
<b>Ago</b>	+0.14	+0.22	+0.28	19.4	32.2	38.7
<b>Sep</b>	+0.08	+0.12	+0.12	12.2	18.0	18.0
<b>Oct</b>	-0.09	-0.16	-0.18	14.8	26.0	29.2
<b>Nov</b>	-0.10	-0.13	-0.19	18.6	26.9	36.8
<b>Dec</b>	-0.03	-0.05	-0.11	17.1	23.7	33.4
<b>Average Heating Season</b>	-0.05	-0.09	-0.13	17.1	28.4	32.8
<b>Average Cooling Season</b>	+0.12	+0.20	+0.24	16.2	24.8	31.6

After that, as previously done, two days profiles are presented, in this case November for the winter season and July for the summer one. These days are chosen to show the maximum variations. The points correspond to the PMV while the lines to the energy saved comparing to the base optimization case (A). When the latter is positive it means that it is actually energy saved, where it is negative, instead, corresponds to an energy increase compared to the base optimization case (A).

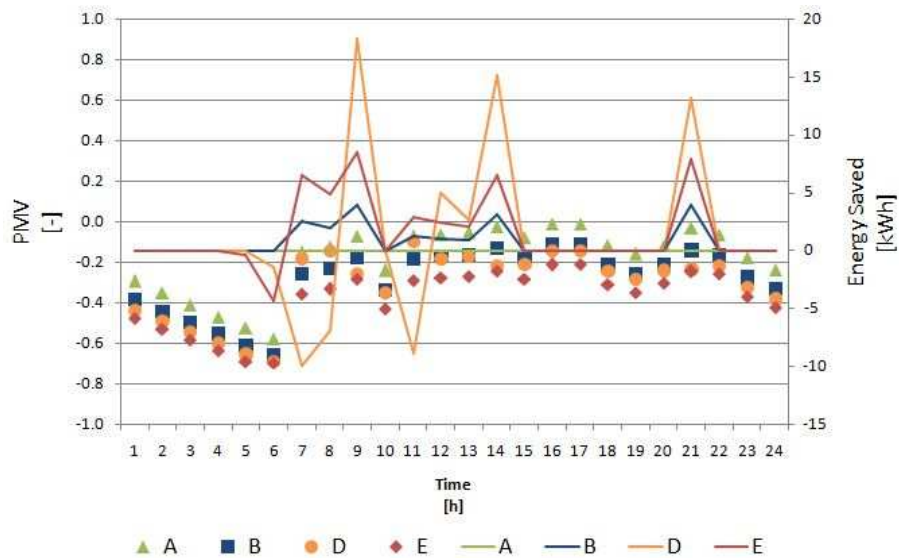


**Figure 59. Hourly Air Temperature and Specific Power trends for the representative days of November.**

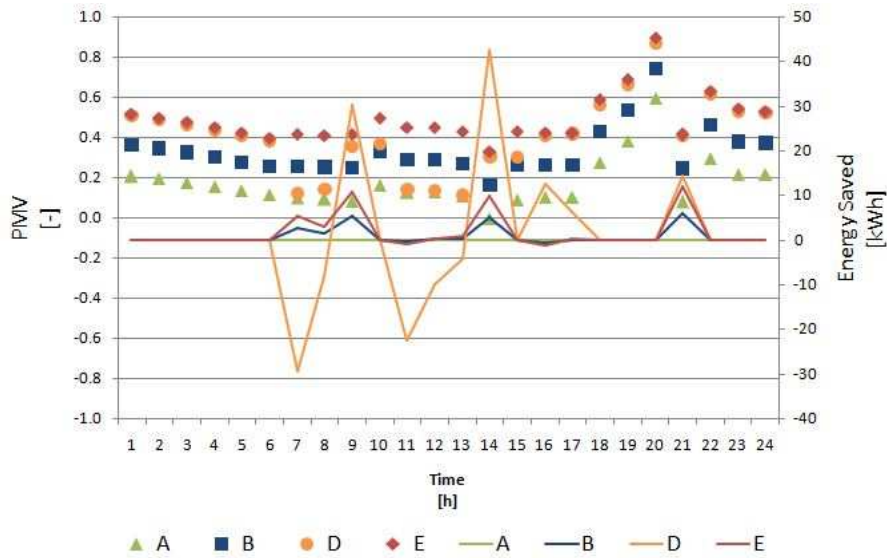


**Figure 60. Hourly Air Temperature and Specific Power trends for the representative days of July.**

Concerning the PMV trend in November, is evident that, following the heating schedules, it is lower during the night but during the day is about -0,2 for all the hours. Regarding July average day, instead, the night and day variation is lower, despite the same schedules are used; in general can be said that the worst PMV is obtained during the evening hours (18-22 pm). Furthermore, it is possible to argue again that, in the summer months the PMV variation is greater while in winter is lower and, in detail, for both the months, the variation between the base case (A) and the cases B and E is quite constant while the variation with the case D is more variable.

As for the energy saved it is mainly concentrated in three hours (9 am, 14 and 21 pm), i.e. during the ventilation peaks where, therefore, being able to reduce/increase the internal temperature required, it is possible to save more energy. Further, also here it is evident the different balance between actually energy saved and wasted between the case D and cases B and E.

Comparing the saved energy and the PMV variation it is possible to conclude that, also during the savings peaks, the PMV variation is sufficiently low because of the low air temperature variation; in conclusion, thus, the energy savings is highly acceptable by the comfort variation point of view.

Finally, in order to have a broad idea to the hourly PMV peaks during the whole winter and summer seasons in Configuration 6, the graphs below are showing the peaks for each optimization case.

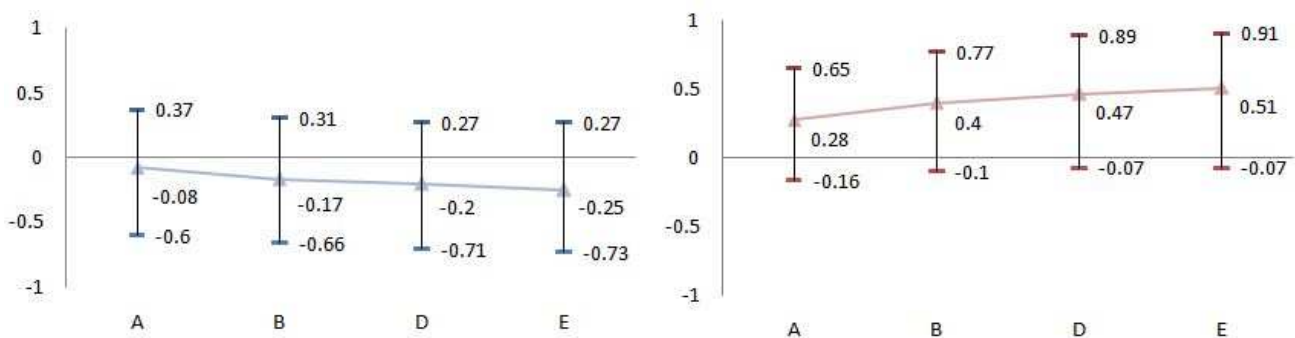


**Figure 61. PMV peaks for winter and summer seasons in Configuration 6.**

Concerning Figure 61, the winter minimum peak varies from -0.60 to -0.73 ( $\Delta = 0.13$ ) while during the summer the maximum PMV rise from 0.65 to 0.91 ( $\Delta = 0.31$ ). It has to be underlined that the inner values, or rather the upper limit in winter and the lower limit in summer, are used for the seasonal PMV average calculation nevertheless are not considered as a "real" peak because are nearest to the 0 (neutral feeling) compared to the other "external" limits. Further, as already assumed, the peak are generally obtained during the middle season months; the winter minimum peaks, in fact, are obtained during October (at 6 am) while the summer maximum peak are, for optimization case 1 in May (at 20 pm) and for the other cases in June (at 20 pm).

Moreover, it has to be remembered that these are the hourly peaks and, for an overall evaluation, the amount of hours for each comfort category has to be considered. Figure 62, splits the previous graph about Configuration 6 (Figure 54) in winter and summer amount of hours belong to each comfort category.

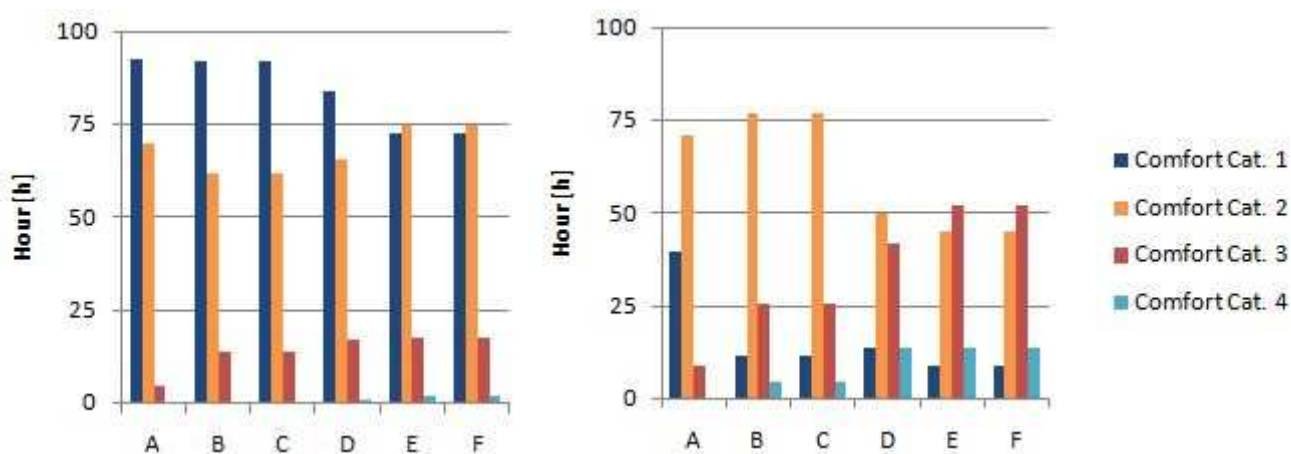


**Figure 62. PMV peaks for winter and summer seasons in Configuration 6.**

It is evident that, in winter, the higher amount of hours with high comfort level (Comfort Category 1 and 2) regards all cases of optimization; the seasonal number of hours belonging to the comfort category 3 rises from 5 to 18 (3% and 11%) while the hours in comfort category 4 go from 0 to 2 (0% and 1%). In summer, instead, the Comfort Category 3 has a substantial hourly increase that rises from 8% to 43% with a decrease of the Comfort Categories 1 and 2 from 93% to 45%. Regarding comfort category 4, it goes from 0% to 12%.

To conclude the comfort evaluation, an explanation about the different calculated internal temperatures is required. As described in Paragraph 4.6.2, The PMV is directly correlated with the operative temperature which is calculated starting from the air temperature and the surface temperatures (Eq. 54). Anyway, the simplified equation for the calculation of the PMV (Eq. 56) that is used here requires the indoor and the surface temperatures.

In order to see the hourly correlation between the internal temperatures, below are highlighted the hourly profiles of air, surface and operative temperatures calculated for the base case A, divided into winter and summer months.

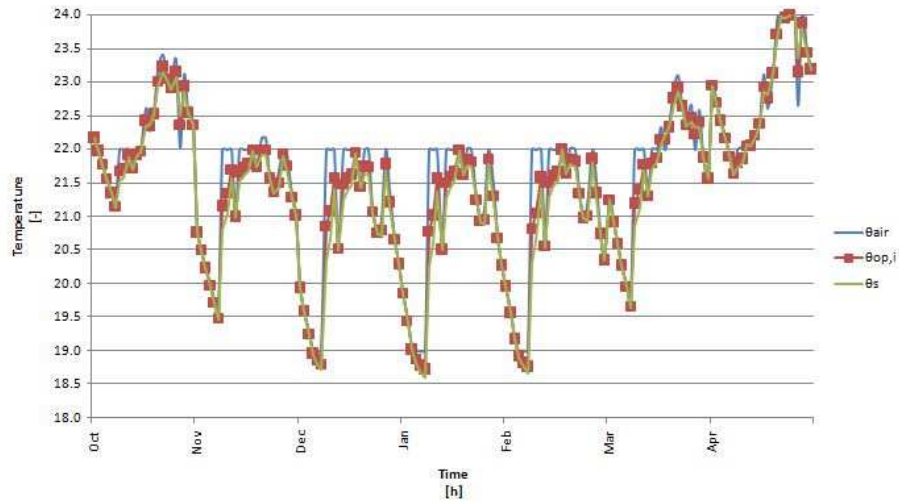


**Figure 63. Internal Air, Surface and Operative Temperature in Configuration 6 (Case A) – Heating Season**

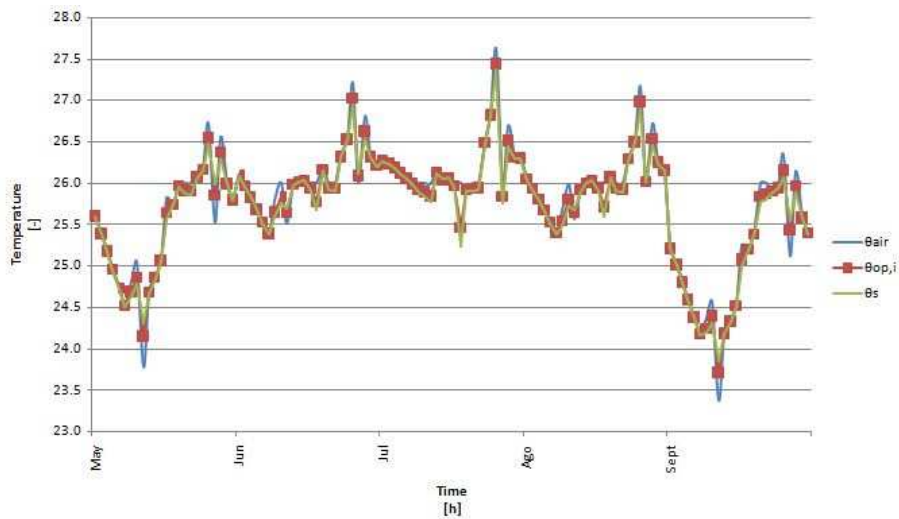


**Figure 64. Internal Air, Surface and Operative Temperature in Configuration 6 (Case A) – Cooling Season**

Concerning Figures 63-64, it can be seen that the greatest variation between the temperatures regards certain peaks in summer while in winter, during daylight hours, the air temperature is almost always about 0.5 °C higher than the surface temperature. This means that, in summer, the variation between air and surface temperature is low while, in winter, the surface temperature deviates the most from the air temperature, reducing significantly the operative temperature. For example, looking at the temperature trend in the early hours of the winter morning, where the set-point is changed from 19 to 22 °C it is possible to see that the surface temperature cannot reach the air temperature immediately, but will need some time. Consequently the operative temperature, that is a dependent on the air and the surface temperature, will be lower than the set-point required. For that reason it is fundamental to not evaluate just the air temperature but also the surface temperature, in order to calculate the comfort level and, although it is not used in order to calculate the PMV, it can be used to better understand the perceived temperature. Then, it's clear that the operative temperature is always between the air and surface temperatures and, with respect to the air temperature, it has a slight variation.

#### 5.4.5. SENSITIVITY ANALYSIS

As already stated above, the goal of the whole process described in the thesis is to improve building energy efficiency in the operational phase through different models and techniques and to use appropriately measured data. In order to verify the sensitivity of some inputs required by the model, here, we will present a generalization of the case study, simulating the possible energy saving indicated by the MPC in different climates and varying both the ventilation rate and the internal gains; therefore it's important to see how the model results depend on these factors.

First, it should be emphasized the fact that the climatic analysis is used in order to generalize the sensitivity analysis of the case study and to show also energy saving ranges achievable in the main national climatic zones for a residential use.

After that, the variation of ventilation rate and of internal gains from a baseline case, instead, will indicate the sensitivity of the model to these input and, thus, how they could impact the final outputs. The sensitivity analysis method used is the One a Time (OAT) one, as one single parameter is varied for each calculation. It is one of the simplest methods for test the most important parameters in a model [7], and, for the reasons already explained, or rather that the MPC is applies to a real building with a certain geometry and envelope characteristics, the main parameters that is important to analyze are the ventilation and internal gains.

Concerning the Italian cities analyzed, the main data used by the MPC are listed in Table 82 and shown in Figure 65. Please note that the data refers to the daily average for each month and that the hourly values are derived by them (see section 4.2.7.).

**Tab. 82 – Main daily climate data used for climate analysis**

	External Temperature			Global Solar Radiation		
	Milan	Rome	Palermo	Milan	Rome	Palermo
	[°C]	[°C]	[°C]	[kJ/m <sup>2</sup> ]	[kJ/m <sup>2</sup> ]	[kJ/m <sup>2</sup> ]
January	0.6	12.1	7.6	2959	5701	4423
February	2.9	13.0	8.0	4679	8306	6515
March	8.5	13.4	10.2	8605	12626	10722
April	12.8	15.8	13.0	13415	17341	15504
May	16.8	19.2	17.2	17476	21829	19881
June	19.9	21.9	21.0	19447	23594	22029
July	23.1	24.8	24.2	19941	24170	22036
August	22.0	25.8	24.0	16121	21506	18564
September	19.0	23.7	21.1	11558	15710	13643
October	13.0	19.9	16.0	6695	10098	8684
November	7.5	17.4	12.4	3088	6510	5166
December	2.4	13.4	8.4	2327	4811	3770

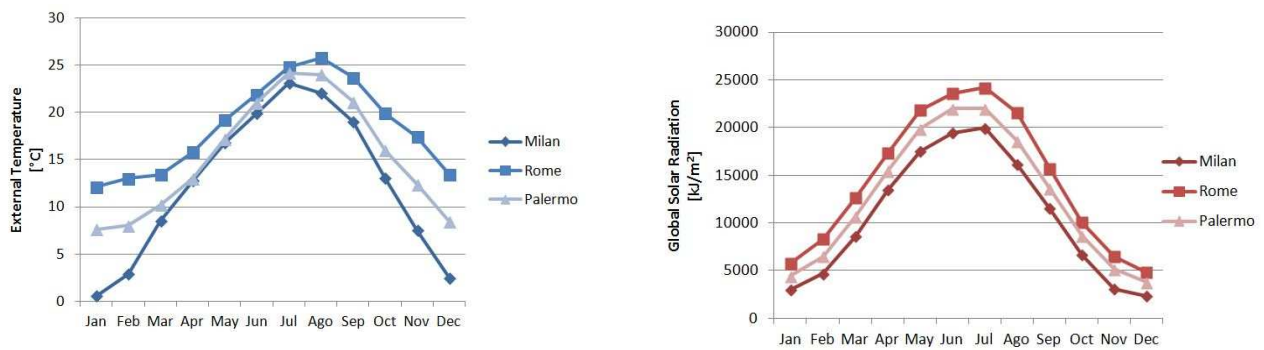


**Figure 65. External Temperature and Global Solar Radiation distributions for different climates used.**

In order to generalize the case study, the Baseline Case is run with the Configuration 1 previously used (Tables 68-69), where the building operation is continuous and the internal temperature required is 20 degree, the air change rate is 0.3 1/h and the internal gains are 4 W/m<sup>2</sup>. The building geometry considered is the same for each climate, but the U values of the components are corrected in line with the limits required by the national standard [8], which depends on the climate zone.

**Tab. 83– Average Transmittance limits for different climate zones as required by [8]**

Average Transmittance		Milan	Rome	Palermo
Exterior Wall	[W/m <sup>2</sup> K]	0.27	0.29	0.41
Transparent components	[W/m <sup>2</sup> K]	1.80	2.00	2.40
Roof	[W/m <sup>2</sup> K]	0.24	0.26	0.32
Ground floor	[W/m <sup>2</sup> K]	0.30	0.34	0.46

Then, both the optimization cases B and F (as in Table 72) are simulated in order to show a sort of energy savings range between a maximum and minimum conditions; the hourly limit violations chosen are, respectively, 0.5 and 1 degree and the daily ones 5 and 15.

According with the previous hypothesis, the following table is showing the possible energy savings obtained with the MPC for the three climate zones analyzed.

**Tab. 84– Possible Energy Savings with different Optimization Cases during Heating and Cooling Seasons for different climate - Baseline Case**

Optimization Cases	Heating Season			Cooling Season		
	Milan	Rome	Palermo	Milan	Rome	Palermo
<b>B</b>	3%	5%	9%	12%	9%	8%
<b>F</b>	8%	13%	24%	25%	19%	18%

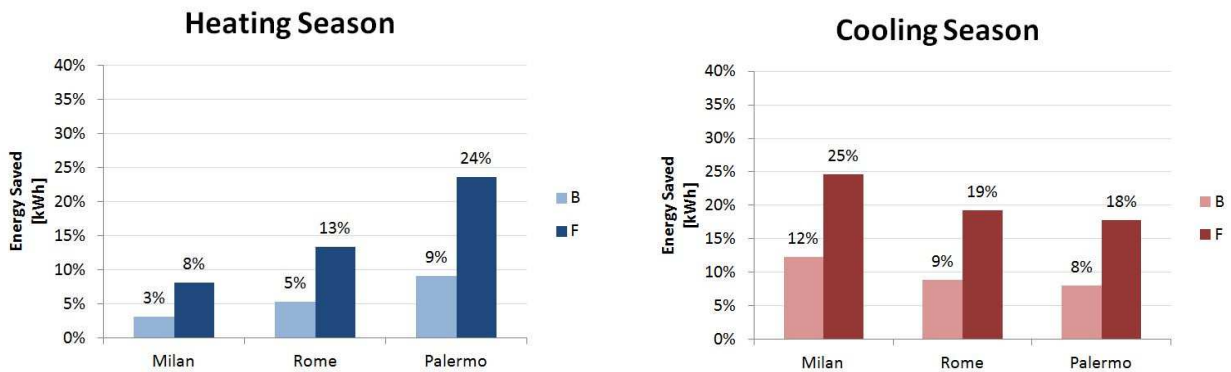


**Figure 66. Possible Energy Savings with different Optimization Cases during Heating and Cooling Seasons for different climate - Baseline Case**

Here, two types of assessments can be done; firstly, during the winter season the higher savings are achieved by the warmer weather (Palermo) while in summer the greater savings are in the colder climate (Milan). This seems to suggest that the lower the energy needs, the higher is the potential savings. However, it should also be assessed the gap between minimum and maximum savings, i.e., the relationship between savings and the violation limits of temperature applied. The greater the violation, the greater the savings gap across the different climatic zones. This is because the smaller the number of hours per day of energy demand, the greater the possibility of exploiting the maximum violation per day applied. Please, remember that the maximum daily violation here is set as 15 degree day and the Conf.1 used has a plant operation schedule of 24 hour per day. In an actual use of the MPC, the maximum violations will be probably different in the three climate zones but in this case they are considered to be equal, in order to enable a meaningful comparison.

After considering the sensitivity with respect to climate, we perform the analysis by changing ventilation rate and the internal gains. In details, the air change rate will be ranging from a minimum of 0.3 and a maximum of 0.5 1/h while the internal gains ranging from a minimum of 2 to a maximum of 6 W/m<sup>2</sup>. It has to be underlined that the case study is a residential building, so, the sensitivity analysis here is done just for this building usage. A radical change of its usage would lead to a change about both geometry and envelope compositions that is difficult to achieve starting from the case study building presented in this thesis. Further, it should be stressed that the sense of this chapter is to show the application of the workflow presented in chapter 4, working with a real building and real data, and evaluate the outcomes from a more general standpoint, employing sensitivity analysis.

In the charts below it is possible to see the results obtained by varying the internal gains from the baseline case, both in winter and summer season (respectively blue and red lines) and for each climate. In detail, the symbol "+" is representing the seasonal energy savings achieved with the higher internal gains level ("IG\_max" is equal to 6 W/m<sup>2</sup>) and the symbol "-" the lower one ("IG\_min" is equal to 2 W/m<sup>2</sup>). The ventilation rate is fixed at 0.3 1/h.

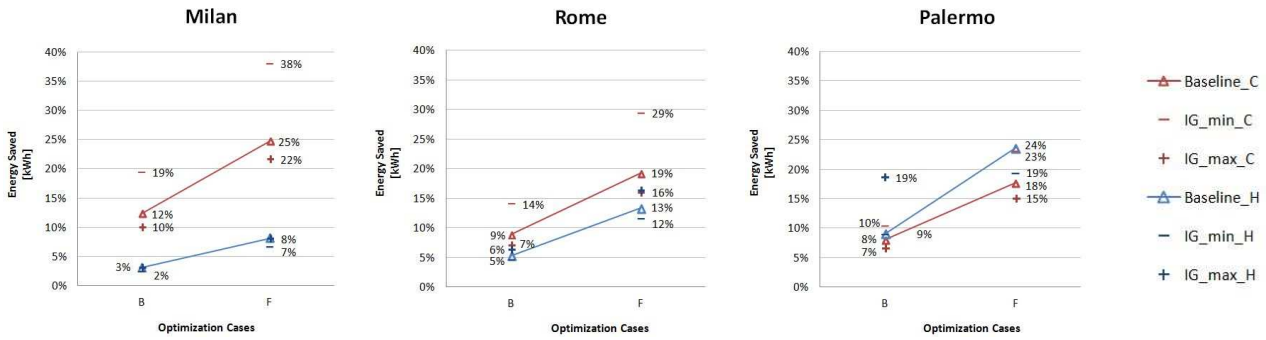


**Figure 67. Possible Energy Savings with different Optimization Cases during Heating and Cooling Seasons in different climate with fixed Ventilation Rate (0.3 1/h) and variable Internal Gains.**

In general, from the obtained results is deduced that the outputs are more sensitive to the internal gains variation in summer and, again, when the energy demand is lower. Both the savings potential that the "uncertainty" of it, therefore, increase with decreasing of the amount of energy needs. This is very important because it supports the importance of using real data in order to calibrate and to use the MPC especially in efficient buildings, or rather where the energy needs are lower.

The following charts, instead, are showing the analysis of the ventilation parameter; starting from the baseline case with a ventilation rate of 0.3 to a maximum of 0.5 1/h (Vent\_max) is possible to see also the sensitivity of this input data. The internal gains, here, are fixed at 4 W/m<sup>2</sup>.

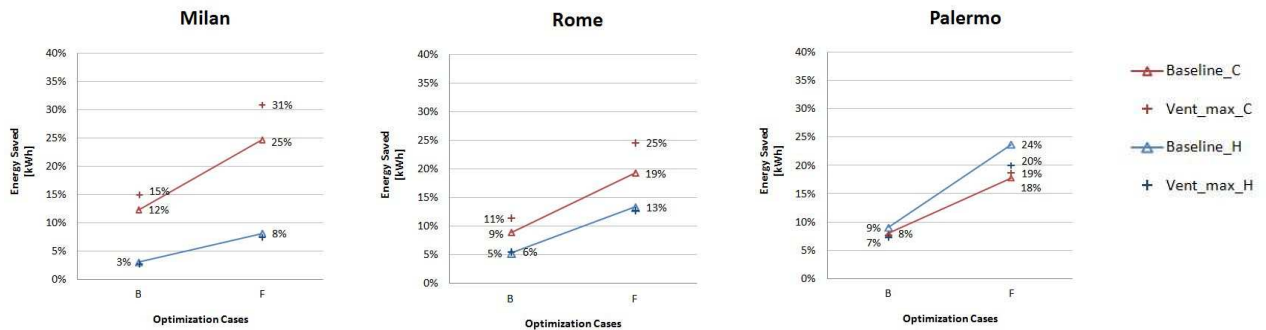


**Figure 68. Possible Energy Savings with different Optimization Cases during Heating and Cooling Seasons in different climate with fixed Internal Gains and variable Ventilation Rate.**

In this case the variations are lower than the ones shown in Figure 76, therefore, it means that the internal gains have a bigger weight than the ventilation rate on the model outputs. The correlation with the amount of energy needs, anyway, is the same as the previous situations and the variation is higher when the energy needs are lower.

Finally, also the case with the maximum ventilation rate (0.5 1/h) and the internal gains variation is run and the results are shown in the following graphs. As a results of the two previous simulations (Fig.67 ad 68) the sensitivity is lower than the first case (Fig. 67) but higher than the second one (Fig. 68).

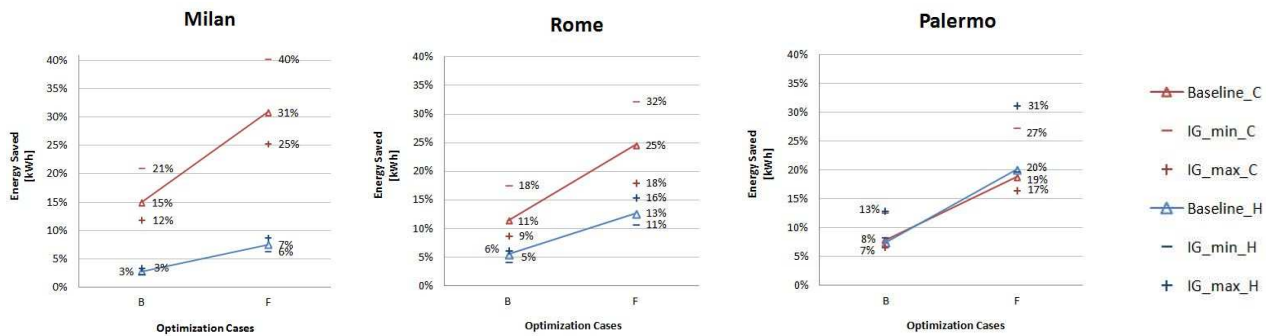


**Figure 69. Possible Energy Savings with different Optimization Cases during Heating and Cooling Seasons in different climate with fixed Ventilation Rate (0.5 1/h) and variable Internal Gains.**

In general it can be said that the amount of energy saved may vary up to 50% with a variation of the same percentage of internal gains; the maximum variation of the simulated cases, in fact, relates to the first analysis presented, namely the winter case in Palermo where the internal gains were increased from 4 to 6 W/m<sup>2</sup> increasing the minimum energy savings (Optimization case B) from 9% to 19% and the maximum ones (Optimization case F) from 24% to 42%. With respect to the other cities, the most significant value relates to an increase of approximately 35% of the possible energy savings in the summer cases decreasing the internal gains from 4 to 2 W/m<sup>2</sup>. In detail, in Milan the minimum energy savings (Optimization case B) rise from 12% to 19% and the maximum one (Optimization case F) from 25% to 38% while in Rome, respectively, from 9% to 14% and from 19% to 29%. Concerning the ventilation analysis the higher variation is about 20% in the same cases said above; increasing ventilation from 0.3 to 0.5 1/h, the winter savings in Palermo decreases from 9% to 7% (Optimization case B) and from 24% to 20% (Optimization case F), in Milan the summer savings increase, respectively, from 12 to 15% and from 25 to 31%, and in Rome from 9 to 11% and from 19 to 25%. Finally, with a fixed ventilation rate of 0.5 1/h and variable internal gains, the maximum variation is about 40%, still in the winter case of Palermo with higher level of internal gains where the energy savings rise up from 7 to 13% and from 20 to 31%. The maximum variations in Milan and Rome are approximately the 25 and 30% still in the same cases, or rather, the summer situation with the lower internal gains level where the energy savings rise up from 15 to 21% and from 31 to 40% in Milan and from 11 to 18% and from 25 to 32% in Rome.

As a conclusion, it can be said that the variation, although not excessive, stresses again the importance of having measured data to enable model calibration, because the optimization process of MPC, and the related outcomes, is highly dependent on these parameters.

## 5.5. DISCUSSION

In conclusion, this chapter shows the entire process of data analysis in order to both monitor and manage optimally building energy demand.

Firstly, the lumped parameter model was calibrated through the analysis of measured data, i.e. the monthly energy demand and the internal free-floating temperature. In detail, transmittances and capacity of the building have been changed, after further on-site measurement sessions. Then, the in-

verse models and the optimization algorithm were tested through different configurations of the case study, created by varying both the thermo-physical characteristics of the building and the schedules for ventilation, internal gains and heating/cooling operation (i.e. building operation modes).

The results obtained indicate that, through inverse models, the main parameters (internal gains, ventilation and envelope transmittances and capacity) can be identified starting from hourly data of air temperature and energy needs. Further, considering the optimization cases tested, it has been shown that is possible to obtain a 10% energy saving with respect to the present state-of-the-art of control, considering a temperature violation limit of 1°C during the heating/cooling operation hours.

The comfort analysis revealed that the average PMV remains almost stable, i.e. energy savings can be obtained without compromising significantly thermal comfort. Furthermore, it should be recalled the fact that it is possible, by formulating the objective function in an appropriate way, to minimize also the running costs and CO<sub>2</sub> emissions, eventually weighting multiple objectives, in a multi-criteria fashion.

In this way, in case of variable electric energy tariffs for example, the optimization algorithm will search the optimal operating trajectories, considering the relevant operation constraints which are present, not only at the building level.

Finally, it can be pointed out that the added value of the approach presented resides not only in the possibility to save energy and to increase operational flexibility, but more in general in the possibility to construct in an incremental way a simplified energy model. This energy model can give a feed-back on the real performance of physical elements and on building operation modes, thus helping to reduce the “performance gap” between simulated and measured performance.

In conclusion, a generalization of the results obtained with the case study is presented using different climate conditions and a sensitivity analysis on internal gains and ventilation rate. Of course, by performing a generalization through simulation it was not possible to calibrate on other real case studies, but the sensitivity analysis enabled us to see how much the output results may vary according to a variation of the relevant input parameters.

By analyzing the whole process applied to the case study, we can conclude that while modelling approached can be verified and validated numerically, the calibration phase is the most delicate and important. In fact, the selection of parameters to be calibrated is not immediate but must be interpreted starting from actual data, that unfortunately in most of the cases are not easily accessible and sufficient to obtain an effective model. Further research work should be necessarily oriented in this sense.

## **LIST OF REFERENCES**

- [1] U.S. Department of Energy (DOE) Building Technologies Office (BTO) and National Renewable Energy Laboratory (NREL), EnergyPlus Energy Simulation Software, <http://apps1.eere.energy.gov/buildings/energyplus/>.
- [2] ANSI/ASHRAE Standard 140-2011, Standard Method of Test for the Evaluation of Building Energy Analysis Computer Programs.
- [3] EN 15265:2007, Energy performance of buildings. Calculation of energy needs for space heating and cooling using dynamic methods. General criteria and validation procedures.
- [4] <http://www2.arpalombardia.it/siti/arpalombardia/meteo/richiesta-dati-misurati/Pagine/RichiestaDatiMisurati.aspx>
- [5] UNI EN ISO 13790:2008, Energy performance of buildings, Calculation of energy use for space heating and cooling.
- [6] ISO 9869-1:2014, Thermal insulation — Building elements — In-situ measurement of thermal resistance and thermal transmittance — Part 1: Heat flow meter method.
- [7] Fabrizio E., Monetti V. Methodologies and Advancements in the Calibration of Building Energy Models. *Energies*. 2015; 8:2548-2574
- [8] D.M. 26 gennaio 2010 “Aggiornamento del decreto 11 marzo 2008 in materia di riqualificazione energetica degli edifici”.

## 6. CONCLUSION

EU environmental and energy policy in the building sector has evolved over time embodying progressively concepts such as sustainability and resource efficiency and European Commission established the long-term objective of decreasing the CO<sub>2</sub> emission levels for the building sector by 88-91% in 2050, compared to 1990 levels. In order to achieve this target, which is also a prerequisite for meeting other EU economic and climate goals (Directive 2009/87/EC), the EU especially needs to tackle the existing building stock and reduce drastically its energy use in the long term.

The “decarbonization” of built environment has to go through increased penetration of renewable energy sources and increased efficiency in end-uses. Energy efficiency practices, in fact, are relevant today for economic development at the EU level and can determine several additional benefits. Building renovation strategies, so, are an essential element in sustainability transition path planning, which have to match short-term goals (i.e. economic growth and job creation) and long-term goals (i.e. sustainability). In a general sustainability perspective, environmental and economic impacts related to building energy use, are strictly correlated with the social (and also behavioural) dimension of the problem (environment, economy and society are the three pillars of sustainability). The social dimension is connected to both the type of activities that are present within the built environment and the internal environmental quality (e.g. air quality, thermal comfort, visual comfort, etc.) perceived by occupants, which has to be controlled in the operation phase.

In the last few decades, control systems in buildings have received much less attention than other areas, but their role is becoming crucial because of the possibility to manage technical functions and to acquire data on real building performance. The relevant gap often present between simulated and measured energy performance is caused by errors committed during the whole building life cycle, i.e. in design phase, construction phase, commissioning and operational phase. In order to be able to bridge this gap, it is necessary first to identify the key factors influencing both predicted and measured energy performance, like design assumptions, modelling tools characteristics, as-built quality and occupants’ behaviour, etc.

In the design phase, on the modelling side, errors are mostly connected to generally optimistic assumptions on building components and technical systems performance, together with an inadequate understanding of occupants’ behaviour. Further, despite the large effort in disciplines such as building physics, building science and energy management, an overall coherent, reliable, robust and interoperable model-based approach for performance optimization across all building life cycle phases, is still currently missing. The evolution of building performance simulation as a discipline is certainly giving a contribution in this sense both on the theoretical and on the applied side, but there exist still relevant issues to be addressed.

In the analysis of the *state of the art* it has been shown that two fundamental elements are crucial: the ability to predict the energy demand so that it can be optimally handled (by means of an appropriate optimization algorithms) and the ability to analyze and use measured data both to diagnose any malfunctioning and to calibrate the predictive models.

Concerning Model Predictive Control (MPC) the major issue is related to the building simulation model: although many detailed dynamic models for the energy assessment are now available, models applicable to control systems are few and not always usable across building life cycle phases. Actually, it is shown that in order to be easily and efficiently implemented in a control system, the model must be simplified and linear. Furthermore, the model could contain both quantities with

physical meaning and quantities that are purely numerical; grey-box models can be used in this sense, but more work is required to develop them. A real integration between physical energy modeling and automation is necessary, in order to obtain sufficiently robust and accurate models to correctly predict the building behavior, but which should be also simple enough to be used for MPC. Concerning the use of data, today it is technically possible to acquire and process large scale data to reconstruct the energy behavior of the building stock at multiple scales but, in practice, this does not happen very often and, when it happens, it is difficult to obtain good data to work on. Despite that, within an appropriate uncertainty analysis framework, data analysis can be done with different levels of detail and can provide several advantages, representing a fundamental tool for the future of energy management practices in buildings. The use of grey-box and black-box models renders possible (computationally cheap and efficient) workflows that can support the sustainability transition of the built environment.

Considering these general issues, the original part of the research presented is given by the overall methodology that aims to address some of the fundamental problems present in monitoring and control systems.

Starting from a linearized lumped parameters model, an optimization algorithm is used to find the optimal operation trajectory that satisfies the constraints while minimizing energy demand.

With a Linear Programming (LP), in fact, it is possible to find the best possible solution given the specific conditions (i.e. find a solution that is certainly a global optimum). Further, the optimization model, working on set-point violations, can be, in principle, simply added an additional layer on existing automation systems, without having to replace completely the technology, but simply working on the top of conventional PI/PID controllers.

In the data analysis workflow presented, two main levels of model calibration are done; firstly with monthly data the main lumped parameters are analyzed through regression models and secondly, using hourly data, an identification technique (ARX model) is used to directly calibrate/built the whole model (suitable for multiple temporal scale of analysis) with the estimated parameters.

In this sense, we can think about a workflow in which there is an overlay of long-term performance monitoring, with low-frequency data (i.e. monthly, daily), and short-term model recalibration based on detailed high-frequency data (i.e. hourly, sub-hourly). An important feature of regression models is that they can work online, and, thus, they can periodically self-calibrate and give a feed-back on performance while the ARX model is helpful to dynamically reconstruct the energy model suitable for optimization starting from actual hourly data. By analyzing the data, it is possible to perform Fault Detection and Diagnosis (FDD) assuring both a good performance of the control system and a prompt corrections in case of energy performance deviation during the operation phase. Parameter identification allows also to analyze the evolution of parameters over time, and, thus, lay the foundations for a machine learning system application which may constantly improve the control system knowledge adapting and learning to building and end-users characteristics.

In summary, the whole analysis workflow proposed is in continuity with present energy management and FDD practices. On the other hand it is also important to unveil the fundamental behavioral dimension of the problem, to promote a behavioral change.

The energy demand reduction, however, is not the only objective to be pursued. Internal environmental quality and energy savings can be conflicting objectives and comfort expectation can cause an “economic rebound effect”, limiting the energy saving potential of efficiency practices and, therefore, compromising the return of investment. The robustness of building performance models

can become an issue, in terms of risk, especially in techno-economic evaluations employing cost-optimal analysis and life cycle cost (LCC) accounting methodologies.

The internal comfort evaluation, thus, is fundamental in order to ensure feasible energy savings, keeping end-user behaviour under control. As shown in Chapter 5, the Predicted Mean Vote (PMV) evaluation acquires a crucial role in the choice of the limits to be set in the optimization algorithm. The latter in fact, needs a limit in terms of degree/days and degree/hours of comfort violation that can be chosen starting from a comfort assessment, done through the PMV evaluation.

Further, a possible evolution of the control scheme is related to the consideration of different comfort models, including adaptive one when HVAC systems are turned-off, leading to a “hybrid” control scheme with two operating models which compete in the optimization.

Through an adaptive control, in fact, the comfort level can be calculated even in case of intermittent “active” (i.e. HVAC on) and “passive” operation (i.e. HVAC off), or rather with a “passive” control scheme.

The advantages provided by a Model Predictive Control (MPC) system such as the one presented in this research are also dependent of the type of objective function adopted. Starting from the minimal energy demand, in fact, it is also possible to minimize costs (using dynamic tariffs) and emissions (using hourly CO<sub>2</sub> emission time-series and emission factors) or considering a combination of both, using weighting factors. Further, it permits to increase the overall energy efficiency, considering both the load matching and the dispatch flexibility problem. The first concerns the possibility to optimize the matching among energy produced onsite and load. Dispatch flexibility, instead, indicates a virtual storage capability able to improve the energy dispatching according to comfort and demand requirements.

As a conclusion, the research aims to give a contribution in the building energy efficiency field, but considering a wider perspective on the use of data at the building scale. Automated data acquisition and processing could, in principles, be used for large-scale performance benchmarking in the building stock. This fact represents a big opportunity for the evolution of the building sector, as pointed out in an ongoing EU Joint Research Centre (JRC) project on “Resource Efficient Building”. The project by the JRC follows European Commission Communication on Resource Efficiency Opportunities in the Building Sector - COM(2014)445, which insist on the use of data to improve the whole life cycle environmental performance, the quality and the value in buildings.

However, while policy initiatives can translate macro-objectives into performance indicators and clarify the general framework, fundamental issues remain that of real environmental performance measurement and benchmarking.

In the past, the limited collection of detailed and reliable building data, as well as the underestimation of the importance of access to high quality data has determined an over-reliance on normative models. Today the possibility of incorporating models for control and diagnostic already from the design phase, as well as the possibility to use automated meter reading system, makes it possible to think about a major breakthrough in the construction sector, by bridging the knowledge from different fields, in particular automatic control, performance diagnostic, energy efficiency and construction technology.